

International Association for Gondwana Research Conference Series 22

International Association for Gondwana Research Conference Series 22

2016 Convention & 13th International Conference on Gondwana to Asia

Editors

A.P.Pradeepkumar, E.Shaji and M.Santosh

Abstract Volume

November 18-22, 2016



ISBN 978-81-923449-6-6



9 788192 344966 >

International Association for Gondwana Research Conference Series 22

**2016 Convention &
13th International Conference on
Gondwana to Asia**

Abstract volume



Organized by

Department of Geology, University of Kerala, Trivandrum, India

Supported by UGC-SAP-DRS II

Sponsored by

University of Kerala

(Reaccredited with A grade by NAAC)

Trivandrum, India, November 18-22, 2016

International Association for Gondwana Research Conference Series 22

**2016 Convention
&
13th International Conference on Gondwana to Asia**

Abstract Volume

Editors

A.P.Pradeepkumar¹ E.Shaji¹ and M.Santosh^{2, 3}

¹ *Department of Geology, University of Kerala, Trivandrum 695 581, India*

² *China University of Geosciences Beijing, No. 29 Xueyuan Road, Beijing 100083, China*

³ *Department of Earth Sciences, University of Adelaide, SA 5005, Australia*

Published by the International Association for Gondwana Research

IGR Conference Series No. 22, pp.1–226

2016

© International Association for Gondwana Research

China University of Geosciences Beijing,
29 Xueyuan Road,
Beijing 100083, China.
E-mail: gondwana@cugb.edu.cn

ISBN 978-81-923449-6-6



9 788192 344966 >

Edited by

A.P.Pradeepkumar, E.Shaji, and M.Santosh

Co-editors

Rajesh S¹, Nandakumar V², Rajesh V J³, Sajeev K⁴

¹Department of Geology, University of Kerala, Trivandrum, India

²NCESS, Trivandrum, India

³IISc, Bangalore, India

⁴IIST, Trivandrum, India

Editorial assistance

Dhanil Dev. S. G., Prasanth. R.S., Dhaneesh. K.J., Prathiba Raveendran., Indu. G.T

Proceedings of the International Association for Gondwana Research Conference Series 22
and

2016 Annual Convention

&

13th International Conference on Gondwana to Asia

18 – 22 November 2016

Department of Geology, University of Kerala, Trivandrum, India

ISBN 978-81-923449-6-6

Printed and bound by University Press, University of Kerala, India

Contents

Crustal development of the North China Craton constrained by geochemical and isotopic data on Neoproterozoic and Paleoproterozoic granitoids, Inner Mongolia Nancy Hui-Chun Chen, Guochun Zhao	1
Structural evolution of the Yeongwol area, Taebaeksan zone, Okcheon fold-thrust belt, Korea Yirang Jang, Sanghoon Kwon	2
Timing of tectonic evolution of the East Kunlun Orogen, Northern Tibet Plateau Dong, Y.P., Sun, S.S., Liu, X.M., Yang, Z., He, D.F., Li, W., Zhang, F.F., Cheng, B. and Zhou, X.H	5
Neoproterozoic trench-arc system in the western segment of Jiangnan orogenic belt, South China Liangshu Shu, Jinlong Yao	7
Crustal architecture and tectonic evolution of the Southern Granulite Terrane, India: an overview T.R.K.Chetty	9
Submarine pumice eruption and evidence for granite forming magma chamber in the Andaman Island arc: A first report Renjith, M.L	13
Structural study of Paramagnetic Karwar Granite in Western Dharwar Craton; Evidences for transpression related tectonic setting and Archean oblique convergence: An AMS based approach Amal Dev J and E Shaji	16
Assessment of Groundwater Condition and Its Environmental Impact on Al Shouaiba Residential District, Al Ain City, UAE A.A. Murad, S.M. Hussein, H. Arman, D. Alshamsia, S. Al Balush and H. Waid Al Balus	19
Dating the collisional events along the Southeast Anatolian Orogenic Belt, Turkey Fatih Karaođlan, Raymond Jonckheere, Di-Cheng Zhu, Willis E. Hames	20
3D geological modeling and metallogenic features of the Mengkelaoangou Pb-Zn-Ag polymetallic ore deposit, Henan Province, Central China Fan Yang, M. Santosh, Gongwen Wang, Nana Guo	24

Petrology, phase equilibria modeling and zircon U-Pb geochronology of Paleoproterozoic mafic granulites from the Fuping Complex, North China Craton Li Tang, M. Santosh, Toshiaki Tsunogae	26
Spectral and chemical features of anorthosite complex in Southern India: Implications for Lunar Highland anorthosite evolution Sam Uthup, V.J. Rajesh and Satadru Bhattacharya	30
Gold mineralization and Neoproterozoic suprasubduction zone signature in Shimoga greenstone belt, Western Dharwar Craton, India Sohini Ganguly, C. Manikyamba and M. Santosh	28
Geochemical fingerprinting of a forearc-arc-backarc association in the Neoproterozoic/Paleoproterozoic Kotri-Dongargarh mobile belt, Central India Sirish Kumar and Deepanker Asthana	32
Depth estimation of BIF in Sandur Schist Belt through ground magnetic from South India K. Satish Kumar	36
New evidence for meteoritic impact at Luna, Gujarat, India G.K. Indu, K.S. Sajin kumar, Keerthy Suresh, V.J. Rajesh	37
A comparison between Cr-diopside of Lattavaram and Kalyanadurgam Kimberlites, Anantapur district, Southern India P. Ramesh Chandra Phani	38
Understanding early Paleozoic orogeny in South China: significance of tectonism and magmatism in the Central Jiangnan Orogen and the North Cathaysia Jianhua Li, Guochun Zhao, Shuwen Dong, Yueqiao Zhang, Stephen Johnston, Jianjun Cui, Yujia Xin	40
Electron microprobe dating on monazites from Mangalwar Complex, Rajasthan: evidences for Meso-Proterozoic and Grenvillian reworking of a Palaeoproterozoic crust Krishnapriya Basak, Siladitya Sengupta and Sandip Nandy	42
Sedimentation in the Baikal Rift Zone: implications for Cenozoic intracontinental processes in the Central Asian Orogenic Belt Krivonogov S.K	45
Glossopteris flora from the Godavari valley coalfield, Telangana, India: basinal correlation and implications in palaeoecology Rajni Tewari	47

Structure and tectonic evolution of the Archean Biligiri Rangan Block, Southern India R.T. Ratheesh-Kumar	52
Petrogenesis and fluid characteristics of sapphirine granulites of the Highland Complex, Sri Lanka P. L. Dharmapriya, Sanjeewa P.K. Malaviarachchi, Andrea Galli, Leo Kriesman, S. Bhattacharya, Y. Osanai, K. Sajeev, T. Tsunogae	56
Geochemistry and petrographic studies of Ordovician sedimentary rocks (Sanguba Group) from Spiti valley, Tethys Himalaya, Northern India: implications for paleoweathering, paleoclimate and tectonic setting Shaik A Rashid and Javid A Ganai	58
New occurrence of unusual carbonatitic lamproites from Sidhi gneissic Complex, Central India Satyanarayanan.M, Subba Rao, D.V, Renjith, M.L, Singh, S.P	60
Advent, acme and decline of the Glossopteris flora: A case study from the Talchir Basin, Son-Mahandi Master Basin, India Kamal Jeet Singh, Anju Saxena, Shreerup Goswami	63
The Mahanadi Shear Zone of the Eastern Ghats Province – strike-slip or extensional Subham Bose and Saibal Gupta	65
Granite remote sensing image recognition and extraction in Taibai area, Shaanxi, China Xiaohu Zhou, Yunpeng Dong, Xiaoming Liu, Shengsi Sun, Zhao Yang	66
Occurrence of magmatism in Sivas-Erzincan region (Centraleastern Turkey) and its implications on the formation of Çöpler, Karakartal and Fındıklıdere ore deposits: A geochronological approach Miğraç Akçay, Oğuzhan Gümrük, Brent McInnes, Noreen Evans, Fred Jourdan, Svetlana Tessalina	68
Petrological, geochemical and fluid inclusion characteristics of mafic granulites from the Mercara Suture Zone, Southern India: implications for deep subduction and subsequent exhumation T. Amaldev, K. R. Baiju, M. Santos, T. Tsunogae, T. Pradeepkumar, K. Sajeev, M. Satyanarayanan	71
Deciphering the Precambrian crust between Shillong Massif and Northeast India S. M. Mahbubul Ameen, Md. Sakawat Hossain, Md. Sakaouth Hossain, Rashed Abdullah, Zahidul Bari, Md. Nehal Uddin, Sudeb Chandra Das, Al-Tamini Tapu, Hasibul Jahan, Md. Shams Shahriar	75

Evidence for melting and metasomatism of lithospheric mantle in an Archean supra subduction zone— A case study from the ultra mafic suites of Wyanad, Southern India J. Arun Gokul, M. Santosh E. Shaji, Qiong- Yan Yang	80
Magma sources of Paleozoic and Mesozoic porphyry Cu-Mo deposits in Southern Siberia (Russia) and Mongolia: evidence from geochemical and isotopic data A.N. Berzina, A.P. Berzina and V.O. Gimon	82
Preliminary works on the structural geometry of the Pyeongchang area, Taebaeksan zone, Okcheon Belt, Korea Hee Jun Cheong, Jungrae Noh, Sanghoon Kwon	86
Subduction record of the East African Orogen in a whole plate topological framework Alan S. Collins, Andrew Merdith, John Foden, Donnelly Archibald, Morgan Blades, Brandon Alessio, Haytham Sehsah, Simon Williams, Dietmar Müller	88
Characterization of the crystalline basement in Voktipur, Northwest Bangladesh Sudeb Chandra Das, S. M. Mahbulul Ameen, Zahidul Bari, Mohammad Nazim Zaman, Md. Sakaouth Hossain, Al-Tamini Tapu	89
Petrology and crystallization condition of granitic rocks in Wang Nam Khiao area, Nakhon Ratchasima, Northeastern Thailand Alongkot Fanka, Toshiaki Tsunogae and Chakkaphan Sutthirat	91
A geophysical over view of the lithospheric structure and evolution of the sahyadris of Central Kerala, India Ajayakumar P and Mahadevan T.M	92
Petrology and geochemistry of orthogneisses from Austhovde in the Lützow-Holm Complex, East Antarctica: implications for arc magmatism and high-grade metamorphism Kazuki Takahashi, Toshiaki Tsunogae, Yusuke Takamura, Yohsuke Saitoh	95
P-T fluid evolution of partially retrogressed pelitic granulite: A case study of the southern marginal zone of the Neoproterozoic Limpopo Complex, South Africa Tatsuya Koizumi, Toshiaki Tsunogae, Dirk D. van Reenen	98
U-Pb geochronology of detrital zircon from Sri Lanka and East Antarctica: Implications for the regional correlation of Gondwana fragments Yusuke Takamura, Toshiaki Tsunogae, M. Santosh, Sanjeeva Malaviarachchi, Yukiyasu Tsutsumi	100

Decarbonation of carbonate and formation of incipient charnockite in South-Central Madagascar Toshiaki Tsunogae, Takahiro Endo, M. Santosh, E. Shaji, Roger A. Rabeloson	103
Petrology and geochemistry of orthogneisses from Austhovde in the Lützow-Holm Complex, East Antarctica: implications for arc magmatism and high-grade metamorphism Kazuki Takahashi, Toshiaki Tsunogae, Yusuke Takamura, Yohsuke Saitoh	105
Mylonites in the Achankovil shear zone, Southern India: Microstructural evolution and deformation mechanisms Vikas C, Pratheesh P	108
PT-parameters and time UHT metamorphism in South-Western Siberian craton (Yenisei Ridge, Russia) V.P. Sukhorukov and O.M. Turkina	112
Occurrence and Characterization of Ferberite: Implications to Tungsten Mineralization in high temperature shear zone of the Eastern Ghats Mobile Belt, India G. Parthasarathy, T.R.K. Chetty and M. Satyanarayanan	115
Precambrian crustal growth in Kotri belt, Bastar Craton, Central India C. Manikyamba, M. Santosh, B. Chandan Kumar, S. Rambabu, Li Tang, Abhishek Saha, D.V Subba Rao	117
Mesoproterozoic Mafic complexes of south east central continental margin of Indian plate: Zircon trace element signatures and petrogenesis K.S.V. Subramanyam, M. Santosh, Qiong-Yan Yang, Ze-ming Zhang, V. Balaram, U.V.B. Reddy	120
A re-evaluation of the Kumta Suture in Southwest India and its extension into Madagascar Sheree E. Armistead, Alan S. Collins, William H. Mansfield, M. Santosh, E. Shaji	122
The Dhala crater, Madhya Pradesh, India: Impact crater or volcanic caldera? Keerthy Suresh, K.S. Sajinkumar, M. Santosh, S.P Singh, G.K. Indu	124
Studying field geology in the Nepal Himalaya - The 5th student exercise tour in March 2016 Masaru Yoshida, Kazunori Arita, Tetsuya Sakai and Bishal Nath Upreti	126
Radiogenic heat production and the formation of regional scale granulite and UHT metamorphic terranes through Earth history Chris Clark	128

Vegetational changes in the late Palaeozoic-early Mesozoic sediments of Kashmir, Tethys Himalaya, India Deepa Agnihotri and Rajni Tewari	131
Detrital zircon age data from quartzites in the southern Madurai Block, India and their bearing on Gondwana assembly G. Indu, Shan-Shan Li, M. Santosh, E. Shaji, T. Tsunogae	134
Facies distribution, heavy mineral sediment provenance and zircon geochronology of the Neoproterozoic succession of Oman: implications for tectonic setting and evolution of the Arabian peninsula Irene Gomez-Perez, Andrew Morton and Dirk Frei	136
Petrological characteristics of basement rocks in Voktipur, Rangpur District, Bangladesh Md. Rezaul Islam, Ismail Hossain, Toshiaki Tsunogae, Mowsumi Nahar, Md. Sazzadur Rahman	138
Prograde and retrograde growth of monazite in migmatites: a Gondwanan example from the Nagercoil Block, Southern India Tim E. Johnson, Chris Clark, Richard J. M. Taylor, M. Santosh, Alan S. Collins	142
1.6 billion years of granitoid magmatism and crustal growth in the Singhbhum craton: insights from zircon U-Pb-Hf isotopic study Sukanta Dey	144
Assessment of river banks in Kerala: A participatory approach Shaji J	146
Petrology and geochemistry of dacites from the Coorg Block, Southern India. S G Dhanil Dev, S Chinchu Nair, E Shaji, Mifthah Koya Thangal	148
Migmatites, charnockites and crustal fluid flux: the Pan-African granulites of Southern India. C.W. Fitzsimons, C. Clark, M. Santosh	149
Spatial variability in free phase gas dynamics Using common offset ground penetrating radar in South West Indian Peatlands Devi K and Rajesh R. Nair	154
Metasomatic origin of some microcline granites in Northeast Botswana K.V. Wilbert Kehelpannala, L. Richard, B.A. Bathobakae and L. Mokane	155
Petrological study of rodingite of the ophiolite belt of Manipur, Northeastern India Kakchingtabam Anil Sharma and Bidyanada Maibam	161

Deformation along southeastern margin of Cauvery Suture Zone: Critical consequences related to evolution of Southern Granulite Terrain D.P. Mohanty	164
Geochronological and geochemical study of detrital zircons from the Naga Metamorphites, Northeastern India: Provenance and Paleogeographic implications Bidyananda Maibam, Stephen F. Foley and Klemens Link	167
Seismic imaging of a new Gondwana basin around Vinjamuru region of Nellore Schist Belt, south Indian shield and its possible geodynamic implications O. P. Pandey and K. Chandrakala	170
Lifestyles of the Palaeoproterozoic stromatolite builders in the Vempalle Sea, Cuddapah Basin, India Sarbani Patranabis-Deb	172
New views on the composition and character of earth's mantle: Insights from ophiolites Paul T. Robinson ^{1,2} , Jian-Wei Li ¹ , Jingsui Yang ² , Mei-Fu Zhou ³ , and Fahui Xiong	173
Petrology and geochemistry of basement rocks in Bangladesh: implications for Paleoproterozoic tectonic evolution Ismail Hossaina, Toshiaki Tsunogae and Most Momotaz Khatun	175
Glossopteris flora from the Pali formation, Johilla coalfield, Umaria District, Madhya Pradesh: Palynological implications for a late Permian age S.Suresh Kumar Pillai	177
Neoproterozoic lamprophyres from Halaguru area, Harohalli dyke swarm, Dharwar Craton, India: Insight on the Rodinia break-up and addition of juvenile crust Kirtikumar Randive and Shubhangi Lanjewar	179
200 Myr history of crustal melting in Gongga Shan; constraints on the tectonics of eastern Tibet from the Triassic to present-day Nick M W Roberts and Michael P Searle	183
Late Paleozoic supra-subduction and intra-plate volcanism of the Tianshan-Junggar region: evidence for oceanic closure I.Yu. Safonova, V.A. Simonov, A.V. Mikolaichuk, A.V. Kotlyarov	187
The mystery of Hadean Earth and primordial life M. Santosh	190

Connecting India and Antarctica in Gondwanaland – the Rauer-Rengali link Saibal Gupta and Amol Dayanand Sawant	192
Geochemical and Geochronological studies of the granitoids around chhota shigri area, Himachal Himalayas, India Yengkhom Rajiv Singh, Bidyananda Maibam, Anil D. Shukla, Jasper Berndt, A.L. Ramanathan	194
Permian-Triassic palynomorphs from Talcher Coalfield, Mahanadi Basin, India: implications in biostratigraphy Srikanta Murthy	197
Provenance, palaeoclimate and tectonic settings of the Gondwana sediments of the Upper and Lower Palar Basin, Southern India, Tamil Nadu R. Subin Prakash and S. Ramasamy	200
Metamorphic zircon formation of Paleoproterozoic metasedimentary rocks in the Korla Complex, NW China: implications for the late Paleoproterozoic collisional orogenic event in the Tarim Craton Wenbin Zhu, Rongfeng Ge, Hailin Wu	202
Spatial and temporal provenance analysis of the Upper part of the Roper Group, Beetaloo Sub-basin, North Australia Bo Yang, Todd Smith, Alan S. Collins	204
Continental growth through microblock amalgamation: example from the North China Craton Qiong-Yan Yang, M. Santosh	205
Was there Neotethys Ocean's northern branch? A new look to Meso-Cenozoic tectono magmatic evolution of eastern Mediterranean region Yener EYUBOGLU	207
Mineral chemistry and petrology of mantle peridotites from the Guleman Ophiolite (SE Anatolia, Turkey): Evidence of a forearc setting Mustafa Eren RIZELI, Melahat BEYARSLAN, Kuo-Lung WANG, A. Feyzi BINGÖL	210
Dehydration patches (Incipient charnockite) within the granite gneiss: A report from Munnar area Southern India S Rajesh, A.P. Pradeepkumar	213

Evidences of extensive crustal melting in the Kerala Khondalite Belt, southern India during assembly of Eastern Gondwana V Nandakumar, SL Harley, Vinod Samue, JK Tomson, Jayanthi J L, Batuk Joshi & Nilanjana Sorcar	216
HT-UHT metamorphism of the Kerala Khondalite Belt: Complexity and interpretations Durgalakshmi, I.S. Williams, V.O. Samuel, V.J. Rajesh and K. Sajeev	218
Metamorphism and plate tectonic implications of the BIF, TTG and associated rocks of the Nilgiri Block, with special reference to Calicut District, Kerala, South India R. S. Prasanth and A. P. Pradeepkumar	221
Geochemistry and Metamorphism of the migmatised gneiss and dehydrated charnockite around Marthandam, Tamil Nadu, India J. Remya and A. P. Pradeepkumar	223
Mineral magnetic characterisation of tropical soil profiles from Northern Kerala, India Linu Babu and Reethu Mohan	225

Crustal development of the North China Craton constrained by geochemical and isotopic data on Neoproterozoic and Paleoproterozoic granitoids, Inner Mongolia

Nancy Hui-Chun Chen and Guochun Zhao*

Department of Earth Sciences, The University of Hong Kong, Hong Kong

*Corresponding Author e-mail: gzhao@hku.hk

The North China Craton is the oldest continental fragment in China. It contains magmatic rocks as old as 3.8 Ga, but is dominated by crustal components that formed in the Neoproterozoic at ca. 2.7 and 2.5 Ga, and also includes Paleoproterozoic rocks dated at 1.9-1.8 Ga. The craton has been incorporated into Precambrian supercontinents, although its exact position within, as well as the overall configuration of, these supercontinents is poorly understood. In order to constrain the paleogeographic setting of the North China Craton, we undertook a geochemical and geochronological study of granitoids in the Siziwangqi area of central Inner Mongolia, on the northern margin of the craton. The granitoids comprise a tonalite-trondhjemite-granodiorite (TTG) association and alkali feldspar granite. U-Pb zircon dating of the TTG association yielded crystallization ages of 2.52-2.49 Ga with inherited crystals as old as 2.7 Ga, whereas the alkali feldspar granites gave ages of 2.47 and 1.87 Ga.

Geochemically, the rocks are metaluminous to peraluminous and belong to the calc-alkaline (TTG) and subalkaline to alkaline (alkali feldspar granite) series. The TTG granitoids are characterized by light LREE enrichment, a weak positive Eu anomaly, and flat heavy HREE profiles. The alkali granite is also enriched in the LREE but has a strong positive chondrite-normalized Eu anomaly and displays weak HREE enrichment. Our compositional and geochronological data, in combination with similar regional data, indicate that in the Neoproterozoic the craton constituted part of an accretionary convergent plate margin that lay on the edge of a supercontinent. According to this model, the Paleoproterozoic alkali feldspar granite was associated with collisional assembly of the craton into the Nuna (Columbia) supercontinent.

Structural evolution of the Yeongwol area, Taebaeksan zone, Okcheon fold-thrust belt, Korea

Yirang Jang^{*}, Sanghoon Kwon

Department of Earth System Sciences, Yonsei University, Seoul 120-749, Republic of Korea

^{*}Corresponding Author e-mail: yirang@yonsei.ac.kr

Since the concept of the thrust duplex was first suggested by Boyer and Elliott (1982) in the Mountain City Window, the thrust system has been studied in worldwide fold-thrust belts (FTBs) as an important mechanism for accommodating a large amount of shortening during their evolution (e.g. Mitra, 1990; Suppe and Medwedeff, 1990; DeCelles et al., 2002; Kwon and Mitra, 2006; Bhattacharyya and Mitra, 2009; Mitra et al., 2010). Because kinematic and deformation complexities of FTBs are clearly reflected in its arcuate patterns, the 3-D structural interpretation of the thrust system combined with the fault activation/reactivation information is crucial to understand its 3D evolutionary history.

Thrust systems can be classified into two distinct systems (i.e., duplex vs. imbricate fan) (Boyer and Elliott, 1982). The duplex system is recognized as a distinct map pattern of highly connected thrust traces in contrast to the isolated thrust traces of the imbricate fan (e.g. Boyer and Elliott, 1982; Mitra, 1997; Mitra and Sussman, 1997; Kwon and Mitra, 2006). A possible natural examples of duplex system is exposed in the Yeongwol area, the western part of the Taebaeksan

zone in the Okcheon FTB of the Korean Peninsula. In this area, the Cambrian-Ordovician Yeongwol group is overlain by the Carboniferous-Triassic Pyeongan supergroup or Jurassic Bansom group by N-S trending thrusts, defining highly connected thrust traces having branch lines with the Machari thrust in map view. This defines a thrust system, namely the Yeongwol thrust system in this area. Based on 3-D geometric interpretations based on down-plunge projections (Wojtal, 1988) and branch line and cutoff line rules (Diegel, 1986), this thrust system has been interpreted by alternative duplex models in terms of a hinterland dipping duplex vs. a combination of major thrusts and connecting splays (Jang et al, 2015).

Newly obtained SHRIMP U-Pb zircon ages from igneous intrusions cross-cut by a thrust and synorogenic sedimentary rocks at the footwall of the Gongsuwon thrust give the relative (re)activation ages of the thrusts. The results indicate that faults are reactivated after the early Jurassic, the late Cretaceous and the early Tertiary, respectively. In addition, the illite-age-analysis (IAA) from the fault gouges of the thrusts in the Yeongwol area is conducted

to figure out additional age constraints for the formation and reactivation ages of them. This method uses optimized illite-polytype quantification that can provide reliable age constraints for the timing of faulting (e.g. Pevear, 1992; van der Pluijm et al., 2001; Haines and van der Pluijm, 2008; Rahl et al., 2011; Song et al., 2014). We anticipate that the results from this analyses will help to estimate direct ages for the formation and/or reactivation of the thrusts consisting the Yeongwol thrust system. These age analyses, together with previously reported evidence from the Yeongwol area, indicate the late reactivations of the faults reflected in the modification of earlier structures that formed present-day structural style of the Yeongwol thrust system. It further suggests the preservation of polyphase tectonic events in this area at least after the Permo-Triassic. This further indicate the broader implications in that how detailed 3D structural studies combined with precise age constraints of the faults can support the interpretation of the tectonic evolution of the Okcheon FTB as a whole, and can be extended to the interpretation of other FTBs in general.

References

- Bhattacharyya, K., Mitra, G., 2009. A new kinematic evolutionary model for the growth of a duplex – an example from the Rangit duplex, Sikkim Himalaya, India. *Gondwana Research* 16, 697-715.
- Boyer, S.E., Elliott, D., 1982. Thrust Systems. *The American Association of Petroleum Geologists Bulletin* 66, 1196-1230.
- DeCelles, P.G., Robinson, D.M., Zandt, G., 2002. Implications for shortening in the Himalayan fold-thrust belt for uplift of the Tibetan Plateau. *Tectonics* 21, 1062. doi: 10.1029/2001TC001322.
- Diegel, F.A., 1986. Topological constraints on imbricate thrust networks - examples from the Mountain City Window, Tennessee, U.S.A. *Journal of Structural Geology* 8, 269-279.
- Haines, S.H., van der Pluijm B.A., 2008. Clay quantification and Ar–Ar dating of synthetic and natural gouge: application to the Miocene Sierra Mazatan detachment fault, Sonora, Mexico. *Journal of Structural Geology* 30, 525-538.
- Kwon, S., Mitra, G., 2006. Tree-dimensional kinematic history at an oblique ramp, Leamington zone, Sevier belt, Utah. *Journal of Structural Geology* 28, 474-493.
- Mitra, G., 1997. Evolution of salients in a fold-and-thrust belt: the effects of sedimentary basin geometry, strain distribution and critical taper. In: Sengupta, S. (Eds.), *Evolution of Geological Structures from Macro- to Micro-scales*. Chapman and Hall, London, 59-90.
- Mitra, G., Bhattacharyya, K., Mukul, M., 2010. The Lesser Himalayan Duplex in Sikkim: Implications for variations in Himalayan shortening. *Journal Geological Society of India* 75, 289-301.
- Mitra, G., Sussman, A.J., 1997. Structural evolution of connecting splay duplexes and their implications for critical taper: an example based on geometry and kinematics of the Canyon Range culmination, Sevier Belt, central Utah. *Journal of Structural Geology* 19, 503-521.
- Mitra, S., 1990. Fault-propagation folds: Geometry, kinematic evolution, and hydrocarbon traps. *The American*

- Association of Petroleum Geologists Bulletin 74, 6, 921-945.
- Pevear, D.R., 1992. Illite age analysis, a new tool for basin thermal history analysis. In: Kharaka, Y.K., Maest, A.S. (Eds.), *Water-Rock Interaction*. Balkema, Rotterdam, pp. 1251-1254.
- Rahl, J.M., Haines, S.H., van der Pluijm, B.A., 2011. Links between orogenic wedge deformation and erosional exhumation: evidence from illite age analysis of fault rock and detrital thermochronology of syn-tectonic conglomerates in the Spanish Pyrenees. *Earth and Planetary Science Letters* 307, 180-190.
- Song, Y., Chung, D., Choi, S.-J., Kang, I.-M., Park C., Itaya, T., 2014. K–Ar illite dating to constrain multiple events in shallow crustal rocks: Implications for the Late Phanerozoic evolution of NE Asia. *Journal of Asian Earth Sciences* 95, 313-322.
- Suppe, J., Medwedeff, D.A., 1990. Geometry and kinematics of fault-propagation folding. *Eclogae Geologicae Helvetiae* 83/3, 409-454.
- van der Pluijm, B.A., Hall, C.M., Vrolijk, P.J., Pevear, D.R., Covey, M.C., 2001. The age dating of shallow faults in the Earth's crust. *Nature* 412, 172-175.
- Wojtal, S., 1988. Objective methods for constructing profiles and block diagrams of folds. In: Marshak, S., Mitra, G. (Eds.), *Basic Methods of Structural Geology*. Prentice Hall, Englewood Cliffs, New Jersey, pp. 269-302.

Timing of tectonic evolution of the East Kunlun Orogen, Northern Tibet Plateau

Dong, Y.P.*, Sun, S.S., Liu, X.M., Yang, Z., He, D.F., Li, W., Zhang, F.F., Cheng, B. and Zhou, X.H.

State Key Laboratory of Continental Dynamics, Department of Geology, Northwest University, Northern Taibai Str. 229, Xi'an 710069, China.

* Corresponding author e-mail: dongyp@nwu.edu.cn

The East Kunlun Orogen, located at the northern Tibet Plateau, represents the western segment of the Central China Orogenic Belt which was formed by amalgamation of the North China blocks and South China blocks. It is a key to understanding the formation of Eastern Asian continent as well as the evolution of the Pangea supercontinent. Based on detailed geological mapping, geochemical and geochronological investigations, the orogen is divided into three main tectonic belts, from north to south, including the Northern Qimantagh, Central Kunlun and Southern Kunlun Belts by the Qimantagh suture, Central Kunlun suture and South Kunlun fault.

The Qimantagh suture is marked by the Early Paleozoic ophiolite suture cropped in the Yangziquan, Wutumeiren, and Tatu areas, which consist mainly of peridotites, gabbros, diabases and basalts. Besides, the ophiolite in the Wutumeiren is characterized by occurring anorthosite while the ophiolite in the Tatu occurring chert. The basalts and diabases from both Yaziquan and Tatu areas display depletion of Nb, Ta, P and Ti, and enrichment of LILE, suggesting a

subduction related tectonic setting. LA-ICP-MS zircon U-Pb age of 421 Ma for the diabase represents the formation age of the Yaziquan ophiolite, while the U-Pb ages of 490 Ma and 505 Ma for gabbro and anorthosite, respectively, constrain the formation age of the Tatu ophiolite. The basaltic rocks in the Wutumeiren area display flat distribution of HFSEs (such as Nb, Ta, K, La, Ce, Pr, Nd, Zr, Sm, Eu, Ti, Dy, Y, Yb and Lu) and slightly enrichment in LREEs, while the peridotites showing depletion in MREEs. The LA-ICP-MS zircon U-Pb age of 431 Ma for the gabbro represents the formation age of the Wutumeiren ophiolite. Together with regional geology, we suggest herewith a back-arc basin tectonic setting during ca.505-421 Ma at least for the Qimantagh suture.

The Central Kunlun suture is represented by the ophiolite in the Wutuo area, which is characterized by depletion of Nb, Ta, P and Ti, and enrichment of LILEs, LREEs, K, Pb, Sr and Nd, accounting for a subduction relation setting. The gabbro yields a LA-ICP-MS zircon U-Pb age of 243 Ma, representing the formation age of the ophiolite. Taking into account of evidence

from the Early Paleozoic ophiolites in the Buqinshan (BianQiantao et al., 2001, 2007; Li Zuochen et al., 2013; Li Ruibao et al., 2014; Liu Zhanqing et al., 2011) and the

Derni areas (Chen Liang et al., 2001, 2003), the Central Kunlun ocean might be existed from Early Paleozoic to Middle Triassic time.

Neoproterozoic trench-arc system in the western segment of Jiangnan orogenic belt, South China

Liangshu Shu*, Jinlong Yao

School of Earth Sciences and Engineering, Nanjing University, Nanjing 210093, China

* Corresponding author e-mail: lsshu@nju.edu.cn

The Jiangnan orogenic belt in South China is a key to understanding of the Neoproterozoic tectonic evolution of the South China Craton. We investigate the mafic-ultramafic suites of lherzolite, pyroxenite, gabbro, pillow basalt and gabbroic diorite as well as red jasper interbedded with marine marbles that are mainly exposed in the Yuanbaoshan and Longsheng domains of the western Jiangnan belt along the recent Shaoxing-Pingxiang-Qidong-Guilin fault zone. The post-collisional granite plutons that intruded the ultramafic-mafic rocks are developed well. We present new data from field investigations, LA-ICP-MS zircon U-Pb data, Hf isotopes and whole rock geochemistry on these rock suites. Zircons in the gabbro yield crystallization ages of 867 ± 10 , 863 ± 8 , 869 ± 9 and 855 ± 5 Ma, with positive $\epsilon_{\text{Hf}}(t)$ values whereas those from the granites show ages of 823 ± 5 , 831 ± 5 , 824 ± 5 and 833 ± 6 Ma. The Neoproterozoic serpentinised ultramafic samples display minor REE enriched pattern with depletion of Rb, Ba, Nb, Ta and Ti, similar to those of SSZ type ophiolite. The coeval gabbro

shows tholeiitic features and is characterized by negative Ba, Nb, Ta, Zr, Hf and Sr anomalies and LREE enriched patterns, with a minor negative Eu anomaly. Geochemical signature of the mafic-ultramafic rocks is consistent with subduction related setting. The pyroxene-bearing diorite exhibits a distinctive arc affinity. The zircons from the gabbro show positive $\epsilon_{\text{Hf}}(t)$ values ranging from 3.9 to 13.8. The granitoids are typical S-type granites with high ACNK values (1.15–1.40) and negative $\epsilon_{\text{Hf}}(t)$ values (–15.1 to –3.2), and are classified as collision-related granites. Combined with the occurrences of mafic-ultramafic rocks, siliceous marble and red jasper mixed with basalt, our new results suggest the presence of a Tonian (863–869 Ma) SSZ ophiolite system and arc-type magmatism in the western Jiangnan orogen. This is different from previous proposals of the Neoproterozoic plume and bimodal magmatic settings dated around 830 Ma both in the SE Yangtze Blocks.

References

- Shu, L.S., Charvet, J., 1996. Kinematics and geochronology of the Proterozoic Dongxiang - Shexian ductile shear zone: with HP metamorphism and ophiolitic melange (Jiangnan region, South China). *Tectonophysics* 267, 291–302.
- Shu, L.S., 2012. An analysis of principal features of tectonic evolution in South China Block. *Geological Bulletin of China* 31(7), 1035-1053.
- Yao, J., Shu, L.S., Santosh, M., Li, J.Y., 2012. Geochronology and Hf isotope of detrital zircons from Precambrian sequences in the eastern Jiangnan Orogen: Constraining the assembly of Yangtze and Cathaysia Blocks in South China. *Journal of Asian Earth Sciences* 74, 225–243.
- Yao, J., Shu, L.S., Santosh, M., Zhao, G.C., 2014. Neoproterozoic arc-related mafic–ultramafic rocks and syn-collision granite from the western segment of the Jiangnan Orogen, South China: constraints on the Neoproterozoic assembly of the Yangtze and Cathaysia Blocks. *Precambrian Research, Precambrian Research* 243, 39–62.

Crustal architecture and tectonic evolution of the Southern Granulite Terrane, India: an overview

T.R.K.Chetty

CSIR-National Geophysical Research Institute, Hyderabad- 500 007, India
E-mail: trkchetty@gmail.com

The Southern Granulite Terrane (SGT), central to many reconstruction models of Rodinia and Gondwana supercontinents, occurs at the intersection of two global orogenies of East African Orogen and the Kuunga Orogen. Several modern concepts and innovative ideas emerged from recently acquired large volumes of data, but with variable and contradicting interpretations. The debatable points include: the definition of SGT and its extensions; transition zone where the low grade tonalitic and granitic gneisses gradually transformed into granulite facies metamorphic charnockitic rocks; division and extensions of different tectonic blocks, suture zone/ shear zones and their kinematics; existence of terrane boundaries; timing of subduction, accretion and collisional processes. This could be a direct consequence of limited field observations, lack of field and structurally constrained geochronological data, and limitations of accessibility due to high elevation and dense vegetation.

The SGT is believed to be of lower crustal origin through a complex

evolutionary history with multiple deformations, anatexis, intrusions and polyphase metamorphic events. The major rock types are high-grade granulite facies rocks that include essentially Neoproterozoic charnockites and their variably retrograded assemblages, pyroxene granulites, metasedimentary assemblages, which were subsequently intruded by Cryogenian anorthositic rocks, alkaline plutons, granitoids and mafic-ultramafic rocks including ophiolites. The metasedimentary assemblages include Banded Iron formations (BIF), calc silicates and metapelites. Intense shearing and migmatization gave rise to a variety of amphibole-biotite bearing migmatitic gneisses. The SGT can be divided into five distinct crustal/tectonic units based on lithological assemblages, structural styles, geochronological characteristics and geophysical signatures. From north to south, they are: (i) Northern Granulite Block (NGB) (ii) Cauvery suture/ shear zone (CSZ), (iii) Madurai Granulite Block (MGB), (iv) Achankovil suture/ shear zone (AKSZ), and (v) Trivandrum Granulite

Block (TGB) (see Figure).

The Mettur Shear Zone (MTSZ) within the NGB hosts a series of Neoproterozoic syenite, alkali granite and carbonatite plutons, which were dated showing broadly Cryogenian ages (750–800 Ma) and the source for them could be the melts derived from the ca. 2.5 Ga old delaminated/ eclogitised slab (Santosh et al., 2014a). Dismembered and agmatized bodies of gabbro, anorthosite, pyroxenite, and norite are also recorded indicative of thrust-transported ophiolitic rocks within the MTSZ (Gopalakrishnan, 1996). Further, the geochemical characteristics of granites from the NGB indicate a convergent margin in an island arc setting at around 2.5 Ga derived possibly from the Neoarchean subduction. Significantly, the Mesoarchean exotic Coorg block described from the north western part of the CSZ, escaped the subsequent major thermal events witnessed by the other crustal blocks (Santosh et al., 2014b).

The regional disposition, structural geometry, consistent dextral kinematics, complex behaviour of foliation trajectories and stretching lineations, heterogeneous strain patterns and the contemporaneity of mylonitic fabrics (750–500 Ma) and the crustal architecture of the CSZ are interpreted as a crustal-scale positive 'flower structure' typical of transpressional tectonics in a convergent regime (Chetty and Bhaskar Rao, 2006). The Precambrian ophiolite complexes from within the CSZ provide a clue for the different stages of Wilson cycle of the Mozambique Ocean associated with the subduction-accretion-collision history during the amalgamation of the Gondwana supercontinent. The UHT metamorphism with peak conditions of pressure and temperature in the range of

7–11 kbar and 950–1150°C yielded ages between 600 and 480 Ma (Jayananda et al., 1995), and at c. 900 Ma (Braun et al., 2007).

The division of MGB into distinct subdomains differently by different workers based on geochronological data is intriguing. Based on U-Pb ages of orthogneisses, two distinct terranes were identified: an Archaean basement terrane (~2.7–2.5 Ga) to the north and west and a Proterozoic terrane (1007 ± 23 Ma and 784 ± 18 Ma) dominated by metasedimentary rocks to the south, separated broadly by KKPTSZ (Plavsa et al., 2012). In contrast, the MGB was delineated into western (2.53–2.46 Ga) and eastern domains (1.74–1.62 Ga) based on the data of LA-ICPMS U-Pb zircon and U-Th-Pb monazite ages (Brandt et al., 2014). The wide ranging ages in significant amounts obtained from U-Pb and Hf isotopic data for different lithologies and the contrasting interpretations for the MGB emphasize the need for more detailed field observations and comprehensive understanding of structural architecture.

The geophysical data in conjunction with geological observations suggest a high density and moderately conductive mantle material brought up to the mid-lower level and a thermally eroded crust with a 'flower structure' at depth (~10 km) revealing that the AKSZ also represents the trace of a collisional suture. However, the debate about kinematics along the AKSZ still remains unresolved, thus the correlations with the shear zones of other Gondwana terranes requires cautious approach.

The available geochronological data of protolith emplacement ages between 1765–2100 Ma, the generation of small

plutons of syenites and granites between 770-560 Ma and the metamorphic age around 540 Ma (Kroner et al., 2015) suggest that the rocks of TGB must have witnessed two thermal events during Paleoproterozoic and Neoproterozoic-Cambrian.

Despite growing geological and geophysical evidence that the SGT was evolved through subduction-accretion and collisional processes, the polarity and the timing of subduction is not clear. The evolution of the SGT involves accretion processes of island arc magmatic suites;

thrust stacking with duplex structures and deformed sheath fold geometries, granitic emplacements, obduction of ophiolite complexes: all show a complete range of geological processes, typical of modern orogenic belts. The SGT may represent a distinct part of East African Orogen, which comprises a collage of individual oceanic domains and continental fragments with different geodynamic settings of different orogenic styles encompassing the period between break up of Rodinia and the final amalgamation of Gondwana.

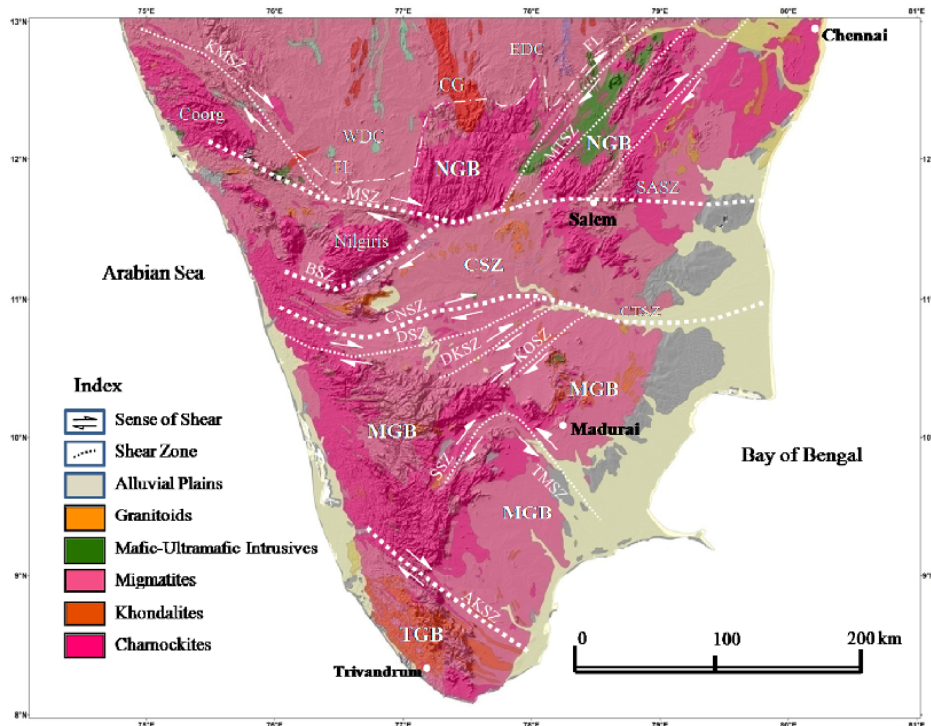


Fig. Geological map showing major rock types and tectonic features along with the digital elevation model of the Southern Granulite Terrane: NGB- Northern Granulite Block; CSZ- Cauvery shear zone; MGB- Madurai Granulite Block; AKSZ- Achankoil shear zone; TGB- Trivandrum Granulite Block; EDC- Eastern Dharwar craton; WDC- Western Dharwar craton; CG- Closepet Granite; FL- Fermor's Line; MTSZ- Mettur shear zone; KMSZ- Kasargod-Mercara shear zone; MSZ- Moyar shear zone; BSZ- Bhavani shear zone; CNSZ- Chennimalai Noil shear zone; SASZ- Salem-Attur Shear Zone; CTSZ- Cauvery-Tiruchinapalli shear zone; DSZ- Dharapuram shear zone; DKSZ- Devathur-kallimandayam shear zone; KOSZ- Kodaikanal Oddanchathram shear zone; SSZ- Suruli shear zone; TMSZ- Theni-Madurai shear zones.

References

- Brandt, S., Raith, M.M., Schenk, V., Sengupta, P., Srikantappa, C., Gerdes, A., 2014. Crustal evolution of the Southern Granulite Terrane, South India: New geochronological and geochemical data for felsic orthogneisses and granites, *Precambrian Research* 246, 91-122.
- Braun, I., Cenko-Tok, B., Paquette, J.L., Tiepolo, M., 2007. Petrology and U–Th–Pb geochronology of the sapphirine-quartz-bearing metapelites from Rajapalayam, Madurai Block, Southern India: evidence for polyphase Neoproterozoic highgrade metamorphism. *Chemical Geology* 241, 129–147.
- Chetty, T.R.K., Bhaskar Rao, Y.J., 2006. The Cauvery Shear Zone, Southern Granulite Terrain, India: A crustal-scale flower structure. *Gondwana Research* 10, 77-85.
- Gopalakrishnan, K., 1996. An overview of Southern Granulite Terrain, India-constraints in reconstruction of Precambrian assembly of Gondwanaland. *Gondwana Nine* 2, Oxford and IBH Pub. 1003-1026.
- Jayananda, M., Martin, H., Peucat, J. J., Mahabaleswar, M., 1995. Late Archaean crust– mantle interactions: geochemistry of LREE-enriched mantle derived magmas. Example of the Closepet batholith, southern India. *Contributions to Mineralogy and Petrology* 119, 314–329.
- Kröner, A., Santosh, M., Hegner, E., Shaji, E., Geng, H., Wong, J., Xie, H., Wan, Y., Shang, C.K., Liu, D., Sun, M., Nanda-Kumar, V., 2015. Palaeoproterozoic ancestry of Pan-African high-grade granitoids in southernmost India: Implications for Gondwana reconstructions. *Gondwana Research* 27 () 1–37.
- Plavsa, D., Collins, A.S., Foden, J.F., Kropinski, L., Santosh, M., Chetty, T.R.K., Clark, C., 2012. Delineating crustal domains in Peninsular India: age and chemistry of orthopyroxene-bearing felsic gneisses in the Madurai Block. *Precambrian Research* 198–199, 77–93.
- Santosh, M., Qiong-Yan Yang, Ram Mohan, M., Tsunogae, T., Shaji, E., Satyanarayanan, M., 2014a. Cryogenian alkaline magmatism in the Southern Granulite Terrain, India: petrology, geochemistry, zircon U-Pb ages and Lu-Hf isotopes. *Lithos* 208-209, 430-445.
- Santosh, M., Qiong-Yan Yang, Shaji, E., Tsunogae, T., Ram Mohan, M., Satyanarayanan, M., 2014b. An exotic Mesoarchean microcontinent: The Coorg Block, southern India *Gondwana Research*, <http://dx.doi.org/10.1016/j.gr.2013.10.005>.

Submarine pumice eruption and evidence for granite forming magma chamber in the Andaman Island arc: A first report

Renjith, M.L.

Geo-Data Division, Southern Region, Geological Survey of India, Hyderabad-500068, India

E-mail address: mlrenjith78@gmail.com

Island arc plate tectonic systems operate in the Andaman Sea region of N-W Indian Ocean is the northern extension of Burma-Java subduction complex formed by oblique subduction of Indian plate beneath the SE Asian plate (Curry, et al., 2005; McCaffrey, 2009; Cochran, 2010). Active magmatism triggered by the east dipping Benioff zone manifest basalt to dacite erupting two subaerial volcanoes (Barren and Narcondam) (Luhr and Haldar, 2006; Pal et al., 2006, 2010; Sheth, et al., 2009; Renjith, 2014) and a few submarine arc volcanoes in the Andaman Sea region (Curry et al., 2005; Kameshraj, et al., 2012). Geology and nature of magmatism particularly of submarine volcanoes are yet to be fully known. This study explores one of the submarine volcanoes situated 50 km south of Barren volcano using high-resolution multibeam swath bathymetric (MBSB) map and pyroclastic materials to bring out underwater pumice eruption and silicic magmatism in the Andaman arc for the first time. MBSB 3D map reveals that submarine volcano has near circular dome shaped edifice with ~21 km diameter at the

base and with a maximum height of ~1800 m from the seafloor, which is having average water depth of ~3400 m. A cryptic double wall near circular caldera structure is identified from the bathymetric maps.

Grab samples collected on board R.V. Samudra Ratnakar from the inner caldera wall yielded abundant pyroclastic materials, dominantly containing larger pumice clasts (upto 15 cm size) along with fine-size fractions of pumice, mineral grains and ash size volcanic materials. Pumices are found weathered (black in colour; older eruption) or fresh (whitish colour; younger eruption) and carry moderate abundance (<30%) of phenocrysts of quartz, plagioclase, amphibole and crystal clots embedded in vesiculated matrix as visible in hand specimen-scale. Many of them are foliated by having stretched vesicles, asbestose-like appearance and linearly arranged mineral phases. They exhibit wide range of vesicle flow structures in microscopic scale and these magmatic deformation textural patterns are interpreted to be the frozen movements of magma froth during its

various magma plumbing stages starting from the bubble nucleation to the final underwater eruption. Vesicle walls of pumices represent glassy form of the magma (melt). Electron micro-probe data reveals that they are rhyolitic in composition (SiO_2 : 72.2-77.5 wt.%; MgO : <0.2 wt.%; Al_2O_3 : 11-12 wt.%; CaO : ~1 wt.%; K_2O : ~2.0 wt.%; $\text{K}_2\text{O}+\text{Na}_2\text{O}$: 3-5 wt.%; $\text{K}_2\text{O}/\text{Na}_2\text{O}$: ~1). The trapped melt inclusions in various mineral phases also yielded similar range of composition and strengthen the evidence for rhyolite magmatism in the Andaman subduction zone.

Crystal clots mainly of plagioclase, amphibole, quartz, magnetite, ilmenite, zircon and apatite are found in textural equilibrium with embayed grain boundaries (Fig.1). Modal content and texture strongly indicate that they represent granitic cumulate fraction (autolith) of the rhyolite magma. Similar mineral phases are also occurring as individual phenocrysts in the pumice and in both cases minerals show similar and narrow range of compositions such as plagioclases (restricted to andesine ($\text{Ab}_{68-47}\text{An}_{29-58}$); amphiboles are magnesio-hornblende with low Mg-number (67-77); Opx is mainly pigeonite and Fe-Ti oxides are titanomagnetite and ilmenite. Apatite and zircons are the first liquidus phases along with opx as indicated by their inclusions in amphiboles and ilmenite. Intensive parameters calculated following the methods of Rudolphi et al., (2010) for amphibole compositions reveal that they have crystallized at 772 to 865°C and 66 to 98 Mpa pressure range from a melt contain 3.2-5.2 wt.% water and high oxygen fugacity ($\log f_{\text{O}_2}$: -12.5 to -10.8; ΔNNO : 1.6-2.9). Crystallization pressure of amphibole is corresponding to the oceanic crust depth of 2 to 3 km and indicates an existence of a shallow magma chamber below the studied submarine volcano. The crystal clots are also show similar range of crystallization pressure and in turn strongly advocates granite forming magma chamber at the shallow chamber. Larger amphibole phenocrysts show dissolution features and are filled with rhyolite glasses suggesting that reheating of the pre-

existing crystals has happened in the magma chamber due to the input of new batches of hotter magma. This incremental magma addition must have enhanced the disaggregation and dispersion of the granitic cumulate as crystal clots in the magma chamber.

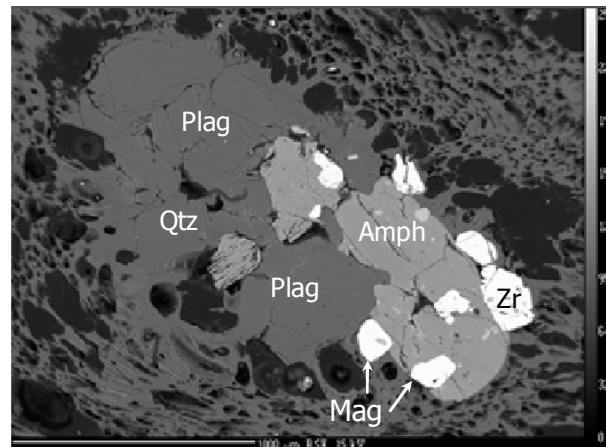


Fig.1 BSE image show crystal clot of granitic cumulate fragment constitute of plagioclase, amphibole, magnetite, quartz and zircon embedded in rhyolitic pumice matrix.

Reference

- Cochran, J.R., 2010. Morphology and tectonics of the Andaman Forearc, northeastern Indian Ocean. *Geophysical Journal International*, 182, 631-651.
- Curray, J.R., 2005. Tectonics and history of the Andaman Sea region. *Journal Asian Earth Science*, 25, 187-232.
- Kameshraj, K.A., Ray, D., Murty, G.P.S., Gahalaut, V.K., Samudrala, K., Paropkar, A.L., Ramachandran, R., Prakash, L.S. 2012. Tectonic and volcanic implications of a cratered seamount off Nicobar Island, Andaman Sea. *Journal of Asian Earth Science*, 56, 42-53.
- Luhr, J.F., Haldar, D., 2006. Barren Island Volcano (NE Indian Ocean): island-arc high-alumina basalts produced by troctolite contamination. *Journal of Volcanology and Geothermal Research*, 149 (3-4), 177-212.

- McCaffrey, R., 2009. The tectonic Subduction zone. *Annual Reviews in Earth and Planetary Science*, 37, 345-366.
- Pal, T., Sengupta, S., Katari, A., Bandopadhyay, P.C., Ashok K. 2007. Dacite–andesites of Narcondam volcano in the Andaman Sea—An imprint of magma mixing in the inner arc of the Andaman–Java subduction system. *Journal of Volcanology and Geothermal Research*, 168, 93-113.
- Pal, T., Raghav, S., Bhattacharya, C.A., Bandopadhyay, P.C., Renjith, M.L., Sankar, M.S., Ghosh, B., 2010. The 2005-2006 eruption of the Barren Volcano, Andaman Sea: evolution of basaltic magmatism in island arc setting of Andaman-Java subduction complex. *Journal of Asian Earth Sciences*, 39 (1-2), 12-23.
- framework of the Sumatra
- Renjith, M.L. 2014. Micro-textures in plagioclase from 1994-1995 eruption, Barren Island Volcano: Evidence of dynamic magma plumbing system in the Andaman subduction zone. *Geoscience Frontiers*, 5, 113-126.
- Ridolfi, F., Renzulli, A., Puerini, M. 2010. Stability and chemical equilibrium of amphibole in calc-alkaline magmas: an overview, new thermobarometric formulations and application to subduction-related volcanoes. *Contribution to mineralogy and Petrology*, 160, 45-66.
- Sheth, H.C., Ray, J.S., Bhutani, Kumar, A., Smitha, R.S., 2009. Volcanology and eruptive styles of Barren Island: an active mafic stratovolcano in the Andaman Sea, NE Indian Ocean. *Bulletin of Volcanology*, 71 (9), 1021-1039.

Structural study of Paramagnetic Karwar Granite in Western Dharwar Craton; Evidences for transpression related tectonic setting and Archean oblique convergence: An AMS based approach

Amal Dev J^{*} and E Shaji

Department of Geology, University of Kerala, Trivandrum

* Corresponding author e-mail: amaldevj@gmail.com

Karwar granite pluton along the Konkan coast extends as an irregular shaped body along the western margin of Dharwar Craton with an aerial extend of 280 square kilometer having a length of 40 km and maximum width up to 20 kilometer. The granite body is bounded by Peninsular Gneiss and metabasalts in south eastern margin, laterite and Quaternary alluvial soil in the southwestern part. It is fringed by the Kumta shear zone/ Suture Zone (Kumar et al., 2103) trending NW-SE with of 50km. Rekha et al., (2013) dated this granite body as Mesoarchean (~3.0 Ga) based on monazite dating. Petrography shows wide variety of textures and mineral assemblages. High-T solid-state deformation fabrics such as chessboard pattern in quartz, which is characterized by square sub grains with boundaries parallel to both prism and basal planes. Three generations of quartz have been recognized and occurrence of automorphic

crystals with occasionally corroded margin or rounded blebs of quartz occurring as inclusion in large crystals of plagioclase indicate early crystallization at high temperature above 573°C.. The vermicular quartz closely associated with albite and orthoclase forms myrmekitic texture indicating late-low temperature crystallization between pre-aqueous and post-aqueous phase. Plagioclase laths show complex twinning and occasionally these twins are deformed and show micro fractures. Three generations of plagioclase have been recognized with wide variety of twins such as polysynthetic, albite, simple and complex or mechanical twins. Low-T solid-state fabrics defined by deformation twins in plagioclase are very prominent in the granites. Interestingly, zoned feldspars and other magmatic to sub-magmatic microstructures are present in the granite indicate their crystallization from a magma. Alkali feldspar occurs as

early crystallized phenocrysts and interstitial xenomorphic grains. Potash feldspars are generally characterized by perthite intergrowth indicating exsolution of sodic phase from the homogenous sodalite-potash feldspar. Biotite crystals shows different forms as elongated grains oriented in parallel and sub parallel manner creating primary gneissosity.

Joints from the pluton show maximum concentration around N336 close to the regional compression direction (WNW-ESE) and perpendicular to the regional extension direction. Since maximum concentration direction is almost parallel to the regional compression direction, the fractures oriented in this direction are considered as tensile with some hybrid character. The high angle nature of joints suggests the possibility of normal or reverse faulting mechanism in the region during compression. Paleostress analysis shows that orientation of σ_1 and σ_2 swings around WNW-ESE regional compression direction often changing its orientation from high angle to parallel nature. This type of orientation clearly indicates the dominance stress condition related to strike-slip faulting and normal faulting. Orientation of σ_3 mostly swings around N-S direction and this could be correlated with regional stretching/elongation in NNE-SSW direction. Field foliations shows two compact concentrations with a mean direction of $245/64^0$ (WNW-ESE) with westward dip showing parallel relation with the trend of shear zone. It is also identified that the orientation of foliations and adjacent gneisses were almost parallel so that foliation development in both these rock units was synchronous.

Magnetic fabric in Karwar granite

and its temporal relationship with regional deformation has done based on the combination of field, microstructural and AMS investigations. Most of the bulk susceptibility values of the Karwar granite are low and fall within the domain of paramagnetic granites and fabric is dominantly controlled by minerals such as biotite and hornblende. The emplacement of Karwar granite is identified as syntectonic with the deformation of adjacent Peninsular gneiss during the Mesoarchean and it developed synmagmatic as well as high-T solid-state deformation fabrics. It is also identified that the evolution of granite body and shear zone formations and deformation of adjacent gneisses where syntectonic and same process could have been triggered all these events. This processes resulted in the fabric development of Karwar granite was influenced by the accretion of WDC that led to the formation of the Kumta Shear Zone during the Neoarchean time. The granite is also believed to be formed in a transpression regime which is clearly demonstrated by the pattern of magnetic foliation and magnetic lineation. This resulted in sinistral shearing along the NW and SE margin of granite and also along the SE margin of Kumta Shear Zone. This transpression regime associated KGP was believed to be produced due to the WNW-ESE directed oblique convergence. The age of emplacement, synmagmatic deformation and fabric development where synchronous and this can be a possible extend WNW-ESE directed oblique convergence to Mesoarchean.

Based on the results of this study, Karwar granite pluton is considered as paramagnetic granite originated in a transpression regime associated with

Archean oblique convergence in West Dharwar Craton that has undergone synmagmatic deformation during emplacement. The formation of KSZ and stabilization of Dharwar Craton were proposed as continuous process that was initiated within the Mesoarchean itself.

Assessment of Groundwater Condition and Its Environmental Impact on Al Shouaiba Residential District, Al Ain City, UAE

A.A. Murad¹, S.M. Hussein^{1*}, H. Arman¹, D. Alshamsia¹, S. Al Balush¹ and H. Waid Al Balusi¹

¹United Arab Emirates University, College of Science, Department of Geology, P.O 15551, Al Ain, United Arab Emirates

* Corresponding author e-mail: S_Hussein@uaeu.ac.ae

The groundwater plays a significant role as destructive or constructive upon the environment. The constructive impact can be seen easily in the development process such as domestic, agriculture and industrial water use. Also, it can play destructive role as groundwater level rise and effects foundations of structures. On the hand, water quality deterioration of some elements such as chloride (Cl^-), sulfates (SO_4^{4-}), Total Dissolved Solids (TDS), and etc. attack the concrete material and causes losing of its strength. Accordingly, Al Shouaiba district is most likely affected by water level rise as well as water quality. So, this study targeted to state how far the effective elements of direct interaction with concrete and foundations materials such as TDS, SO_4^{4-} , Cl^- and groundwater level depth affected the buildings in the study area.

The results of chemical analysis of these ions and water level measurements point out increase in the concentration of TDS, SO_4^- and Cl^- more than permissible limits and decrease of groundwater level depth. The TDS concentration varies from 1000 to ≥ 8000 ppm, SO_4^{4-} variation between 500 – 9000 ppm Cl^- ranges from 500 to 9500 ppm and groundwater level depth that measured from the casing top level fluctuate from 1- 29 m respectively. Consequently, this situation of the investigated parameters makes the study area under true environmental risk and warns the decision makers to take urgent action to prevent or mitigate the hazards from the extension to new zones among the area.

Dating the collisional events along the Southeast Anatolian Orogenic Belt, Turkey

Fatih Karaoğlan¹, Raymond Jonckheere², Di-Cheng Zhu³, Willis E. Hames⁴

¹Çukurova University, Geological Engineering Department, 01330 Balcalı, Adana, TURKEY

²Freiberg Mining Academy and Technical University, Department of Geology, Freiberg, Germany

³School of Earth Science and Mineral Resources, China University of Geosciences, Beijing, P. R. China

⁴Auburn University, Department of Geology and Geography, Auburn, Alabama 36849, USA

The Anatolian Peninsula formed by several blocks (micro-continents) rifted away from the major continents, especially from Gondwanaland. The subsequent drifting of these micro-continents led to the growth of Neotethyan Ocean basins during early Mesozoic. The Anatolian segment of the Alpine-Himalayan orogen resulting from the Neo-Tethyan evolution is divided into a number of E-W trending belts, which are separated from each other by suture zones (Şengör and Yılmaz, 1981; Okay and Tüysüz, 1999; Stampfli, 2000; Garfunkel, 2004; Garfunkel, 2006; Robertson et al., 2012). The Neotethys Ocean, survived along Alpine–Himalayan orogenic belt, was splitted into two parts namely northern and southern branches during the Jurassic in the west and the Cretaceous in the east (Garfunkel, 2004; Garfunkel, 2006; van Hinsbergen et al., of the northern margin of the Gondwana (Anatolid-Torid block) during Triassic-Jurassic (Permian?) (Yılmaz, 1993; Yılmaz et al., 1993; Okay and Tüysüz, 1999; Robertson, 2004; Robertson et al., 2013a; Robertson et al., 2013b). The

oceanic lithosphere, formed in Mesozoic seaways that existed between Eurasia and Gondwana, began to close and gave rise to the Alpine orogenic chain resulting in the obduction of the Alpine and the Anatolian ophiolites during Jurassic in the west and north, and late Cretaceous in the east and south (Şengör and Yılmaz, 1981; Stampfli, 2000; Stampfli and Borel, 2002; Robertson, 2004; Robertson et al., 2012; Karaoğlan et al., 2013a; Karaoğlan et al., 2016).

The Southeast Anatolian Orogenic Belt (SAOB), formed as a result of the closure of the southern branch, is one of the key areas along the Alpine-Himalayan orogeny to study the temporal evolution and uplifting history of continental margins. The SAOB is resulted from the north-dipping subduction of distinct oceanic lithospheres separated by continental fragments (i.e. Bitlis and Pütürge metamorphics) within the southern branch of Neotethys Ocean during late Mesozoic and early Cenozoic. The arc magmatism emplaced within the active margin of the SAOB during late Cretaceous and Eocene

(Yazgan and Chessex, 1991; Parlak, 2006; Rızaoğlu et al., 2009; Karaoğlu et al., 2013b; Lin et al., 2015; Karaoğlu et al., 2016). These magmatic bodies recorded the conditions and the timing of the subduction processes and timing and the rate of the continental collisions.

The U-Pb zircon ages range from 81 to 88 Ma for late Cretaceous granitoids. The ^{39}Ar - ^{40}Ar ages indicate that these late Cretaceous granitoids cooled below 300°C in 6-10 Ma. The formation ages and the timing of the gradual cooling of the late Cretaceous granitoids are similar to metamorphism age and the timing of the exhumation of the HP/LT Bitlis metamorphics during this stage. The combined field, geochemistry and geochronological data suggest that the first continental collision event occurred between Bitlis-Pütürge micro-continents to the south and Tauride platform to the north in an oblique subduction zone between 84 and 74 Ma. The granitoids continued uplifting during early-middle Eocene together with the exhumation of HP/UHT Berit metaophiolite in an extensional regime related to the opening of the Maden back-arc basin. This period also let the intrusion of the arc magmatism, intruding the Pütürge and Malatya-Keban metamorphics, Berit metaophiolite, and Maden back-arc basin units. The Eocene granitoid has similar U-Pb and ^{39}Ar - ^{40}Ar ages, suggesting a fast cooling as a result of either shallow emplacement or fast uplifting. The apatite fission track (AFT) data for all granitoid bodies suggest that they were mainly cooled or uplifted in two episodes, where the first one is in the Eocene in an extensional setting. The AFT age data suggest that the granitoids uplifted during Oligocene and uplift rate

increases during middle-late Miocene

Thus the AFT data marked the final continental collision between the Taurides and the Arabian platform first in Oligocene and the break-off of the subducted slab and the delamination process caused fast uplift of the Eastern Anatolia during middle to late Miocene. Several foreland basins formed above the suture zone during Miocene (i.e. Malatya Basin, Elazığ Basin and Kahramanmaraş basin) (Fig. 1). The detrital U-Pb and Ar-Ar data show that these basins were fed by Late Cretaceous, Eocene and Miocene magmatic bodies similar to those dated in the region, previously. The detrital AFT data collected from the Eocene Darende Basin show that this basin experience a burial event and exhumed during Oligocene suggesting that the collisional event already took place at that time. The detrital AFT data extracted from the Miocene Malatya Basin suggest that the cooling and unroofing of the magmatic and metamorphic bodies in the region started in Paleocene and continued until late Miocene (Fig. 1).

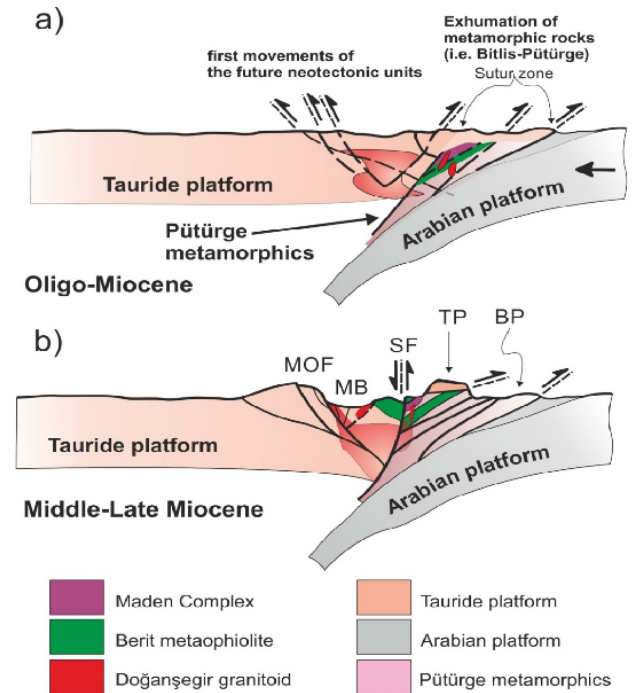


Figure 1. The geodynamic model of the southeast Anatolian Orogenic Belt during Oligocene and Miocene. MOF: Malatya-Ovacık Fault, MB: Malatya Basin, SF: Sürgü Fault, TP: Tauride Platform, BP: Bitlis-Pütürge metamorphics (modified after Karaoğlan et al., 2016)

Acknowledgement

This study was financially supported by National Science Foundation of Turkey - TÜBİTAK (project no: 112Y347)

References

- Garfunkel, Z., 2004. Origin of the Eastern Mediterranean basin: a reevaluation. *Tectonophysics* 391, 11-34.
- Garfunkel, Z., 2006. Neotethyan ophiolites: formation and obduction within the life cycle of the host basins, In: Robertson, A.H.F., Mountrakis, D. (Eds.), *Tectonic Development of the Eastern Mediterranean Region*. Geological Society, London, Special Publications, pp. 301-326.
- Karaoğlan, F., Parlak, O., Hejl, E., Neubauer, F., Klötzli, U., 2016. The temporal evolution of the active margin along the Southeast Anatolian Orogenic Belt (SE Turkey): Evidence from U–Pb, Ar–Ar and fission track chronology. *Gondwana Research* 33, 190-208.
- Karaoğlan, F., Parlak, O., Klötzli, U., Thöni, M., Koller, F., 2013a. U–Pb and Sm–Nd geochronology of the ophiolites from the SE Turkey: implications for the Neotethyan evolution. *Geodinamica Acta* 25, 146-161.
- Karaoğlan, F., Parlak, O., Robertson, A., Thöni, M., Klötzli, U., Koller, F., Okay, A.İ., 2013b. Evidence of Eocene high-temperature/high-pressure metamorphism of ophiolitic rocks and granitoid intrusion related to Neotethyan subduction processes (Doğanşehir area, SE Anatolia), In: Robertson, A.H.F., Parlak, O., Ünlügenç, U.C. (Eds.), *Geological Development of Anatolia and the Easternmost Mediterranean Region*. Geological Society, London, Special Publications, London, pp. 249-272.
- Lin, Y.-C., Chung, S.-L., Bingol, A.F., Beyarslan, M., Lee, H.-Y., Yang, J.-H., 2015. Petrogenesis of Late Cretaceous Elazığ Magmatic Rocks from SE Turkey: New Age and Geochemical and Sr-Nd-Hf Isotopic Constraints, *Goldschmidt 2015*, Prague, p. 1869.
- Okay, A.İ., Tüysüz, O., 1999. Tethyan sutures of northern Turkey, In: Durand, B., Jolivet, F.L., Horváth, F. (Eds.), *The Mediterranean Basins: Tertiary Extension within the Alpine Orogen*. Geological Society, London, Special Publications, pp. 475-515.
- Parlak, O., 2006. Geodynamic significance of granitoid magmatism in the southeast Anatolian orogen: geochemical and geochronological evidence from Goksun-Afsin (Kahramanmaraş, Turkey) region. *International Journal of Earth Sciences* 95, 609-627.
- Rızaoğlu, T., Parlak, O., Höck, V., Koller, F., Hames, W.E., Billor, Z., 2009. Andean-type active margin formation in the eastern Taurides: Geochemical and geochronological evidence from the Baskil granitoid (Elazığ, SE Turkey). *Tectonophysics* 473, 188-207.
- Robertson, A., Parlak, O., Ustaömer, T., Taslı, K., İnan, N., Dumitrica, P., Karaoğlan, F., 2013a. Subduction, ophiolite genesis and collision history of Tethys adjacent to the Eurasian

- continental margin: new evidence from the Eastern Pontides, Turkey. *Geodinamica Acta* 26, 230-293.
- Robertson, A.H.F., 2004. Development of concepts concerning the genesis and emplacement of Tethyan ophiolites in the Eastern Mediterranean and Oman regions. *Earth-Science Reviews* 66, 331-387.
- Robertson, A.H.F., Parlak, O., Metin, Y., Vergili, Ö., Tasli, K., Inan, N., Soykan, H., 2013b. Late Palaeozoic–Cenozoic tectonic development of carbonate platform, margin and oceanic units in the Eastern Taurides, Turkey, In: Robertson, A.H.F., Parlak, O., Ünlügenç, U.C. (Eds.), *Geological Development of Anatolia and the Easternmost Mediterranean Region*. Geological Society, London, Special Publications, London, pp. 167-218.
- Robertson, A.H.F., Parlak, O., Ustaomer, T., 2012. Overview of the Palaeozoic-neogene evolution of neotethys in the Eastern Mediterranean region (Southern Turkey, Cyprus, Syria). *Petroleum Geoscience* 18, 381-404.
- Robertson, A.H.F., Parlak, O., Ustaömer, T., 2013c. Late Palaeozoic–Early Cenozoic tectonic development of Southern Turkey and the easternmost Mediterranean region: evidence from the inter-relations of continental and oceanic units, In: Robertson, A.H.F., Parlak, O., Ünlügenç, U.C. (Eds.), *Geological Development of Anatolia and the Easternmost Mediterranean Region*. Geological Society, London, Special Publications, London, pp. 9-48.
- Şengör, A.M.C., Yılmaz, Y., 1981. Tethyan Evolution of Turkey - a Plate Tectonic Approach. *Tectonophysics* 75, 181-241.
- Stampfli, G.M., 2000. Tethyan oceans, In: Bozkurt, E., Winchester, J., A., Piper, J., A. (Eds.), *Tectonics and Magmatism in Turkey and the Surrounding Area*. Geological Society, London, Special Publications, London, pp. 1-23.
- Stampfli, G.M., Borel, G.D., 2002. A plate tectonic model for the Paleozoic and Mesozoic constrained by dynamic plate boundaries and restored synthetic oceanic isochrons. *Earth and Planetary Science Letters* 196, 17-33.
- van Hinsbergen, D.J.J., Edwards, M.A., Govers, R., 2009. Geodynamics of collision and collapse at the Africa–Arabia–Eurasia subduction zone, In: Pankhurst, B. (Ed.). *Geological Society, London, Special Publications*, London, p. 368.
- Yazgan, E., Chessex, R., 1991. Geology and Tectonic Evolution of the Southeastern Taurides in the Region of Malatya. *TPJD Bülteni* 3, 1-42.
- Yılmaz, Y., 1993. New Evidence and Model on the Evolution of the Southeast Anatolian Orogen. *Geological Society of America Bulletin* 105, 251-271.
- Yılmaz, Y., Yiğitbaş, E., Genç, Ş.C., 1993. Ophiolitic and Metamorphic Assemblages of Southeast Anatolia and Their Significance in the Geological Evolution of the Orogenic Belt. *Tectonics* 12, 1280-1297.

3D geological modeling and metallogenic features of the Mengkelaoangou Pb-Zn-Ag polymetallic ore deposit, Henan Province, Central China

Fan Yang^{a*}, M. Santosh^{a b}, Gongwen Wang^a, Nana Guo^c

^aSchool of Earth Sciences and Resources, China University of Geosciences Beijing, 29 Xueyuan Road, Beijing 100083, China

^bDepartment of Earth Sciences, University of Adelaide, SA 5005, Australia

^cLuanchuan Bureau of Geology and Resources, Luoyang 417500, China

*Corresponding author e-mail: yang_fan1989@126.com

The Mengkelaoangou Pb-Zn-Ag polymetallic deposit is a hydrothermal vein deposit of Luanchuan ore district, and located in the East Qinling orogenic belt in China. Three stages of mineralization are recognized at the Mengkelaoangou, including the early quartz-pyrite (Stage I) characterized by the early quartz sporadically distributed in the dolomite or associated with pyritization, followed by the main ore stage of superimposed transformation of ore-bearing fluid (Stage II) represented by the pyrites which were metasomatically transformed to sphalerite and galena, and the late stage of iron oxides (Stage III) featured by the oxidation of galena, sphalerite and pyrite

forming anglesite, magnesite and limonite. Here, a deposit-scale metallogenic model based on the data of 1:1000 scale geological map, 53 boreholes (total core length of 16,800 m), and 38 1:2000 scale sections of exploration line is constructed for extracting spatial features which provides insights into the regional geology and processes of ore-formation. Based on analysis for the extracted spatial features, we delineated the orebodies, and constructed the stratigraphic model and the tectonic model which reveal that the fault zone and the margin of meta-gabbro are potential locales for ore prospecting (Fig. 1).

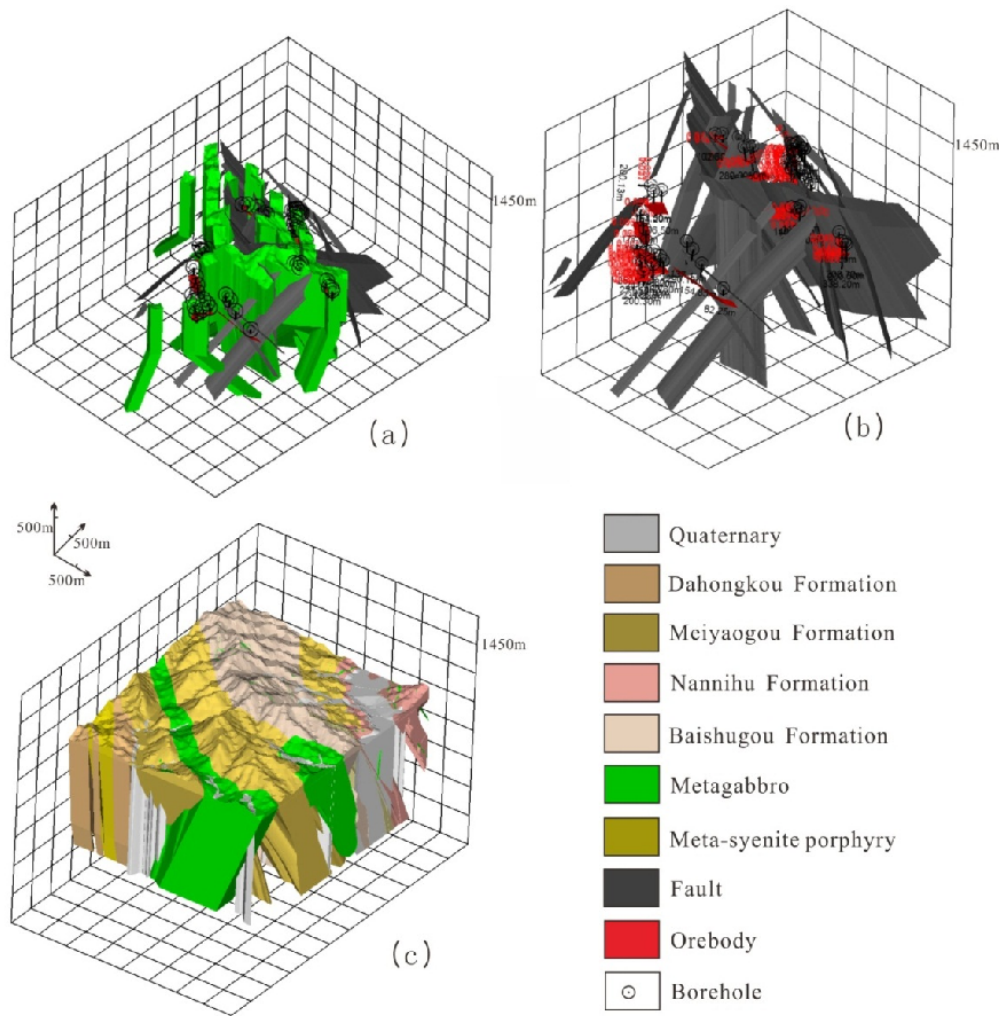


Fig. 13D geological models of the Mengkelaoangou Pb-Zn-Ag polymetallic ore deposit. a: Fault+metagabbro+orebody; b: Fault+orebody; c, Stratum.

Petrology, phase equilibria modeling and zircon U-Pb geochronology of Paleoproterozoic mafic granulites from the Fuping Complex, North China Craton

Li Tang^{1, 2}, M. Santosh^{1, 3}, Toshiaki Tsunogae^{2, 4}

¹ School of Earth Sciences and Resources, China University of Geosciences Beijing, 29 Xueyuan Road, Beijing 100083, China;

² Graduate School of Life and Environmental Sciences, University of Tsukuba, Ibaraki 305-8572, Japan

³ Centre for Tectonics, Exploration and Research, University of Adelaide, Adelaide SA 5005, Australia

⁴ Department of Geology, University of Johannesburg, Auckland Park 2006, South Africa

The North China Craton (NCC) witnessed the collisional assembly of major continental blocks during 2.1-1.8 Ga broadly coeval with the incorporation of the craton within the global supercontinent Columbia. Paleoproterozoic granulites are widespread in the NCC, including mafic granulites that are well preserved in the basement terranes along the Trans-North China Orogen (TNCO). These high-grade metamorphic rocks are proposed to have been formed during the collisional event which resulted in the final cratonization of the NCC. Systematic studies on the petrology and phase equilibria modeling of granulites in combination with precise geochronological studies can provide important insights into the metamorphic history and tectonic processes.

The Fuping Complex is one of the important basement terranes within the

central segment of the Trans-North China Orogen. Mafic granulites are exposed in this complex as boudins or enclaves within tonalite-trondhjemite-granodiorite (TTG) gneisses. Garnet in these granulites shows compositional zoning with homogeneous cores formed in the peak metamorphic stage, surrounded by thin rims that developed during the retrograde cooling that show increase of almandine and decrease of grossular. Petrologic and phase equilibria studies including pseudosection calculation by using THERMOCALC define clock-wise P-T paths for three mafic granulites. The final phase assemblages for the peak metamorphic stages probably correspond to the field just above the solidus because field observations and petrographic studies suggest very limited amount of *in situ* melt was involved during the metamorphism.

The peak metamorphic P-T conditions are estimated at 8.2-9.2 kbar, 870-882 °C (15FP-02), 8.4-11.5 kbar, 855-885 °C (15FP-03) and 9.7-10.5 kbar, 880-900 °C (15FP-06), respectively. The pseudosections for the subsequent retrograde stages based on relatively higher H₂O contents from P/T-M(H₂O) diagrams define the retrograde P-T conditions of <6.1 kbar, <795 °C (15FP-02), 5.6-5.8 kbar, <795 °C (15FP-03), and <9 kbar, <865 °C (15FP-06), respectively. Data from LA-ICP-MS zircon U-Pb dating show that the mafic dyke protoliths of the granulite were emplaced at ~2327 Ma. The metamorphic zircons show two groups of ages at 1.90-1.96 Ga (peak at 1.92-1.93 Ga) and 1.80-1.89 Ga (peak at 1.83-1.86

Ga), consistent with the two metamorphic events widely reported from different segments of the Trans-North China Orogen. The metamorphic ages of 1.93-1.92 Ga are considered to represent the peak granulite-facies metamorphism, whereas the 1.83-1.86 Ga ages are correlated with the retrograde event. Thus, the collisional assembly of the major crustal blocks in the North China Craton might have occurred during 1.93 to 1.90 Ga, marking the final cratonization of the North China Craton.

Gold mineralization and Neoproterozoic suprasubduction zone signature in Shimoga greenstone belt, Western Dharwar Craton, India

Sohini Ganguly^a, C. Manikyamba^b and M. Santosh^c

^aDepartment of Earth Science, Goa University, Goa 403206

^bNational Geophysical Research Institute (Council of Scientific and Industrial Research)
Uppal Road, Hyderabad 500 007

^cSchool of Earth Science and Resources, China University of Geosciences, Beijing, China

Gold mineralization hosted in mafic volcanic rocks from the Kudrekonda Formation and in Banded Iron Formations (BIF) of Ganajur, Karajgi and Palvanahalli areas of the Shimoga greenstone belt (SGB) in western Dharwar Craton (WDC) India have been studied. The geochemical characteristics for mafic volcanic rocks of Kudrekonda Formation of Shimoga greenstone belt, classify them as boninites generated in intraoceanic island arc setting. The petrogenesis of Kudrekonda boninites invoke (i) fluid-fluxed metasomatism of a refractory mantle wedge during initial stage of intraoceanic subduction (ii) partial melting of metasomatized mantle wedge triggered by heat from upwelling asthenosphere and lowering of solidus by subduction-derived fluids. Gold occurring within the quartz veins of Kudrekonda boninites is

syngenetic with a mesothermal origin and is genetically linked with previous tectonothermal events and accretionary processes related to convergent margin activity. Hydrothermal fluids derived from devolatilization reactions during prograde metamorphism at deeper crustal levels served as potential precursor for Au precipitation (Fig. 1). The BIFs from Ganajur, Karajgi and Palvanahalli areas of Shimoga greenstone belt are silicified, carbonatized, sulfidized and their immobile trace element abundances and ratios reflect chemical precipitation from paleo-seawater enriched in dissolved iron and silica with input from hydrothermal fluids. These observations indicate their deposition in a marine off-shelf environment proximal to a mid-oceanic ridge-rift system. The BIF hosted gold-sulphide mineralization of Shimoga

greenstone belt is epigenetic, epithermal type associated with hydrothermal activity at mid-oceanic spreading centre. Auriferous hydrothermal solutions of volcanic origin were released under low oxygen fugacity conditions and these fluids migrated to the site of BIF deposition that acted as chemical traps for the sulphide rich auriferous fluid (Fig. 1). Gold in Kudrekonda boninites is genetically related to auriferous fluids of intraoceanic subduction zone, while genesis of BIF-hosted gold is attributed to hydrothermal activity at midoceanic ridge-rift system. Occurrence of gold in quartz veins cutting across Kudrekonda boninites and Karajgi BIF is interpreted as late-stage process involving syntectonic remobilization of gold, its transportation and precipitation through shear zone-controlled faults and fractures during collision-accretion at ocean-continent convergence. The Kudrekonda boninites represent accretion and preservation of a slice of older, subduction-derived oceanic crust onto a relatively younger, active continental margin through arc-continent collision in a Neoproterozoic suprasubduction zone environment.

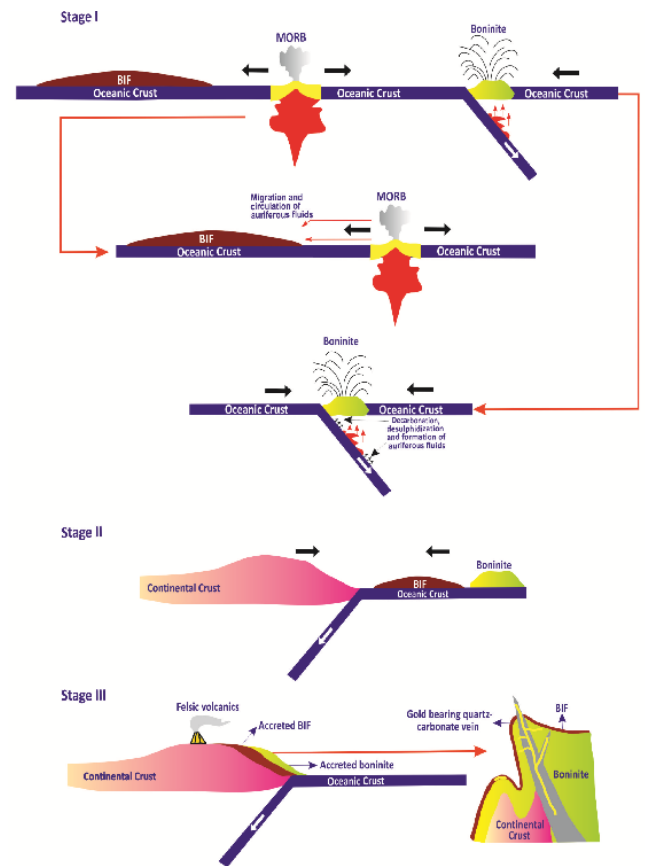


Fig. 1 Slab-devolatilization and hydrothermal process for gold mineralization at diverse tectonic settings.

Spectral and chemical features of anorthosite complex in Southern India: Implications for Lunar Highland anorthosite evolution

Sam Uthup¹, V.J. Rajesh¹ and Satadru Bhattacharya^{2,*}

¹Department of Earth and Space Sciences, Indian Institute of Space Science and Technology, Valiamala P.O., Thiruvananthapuram 695 547, Kerala

²Space Application Centre, Indian Space Research Organization, Ahmedabad 380-015, Gujarat

*Corresponding Author e-mail: samuthup@gmail.com

Planetary analogue research is an important topic in planetary geoscience to understand the planetary origin and its evolutionary processes. Terrestrial analogue sites established, will give us more insight into the mineralogy and mineral chemistry of planetary surfaces. Several landforms in India show close resemblance with the lunar landforms and is being studied by researchers, in order to get better understanding of lunar geological process. The lunar highland region (terrae) is mainly composed of anorthosite suite of rocks. Geoscientists believe that these anorthosites found on the lunar highland are the remnants of initial lunar crust formed from a global basic magma ocean due to floatation. The Archean crust of southern Indian peninsula has many anorthosite exposures, which are similar to those of lunar highland anorthosites. Spectral and chemical characterization of these anorthosite complexes and their petrological studies will provide further

insights into the evolutionary processes of the lunar highland crust. The reflectance spectral features of these anorthositic rocks will also help us in future planetary missions in lunar highland region. Anorthosites from Sittampundi, Kadavur and Oddanchathram were characterized for this study. The reflectance spectroscopy of rocks from our terrestrial study areas showed close resemblances to the lunar highland rock absorption spectra with peaks at 1000nm, 1150nm, 1250nm, 1415nm and 1915nm. The absorption peaks at 1150nm and 1250 nm are observed due to the plagioclase feldspar absorption. The powdered anorthosite samples when subjected to X-ray Diffraction (XRD) gave peaks at 27.99 which are the characteristic peak of plagioclase feldspar. The Laser Raman spectroscopy was also done to characterize the analogue anorthosites. Electron Probe Micro Analyzer (EPMA) studies of the anorthosite rocks collected

from Sittampundi, Kadavur and Oddanchathram gave An95-97, An55-60 and An94 respectively. The lunar anorthosites have very high An content (An

98). Sittampundi anorthosite complex show high degree of closeness to the lunar highland anorthosites when compared with other studied analogue sites.

Geochemical fingerprinting of a forearc-arc-backarc association in the Neoproterozoic/Paleoproterozoic Kotri-Dongargarh mobile belt, Central India

Sirish Kumar and Deepanker Asthana*

Department of Applied Geology, Indian School of Mines, Dhanbad-826004, INDIA

*Corresponding author e-mail: dasthana@hotmail.com

The Bastar craton of central India is an important Archaean protocontinental nuclei and a geological archive of the Earth's early crustal formation events (Bleeker, 2003, Naqvi, 2005). It is surrounded by ENE-WSW trending Central Indian Tectonic Zone (CITZ) towards the north and cross-cut by the prominent N-S trending Kotri-Dongargarh mobile belt (KDMB) (Asthana et al 2014). The CITZ separates the Bastar craton from the Bundelkhand craton and represents a continental scale continent- continent collisional belt, whereas the KDMB is a collage of Archaean/Paleoproterozoic supracrustal assemblages with thick volcano-sedimentary sequences and vast tracts of granitoids. What is not clear, and currently a matter of debate is whether mobile belts of the northern, central and southern KDMB are related to each other or not? If they are indeed related to each other, as shown here, are these mobile belts subduction-related or rift-related?

Furthermore, if they are subduction-related, can they be linked to the CITZ? Alternatively, if they are rift-related, do they belong to the Dongargarh LIP (Sensarma, 2007) or they are rift-related mobile belts (Srivastava et al 2004, Ramakrishnan and Vaidyanadhan, 2010)? Several episodes of orogeny and tectonothermal events in the Bastar craton (Mohanty, 2015) have resulted in metamorphism, alteration and deformation resulting in obliteration of vital field relationships, igneous textures and destruction of magmatic phases as well as mobility of several key elements in the volcanics/dykes. Cumulates appears to have had significant effect on whole rock geochemistry (Kemp, 2004). In order to circumvent the issues related to destruction of magmatic phases, elemental mobility and to understand the petrogenesis and tectonic setting of the KDMB volcanics/dykes we primarily use Al, Ti, REE, HFSE and transition metals that remain relatively immobile during

hydrothermal alteration and low grade metamorphism (Kerrick et al., 1998; Polat et al., 2002; Pearce, 2008). Furthermore, relict clinopyroxene chemistry of the Pitepani volcanics are employed to unravel their petrogenesis, since relict clinopyroxene of magmatic rocks that have suffered low grades of metamorphism retain their magmatic compositions (Leterrier et al., 1982; Asthana, 1991).

The felsic suite of the Bastar craton, termed Bijli rhyolites are restricted to the northern and central parts of the craton. They are made up of high silica rhyolites with pyroclastic textures. They have moderate Al_2O_3 , predominantly peraluminous and magnesian (i.e., calc-alkaline). Rhyolites have high Zr/Y ratios (~3 to ~10), strongly fractionated REE patterns (La/Yb ~9 to ~29), high Th as well as high Th/Ta and Th/Hf ratios. Their REE and mantle normalized plots are similar to F1 rhyolites, which are primarily calc-alkaline rhyolites (Barrie et al., 1993; Hart et al., 2004; Gaboury and Pearson 2008).

The mafic suites of the KDMB are divided into calc-alkaline suite and tholeiitic suites, respectively. The majority of the calc-alkaline suites of KDMB are relatively primitive basaltic andesites to andesites, with high MgO, Mg#, Ni, Cr and low TiO_2 (< 0.8 wt. %). The Pitepani HMA (Asthana et al., 2016) and all reported basaltic andesites (BA), boninites and high-Mg norites of the north, central and south Bastar craton that includes the Dongargarh-Chhuradykes (Srivastava and Gautam, 2015), boninite dyke (Rao and Srivastava, 2009), the “boninites” and “high-Mg norites” (SubbaRao et al., 2008), siliceous high magnesian basalts (Sensarma et al., 2002), “BN” dykes and related volcanics of the central and south

Bastar craton (Srivastava et al., 2004; Srivastava and Gautam, 2012) have similar REE patterns and primitive mantle normalized plots. However, they are neither boninites (*sensu stricto*) nor belong to the boninite-norite suite, since: (a) the REE patterns are neither U-shaped (Sun et al., 1989; Cadman et al., 1997; Nielsen et al., 2002) nor there is a Zr spike in the primitive mantle normalized plots, (b) the Zr contents and La/Yb and Gd/Yb ratios are an order of magnitude higher compared to Whundo-type second stage melts [(i.e., the Archean boninites; Smithies et al., (2004)] and (c) there was no major crust forming events prior to ~2.5 Ga in the Bastar craton (Mohanty, 2015), whereas “norite suites appear in the geological record only after the major late Archean crust forming event (Hall and Hughes, 1990; Cadman et al., 1997)”. The calc-alkaline suites of KDMB have also been termed as siliceous high magnesian basalts (SHMB, Sensarma, 2007). However, Whitney-type second stage melts (i.e., SHMB) are closely associated with komatiites, both in space and time (Smithies et al., 2004). Significantly, till date, neither spinifex textured komatiites/related rocks (Srivastava and Gautam, 2009; Asthana et al., 2015), nor layered igneous complexes with chromite/Ni-Cu-sulfides/platinum group elements (PGE)/Ti-V-bearing magnetite deposits have been reported from the Bastar craton (c.f., Seitz and Keays, 1997; Bryan and Ernst, 2008). The Gd/Yb ratios of the calc-alkaline suite are similar to the Early Archean Barbeton-type komatiites; however their Al_2O_3/TiO_2 ratios are unlike the Barbeton-type komatiites and instead are similar to the Late Archean Munro-type komatiites, and vice-versa. The calc-alkaline basaltic andesites and

andesites are classified as HMA based on: (a) SiO_2 vs MgO diagram and (b) TiO_2 vs. $\text{MgO}/(\text{MgO}+\text{FeO}^{\text{T}})$, Sr/Y vs. Y and $(\text{La}/\text{Yb})_{\text{N}}$ vs. Yb_{N} discriminant diagrams of Kamei et al (2004). Furthermore, the later discriminant diagrams reveal subtle geochemical differences with Cenozoic boninites, and this is further corroborated by their Dy concentrations (Saccani, 2015). Significantly, the REE patterns and the mantle normalized plots reveal consistent and coherent patterns that are remarkably similar to the Cenozoic sanukitic HMA. The similarities demonstrate that magmatic signatures dominate over affects due to secondary process, such as alteration and metamorphism. HMA forms over a very limited period of time, under unusual subduction-related tectonic settings and represent excellent regional and tectonic time markers (McCarron and Smellie, 1998; Katz et al., 2004; Tatsumi, 2008; Yin et al., 2013). Accordingly, all the calc-alkaline suites of the Bastar craton are geochemically similar, consanguineous, and coeval belonging to a single HMA.

The inferences drawn from the whole-rock geochemistry are independently corroborated by the relict clinopyroxene chemistry of the Pitepani HMA [reported as siliceous high magnesian basalts (SHMB, Sensarma et al., 2002) and boninite dyke (Rao and Srivastava, 2009)]. The Pitepani HMA clinopyroxenes plot in the field of HMA in the Si vs Mg# diagram (Asthana et al., 2010), implying that these clinopyroxenes crystallized from a magma that had high MgO contents and high $\text{SiO}_2/\text{Al}_2\text{O}_3$ ratios (Kamei et al., 2004). The presence of clinopyroxenes, both as phenocrysts and in the groundmass (Sensarma et al., 2002; Rao and Srivastava, 2009) have

much in common with sanukitic HMA (Kepezhinskias et al., 1997; Tatsumi et al., 2003; Kamei et al 2004). Pressure and temperature (P&T) of clinopyroxene crystallization in the Pitepani HMA as estimated with clinopyroxene-whole-rock pairs, for which equilibrium was established by comparing and calculating equilibrium clinopyroxene compositions and T for clinopyroxene saturation using whole-rocks and calculated P as input (Putirka 1999). The estimated P&T conditions indicate relatively high clinopyroxene crystallization temperatures between $\sim 1200^\circ\text{C}$ to $\sim 1240^\circ\text{C}$ at shallow depths (0 to ~ 4 kbars) indicating a hot subduction environment (c.f., Bryant et al., 2011) but not hot enough to support a mantle plume-related bimodal Large Igneous Province, (Sensarma, 2007).

KDMB tholeiites plot in the island arc (IAT) and back arc basin basalt (BABB) field in the Ti/Zr vs Zr plot (Woodhead, 1993). IAT is characterized by a distinctly more depleted mantle source (Ti/Zr ratios >70), compared to BABB (Ti/Zr <70). The REE patterns and the mantle normalized plots of the IAT and BABB suites are distinct and reveal consistent and coherent patterns. The IAT suites are present throughout KDMB and their identical geochemistry suggest that they belong to a single magmatic suite. They are represented by the North Bastar dykes (Srivastava and Gautam, 2015), sub-alkaline mafic dykes (BD1-CBC, Srivastava and Gautam, 2012), sub-alkaline basalts (SAB, Srivastava et al., 2004) and Kotri basalt (KB 95, Manikyamba et al 2016). In contrast, the BABB suites are confined to the northern and central parts of the Bastar craton only. They have been reported from the Pitepani tholeiites (Pophare, 2000;

Asthana et al 2010) and are represented by all the Kotri basalts, except KB95 (Manikyamba et al., 2016). The similar geochemistry of the BABB from KDMB indicates that they are consanguineous,

and coeval belonging to a single BABB suite. The compositional range of important HFSE, LILE and REE of HMA, IAT and BABB is given in the table.

Major and Minor elements	HMA (forearc)	Island tholeiites	Arc	Back Arc Basalts	Basin
TiO ₂	0.25-0.78	0.86-1.29		0.73-1.77	
Al ₂ O ₃	8.05-14.98	12.31-15.36		11.6-16.11	
Nb	1-6.03	2-5		1.51-10.81	
Ta	0.03-1.87	0.1-0.4		0.02-0.57	
Zr	35-107	42-102		113-250	
Hf	0.4-2.6	1-2.7		2.63-5.52	
Y	6-20	15-30		17.15-40.59	
Th	1-7.1	0.4-2.2		3.78-9.55	
La	5.1-23.3	4.3-11.6		16.59-48.19	
Ce	9-44.6	9.7-25		34.71-94.4	
Pr	0.92-6	1.32-3.12		3.67-8.05	
Nd	3.9-18.68	5.9-13		17-41.57	
Sm	0.9-3.9	1.8-3.6		3.95-9.51	
Eu	0.33-1.06	0.7-1.23		0.98-2.21	
Gd	1.1-4	2.5-4.6		3.19-7.38	
Tb	0.2-0.7	0.5-0.8		0.5-1.15	
Dy	1.3-4	3-5.2		2.68-6.27	
Ho	0.3-0.9	0.6-1.2		0.56-1.31	
Er	0.9-2.5	1.9-3.4		1.77-4.37	
Tm	0.14-0.39	0.29-0.51		0.26-0.65	
Yb	0.8-2.5	1.9-3.3		1.7-4.34	
Lu	0.13-0.4	0.3-0.51		0.25-0.62	
(La/Yb) _N	2.66-8.43	1.19-2.56		3.9-8.46	
(Gd/Yb) _N	0.98-2.28	0.99-1.25		1.24-1.52	

Depth estimation of BIF in Sandur Schist Belt though ground magnetic from South India

K. Satish Kumar

CSIR- National Geophysical Research Institute, Uppal Road, Hyderabad

E-mail: satish_marine777@yahoo.co.in

Intense ground magnetic anomalies are observed in the western basin of the Sandur Schist belt near Muraripura village, Karnataka. Sources for these anomalies are inferred due to the presence of the exposed Banded Iron formations hosted by metabasalts, arenaceous and argillaceous rocks associated with the Donimali formation of the schist belt. Geologically two varieties of BIF bands are observed in the study area i.e Band 1 and Band 2. Band 1 is dominantly composed of banded iron formation, rich in iron ore minerals and silica chert. Band 2 is largely composed of ferruginous quartzite and quartz arenites. Analysis of Major trace elements of samples from Band 1 & Band 2 reveals, BIFs of the study area is post Precambrian of hydrothermal affinity. Qualitative analysis of the magnetic data indicates, study area can be divided into three lithologically important BIF/BQ formations. Spectral and quantitative analysis of the magnetic data indicates, band 1 is extended up to average depth of 70 m with an average thickness of 70 m. The average depth of Band 2 is 130 m with an average thickness

of 70m. Further, it is observed band 1 & 2 are separated by a strike-slip fault (Fig 1).

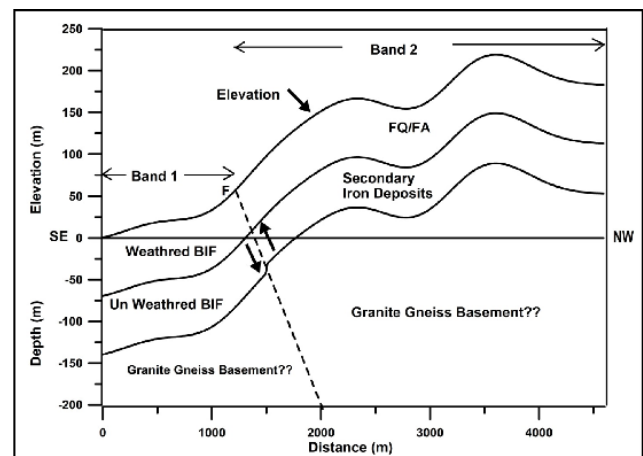


Fig1. Inferred Depth Model of the Study area from Spectral and Quantitative Analysis.

New evidence for meteoritic impact at Luna, Gujarat, India

G.K. Indu^{1*}, K.S. Sajin kumar¹, Keerthy Suresh¹, V.J. Rajesh²

¹Department of Geology, University of Kerala, Kariavattom, Thiruvananthapuram-695 581, India

²Department of Earth and Space Sciences, Indian Institute of Space Science and Technology, Valiamala, Thiruvananthapuram-695 547, India;

*Corresponding Author e-mail: sajinks@gmail.com

Luna Crater, in western Gujarat (latitude 23°42'17"N; longitude 69°15'37"E), is one of the unconfirmed impact craters in India, located in the Kachchh district of Gujarat State. The crater exhibits typical features of a simple impact crater such as circular depression, raised rims and ejecta layer. The presence and preservation of this crater morphology indicate the possibility of meteoritic impact. The SRTM data analysis shows radial drainage pattern with the nearest area showing dendritic and parallel patterns, similar to younger impact craters.

This crater was formed in the younger Quaternary sediments, characterized by 200m thick clay layer. The 2m raised inner and outer rims have ejecta of thickness 0.7m. This ejecta layer is characterized by impactite nodules at some places. Some of these are completely glassy and have low specific gravity and some nodules are Fe rich with high specific gravity. Lumps of ferricrete/laterite are associated with these nodules and are suspected to represent an inverted

topography. These are limited to 0.7m depth below which pure kaolinite clay layer is present. These nodules are identified as melt rock through petrographic study and EPMA. The Hyperspectral and XRD analysis of the high specific gravity nodules show well defined peaks corresponding to goethite, a common weathering product of primary iron bearing minerals. SEM EDX data show anomalous concentration of metallic phases like Ni, Co and Cr in this nodule. The hyperspectral data also reveal magnetite in the nodule. The glassy melt rock shows a composition corresponding to potassic hastingsite which is a high temperature mineral, usually associated with some catastrophic events like meteoritic impact. All these primary results from morphological, stratigraphic, mineralogical and geochemical studies suggest the impact origin of Luna crater.

A comparison between Cr-diopside of Lattavaram and Kalyanadurgam Kimberlites, Anantapur district, Southern India

P. Ramesh Chandra Phani

Senior Subject Matter Expert (Mining), Cyient Limited, Plot #11, Software Layout, Infocity, Madhapur, Hyderabad 500 081, India.

E-mail: Ramesh.Pothuri@cyient.com

Wajrakarur Kimberlite Field (WKF) comprises number of kimberlite clusters with diamondiferous pipes, among which Lattavaram, Chigicherla, Anumpalli, Timmasamudram and Kalyanadurgam kimberlite pipes are significantly well known. Many workers have attempted in the past to study the mineral chemistry of WKF pipes. In this paper, a comparison of major elements in Cr-diopside mineral grains of kimberlites of Lattavaram and Kalyanadurgam of WKF has been presented; the former are exposed at Lattavaram village and the latter at Pillalapalli and Muppalakunta respectively. These kimberlites are reported to be similar to South African Group I kimberlites and exhibit hypabyssal brecciated nature owing to their textural, lithological and mineralogical assemblages. These kimberlites invariably possess mantle derived xenocrystic minerals like pyrope garnet, Cr-diopside, ilmenite, chromite and

olivine which provide inferences on the source region of these kimberlites. Cr-diopside is a prominent mantle derived mineral in both these locations and is used as an indicator mineral in reconnaissance diamond exploration. In this study, *in-situ* loam sampling was carried out, on diamondiferous pipes viz., P-3 and P-4 of Lattavaram and KL-1 and KL-2 pipes of Kalyanadurgam. From the *in-situ* loam sample, heavy indicator minerals were concentrated through panning and jigging and about 66 Cr-diopside grains; 26 from Lattavaram and 40 from Kalyanadurgam were picked under stereoscopic microscope and studied for their major element geochemistry by EPMA. In Lattavaram area, 25 grains were identified to be of C5 class and one grain belongs to C3. Among the Cr-diopsides of Kalyanadurgam, it is observed that 39 grains belong to C5 category and one grain C2 class. The ranges of weight% for

Cr₂O₃ in Lattavaram samples is 0.94 – 2.8 and that in Kalyanadurgam samples is 0.54- 6.34. It is envisaged that the entries of Fe, Al, Na, Ca, and Cr into the clinopyroxene structure are strongly affected by the P-T-X conditions during mineral crystallization; hence atomic cation proportions are also used in this study to

illustrate the chemical variation of mantle-derived kimberlite Cr-diopside relative to the more Fe-rich non-kimberlitic (crustal) grains. The analysis reveals that Cr-diopsides of Lattavaram and Kalyanadurgam are of kimberlitic nature and have bearing on diamond potentiality of these pipes.

Understanding early Paleozoic orogeny in South China: significance of tectonism and magmatism in the Central Jiangnan Orogen and the North Cathaysia

Jianhua Li^{*1, 2}, Guochun Zhao¹, Shuwen Dong³, Yueqiao Zhang³, Stephen Johnston⁴, Jianjun Cui², Yujia Xin²

¹Department of Earth Sciences, James Lee Science Building, The University of Hong Kong, Pokfulam Road, Hong Kong, China

²Institute of Geomechanics, Chinese Academy of Geological Sciences, Beijing 100081, China

³State Key Laboratory for Mineral Deposits Research, Nanjing University, Nanjing 210093, China

⁴Earth & Atmospheric Sciences, Earth Sciences Building, University of Alberta, Edmonton, Alberta, Canada

*Corresponding Author e-mail: jianhua1@hku.hk

The early Paleozoic orogeny in South China, involving significant crustal shortening, is manifested by a conspicuous Middle or Late Devonian unconformity, early Paleozoic metamorphism, ductile shearing, folding, and Silurian plutonism. Despite numerous geological records, the paucity of structural data inhibits our ability to delineate the synorogenic structural framework. This in turn leads to many controversies and uncertainties regarding (1) how the orogeny involved and (2) what drove the orogeny. To address the controversies and uncertainties, we conducted structural coupled with thermochronological and geochronological studies in the central Jiangnan Orogen and the north Cathaysia. In the central

Jiangnan Orogen, the early Paleozoic deformation was characterized by combined dextral and thrust shearing that was variably partitioned into arrays of anastomosing high-strain zones. Dextral arrays strike dominantly E-ESE and dip steeply to the south; thrust arrays strike NE, dip 20~80° to the SE and bear top-to-the-NW shear criteria. In the north Cathaysia, early Paleozoic deformation corresponds to sinistral shearing along arrays of NNE-oriented, steep-dipping zones. Synkinematic recrystallized microstructures and lattice-preferred orientation (LPO) patterns indicate that the above-stated ductile shearing commenced under upper greenschist to low amphibolite facies conditions at temperatures of ~400-

600 Ma. Combined dating by U-Pb and $^{40}\text{Ar}/^{39}\text{Ar}$ shows that the orogenic shortening commenced at ~460 Ma, terminated around 420 Ma and was followed by cooling through ~450-350 Ma at ~400-370 Ma. Synthesis of our structural data with previous work allows tracing the early Paleozoic orogen that extends through the Jiangnan Orogen into the north Cathaysia, with the southern part of the Jiangnan orogen marking its core and the southeast Yangtze acting as its foreland fold-and-thrust zone. The orogeny involved prominent NW-SE shortening, and was related to intracontinental convergence between the Yangtze and Cathaysia Blocks, externally induced by the

amalgamation of South China and Australia during final assembly of Gondwana.

Acknowledgements

This research was financially supported by a NSFC Project (41190075) entitled "Final Closure of the Paleo-Asian Ocean and Reconstruction of East Asian Blocks in Pangea," which is the fifth research project of NSFC Major Program (41190070) "Reconstruction of East Asian Blocks in Pangea", Hong Kong RGC GRF (HKU7063/13P and 17301915), and Natural Science Foundation of China (No. 41502197). Jianhua's work in Hong Kong has been supported by grants from Hong Kong Scholars Program.

Electron microprobe dating on monazites from Mangalwar Complex, Rajasthan: evidences for Meso-Proterozoic and Grenvillian reworking of a Palaeoproterozoic crust

Krishnapriya Basak, Siladitya Sengupta and Sandip Nandy

Geological Survey of India, Kolkata

The polymetamorphic terrane of northern Mangalwar Complex (MC), western Indian Craton, Rajasthan provides insight into the multiple episodes of thermal events. Here formation of a supercontinent is recorded in regional NE-SW trending orthogneisses and granitoids of MC having enclaves of migmatitic paragneisses and metasedimentary rocks. The metasedimentary rocks having garnet-staurolite-tourmaline porphyroblasts in matrix of biotite, sillimanite (\pm kyanite), indicate amphibolite facies metamorphic condition ($P= 5.5\text{-}6.4\text{ kb}$ and $T 550\text{-}600^\circ\text{C}$) whereas the paragneisses with stromae of garnetiferous leucosomes are of relatively higher grade. The host orthogneisses along with the enclaves of migmatites and metasediments bear evidences of multiple phases of deformation which are considered to be related to sequential episodes of NW'ly -directed thrusting in a NE-SW trending compressional orogeny. The syntectonic granitic intrusion at 1.72 Ga constraint the upper age limit of the

deformation phase (Sengupta & Basak, 2014)1.

Monazites in paragneisses and metasediments occur either as included phase in garnet/staurolite porphyroblasts or as matrix phase. EMP data reflects multiple episodes of monazite growth related to metamorphic events.

Electron microprobe (EMP) dating on monazite of metasediments (garnetiferous mica schist, tourmaline-kyanite schist and staurolite schist) (Fig.1) has yielded dominant ages of ~ 1345 (1342 ± 30 Ma) and ~ 1000 Ma (942 ± 17 Ma) on matrix monazites. Monazites of paragneisses of MC have experienced at least three stages of metamorphic evolution at 1.8 , 1.35 and 1.0 Ga (Fig.2). Older ages around $1900\text{-}1800$ Ma (1808 ± 13 Ma) are only detected in monazite cores and in monazite inclusions in garnet porphyroblasts of migmatitic paragneisses. The recrystallised part and outer rim of the older matrix monazites of migmatitic rocks have also yielded Meso- (1288 ± 22 Ma) to

Neo-Proterozoic ($921\pm 40\text{Ma}$) ages. It becomes evident that the high – grade metasediments of Mangalwar Complex have suffered a major phase of tectonothermal Orogeny high grade metamorphism at 1.9-1.8Ga succeeded by emplacement intrusion of a number of granitoids at 1.75-1.71Ga.

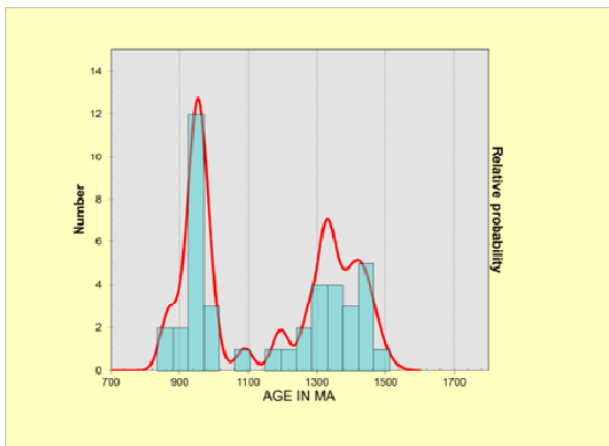


Fig.1. Two age populations from monazites of metasedimentary rock of MC; plotted in probability density plots showing statistically significant age peaks at $942\pm 17\text{Ma}$ ($n=53$) and $1342\pm 30\text{Ma}$ ($n=67$).

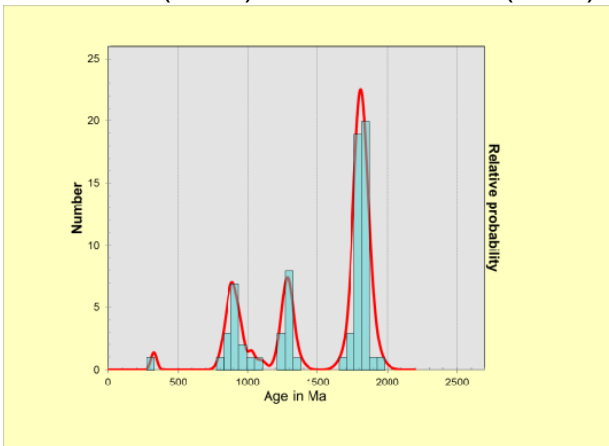


Fig.2 Density probability plots of EPMA dates of monazites of paragneisses of MC showing significant age peaks at $1808\pm 13\text{Ma}$ ($n=44$), $1288\pm 22\text{Ma}$ ($n=15$) and $921\pm 40\text{Ma}$ ($n=25$).

On the other hand, the metasediments of MC have recorded only

$\sim 1.35\text{Ga}$ and $\sim 1.0\text{Ga}$ events. These dates are also recorded from Hindoli-Jahazpur Group (HJG) (Sengupta & Basak, 2016)² occurring at eastern part and from southern part of study area near Pur-Banera (Ozha et al., 2016)³. At the eastern part, the 1.4 Ga age is marked as a major thrusting event followed by Grenvillian reactivation of a crustal scale shear zone occurring between HJG and MC whereas at the southern part these ages were correlated to rift-induced collisional orogeny pertaining to breaking up of Columbia and assembly of Rodinia supercontinent. Hence, orogenic events recorded in Mangalwar Complex of western Indian Craton can be correlated with the amalgamation (1.9-1.8Ga) and break-up (1.4Ga) of a major supercontinent Columbia (Zhao et al. 2004, Bhowmick and Dasgupta, 2012⁵) with emplacement of voluminous granitic melt at 1.72Ga.

References

- Bhowmick, S.K. & Dasgupta, S. (2012). Tectonothermal evolution of the Banded Gneissic Complex in central Rajasthan, NW India: Present status and correlation. *Jour. Asian Earth Sciences* 49; 339-348.
- Ozha, M.K., Mishra, B., Hazarika, P., Jeyagopal, A.V., Yadav, G.S. (2016). EPMA monazite geochronology of the basement and supracrustal rocks within the Pur-Banera basin, Rajasthan: Evidence of Columbia breakup in Northwestern India. *Jour. Asian Earth Sciences* 117, 284-303.
- Sengupta, S & Basak, K, (2015). Palaeoproterozoic tectonothermal event in the northern part of Mangalwar Complex: A Rb-Sr whole-rock study. (abstract) National Seminar on Recent Advances in Research on Precambrian

Terrains in India, organized by University of Mysore.

Sengupta, S & Basak, K. (2016). Mesoproterozoic orogeny along Eastern Boundary of Aravalli Craton, Northwestern India: a tectonostratigraphic and geochronologic study (abstract); accepted in 35th IGC 2016.

Zhao, G.C., Sun, M., Wilde, S.A., Li, S., 2004. A Palaeo-Mesoproterozoic supercontinent: assembly, growth and break-up, Earth Science Reviews 67, 91-123.

Sedimentation in the Baikal Rift Zone: implications for Cenozoic intracontinental processes in the Central Asian Orogenic Belt

Krивonogov S.K.^{1, 2}

¹ Sobolev Institute of Geology and Mineralogy SB RAS, Koptyuga ave. 3, Novosibirsk 630090, Russia

² Novosibirsk State University, Pirogova St. 2, Novosibirsk 630090, Russia

We present a review of sedimentological, geomorphological, lithological, geochronological, geophysical and geological data from major, minor and satellite basins of the Baikal Rift Zone (BRZ) and discuss various aspects of its evolution. Previously, the most detailed sedimentological data have been obtained from the basins of the central BRZ, e.g., Baikal, Tunka and Barguzin, and have been used by many scientists worldwide. We add new information about the peripheral part and make an attempt to provide a more comprehensive view on BRZ sedimentation stages and environments and their relations to local and regional tectonic events. A huge body of sedimentological data was obtained many years ago by Soviet geologists and therefore is hardly accessible for an international reader. We pay tribute to their efforts to the extent as the format of a journal paper permits. We discuss structural and facial features of BRZ

sedimentary sequences for the better understanding of their sedimentation environments. In addition, we review tectono-sedimentation stages, neotectonic features and volcanism of the region. Finally, we consider the key questions of the BRZ evolution from the sedimentological point of view, in particular, correlation of Mesozoic and Cenozoic basins, bilateral growth of the Baikal rift, Miocene sedimentation environment and events at the Miocene/Pliocene boundary, Pliocene and Pleistocene tectonic deformations and sedimentation rates. The data from deep boreholes and surface occurrences of pre-Quaternary sediments, the distribution of the Pleistocene sediments, and the data from the Baikal and Hovsgol lakes sediments showed that 1) BRZ basins do not fit the Mesozoic extensional structures and therefore hardly inherited them; 2) the Miocene stage of sedimentation was characterized by low topography and weak tectonic processes;

3) the rifting mode shifted from slow to fast at ca. 6-5 Ma; 4) the late Pleistocene high

sedimentation rates reflect the fast subsidence of basin bottoms.

***Glossopteris* flora from the Godavari valley coalfield, Telangana, India: basinal correlation and implications in palaeoecology**

Rajni Tewari

Birbal Sahni Institute of Palaeosciences, 53 University Road, Lucknow 226007, India

The NNW-SSE trending Pranhita-Godavari Basin is the only coal producing area in South India with as much as 10528.40 million tons of coal reserves exploited by the Singareni Collieries Company Limited (SCCL). The north-west extension of the Pranhita-Godavari Basin across the Maharashtra State is known as the Wardha Valley Coalfield. The Basin covers an area of about 17000 sq. km and is bounded by the latitudes 16°38' and 19° 32' and the longitudes 79° 12' and 81° 39'. It rests on the Precambrian platform following the course of Pranhita and Godavari rivers over a strike length of 470 km. The south eastern sector of over 350 km length and 55 km width including a 6 km wide constriction in the Paluncha-Kothagudem area, is referred to as the Godavari Valley Coalfield. This coalfield encompasses the districts of Adilabad, Karimnagar, Warangal and Khammam of Telangana State. On the basis of the tectonic setting and the lithic fill, the Pranhita-Godavari Basin is subdivided into Godavari, Kothagudem, Chintalapudi and Krishna-Godavari coastal sub-basins (Fig.1A). An almost complete succession of

the Lower and the Upper Gondwana deposits is exposed in the Pranhita-Godavari Basin. The Lower Gondwana sediments consisting of Talchir, Barakar and Kamthi (lower part) formations are exposed both along the eastern and western margins while the Upper Gondwana sediments comprising the Kamthi (upper part), Maleri and Kota formations, and Chikiala Sandstone cover the central/axial portion (Raja Rao, 1982). The coal seams are discontinuous at places due to faulting. Therefore, the different coal bearing areas are treated as different coal belts. The coal seams of economic value are mainly confined to the Godavari and Kothagudem sub-basins and the Yellandu outlier.

Although, the studies on the *Glossopteris* flora of India have been carried out in detail from different Lower Gondwana basins like Damodar, Wardha, Satpura, Mahanadi, South Rewa and Rajmahal (Lakhanpal et al., 1976; Chandra and Tewari, 1991; Bajpai and Singh, 1994; Tewari, 2007, 2008; Srivastava and Agnihotri, 2010; Singh et al., 2011, 2012; Goswami and Singh 2013; Tewari et al.,

2013), records of megafossils from the Pranhita-Godavari Basin are sporadic and include equisetalean axes, *Phyllothea*, *Gangamopteris* sp., *Glossopteris communis*, *G. indica*, *G. subtilis*, *G. sastrii*, *G. stenoneura*, *G. tenuinervis*, *Glossopteris* sp., *Vertebraria indica*, *Vertebraria* sp., *Noeggerathiopsis hislopii* and *Araucarioxylon* (Feistmantel, 1880, 1881; King, 1881; Jacob, 1950; Lakshminarayana and Murty 1990; Tewari and Jha 2006; Jha and Tewari 2007; Joshi et al., 2015). For a better understanding of the *Glossopteris* flora and the palaeoclimate that was responsible for the formation of coal in the Pranhita-Godavari Basin, it was imperative to study in a comprehensive manner, the floral elements that constituted this vegetation and their correlation with the palaeofloral composition of the other Indian Lower Gondwana basins.

To minimize the knowledge gap between the scantily studied *Glossopteris* flora of the Pranhita-Godavari Basin and those of the other Indian Lower Gondwana basins, and, to carry out the basinal correlation based on the flora, a detailed survey to different coal belts such as Golet-Belampalli, Somagudem-Mandamari-Ramkrishnapuram-Srirampur-Indaram, Adilabad District; Ramagundam-Godavari, Karimnagar District and Chilpur-Venkatapur-Lingala, Kothagudem, Cherla-Manuguru, and Godavaridevipeta-Madharam-Amravaram, Khammam District, was undertaken for the collection of the plant fossils. The plant mega remains, however, could only be collected from the early Permian Barakar Formation of the Prakasham Khani open cast mines II and IV, Manuguru Area of Cherla-Manuguru Belt and the Goutham Khani Open Cast Mine, Kothagudem Area

(Fig.1A) of Kothagudem Belt. Cherla-Manuguru coal belt is located in the south eastern part of the Godavari Valley Coalfield. The river Godavari divides the area into Cherla sector in the north and Manuguru sector in the south. The coal belt is located on the west of river Godavari and extends over a strike length of about 13 km from its bank on the north-east to Bugga in the south west. The Kothagudem belt stretches for about 18 km from Kothagudem in the north and up to Pengadapa in the south. Other than the previously known taxa, *Glossopteris communis*, *G. indica* and *Noeggerathiopsis hislopii* from the bore core 726 of the Manuguru Area, the new records from the Prakasham Khani open cast mines II and IV include *Phyllothea indica*, *Glossopteris arberi*, *G. cordatifolia*, *G. damudica*, *G. gigas* (Fig. 1B), *G. karanpuraensis*, *G. longicaulis*, *G. mohudaensis*, *G. musaefolia*, *G. pseudocommunis*, *G. rhabdotaenioides*, *G. taenioides*, *G. tenuifolia* and *Cordaites* sp. In the Goutham Khani Open Cast Mine, only *Vertebraria indica*- the root of *Glossopteris*, were preserved. Though, the *Glossopteris* leaves were curiously absent in this coal mine, a variety of dispersed megaspores- the female reproductive units of the early land plants could be recovered after the maceration of the rock samples.

Earlier records of abundant megaspores- from the Barakar and Raniganj formations of different areas of the Godavari Valley Coalfield such as, Ramagundem, Chelpur, Rampuram, Mailaram, Gundala, Kachinapalli and Goutham Khani (Tewari and Jha, 2007; Tewari et al., 2007; Joshi and Tewari, 2015- Fig.1A, C-E) include the genera *Ancorisporites*, *Bokarosporites*, *Banksisporites*, *Biharisporites*,

Gundalasporea, *Jhariatriteles*, *Kamthisporea*, *Singhisporites* (1C-E), *Ramispinatispora* and *Talchirella*. The different kinds of ornamentations like grana, verrucae, bacula, coni and spines with simple, bifurcate and multifurcate apices present on the exosporia (the outer wall) of the megaspores reveal the diversity of the source vegetation—the lycopsids (with which the affinity of the dispersed Gondwana megaspores is well established), the megafossils of which are not recorded from this Coalfield, so far. The lycopsids are an important group of early land plants usually growing in aquatic, fresh water conditions. The presence of different ornamentations on the megaspore exosporia during the early and late Permian indicates that these were acquired as an adaptation to the changing environment. Hence, megaspores are not only of evolutionary significance but also bear palaeoecological implications. Besides, temporal and spatial distribution of the megaspores is useful in biostratigraphy and basinal correlation.

An analysis of the new and the existing data from the Godavari Valley Coalfield of the Pranhita-Godavari Basin reveals the presence of the pteridophytes and the gymnosperms during the Permian. The pteridophytes are represented by Lycopodiales and Equisetales, and the gymnosperms by Glossopteridales, Cordaitales and Pinales. The floral assemblage compares fairly well with those of the other Lower Gondwana basins of India. This study adds to the knowledge of the *Glossopteris* flora of India, especially that of the Godavari Valley Coalfield from where the plant fossil records are poor or without detailed systematic analysis. Besides, the richness of the flora reflects warm, temperate and humid climatic

conditions necessary for the formation of thick coal seams during the Barakar Formation.

References

- Bajpai, U. and Singh, K.J., 1994. Indian Gondwana Annotated Synopsis III. Permian Megaplants—2, Birbal Sahni Institute of Palaeobotany, Lucknow, 82 pp.
- Chandra, S. and Tewari, R., 1991. A Catalogue of Fossil Plants from India—B. Palaeozoic and Mesozoic Megafossils. Part 2, Birbal Sahni Institute of Palaeobotany, Lucknow, 81 pp.
- Feistmantel, O., 1880. The fossil flora of Gondwana System (Lower Gondwana) II. The flora of Damuda–Panchet Divisions. Memoirs of Geological Survey of India. Palaeontologia indica 12, 1–77.
- Feistmantel, O., 1881. The fossil flora of Gondwana System II. The flora of the Damuda and Panchet Divisions. Memoirs of Geological Survey of India Palaeontologia indica 12, 78–149.
- Jacob, K., 1950. *Dadoxylon* from the Kothagudem Coalfield of Hyderabad. Palaeobot. India 7, Journal of Indian Botanical Society 29, 28.
- Jha, N. and Tewari, R., 2007. Occurrence of Late Permian palynomorphs and equisetalean axes in Sattupulli Area, Chintalapudi sub-basin, Andhra Pradesh, in: Chaudhury US, Tidke JA, Manik SR & Nathar VN (Editors)—Proceedings of the International Conference on Modern Trends in Plant Science with Special Reference to the Role of Biodiversity in Conservation 2005. Sant Gadge Baba Amravati

- University, Amravati, 208–213.
- Jha, N., Sabina, P.K., Aggarwal N. and Mahesh, S., 2014. Late Permian Palynology and depositional environment of Chintalapudi sub basin, Pranhita–Godavari basin, Andhra Pradesh, India. *Journal of Asian Earth Sciences* 79, 382–399.
- Joshi, A. and Tewari, R., 2015. Early Permian megaspores from Gouthamkhani Open Cast Mine, Kothagudem area, Godavari Graben, Telangana. *The Palaeobotanist* 64(2), 139–150.
- Joshi, A., Tewari, R., Agnihotri, D., Pillai, S.S.K. and Jain R.K., 2015. Occurrence of *Vertebraria indica* (Unger) Feistmantel, 1877 – an evidence for coal-forming vegetation in Kothagudem area, Godavari Graben, Telangana. *Current Science* 108 (3), 330–333.
- King, W., 1881. The geology of Pranhita–Godavari Valley. *Memoirs of Geological Society of India* 18, 150–311.
- Lakhanpal, R.N., Maheshwari, H.K. and Awasthi, N., 1976. A Catalogue of Indian Fossil Plants. Birbal Sahni Institute of Palaeobotany, Lucknow, 1–318.
- Lakshminarayana, G. and Murty, K.S., 1990. Stratigraphy of the Gondwana formations in the Chintalapudi sub-basin, Godavari Valley, Andhra Pradesh. *Journal of Geological Society of India* 36, 13–25.
- Raja Rao, C.S., 1982. Coalfields of India-2. Coal resources of Tamil Nadu, Andhra Pradesh, Orissa and Maharashtra. *Bulletin of the Geological Survey of India Series A* 45, 9–40.
- Singh, K.J., Goswami, S and Srivastava, G., 2011. Palaeodiversity in the genus *Glossopteris* from the Lower Gondwana rocks of the Korba Coalfield, Chhattisgarh State, India. *Journal of the Palaeontological Society of India* 56, 39–59.
- Singh, K.J., Saxena, A. and Goswami, S., 2012. Palaeobiodiversity of the Lower Gondwana rocks in the Korba Coalfield, Chhattisgarh, India and observations on the genus *Gangamopteris* McCoy. *The Palaeobotanist* 61, 145–163.
- Goswami, S. and Singh, K.J., 2013. Floral biodiversity and geology of the Talcher Basin, Orissa, India during the Permian–Triassic interval. *Geological Journal* 48, 39–56.
- Srivastava, A.K. and Agnihotri, D., 2010. Upper Permian plant fossils assemblage of Bijori Formation: a case study of *Glossopteris* flora beyond the limit of Raniganj Formation. *Journal of the Geological Society of India* 76, 47–62.
- Tewari, R., 2007. The *Glossopteris* flora from the Kamptee Coalfield, Wardha Basin, Maharashtra, India. *Palaeontographica B* 277, 43–64.
- Tewari, R., 2008. The genus *Glossopteris* Brongniart from the Kamthi Formation of Camp IV area, Wardha Valley Coalfield, Wardha Basin, Maharashtra, India. *Journal of Palaeontological Society of India* 53, 19–30.
- Tewari, R. and Jha, N., 2006. Occurrence of plant mega and microfossils of Barakar and Raniganj formations of Manuguru area, Godavari Graben, Andhra Pradesh. *Journal of Geological Society of India* 67, 101–112.

Tewari, R. and Jha, N., 2007. Permian megaspores from Godavari Graben, India: Present Status. *The Palaeobotanist* 56, 133–138.

Tewari, R., Jha, N. and Saleem, M., 2007. Permian megaspores from Kachinapalli Area, Godavari Graben, India. *Phytomorphology* 57, 21–32.

Tewari, R., Pandita, S.K., Agnihotri, D., Pillai, S.S.K. and Bernardes-De-Oliveira, M.E.C., 2012. An early Permian *Glossopteris* flora from the Umrer Coalfield, Wardha Basin, Maharashtra, India. *Alcheringa* 36(3), 355–371.

Structure and tectonic evolution of the Archean Biligiri Rangan Block, Southern India

R.T. Ratheesh-Kumar

Xinjiang Institute of Ecology and Geography, Chinese Academy of Sciences, 818 South Beijing Road, Urumqi, Xinjiang, China-830011

The Southern Granulite Terrain (SGT) in India is a collage of crustal blocks ranging in age from Archean to Neoproterozoic. This study contributes towards the tectonic evolution of one of the least studied terrain in the northern part of the SGT comprising BiligiriRangan (BR) – Male Mahadeshwara (MM) Hills domain (Fig. 1a and b), which was previously considered as the lower crust of the DharwarCraton. A multidisciplinary approach has been implemented for this study that integrates field relations, petrography, mineral chemistry, thermodynamic modeling of metamorphic *P-T*-evolution, and LA-ICPMS U-Pb and Lu-Hf analyses of zircons on representative rocks from the BR Hill-MM Hill domain together with crustal thickness model derived using gravity inversion and flexure inversion geophysical techniques. The results suggest Meso- to Neoproterozoic tectonic evolution of this terrain as a discrete crustal block, and we named this terrain as BiligiriRangan Block (BRB) (Ratheesh-Kumar *et al.*, 2016).

The BRB is identified as one of the ancient high-grade granulite terrains of

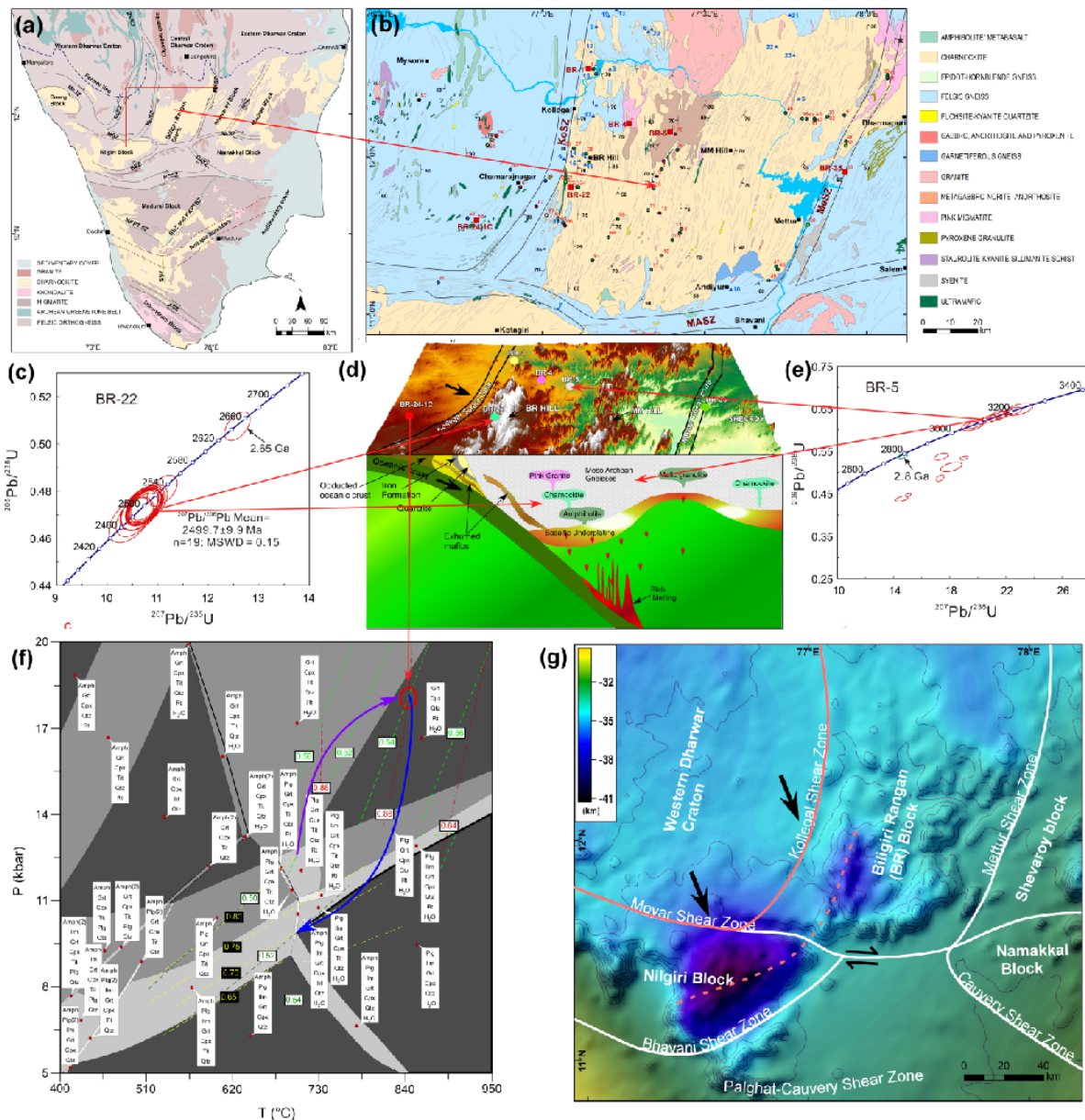
southern India, characterized by distinct lithology and geochemical and isotopic signature. The block is bounded by the EW-trending Moyar-Attur shear zone in the south, in the west by NNE-trending Kollegal shear zone against the Western DharwarCraton (comprising the mafic-ultramafic suites and metasediments of the Sargur Group), and in the east by the NE-trending Mettur shear zone against the Eastern Dharwar Province (comprising the Shevaroy Block). Systematic field investigations (Fig. 1b) have been carried out in and around the BRB that reveals Charnockite as the major rock-type that are in association with mafic granulite, granites and metapelites. The westernmost periphery of the BRB, adjacent to the Kollegal shear zone, is characterized by the occurrence of enclaves and lenses of ultramafics, gabbro and amphibolites oriented along the Kollegal shear zone. Metasedimentary rocks including quartzofeldspathic gneisses, quartzite and banded iron formation (BIF) are exposed in several localities in and around the Kollegal shear zone. Representative samples from the BRB selected for the present study

including the charnockite, pink granite and garnet bearing gneiss samples (exposed within the terrain), quartzite and metagabbro samples (from the Kollegal shear zone), and mafic granulite sample (from the Mettur shear zone).

Zircons in the quartzite from the Kollegal shear zone show a wide range of ages between 3315 ± 24 and 2972 ± 20 Ma. The data indicate different zircon populations with a wide range of $\epsilon\text{Hf}(t)$ values from negative to positive (-6.4 to 5.1). The distribution in age and Hf isotope values are suggestive of multiple sources of both juvenile and reworked components. Zircons in the garnet-bearing gneiss (sample BR-5) show upper concordant age at 3207 ± 22 Ma and lower concordance at 2806 Ma (Fig. 1e). The spread in ages may suggest a sedimentary protolith for this garnet-bearing gneiss. The age ranges obtained from this sample can be correlated with the similar age range yielded by the zircons in quartzite (sample BR-1). This may indicate that both the garnet-bearing gneiss and the quartzite represent contemporary sedimentary units, with detritus derived from the continental crust that existed during Mesoarchean. The age of TTG (3100-3360 Ma) reported from this region (Peucat et al., 2013) and the high positive ϵHf isotope values of the zircons from quartzite ($\epsilon\text{Hf}(t) \sim +5.1$) and garnet-bearing gneiss ($\epsilon\text{Hf}(t) \sim +2.7$) obtained in the present study are suggestive of a primitive juvenile continental crust with ages between 3100 and 3400 Ma. The age data from charnockite (Fig. 1c) reveal 2600 Ma as the age of charnockite formation and 2513 ± 5 Ma as the granulite-facies metamorphism in the BR Hill. The age estimates of other samples including pink granite that yields

an upper intercept age of 2490 ± 13 Ma, and the mafic granulite (BR-35) that shows a wide range of discordant ages between 2632 to 2498 Ma are also broadly consistent with the age range obtained from zircons in the charnockite, suggesting that the protoliths of these rock types are cogenetic (at. ca. 2600 Ma) and witnessed a common metamorphic event (at ca. 2500 Ma).

The occurrence of quartzite-iron formation intercalation as well as ultramafic lenses along the western boundary of the BRB is interpreted to indicate that the Kollegal structural lineament is a possible paleo-suture. Phase diagram computation (using mineral chemistry data and thermodynamic modeling) of a metagabbro from the western periphery of the Kollegal suture zone reveals a clockwise P-T path with a peak pressure ~ 18.5 kbar and temperature ~ 840 °C (Fig. 1f), clearly suggest high-pressure granulite facies metamorphism in a subduction setting, and subsequent exhumation. Based on these results, this study proposes a new tectonic model for the evolution of the BRB (Fig. 1d) that envisages eastward subduction of the Western Dharwar oceanic crust beneath the BRB along the Kollegal suture zone resulted in the arc magmatism during the Neoproterozoic. The anomalously high crustal thickness patterns (Fig. 1g) in Nilgiri and in BRB are interpreted as a more competently thickened crust resulted by the subduction of the western Dharwar crust beneath these block segments. This model better explains existing chaos in the plume model (Jayananda et al. (2000) and westward subduction of the Eastern Dharwar Craton beneath the Western Dharwar Craton as proposed by Chadwick et al. (2000) and Chardon et al. (2008).



Figs. 1(a) General tectonic framework map of southern India showing the study window (b) detailed geological map of the study area (BiligiriRangan Block) (c) Age of the charnockite indicating the age of arc magmatism (d) A schematic tectonic model depicting the subduction of the Western Dharwar Oceanic crust and associated slab melting and arc magmatism in the BRB (e) Age of the garnet bearing gneiss indicating MesoArchean primitive crust in the BRB (f) P - T phase diagram showing the high-pressure (18-19 kbar) and medium temperature (~840°C) metamorphic evolution of metagabbro in the Kollegal suture zone (g) Crustal thickness map showing the subduction polarity of the western Dharwar oceanic crust beneath the BRB and Nilgiri Block along the Kollegal-Moyar suture zone and the resulting high-crustal thickness patterns (Ratheesh-Kumar *et al.*, 2016).

References

- Chadwick, B., V. N. Vasudev, and G. V. Hedge (2000), The Dharwarcraton, southern India, interpreted as the result of Late Archaean oblique convergence, *Precambrian Res.*, 99, 91– 101.
- Chardon, D., Jayananda, M., Chetty, T.R.K., Peucat, J.J., 2008. Precambrian continental strain and shear zone patterns: South Indian case. *Journal of Geophysical Research* 113, <http://dx.doi.org/10.1029/2007JB005299>.
- Jayananda, M., Moyen, J.-F., Martin, H., Peucat, J.-J., Auvray, B., Mahabaleswar, B., 2000. Late Archaean (2550–2520 Ma) juvenile magmatism in the eastern Dharwarcraton, southern India: constraints from geochronology, Nd–Sr isotopes and whole rock geochemistry. *Precambrian Research* 99, 225–254.
- Peucat, J.J., Jayananda, M., Chardon, D., Capdevila, R., Fanning, C.M., Paquette, J.L., 2013. The lower crust of the DharwarCraton, Southern India: Patchwork of Archean granulitic domains. *Precambrian Research* 227, 4–28.
- Ratheesh-Kumar, R.T., Santosh, M., Yang, Q-Y., Ishwar-Kumar, C., Chen, N-S., Sajeew, K. Archean tectonics and crustal evolution of the BiligiriRangan Block, southern India, *Precambrian Research*, In Press, <http://dx.doi.org/10.1016/j.precamres.2016.01.022>

Petrogenesis and fluid characteristics of sapphirine granulites of the Highland Complex, Sri Lanka

P. L. Dharmapriya^{a, b}, Sanjeewa P. K. Malaviarachchi^{a, b}, Andrea Galli^c, Leo Kriesman^d, S. Bhattacharya^e, Y. Osanai^f, K. Sajeev^e, T. Tsunogae^h

^aPostgraduate Institute of Science, University of Peradeniya, 20400, Sri Lanka

^bDepartment of Geology, Faculty of Science, University of Peradeniya, 20400, Sri Lanka

^cDepartment of Earth Sciences, ETH Zurich, Sonneggstrasse 5, CH-8092 Zurich, Switzerland

^dDepartment of Geology, Naturalis Biodiversity Center, Leiden, Netherlands

^eCentre for Earth Sciences, Indian Institute of Science, Bangalore 560012, India

^fDivision of Earth Sciences, Department of Environmental Changes, Faculty of Social and Cultural Studies, Kyushu University, 744 Motooka, Fukuoka, 819-0395 Japan

^hFaculty of Life and Environmental Sciences, University of Tsukuba, Ibaraki 305-8572, Japan

Sapphirine granulites are important to understand high-grade metamorphism in the hot-deep crust. Here we report petrogenesis and fluid characteristics of sapphirine granulites from Gampola and Kotmale in the Highland Complex, Sri Lanka. The studied rocks from Gampola are sapphirine bearing garnet-sillimanite-orthopyroxene gneisses and those from Kotmale includes sapphirine bearing garnet-sillimanite gneisses and garnet-orthopyroxene gneisses. Multiple thin sections from each sample and wafers for fluid inclusion studies were prepared at the National Institute of Fundamental studies, Kandy. Detailed petrographic studies were performed at the Department of Geology, University of Peradeniya. Mineral chemical analyses were carried out at the Kyushu

University, Japan and Whole rock geochemical analyses and pseudosection calculations were done at the Department of Earth Sciences, ETH Zurich. Fluid inclusion studies were performed at the Indian Institute of Science, Bangalore, India.

Sapphirine is present in multiple textural settings such as: isolated inclusions in garnet; coexisting with kyanite/sillimanite or spinel inside garnet porphyroblasts; associated with plagioclase bearing leucosomes in the matrix; intergrowth with plagioclase in plagioclase+orthopyroxene corona after garnet; and coexistence with magnetite in orthopyroxene+cordierite symplectite after garnet. The presence of Al-rich orthopyroxene (Al_2O_3 up to 9 wt %) and

coexistence of orthopyroxene + sillimanite + quartz assemblage are considered as diagnostic evidence for UHT metamorphism of the studied samples. Above textural observations coupled with conventional thermobarometric calculations and pseudosection modeling indicate that the rocks have reached up to temperature (T) of 800 - 850 °C at pressure (P) of 11 – 12 kbar during prograde metamorphism followed by a prograde decompression event up to the peak UHT metamorphism. The calculated peak metamorphic conditions are T of 920 – 950 °C at P of 10 – 10.5 kbar under relatively high oxidizing conditions. Subsequently, the rock has followed a near isobaric cooling path up to T of 890 – 860 °C, prior to near isothermal decompression up to 6 kbar.

Three types of fluid inclusions [carbonic (type-I), aqueous carbonic (type-II) and aqueous biphasic (type-III)] were

identified mainly from leucosomes of the studied sapphirine granulites. Type-I inclusions are of primary or pseudosecondary nature and lie in the density range of 0.54 to 0.85 g/cc. Due to their low densities, the corresponding isochores pass well below the peak metamorphic P - T conditions occupying a broad region of the P - T space, probably due to density reversals in response to their volume changes. The post-metamorphic isothermal decompressional processes may have caused the internal pressure in inclusions to be greater than the confining pressure. The Type II and Type III fluid inclusions were observed to be of secondary origin.

Acknowledgement

The financial support by the Ministry of Technology and Research, Sri Lanka (Grant: MTR/TRD/AGR/3/1/04) is gratefully acknowledged.

Geochemistry and petrographic studies of Ordovician sedimentary rocks (Sanguba Group) from Spiti valley, Tethys Himalaya, Northern India: implications for paleoweathering, paleoclimate and tectonic setting

Shaik A Rashid and Javid A Ganai

Department of Geology, AMU, Aligarh-202002, India

A marine sedimentary (sandstone-shale) succession of Ordovician age (Thango Formation), exposed at Spiti region, Himachal Pradesh, Tethys Himalaya has been examined thoroughly to understand the processes that control sediment geochemistry with a specific focus on weathering processes, provenance, paleo-climatic conditions. Microscopic examination of the thin sections revealed that the sandstones are generally fine grained, sometimes medium to coarse grained, poor to moderately sorted with fair amount of matrix. Quartz, microcline, plagioclase and lithic fragments form the main framework mineralogy. Mono-crystalline quartz dominates over polycrystalline quartz showing straight to strong undulose extinction. Chert is the most prominent lithic fragments. Sandstones have higher SiO₂ contents (66 to 90 wt.%) than shales which ranges from 58 to 71wt.%. Shales contain higher in

Al₂O₃, (13-18wt.%), K₂O (12-18wt.%) and Fe₂O₃ (3 - 6wt.%) concentrations. Majority of the sediments display similar patterns typical of post-Archaean sediments (such as UCC and PAAS) with LREE enrichment (La_N/Yb_N= 6.03 to 73.79) and fairly flat HREE patterns (average Gd_N/Yb_N ratios of 0.9) with marked negative Eu anomalies (Eu/Eu* = 0.31–0.51). The sandstone and shales of Sanguba group has CIA (chemical index of alteration) values ranging from 55 to 72 which reflect composition of muscovite and illite, indicating low to moderate degree of chemical weathering in the source region. Average La/Th and Th/Yb values determined for these rocks are 2.5 and 15.7, respectively, which corresponds to a relatively felsic composition. The Cr/Th ratios of the Sanguba Group sedimentary rocks ranging from 0.7 to 9.1 (average = 3.3) thus strongly suggest to have been derived from mainly silicic source rocks.

High silica contents (>69%) and K_2O/Na_2O ratios (>1) of these sediments are consistent with passive margin tectonic setting defined by Roser and Korsch (1986). In the provenance discrimination diagram of Roser and Korsch (1988), all the shales and sandstones of the present study plot in the fields of quartzose sedimentary and felsic igneous provenance, thus substantiating the above inference. The striking similarities between

the trace element (including REEs) patterns of the Thango Formation shales of Spiti region and different Proterozoic granites of the Himalayan region strongly support the hypothesis that the upliftment and erosion of these S-type syn-collisional granites from the Proterozoic granitoid belts may have supplied significant amounts of detritus to the Tethyan sedimentary basin.

New occurrence of unusual carbonatitic lamproites from Sidhi gneissic Complex, Central India

Satyanarayanan M^{1*}, Subba Rao, D.V¹, Renjith, M.L³, Singh, S.P²

¹CSIR-National Geophysical Research Institute, Hyderabad 500007, India

²Department of Geology, Bundelkhand University, Jhansi 284128, India

*Corresponding author e-mail: msnarayanan@ngri.res.in

The Precambrian Central Indian Shield (CIS) comprises of two cratonic blocks which are represented by Bundelkhand craton and Bastar craton. The ENE-WSW trending Satpura belt record a period of geodynamics, continental/cratonic stability and signatures of amalgamation of the these cratonic nuclei during the early Proterozoic. The Central Indian Tectonic Zone (CITZ) is a consequence of such tectonic structure ~500 km in length and about 100 km in width which incorporates the different metamorphic belts and magmatic domains developed in time and space. The Son-Narmada North Fault (SNNF) and CIS are the two large crustal scale structures that occur in northern and southern part of CITZ. The Sidhi granite-gneissic belt / Sidhi gneissic complex (SGC) occurs in the northern part of CITZ and is about 80 km in length and represents early Precambrian tectonic relics. The SGC predominantly contains medium to high grade regional metamorphic of pelitic, quartzofeldspathic, basic and ultrabasics including the BIF (Table 1). The metamorphite shows atleast

two phases of deformation and are invaded by several phases of granitoids/ granite, pegmatites, quartzofeldspathic veins, dolerites, gabbro, syenite and lamprophyre dyke magmatism. The polyphase metamorphosed and multiphase deformed gneissic rocks of SGC show a regional foliation trend of ENE-WSW with moderate to steep dips towards north. The alkaline rocks associated with mafic, ultramafic, alkali gabbro and occasionally lamprophyres and carbonatites either occur as small isolated dykes within SGC or at the contact of SNNF (Roy and Bandyopadhyay, 1988). These alkaline and lamprophyres are not affected by E-W and NE-SW trending shears of SCG and is not extending into Vindhyan supergroup. Thus the alkaline suit and lamprophyre occurrences are limited in time and space and are confined between SNNF and Kargil fault in the north.

Petrography, mineral chemistry and whole-rock geochemistry of two newly found lamproite dykes (Dyke-1 located at E 81°48'39"; N 24°24'33"; Dyke-2 located at E 81°50'1"; N24°28'57") from Sidhi

Gneissic Complex (SGC), central India, are presented here and discussed their various petrogenetic intricacies. Both dykes have almost similar sequence of mineral-textural patterns resulted from crystallization accompanied at various stages of magma plumbing such as: i) an early cumulate forming event at a deeper magma chamber giving rise to megacrystic and/or large phlogopites with subordinate amount of olivine and cpx; ii) ground mass crystallization at shallow crustal levels resulting in crystallization of fine-grained matrix of phlogopite, K-feldspar, Fe-Ti oxides and calcite; iii) Dyke emplacement related quench texture (plumose K-feldspar, acicular phlogopites) and finally iv) autometasomatism by hydrothermal alteration of mafic phases and injection of hydrothermal fluids. Phlogopite phenocrysts often display resorption morphologies and the prominent growth zones reveal disruption of equilibrium at the crystal-melt interface at a certain period of crystallization by incremental addition of similar magma or chaotic dynamic mixing, which probably occurred at deeper magma chamber. Carbonate aggregates in late

stage melt segregation is common feature in both dykes, however, their micro-xenolith forms reveals assimilation with plutonic carbonatite body and enhanced the carbonatitic nature of these dykes. Geochemically both dykes are ultrapotassic (K_2O/Na_2O : 3.0-9.4) together with low CaO , Al_2O_3 , Na_2O , and high K_2O/Al_2O_3 (0.51-0.89) are thus classified as lamproite. In contrast to these similarities, evidences prove that both dykes have evolved independently from two distinct magmas. In Dyke 1, phlogopite composition evolved towards minette trend (Al-enrichment) from a differentiated parental magma with low MgO , Ni and Cr contents, whereas in Dyke 2, the phlogopite composition evolved towards lamproite trend (Al-depleting) from a more primitive magma having high MgO , Ni and Cr contents (Figure 1). Whole-rock trace-elements signatures like enriched LREE, LILE, negative Nb-Ta and positive Pb anomalies; high Rb/Sr, Th/La and Ba/Nb, and low Ba/Rb, Sm/La and Nb/U ratios indicate that both lamproite dyke magmas have sourced from a subduction modified garnet facies mantle containing phlogopite.

Table 1. Lithostratigraphic succession of SGC (Modified after Roy and Bandyopadhyay, 1988)

Rock type	Event
Alkaline, lamprophyres, ultrapotassic granite, syenite, gabbro and peridotite, alkali gabbro intrusion into metamorphics, migmatite-gneisses and granite	N-S, E-W and NNE-SSW trending alkaline and lamprophyre activity.
Mafic intrusion (gabbro and dolerite) trending in E-W and NE-SW directions. Development of NE-SW trending quartz reefs and shear system	Mafic magmatic event
Pink granite, leucogranite, graphic granite, Hbl granodiorite, pegmatite intrusions	Granite magmatic event

Development of amphibolite facies metamorphism of pelitic, mafic and BIF (bitite gniess, amphibolite, para gneisses, migmatites, qurtzo- felspathic gneiss and schist, anthophyllite schist, magnetite-grunerite schist)	Deformation and metamorphism
Upper part dominated by meta andesites, diabase quartzo feldspathic and pelite rocks. Lower part dominated by mafic and ultramafic along with BIF and quartzite sediments	Volcanism and supracrustal deposition in shallow basin
----- Basement not exposed -----	

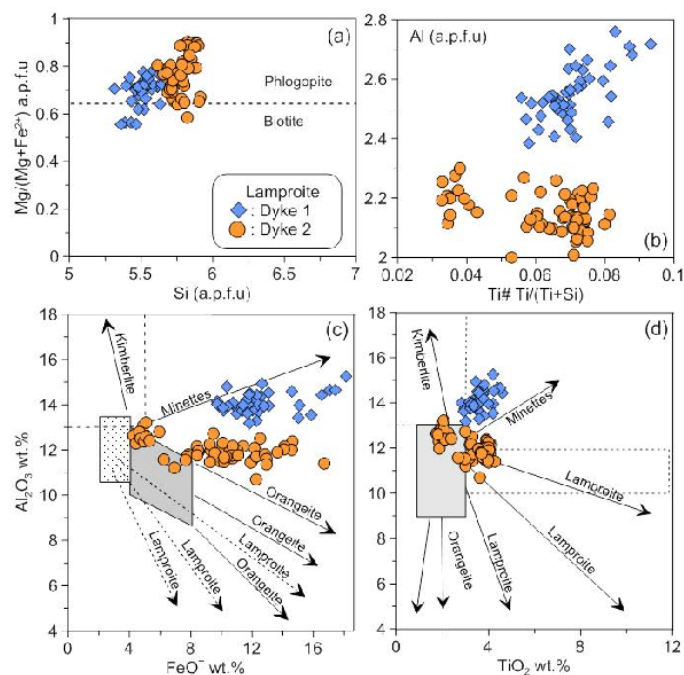


Figure 1. Compositional variation of micas from lamproite dykes, Sidhi area, Central India. (a) Si vs. Mg/(Mg+Fe²⁺) (a.p.f.u.) mica classification diagram; (b) Al vs. Ti/(Ti+Si) (a.p.f.u.) variation diagram; Al₂O₃ vs. FeO (c) and TiO₂ (d) mica discrimination diagram after Mitchell and Bergman (1991).

References

- Mitchell, R.H., Bergman, S.C., 1991. Petrology of Lamproites. New York, Plenum, 447 pp.
- Roy, A., Bandyopadhyay, B.K., 1988. Tectonic significance of ultramafic and associated rocks near Tal in the

Bijawar belt, Sidhi district, Madhya Pradesh. Journal of Geological Society of India 32, 397-410.

Advent, acme and decline of the *Glossopteris* flora: A case study from the Talchir Basin, Son-Mahandi Master Basin, India

Kamal Jeet Singh^a, Anju Saxena^{a*}, Shreerup Goswami^b

^a Birbal Sahni Institute of Palaeosciences, 53 University Road, Lucknow-226007, India

^b Sambalpur University, Jyoti Vihar, Sambalpur, Odisha- 768019, India

*Corresponding author e-mail: anju_saxena2002@yahoo.co.in; anju_saxena@bsip.res.in

The paper provides an appraisal of *Glossopteris* flora and its distribution throughout the Permian in different Lower Gondwana formations of Talchir Basin, eastern part of Son-Mahanadi master basin. The advent, acme and decline of the *Glossopteris* flora has been envisaged and summarized to depict how the constituent elements of this flora had appeared in this basin in the earliest Permian, Talchir Formation (Asselian-Sakmarian) and evolved and diversified through the Karharbari Formation (Artinskian), Barakar Formation (Artinskian-Kungurian), Barren Measures Formation (Guadalupian) and the Late Permian lower Kamthi Formation (Lopingian) and ultimately vanished in the early Triassic of upper Kamthi Formation (Anisian-Rhaetian). Permian deposits (particularly the Barakar and the lower Kamthi formations) not only have the best preserved flora, but also possess the highest diversity, whereas the upper Kamthi Triassic sediments have a meagre number of taxa. The flora from the

Handapa and Madhupur strata is one of the richest from the Late Permian beds of India. The plant diversity of the basin has been assessed in detail to interpret the development of the flora, evolutionary trends and palaeoenvironment of the basin. The patchy vegetation mosaic (comprising mainly of the genera *Gangamopteris* and *Noeggerathiopsis*) of the Talchir glacial phase has ultimately evolved and diversified through time (Karharbari Formation to Lower Kamthi Formation) and gave rise to the thick dense swampy forests consisting of large *Glossopteris* trees and other shade loving under-storied pteridophytes.

The floral diversity of the Talchir Basin mainly comprises of Pteridophytes, Pteridosperms and Gymnosperms. Among these, the order Glossopteridales (Gymnosperms) is the most dominant (with 88 taxa, including leaf forms, rooting structures, fructifications and seeds) followed by Equisetales (9), Filicales (9), Coristospermales (5), Cordaitales (3),

Cycadales (2), Coniferales (2), Peltaspermales (2) and Lycopodiales (1). Among the Glossopteridales, the genus *Gangamopteris* is represented by 4 taxa whereas the genus *Glossopteris* is represented by 51 species. Amongst fifty one species of the genus *Glossopteris* recorded in all, one species each has been found in the Talchir and upper Kamthi formations and two, sixteen and forty seven species respectively are represented in Karharbari, Barakar and the lower Kamthi formations. Barren Measures Formation is devoid of any megaplant fossil. Similarly, out of twenty seven taxa of fertile organs belonging to the *Glossopteris*, two each are found in the Talchir and Barakar formations respectively, whereas twenty four are recorded from the lower Kamthi Formation. It is observed that *Glossopteris* is less diversified in the Karharbari Formation. However, it diversified and proliferated in the Barakar and lower Kamthi (Late Permian) formations. Further, it shows declination in the Early Triassic (upper Kamthi Formation). The study shows that the lower Kamthi Formation of Talchir

Basin has the maximum diversity of *Glossopteris* (forty seven species) among all the known localities of this formation exposed in Indian Gondwana.

The existence of meagre *Glossopteris* species against many *Gangamopteris* species in the Talchir needle shale confirms its association with the lower floral zone of Talchir Formation instead of the upper floral zone established by previous workers in this basin. Very low diversity of *Glossopteris* in the upper Kamthi Formation of Talchir Basin demonstrates that this palaeogeographic area would have experienced more arid conditions in early-middle Triassic period as compared to the mellowing climatic conditions prevailing during the same time period in the Panchet Formation (=Upper Kamthi Formation) of other areas of Son-Mahanadi Basin and the Damodar Basin. Several groups of plants including spores and pollen have disappeared in a ladder pattern during the Permian-Triassic interval (Lower Kamthi-Upper Kamthi Formation) and, similarly, in steps, many new fore-runners appeared in the Upper Kamthi Formation.

The Mahanadi Shear Zone of the Eastern Ghats Province – strike-slip or extensional

Subham Bose and Saibal Gupta

Department of Geology & Geophysics, I.I.T. Kharagpur, India 721 302.

The Eastern Ghats Belt of India is traversed by a network of ductile shear zones, of which some are boundary shear zones while others are intra-province mega-lineaments. For obvious reasons, boundary shear zones have always been the focus of major structural work. However, the possibility of significant tectonic movements along the intra-province mega-lineaments cannot be ignored. The present study deals with the Mahanadi Shear Zone, an intra-province mega-lineament in the Eastern Ghats Province, the northern part of the Eastern Ghats Belt. Satellite imagery reveals a prominent swing in the broad structural grain from NE-SW in the south to WNW-ESE to the north of the shear zone. Structural studies reveal the presence of a gently plunging lineation on the mylonitic foliation in the vicinity of the shear zone suggesting a significant strike-slip component of movement. Both mesoscopic and microscopic studies further reveal a

dextral sense of movement in near-horizontal sections at right angles to the mylonitic foliation in the shear zone. Moreover, north of the Mahanadi Shear Zone, another prominent zone of strain localization having the same structural trend has been observed within the granulite facies rocks. Here too, the shear sense appears to be broadly dextral in near horizontal sections. These opens up the possibility for a significant strike slip movement along parallel shear zones, which has dextrally displaced the northern part of EGP (comprising of the Angul and Tikarpara domains) with respect to the rest of EGP, south of the Mahanadi Shear Zone. However, earlier studies in this area considered the Mahanadi Shear Zone to be broadly extensional, with an insignificant strike-slip component.

Further studies to investigate the importance of the strike-slip component of movement along the Mahanadi Shear Zone are currently in progress.

Granite remote sensing image recognition and extraction in Taibai area, Shaanxi, China

Xiaohu Zhou^{a, b, c}, Yunpeng Dong^{a, b}, Xiaoming Liu^{a, b}, Shengsi Sun^{a, b}, Zhao Yang^{a, b}

^a State Key Laboratory of Continental Dynamics, Northwest University, Xi'an, Shaanxi, China, 710069

^b Department of Geology, Northwest University, Xi'an, Shaanxi, China, 710069

^c Shaanxi Key Laboratory of Exploration and Comprehensive Utilization of Mineral Resources, Xi'an 710054, China

Remote sensing petrology is one of the most important branches in remote sensing technology. It is based on rock spectroscopy and aims at identify lithology through analyzing remote sensing images. Granite is of huge importance among igneous rocks because the formation and distribution of which has tight relationships with certain geological settings so that indicated information about regional tectonic and mineralization can be inferred. Remote sensing of identifying lithology of granite has long been focused and researched. Large amount of granite develops in Qinling Mountains – Taibai area which is located in the fault belts conjunction part, consequently it is the main tectonic mineralization area. Considering previous geological researches about this area have been done, the efficiency and veracity of extraction can be verified. Hence this area

becomes an ideal region to process remote sensing information extraction of granite. Based on ASTER data, combing other remote sensing data, this paper aims to analyze typical granite spectral characteristics and summarize its regularity of absorbing and reflecting in order to find out a suitable remote sensing identify method for target granite. This method is going to offer basic data support for regional geological survey, as well as provide examples of remote sensing information extraction for similar regional granite. We get some conclusions as follows:

(1) Granitoids rock samples collected from Taibai generally has not obvious spectral features in the VNIR-SWIR region, and the main spectral features come from the accessory minerals contained in the rocks. The main absorption bands could be found at Fe²⁺

centered at 0.55 μm , Fe³⁺ centered at 1.9 μm and hydroxy centered at 2.2 μm and 2.35 μm . Types of granites in different regions have different spectral characteristics because of the various kinds of mineral species and abundance, coupled with different background environment and weathering degree.

(2) Compared with the 432 optimal bands combination based on the optimal index factor (OIF) calculation, the principal component analysis (PCA) processing of 345 components combination is more effective. The granite rock boundaries present brighter color and distinguished features in the false color composite images. Considering the enhancement of spectral characteristics, different band math component combinations are

0.87 μm , H₂O centered at 1.4 μm and selected for different rock mass. The selected ratio of 2/1, 2/4 and band 4 of OLI image are employed to identify lithological information of Taibai rock mass and ratio of 2/1, band 4 of OLI image and relative absorption-band depth (RBD) 8 to Laojunshan rock mass. The granitoids information is obviously easy to identify through the enhancement of band math component combination.

(3) Based on the band math component combination images and PCA 345 components combination image, a relatively accurate extraction information is obtained ultimately, which prove the feasibility of granitoids information extraction based on the ASTER and other auxiliary remote sensing images.

Occurrence of magmatism in Sivas-Erzincan region (Centraleastern Turkey) and its implications on the formation of Çöpler, Karakartal and Fındıklıdere ore deposits: A geochronological approach

Miğraç Akçay^a, Oğuzhan Gümrük^a, Brent McInnes^b, Noreen Evans^b, Fred Jourdan^b, Svetlana Tessalina^b

^a Jeoloji Mühendisliği Bölümü, Karadeniz Teknik Üniversitesi, 61080 Trabzon, Turkey

^b John de Laeter Centre, Curtin University, Perth, Western Australia

Sivas-Erzincan-Tunceli zone (located in central eastern Turkey) is known with the presence of many ore deposits ranging from porphyry systems (Çöpler, Karakartal, Fındıklıdere) to skarns (Yakuplu, Demirmağara, Bizmişen) and to mesothermal-epithermal systems (Çöpler, Fındıklıdere) formed in association with subalkaline intrusions ranging in composition from diorites to tonalites and having a subduction-related affinity. From Karakartal to Fındıklıdere and to Çöpler, the system changes from purely magmatic to magmatic-hydrothermal as shown by magnetite-pyrite-molybdenite-chalcopyrite-Au at Karakartal, pyrite-chalcopyrite-sphalerite-fahlore-galena-Au at Fındıklıdere, and magnetite-pyrite-molybdenite-chalcopyrite-Au-orpiment-realgar-Mn oxides at çöpler (Gümrük et al. 2013). Demirmağara and Bizmişen are

known to contain only skarn systems. This study aims at examining the development of magmatism in the region as a whole and the occurrence of mineralising processes in association with it based on zircon U-Pb and U/Th-He, biotite and sericite Ar-Ar and molybdenite Re-Os geochronology and Sm-Nd isotope data.

Sm-Nd isotopic signatures show some significant differences between intrusives associated with porphyry and skarn type deposits. In contrast to Karakartal and Çöpler intrusions hosting porphyry systems, the Demirmağara, Çaltı and Yakuplu plutons that contain skarn type deposits are more enriched in ⁸⁷Sr/⁸⁶Sr and slightly more depleted in ¹⁴³Nd/¹⁴⁴Nd. Coupled with the fact that the latter intrusions contain a lot more inherited zircons with U/pb ages around 600 Ma, this could be taken as an evidence

to suggest that these intrusives, especially the Yakuplu pluton, was derived from a parental magma contaminated by crustal rocks. Despite large variation in associated mineralised occurrences, all of the intrusions have similar geochemical features as shown by parallel primitive mantle normalised trace element patterns characterised by negative Nb, P and Ti anomalies. These trends are indicative of arc magmatism due to subduction, supported also by discrimination diagrams of Y vs Nb, (Y+Ta) vs Rb, Yb vs Ta and (Y+Nb) vs Rb of Pearce et al. (1984). The similarity of petrogenesis of granites is also represented by average lower and upper crust-normalised trace element plots which indicate that they have similar composition to lower crust but are depleted to some extent relative to upper crust.

Based on zircon U-Pb dating, the intrusions in the Karakartal area was dated as 50-44 Ma, the Çaltı, Demirmağara and Yakuplu plutons as 44.9-42.8 Ma, 43.7 Ma and 43.7-43.0 Ma, respectively, and the one associated with the Çöpler deposit as 43.7-41.4 Ma. Molybdenites obtained from the Karakartal, Fındıklıdere and Çöpler deposits produced respective Re-Os ages of 49.14-48.83 Ma, 45.72-45.08 Ma and 42.66-40.89 Ma. Similarly, Ar-Ar dating on K-feldspars and biotites from the K-silicate alteration zones in the Karakartal and Çöpler deposits yielded respective plateau ages of 49.86-46.83 Ma, and 44.81-44.76 Ma (Fig.1).

U/Th-He dating on zircons, which indicates closing temperatures of around 200°C, put forward that cooling of intrusions of the Karakartal, Fındıklıdere and Çöpler below this temperature took place at 46.2±0.9 Ma, 41.6±0.6 Ma,

36.6±0.7 Ma, respectively. These data can be used to infer that the cooling process for each intrusion occurred in durations of ≥3.7 Ma, ≥5.1 Ma and ≥9.5 Ma, respectively, and that the mineralising processes at these respective sites continued for around ~4 Ma, 2.9 Ma and ~6 Ma (Table 1).

All the data summarised above indicate that the length of duration of mineralising process was much longer in the Çöpler area than in Karakartal and Fındıklıdere, a strong evidence to explain why the Çöpler deposit has the largest resources among all. The data also indicate that zones where late stage magmatic episodes are present have a strong potential for the presence of large scale porphyry Au-Cu occurrences.

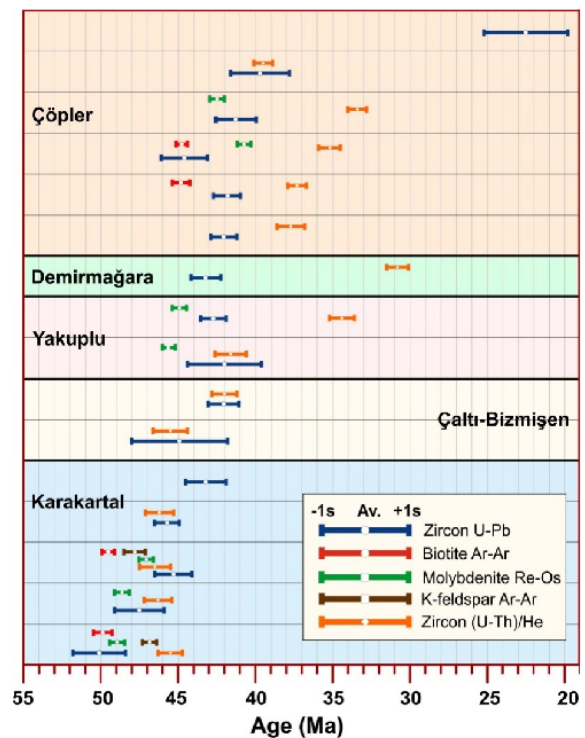


Fig.1. Distribution of zircon U-Pb, biotite and K-feldspar Ar-Ar, molybdenite Re-Os and zircon (U-Th)/He geochronological data for mineral deposits in the Sivas-Erzincan region (centraleastern Turkey).

Table 1. Summary of geochronological data denoting age constraints in relation to various stages of magmatism and mineralisation in Karakartal, Fındıklıdere and Çöpler regions.

Age constraints	Data Source	Method	Karakartal	Fındıklıdere	Çöpler
Intrusion	Zircon	U-Pb	≥ 51.8 Ma	≥ 46.7 Ma	≥ 46.1 Ma
Cooling	Biotite	Ar-Ar	≥ 49.7 Ma	44.4 Ma	44.8 Ma
K-silicate alteration	Secondary biotite & K-feldspar	Ar-Ar	47.8 Ma	43.8 Ma	43.8 Ma
Final cooling	Zircon	(U-Th)/He	46.2 Ma	41.6 Ma	36.6 Ma
Mineralisation	Molybdenite	Re-Os	48.83 Ma	45.08 Ma	40.89
From initiation to the end of magmatism			≥ 5.3 Ma	≥ 5.1 Ma	≥ 9.5 Ma
From onset of magmatism to potassic alteration			≥ 4 Ma	≥ 2.9 Ma	≥ 6 Ma

References

- Gümrük, O., Akçay, M., Aslan, N., 2013. Mineral chemistry of biotite and chlorite from the Karakartal (Kemaliye, Erzincan) porphyry Au-Cu deposit: A geothermometric approach on mineral paragenesis and succession. Mineral Deposit Research For A High-Tech World, 12th SGA Biennial Meeting 2013, Proceedings, 2, 805-808.
- Pearce, J.A., Harris, N.B.W., Tindle, A.G., 1984. Trace element discrimination diagrams for the tectonic interpretation of granitic rocks. J. Petrol. 25, 956-983.

Petrological, geochemical and fluid inclusion characteristics of mafic granulites from the Mercara Suture Zone, Southern India: implications for deep subduction and subsequent exhumation

T. Amaldev^{a*}, K. R. Baiju^a, M. Santosh^{b, c, ,}, T. Tsunogae^{d, e}, T. Pradeepkumar^f,
K. Sajeev^g, M. Satyanarayanan^h

^aDepartment of Marine Geology and Geophysics, Cochin University of Science and Technology, Lakeside Campus, Kochi-16, India

^bCenter for Tectonics, Resources and Exploration, Department of Earth Sciences, University of Adelaide, SA 5005, Australia

^cSchool of Earth Sciences and Resources, China University of Geosciences Beijing, 29 Xueyuan Road, Beijing 100083, China

^dGraduate School of Life and Environmental Sciences, University of Tsukuba, Ibaraki, Japan

^eDepartment of Geology, University of Johannesburg, Auckland Park 2006, South Africa

^fPPOD Laboratory, Geological Survey of India, Bangalore 560070, India

^gCentre for Earth Sciences, Indian Institute of Science, Bangalore 560 012, India

^hCSIR — National Geophysical Research Institute, Hyderabad 500007, India

*Corresponding author e-mail: amaldev302@gmail.com

Major orogenic belts were formed by material recycling through suture zones which involves prolonged subduction and accretion, followed by collision and exhumation (Rogers and Santosh, 2004; Stern, 2011). The mafic granulites found as enclaves, bands or boudins in collisional zones were considered to be traces of deep subduction of continental crust materials and their subsequent exhumation (Santosh et al., 2009, 2010). The metamorphic pressure–temperature–time

histories of mafic granulites provide important insights to the tectonic settings and evolutionary processes of ancient cratons and associated suture zones (Santosh et al., 2010; Shaji et al., 2014; Yano et al., 2016)

The Mercara Suture Zone is recognised as a terrane boundary, and possible Mesoarchean suture (3.0 – 3.2 Ga) along which the Coorg Block in Southern Granulite Terrain has accreted to the

Western Dharwar Craton (Amaldev et al., 2016). The major rock types in the Mercara Suture Zone include charnockite, TTG gneisses, metagabbros, mafic granulites, kyanite-sillimanite bearing metapelites (khondalite) and quartz mica schists (Chetty et al., 2012; Amaldev et al., 2016; Ishwarkumar et al., 2015). The suture is marked by steep gravity gradients reflecting the presence of underplated high-density material, along with the electrical anomalies suggestive for vertical conductive structure extending from the lower crust into the upper mantle coinciding with the geologically marked transition zone between the Coorg Block and the Western Dharwar Craton (Sunil et al., 2010; Azeez et al., 2015). The present work concentrates on the petrology, geochemistry and fluid characteristics of the fluids involved in the genesis of these mafic enclaves and its role in the high grade metamorphism of the terrain.

The mafic granulites in this area are medium to coarse grained rocks predominantly consisting of orthopyroxene, clinopyroxene and plagioclase \pm garnet \pm hornblende \pm biotite \pm quartz. Minor amounts of magnetite, rutile and ilmenite are also present as accessory phases. Clinopyroxene and plagioclase inclusions are found in garnet porphyroblasts suggesting prograde high - pressure metamorphism. Inclusions of hornblende occur within garnet and are interpreted as relics from the prograde path preceding peak metamorphism. The available mineral assemblages and their reaction textures itself gives a better picture on the initial subduction, crustal thickening, subsequent exhumation, followed by cooling and retrogression of the terrain, which in turn can be well established from petrogenetic

grids and thermobarometric data.

Major and trace element chemistry of mafic granulites are suggestive that these rocks are essentially tholeiitic and are characterised by low silica, low alumina, high iron, high FeO/MgO ratio's. The rocks are characterized by a marked enrichment in LILE and LREE, shows relative depletion of HFSE and a weak positive Eu anomaly. The rocks are rich in compatible elements (Cr, Ni, Co, Sc and V) and comparably low incompatible elements (Rb, U, Th, Ba, Nb and K). High concentration of ferromagnesian elements such as Sc, V, Cr, Co and depletion of HFSE indicates mafic source rock. Geochemical signatures are also typical of subduction-related intraoceanic tholeiitic arc basalt.

Fluid inclusions ubiquitously present in quartz grains and garnet grains in these rocks were studied. These inclusions occur either as isolated clusters or arrays that pinch out within grains. The quartz grains were plastically deformed showing grain boundary migration recrystallization, deformation lamellae and deformation bands. Hence, the inclusions preserved in these samples might have resulted from metamorphism of pre-existing rocks with different degrees of reworking of primary inclusions during or after the peak metamorphic condition. The garnet also shows deformational effect in the form of micro cracks. Two types of inclusions are identified at room temperature in quartz grains and garnet: - Type-1, Pure CO₂ fluid inclusion clusters and Type-II, large CO₂ inclusions occurring as isolated inclusions. Sometimes CO₂ + H₂O inclusions are also present, wherein the inclusions appear to consist of two phase (liquid CO₂+ gaseous CO₂) at room temperature. From

microthermometry most inclusions show Tm CO₂ between -56.6° to -58°C and rarely below -56.6°C implying that the trapped fluids consists minor amount of other gases and contaminants mostly of CH₄ and N₂. The lowest homogenization temperature recorded in the sample is -50.2, corresponding to densities between 1.155 g/cc. When considering peak metamorphic temperatures of 750 to 850°C, these densities correspond to trapping pressures of 8 to 10 Kb i.e. at 30 to 35 km depth. The low density CO₂ isochores indicate re-equilibration of high density (peak-metamorphic) fluid inclusions during uplift /retrogression. The fluid inclusion data extracted from the mafic granulites is in conjunction with the thermobarometry of the terrain and suggest deep subduction and subsequent exhumation.

References

- Abdul Azeez, K.K., Veeraswamy, K., Gupta, A.K., Babu, N., Chandrapuri, S., Harinarayana, T., 2015. The electrical resistivity structure of lithosphere across the Dharwar craton nucleus and Coorg block of South Indian shield: Evidence of collision and modified and preserved lithosphere. *Journal of Geophysical Research - Solid Earth* 120, 6698–6721
- Amaldev, T., Santosh, M., Tang, Li, Baiju, K.R., Tsunogae, T., Satyanarayanan, M., 2016. Mesoarchean convergent margin processes and crustal evolution: Petrologic, geochemical and zircon U - Pb and Lu-Hf data from the Mercara Suture Zone, southern India. *Gondwana Research* 37, 182–204
- Chetty, T., Mohanty, D., Yellappa, T., 2012. Mapping of shear zones in the Western Ghats, Southwestern part of Dharwar Craton. *Journal of the Geological Society of India* 79, 151–154.
- Ishwar-Kumar, C., Windley, B.F., Horie, K., Kato, T., Hokada, T., Itaya, T., Yagi, K., Gouzu, C., Sajeev, K., 2013. A Rodinian suture in western India: new insights on India – Madagascar correlations. *Precambrian Research* 236, 227–251.
- Rogers, J.J.W., Santosh, M., 2004. *Continents and Supercontinents*. Oxford University Press, New York
- Santosh, M., Tsunogae, T., Shimizu, H., Dubessy, J., 2010. Fluid characteristics of retrogressed eclogites and mafic granulites from the Cambrian Gondwana suture zone in southern India. *Contributions to Mineralogy and Petrology* 159, 349–369.
- Santosh, M., Maruyama, S., Sato, K., 2009. Anatomy of a Cambrian suture in Gondwana: Pacific-type orogeny in southern India? *Gondwana Research* 16, 321–341.
- Shaji, E., Santosh, M., He, X.-F., Fan, H.-R., Dev, S.G.D., Yang, K.-F., Thangal, M.K., Pradeepkumar, A.P., 2014. Convergent margin processes during Archean– Proterozoic transition in southern India: Geochemistry and zircon U–Pb geochronology of gold-bearing amphibolites, associated metagabbros, and TTG gneisses from Nilambur. *Precambrian Research* 250, 68–96
- Stern, C.R., 2011. Subduction erosion: rates, mechanisms, and its role in arc magmatism and the

evolution of the continental crust and mantle. *Gondwana Research* 20, 284-308.

Sunil, P., Radhakrishna, M., Kurian, P., Murty, B., Subrahmanyam, C., Nambiar, C.G., Arts, K., Arun, S., Mohan, S., 2010. Crustal structure of the western part of the Southern Granulite Terrain of Indian Peninsular Shield derived from gravity data. *Journal of Asian Earth Sciences* 39, 551–564.

Yano, M., Tsunogae, T., Santosh, M., Yang, Q-Y., Shaji, E., Takamura, Y., Ultrahigh- temperature metagabbros from Wynad: implications for Paleoproterozoic hot orogen in the Moyar Suture Zone, southern India, *Journal of Asian Earth Sciences* (2016), doi: <http://dx.doi.org/10.1016/j.jseaes.2016.04.024>

Deciphering the Precambrian crust between Shillong Massif and Northeast India

S. M. Mahbubul Ameen^{a*}, Md. Sakawat Hossain^a, Md. Sakaouth Hossain^a,
Rashed Abdullah^{a,b}, Zahidul Bari^a, Md. Nehal Uddin^c, Sudeb Chandra Das^d, Al-
Tamini Tapu^e, Hasibul Jahan^a, Md. Shams Shahriar^a

^a Department of Geological Sciences, Jahangirnagar University, Savar, Dhaka-1342, Bangladesh.

^b School of Earth Sciences, The University of Queensland, St Lucia QLD 4072, Australia.

^c Geological Survey of Bangladesh, 153 Pioneer Road, Segunbagicha, Dhaka 1000, Bangladesh.

^d Morning Glory School and College, Savar Cantonment, Savar, Dhaka-1342, Bangladesh.

^e Economic Geology, Oulu Mining School, University of Oulu, Oulu, Finland.

*Corresponding Author e-mail: ameensmm@juniv.edu

The Precambrian basement in Bangladesh, occupies a critical position between the two regional crustal provinces, Shillong Massif (1914–500 Ma, Dikshitullu et al., 1995; Yin et al., 2010) and Chotanagpur Granite Gneiss Complex (>2550–800 Ma, Rekha et al., 2011; Sanyal and Sengupta, 2012 and references therein) of the Indian Shield (Fig.1; Table 1). The basement rocks in Bangladesh are only accessible by drillholes and generally underlie beneath ~125 to 2100 m Cenozoic sediments. These basement rocks in Bangladesh have long been thought as subsurface continuation of northeastern part of the Indian Shield, which connects the main shield area with the Shillong Massif and Mikir Hills further to the east (Reimann, 1993). The lack of outcrop and high resolution regional geophysical study

and the paucity of appropriate petrology, geochronology data on the drillcore samples have remained as major obstacles to understand this crustal fragment in northwest Bangladesh. Basement studies in Bangladesh are mostly from Maddhapara (Fig. 1b) where an underground hardrock mine is in operation (Ameen et al., 1998, 2007; Hossain et al., 2007, 2008; Zaman et al., 2001). Two similar Columbia ages (1.72 Ga, Ameen et al., 2007; 1.73 Ga, Hossain et al., 2007) were obtained from granitoid basement in Maddhapara (Fig. 1b) considered to have represented the emplacement age of the Maddhapara granitoid in Dinajpur block (DB). A late monzogranite dyke cutting through the tonalite dated at 1.51 Ga (Ameen, unpub.) represents a minor episode of felsic magmatism in

Maddhapara (Table 1). Studies on core samples in recent years, however, revealed diverse rock association in different

locations of the DB.

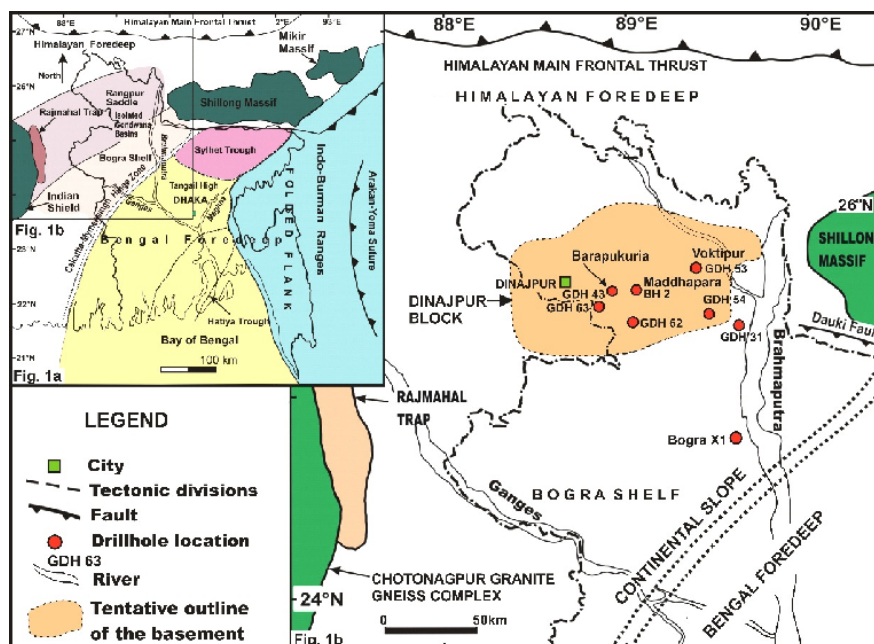


Fig. 1. Northwest Bangladesh and surrounding areas. a) Tectonic map of Bangladesh and adjoining areas (modified from Alam et al., 1990; Khan, 2002); b) Simplified tectonic map of the northwest part of Bangladesh and location of selected drillholes intersected basement (modified from Ameen et al., 2007).

Tonalite-diorite rocks similar to Maddhapara have been reported from drillhole GDH 53 and 54 (Fig. 1b) (Das et al., 2015; Tapu et al., 2012), suggesting a wider areal extent of granitoid rocks similar to Maddhapara, which may or may not belong to the same age bracket. About 30 km southeast of Maddhapara, drillcores from GDH 63 (Fig. 1b) reveal a more felsic phase (foliated leucogranite) in the basement, unlike any other leucocratic phases reported in other drillholes. The basement rocks, in many of these drillholes (Fig. 1b) are dissected by felsic, mafic and ultramafic dykes (hornblendite, picrite porphyry and lamprophyre) (Das et al., 2015). Along with diorites, the basement appeared to contain metasediments (!) in

Barapukuria area (Fig. 1b). Besides, the presence of basemetal sulphides associated with sheeted veins in GDH 62 likely portends a mineralization event, which is yet to be studied (Tapu et al., 2014). The recent discovery of charnockite in GDH 31 (Hossain et al., 2015) may be linked with regional high-grade event in the adjacent parts of the Indian Shield.

These preliminary findings deserve serious consideration and need to be constrained by appropriate studies. These studies are imperative to understand the critical relation of the basement rocks in northwest Bangladesh with those of the regional cratonic blocks of the Indian or other Shields and its place/s in the Paleocontinent cycles.

Table 1: Compilation of Age data on Chotanagpur Granite Gneiss Complex (CGGC), Bangladesh basement and Shillong Massif modified from Mohanty et al. (2012) and references therein.

Time (Ma)	CGGC	Bangladesh basement, Maddhapara	Shillong Plateau
500-750			Arunachal biotite granite (non-foliated) 500±19 Thermal imprint on Sonapahar metapelites 500±14 Nongpoh Granite 550±15
750-1000	Raigarh Granite 972±114 803±49, 815±47, 1005±51 Thermal overprint on Bengal Anorthosite 947±27		Khasi Granite 690±19 Mylliem Granite 607±13 Goalpara Granite 647±122
1000-1200	Purulia Granite 1071±64 Jajawal Granite 1100±20		Thermal imprint on Sonapahar metapelites 1078±31
1200-1500	Purulia Migmatites 1178±61 Mica belt Granite 1238±33, 1284±409 Binda Granite 1242±34		Norite enclave of Khasi batholith 1462 Thermal imprint on Sonapahar metapelites 1472±38
1500-1700	Dumka Granulite 1100±20 Charnockite 1100±20 Granulites 1100±20 Bengal Anorthosite 1100±20	Monzogranite 1511±19 (Ameen unpub.)	Shillong Group (?) 1550 Ziro biotite granite gneiss 1644±40, 1676±122
1700-1900	Chotanagpur/Simultala Orogeny Granulite event Daltonganj granite 1742±65 Barra Bazaar granite 1771±210	Tonalite, 1722±6 (Ameen et al., 2007) Diorite, 1730±11 (Hossain et al., 2007)	Deformation, porphyritic and biotite granite
1900-2600	Intrusion of ultramafic 1925±110 Granulite event (?)		Bomdila augen gneiss 1914±25
2600-2900	CGGC metapelites 2569±18		Granulite grade metamorphism and migmatization

References

- Alam, M.K., Hasan, A.K.M.S., Khan, M.R., Whitney, J.W., 1990. Geological map of Bangladesh. Geological Survey of Bangladesh, Dhaka, Scale 1:1000000.
- Ameen, S.M.M., Khan, S.H., Akon, E., Kazi, A.I., 1998. Petrography and major oxide chemistry of some Precambrian crystalline rocks from Maddhapara, Dinajpur, Bangladesh. Bangladesh Geoscience Journal 4, 1–19.
- Ameen, S.M.M., Wilde, S.A., Kabir, M.Z., Akon, E., Chowdhury, K.R., Khan, M.S.H., 2007. Paleoproterozoic granitoids in the basement of

- Bangladesh: a piece of the Indian shield or an exotic fragment of the Gondwana jigsaw? *Gondwana Research* 12, 280–387.
- Das, S.C., Ameen, S.M.M., Bari, Z., Zaman, M.N., 2015. Petrographic characterization of crystalline basement rocks from Voktipur, northwest Bangladesh. *Jahangirnagar University Journal of Science* 37 (1), 55–74.
- Dikshitullu, G.R., Pandey, B.K., Krishna, V., Dhana Raju, R., 1995. Rb-Sr systematic of granitoids of Central Gneissic Complex, Arunachal Himalaya: implications of tectonics, stratigraphy and source. *Journal of the Geological Society of India* 45, 51–56.
- Hossain, I., Tsunogae, T., Rajesh, H.M., 2008. Geothermobarometry and fluid inclusions of dioritic rocks I Bangladesh: Implications for emplacement depth and exhumation rate. *Journal of Asian Earth Sciences* 101, 65–74.
- Hossain, I., Tsunogae, T., Rajesh, H.M., Chean, B., Arakawa, Y., 2007. Paleoproterozoic U-Pb SHRIMP zircon age from basement rocks in Bangladesh: a remnant of magnetization associated with the Columbia supercontinent. *Comptes Rendus Geosciences* 339, 979–986.
- Hossain, M. S., Ameen, S.M.M., Bari, Z., Zaman, M.N., 2015. Petrography and microtextural characteristics of the basement complex of GDH-31, Gaibandha, Bangladesh. *Jahangirnagar University Journal of Science* 37 (1), 39–54.
- Khan, M.R., 2002. Plate tectonics and Bangladesh. *Journal of Asiatic Society of Bangladesh Science, Golden Jubilee Issue* 28, 39–62.
- Mohanty, S., 2012. Spatio-temporal evolution of the Satpura Mountain Belt of India: A comparison with the Capricorn Orogen of Western Australia and implication for evolution of the supercontinent Columbia. *Geoscience Frontiers* 3, 241–267.
- Reimann, U. K., 1993. *Geology of Bangladesh*. Gebruder - Brontraeger, Berlin-Stuttgart.
- Rekha, S., Upadhyay, D., Bhattacharya, A., Kooijman, E., Goon, S., Mahato, S., Pant, N.C., 2011. Lithostructural and chronological constraints for tectonic restoration of Proterozoic accretion in the eastern Indian Precambrian shield. *Precambrian Research* 187, 313–333.
- Sanyal, S., Sengupta, P., 2012. Metamorphic evolution of the Chotanagpur Granite Gneiss Complex of the East Indian Shield: current status. *Geological Society of London, Special Publications* 365, 117–145.
- Tapu, A.T., Ameen, S.M.M., Abdullah, R. 2012. Petrological and geochemical study of the crustal rocks from Barapaharpur Area, Dinajpur, Bangladesh. MS Thesis (unpub.). Department of Geological Sciences, Jahangirnagar University, Bangladesh.
- Tapu, A.T., Ameen, S.M.M., Abdullah, R. 2014. Basemetals within the basement rocks in Barapaharpur, northwest Bangladesh: Implications for mineralization in the shallow basement of Bangladesh. Abstract volume, 2014 GSA Annual Meeting (19-22 October, 2014), Vancouver, British Columbia.
- Yin, A., Dubey, C.S., Webb, A.A.G., Kelty, T.K., Grove, M., Gehrels, G.E., Burgess, W.P., 2010. Geologic correlation of the Himalayan orogen and Indian craton (part 1): Structural geology, U-Pb zircon geochronology, and tectonic evolution of

the Shillong Plateau and its neighboring regions in NE India the eastern Himalayan orogeny. Geological Society of America Bulletin 122, 336–359.

Zaman, M.N., Ahmed, S.S., Islam, M.B., Islam, M.S., Ishiga, H, Elahi, M.E.,

Daogong, C., Xiachen, Z., 2001. Trace and Rare Earth Element Geochemistry of the Basement Complex in Maddhapara, Dinajpur, Bangladesh. Acta Mineralogica Pakistanica 12, 27–42.

Evidence for melting and metasomatism of lithospheric mantle in an Archean supra subduction zone— A case study from the ultra mafic suites of Wyanad, Southern India

J. Arun Gokul^a, M. Santosh^{b, c}, E. Shaji^a, Qiong- Yan Yang^b

^a Department of Geology, University of Kerala, Kariyavattom Campus, Trivandrum 695 581, India

^b School of Earth Sciences and Resources, China University of Geosciences Beijing, 29 Xueyuan Road, Beijing 100083, China

^c Department of Earth Sciences, University of Adelaide, Adelaide SA 5005, Australia

The Southern Granulite Terrane (SGT) to the south of the Dharwar Craton preserves rock records ranging in age from Mesoarchean to late Neoproterozoic (Santosh et al., 2015, 2016). The southern margin of the Mesoarchean Coorg block contains remnants of rare ultramafic rocks in association with arc magmatic rocks and accreted metasediments. The Coorg Block is bound to the north by the curvilinear NW-SE trending Mercara Shear Zone (MRSZ) and to the south by the WNW-ESE trending Moyar Shear Zone (MOSZ) (Chetty et al., 2012; Santosh et al., 2015) separating the Neoproterozoic Nilgiri block. The Wyanad region is the junction of two major suture zones of Mercara suture zone (Mesoarchean) and Moyar suture zone (Neoproterozoic). Therefore investigations on the ultra mafic and associated rocks from this area are critical in understanding the evolution of the subcontinental lithospheric

mantle and its modification through episodic subduction history. Recent studies revealed that the Mesoarchean ages from the Wyanad suite are consistent with the ages reported from the Coorg Block, whereas the Neoproterozoic ages correspond with those in the Nilgiri Block to the south (Yang et al., 2016). The metaultramafics from this region carry magmatic zircons with crystallization ages of 3.3 to 3.0 Ga and 2.5 Ga. The associated orthopyroxene-bearing felsic charnockite also carry magmatic zircons of 3.2–3.0 Ga, whereas those in metadiorite crystallized at around 2.5–2.6 Ga. Zircon Lu–Hf data yield $\epsilon_{\text{Hf}}(t)$ values in the range of -18.23 to 13.98 and Hf crustal residence model ages (TCDM) of 2576– 4009 Ma, suggesting the involvement of both juvenile and reworked components in magma generation. Here we summarize the evidence for multiple mantle metasomatism through

Mesoarchean and Neoproterozoic subduction systems and discuss their implications on the Archean tectonic history of the SGT.

References

- Chetty, T.R.K., Mohanty, D.P., Yellappa, T., 2012. Mapping of Shear Zones in the Western Ghats, Southwestern Part of Dharwar Craton. *J. Geol. Soc. India* 79 (Feb), 151–154.
- Santosh, M., Yang, Q.Y., Shaji, E., Tsunogae, T., Mohan, M.R., Satyanarayanan, M., 2015. An exotic Mesoarchean microcontinent: the Coorg Block, southern India. *Gondwana Res.* 27, 165–195.
- Santosh, M., Yang, Q.Y., Shaji, E., Mohan, M.R., Tsunogae, T., Satyanarayanan, M., 2016. Oldest rocks from Peninsular India: evidence for Hadean to Neoproterozoic crustal evolution. *Gondwana Res.* 29, 105–135.
- Yang, Q.Y., Santosh, M., Ganguly, S., Arun-Gokul, J., Shaji, E., Tsunogae, T., Dong, Y., Manikyamba, C., Dhanil Dev, S.G., 2016. Melt-fluid infiltration in Archean suprasubduction zone mantle wedge: evidence from geochemistry and zircon U-Pb and Lu-Hf data from Wynad, southern India. *Precambrian Research* 281(2016)101-127.

Magma sources of Paleozoic and Mesozoic porphyry Cu-Mo deposits in Southern Siberia (Russia) and Mongolia: evidence from geochemical and isotopic data

A.N. Berzina, A.P. Berzina and V.O. Gimon

Sobolev Institute of Geology and Mineralogy, Siberian Branch Russian Academy of Sciences, Novosibirsk 630090, Russia

Porphyry-Cu-Mo deposits occur in areas, which were involved in multiple magmatic events and are temporally and spatially associated with porphyry intrusions. The deposits of this type were formed as a result of mantle-crust interaction and they are usually associated with magmas, variable in composition from mafic to intermediate and silicic. Their source composition, relationship and role in ore formation are clearly of primary importance in the modeling of the evolution of porphyry-Cu-Mo systems. To constrain the relationships between magmas of different compositions involved in the formation of porphyry-Cu-Mo and Mo-Cu ore-magmatic systems, the new strontium and neodymium isotopic data, coupled with a new and previously published geochronological data were used.

Southern Siberia (Russia) and Mongolia, a part of the eastern segment of the Central Asian Orogenic Belt is an

important metallogenic province. A number of medium to large porphyry Cu-Mo deposits are located in this region (Fig. 1). In general, the deposits delineate younging trend with decreasing Cu/Mo value from west to east. Geochronological data suggest that the emplacement and mineralization of the porphyries occurred during Early Paleozoic to Late Mesozoic.

The deposits are confined to transregional magmatic belts extending along the southern margin of the Siberian craton. These belts are associated with magmatic events related to the subduction of the Paleasian ocean in Early Paleozoic (Berzin et al., 1994),

Sm-Nd isotope analyses were performed at the Laboratory of Geochronology, Geological Institute of Kola Scientific Center of the Russian Academy of Sciences (Apatity) on a multi-

collector Finnigan MAT-262 (RPQ) thermal ionization mass spectrometer, operating in static mode. SIMS U–Pb analyses of zircons were made using a SHRIMP II ion microprobe at the All Russia Geological Research Institute (VSEGEI, St. Petersburg, Russia). Analysis of Sr isotopes was carried out on an MI 1201AT mass spectrometer in Analytical Center for multi-elemental and isotope research SB RAS (Novosibirsk, Russia).

subduction of the west gulf of the Mongol-Okhotsk ocean in Late Paleozoic–Early Mesozoic (Yarmolyuk & Kovalenko, 2003) and collision of the Siberian and North China - Mongolia continents during the closure of the central part of the Mongol-Okhotsk ocean in Jurassic (Zorin et al., 1997). From Paleozoic to Mesozoic the western margin of Paleasian ocean and Mongol-Okhotsk basin were shifted toward the east. As a result, the intense magmatic activity in the region took place in the western part in Early Paleozoic time, in the central area – in Early and Late Paleozoic and in the eastern part – in Early-, Late Paleozoic and Early Mesozoic time.

Paleozoic porphyry deposits Cu-Mo Aksug and Mo-Cu Sora (Altai-Sayan belt, Russia); Cu-Mo Erdenetiin-Ovoo (Northern Mongolia); Cu-Mo Tsagaan Suvarga and Cu-Au Kharmagtai (South Gobi region of Mongolia) are confined to continental-margin volcanoplutonic belts. Rocks of Paleozoic deposits are characterized by high Sr, Sr/Y and La/Yb values similar to those of typical adakitic rocks, low $(^{87}\text{Sr}/^{86}\text{Sr})_i$ ratios (0.7011–0.7046) and positive $\epsilon\text{Nd}(T)$ values ranging from +0.3 to +8.0 (Table 1). These features, along with

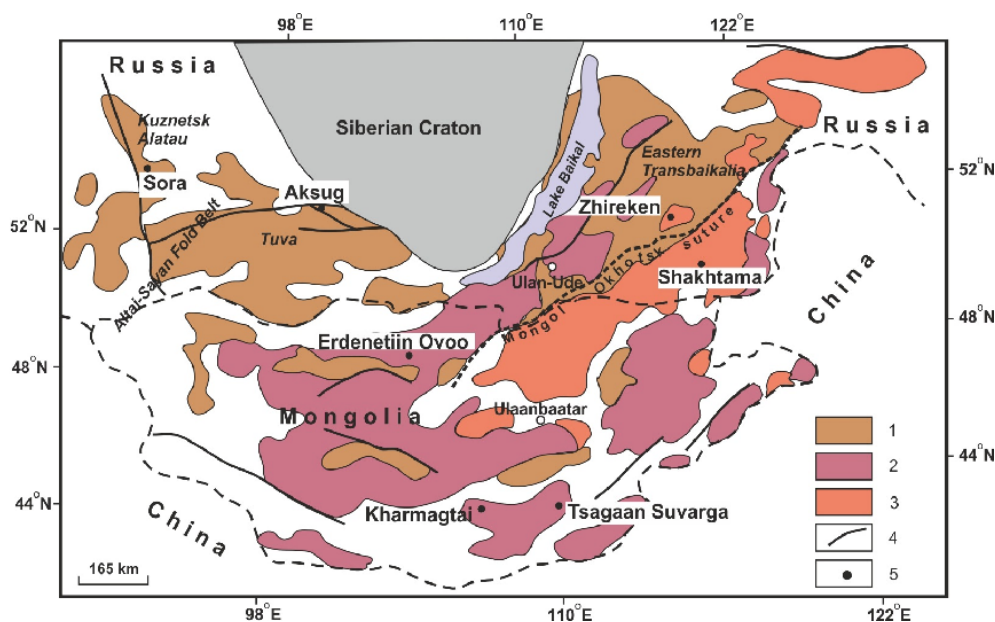
typical arc magma characteristics such as the enrichment in LILE and LREE and depletion in HREE and HFSE indicate that parental magmas for mafic rocks were derived from a lithospheric mantle previously metasomatized by slab fluids/melts. Sr, Nd and Pb isotopic characteristics suggest significant contribution of mantle material in the formation of felsic magmas. Petrological and geochemical data suggest that felsic adakitic rocks at Paleozoic porphyry Cu-Mo deposits were derived from partial melting of mafic rocks at the bottom of the lower crust, while typical arc-type granitoids were probably formed as a result of crystal differentiation of basic magma during its ascent to the upper levels of the crust.

Late Mesozoic porphyry deposits Mo-Cu Zhireken and Mo Shakhtama (Eastern Transbaikalia, Russia) were formed in intra-plate setting after collision of Siberian and North-China continents and closure of the Mongol-Okhotsk Ocean. The rocks are characterized by $\epsilon\text{Nd}(T)$ values ranging from +2.1 to -10.3, elevated I_{Sr} ratios (0.7045–0.7078) and Nd model ages from 0.8 to 1.5 Ga. Both deposits include adakite-like rocks with geochemical characteristics of K-adakites. Geochemical and isotopic data points to the involvement of subduction-modified (metasomatized) mantle source component and/or juvenile crust, contributed by mantle-derived magmatic underplating in response to the subduction of Mongol–Okhotsk Ocean plate and subsequent collision of Siberian and Mongolia – North China continents. Relatively high I_{Sr} values and Nd model ages suggest significant involvement of Precambrian continental crust in the source of Mesozoic deposits. Based on

their relatively high $\epsilon\text{Nd}(T)$ values and relatively high Mg, Cr, V and Ni contents in Shakhtama granitoids, it is suggested that high-Mg# K adakitic Shakhtama magmas were most probably generated by high-T partial melting of mafic juvenile and old lower crust during delamination and interaction with mantle material.

Relatively low contents of compatible elements and MgO in Zhireken rocks probably indicate that Zhireken melts were generated at the bottom of thickened lower crust by mixing of magmas from partial melting of juvenile and Precambrian lower crust.

Figure 1. Paleozoic-Mesozoic magmatism within the southern margin of the Siberian craton and the location of porphyry Cu-Mo deposits. 1 – Early Paleozoic, 2 – Late Paleozoic to Early Mesozoic, 3 – Mesozoic, 4 – faults, 5 – deposits.



Acknowledgments

This research was financially supported by RFBR grant (16-05-00921).

References

Berzin N.A., Coleman R.G., Dobretsov N.L., Zonenshain L.P., Xiao X., Chang E.Z., 1994. Geodynamic map of the Western part of the Paleo-Asian Ocean. *Russian Geology and Geophysics*, 38 (7–8), 5–22.

Berzina A.P., Berzina A.N., Gimon V.O., Krymskii R.Sh., Larionov A.N.,

Nikolaeva I.V., Serov P.A., 2013. The Shakhtama porphyry Mo ore-magmatic system (Eastern Transbaikalia): age, sources, and genetic features. *Russian Geology and Geophysics* 54 (6), 587-605.

Berzina A.P., Berzina A.N., Gimon V.O., Bayanova T.B., Kiseleva V.Yu., Krymskii R.Sh., Lepekhina

- E.N., Paleskii S.V., 2015. The Zhireken porphyry Mo ore-magmatic system (Eastern Transbaikalia): U–Pb age, sources, and geodynamic setting. *Russian Geology and Geophysics* 56 (3), 446-465.
- Kirwin, D.J., Wilson, C.C., Turmagnai, D., Wolfe, R., 2005. Exploration history, geology, and mineralization of the Kharmagtai gold–copper porphyry district, south Gobi region, Mongolia. In: Seltmann, R., Gerel, O., Kirwin, D.J. (Eds.), *Geodynamics and Metallogeny of Mongolia With a Special Emphasis on Copper and Gold Deposits: IAGOD Guidebook Series, vol. 11*. CERCAMS (Centre for Russian and Central EurAsian Mineral Studies), Natural History Museum, London, United Kingdom, 193–201.
- Lamb, M.A., Cox, D., 1998. New $^{40}\text{Ar}/^{39}\text{Ar}$ age data and implications for porphyry copper deposits of Mongolia. *Economic Geology* 93, 521–529.
- Sotnikov V.I., Ponomarchuk V.A., Shevchenko D.O., Berzina A.P., Berzina A.N., 2001. $^{40}\text{Ar}/^{39}\text{Ar}$ geochronology of magmatic and metasomatic events in the Sora porphyry Cu-Mo ore cluster (Kuznetsk Alatau). *Russian Geology and Geophysics* 5, 786-801.
- Sotnikov V.I., Ponomarchuk V.A., Shevchenko D.O., Berzina A.P., 2005. The Erdenetuin-Obo porphyry Cu-Mo deposit, northern Mongolia: $^{40}\text{Ar}/^{39}\text{Ar}$ geochronology and factors of large-scale mineralization. *Russian Geology and Geophysics* 6, 620-631.
- Watanabe, Y., Stein, H.J., 2000. Re-Os ages for the Erdenet and Tsagaan Suvarga porphyry CuMo deposits, Mongolia, and tectonic implications. *Economic Geology* 95, 1537–1542.
- Yarmolyuk V.V., Kovalenko V.I., 2003. Deep geodynamics and mantle plumes: Their role in the formation of the Central Asian Fold Belt. *Petrology* 11 (6), 504–531.
- Zorin, Yu.A., Belichenko, V.G., Turutanov, E.Kh., Mazukabzov, A.M., Sklyarov, E.V., Mordvinova, V.V., 1997. The structure of the earth's crust and geodynamics of the western part of the Mongol-Okhotsk belt. *Otechestvennaya Geologiya* 11, 52-58. (In Russian).

Preliminary works on the structural geometry of the Pyeongchang area, Taebaeksan zone, Okcheon Belt, Korea

Hee Jun Cheong*, Junrae Noh, Sanghoon Kwon

Department of Earth System Sciences, Yonsei University, Seoul 120-749, Republic of Korea

*Corresponding author e-mail: hjcheong@yonsei.ac.kr

The Okcheon belt is NE-SW trending fold-thrust belt in the middle Korean Peninsula, where the study area (Pyeongchang area) is located at its northwestern area as parts of the Taebaeksan zone. The Pyeongchang area is composed of Cambro-Ordovician Joseon supergroup and Carboniferous-Triassic Pyeongan supergroup (GICTR, 1962; Dongah Geological Consultant, 1978; Cheong et al., 1979; Hong et al., 1995; Kim et al., 1999). The Joseon supergroup includes Ordovician strata of the Jeongseon Limestone, which belongs to Pyeongchang group. The Pyeongan supergroup consists of the Hongjeom, Sadong, Gobangsan and Nokam formations in ascending order. The Jeongseon Limestone is unconformably overlain by the Hongjeom Formation. Major structures in the Pyeongchang area include the Imhari anticline, the Jeongseon Great syncline, and the Pyeongchang fault. The Imhari anticline trends NNE, and shows complex outcrop scale folds. The Jeongseon Great syncline has the map-

scale folded western limb (viz. Jidongri anticline, Nambyeongsan syncline), and is clearly reflected in map pattern of the area (GICTR, 1962; Dongah Geological Consultant, 1978). The NNE-trending Pyeongchang fault cuts the folded western limb of the Jeongseon Great syncline.

To figure out the structural geometry of the Pyeongchang area, we have carried out detailed field surveys and down-plunge projections. In northern part of the study area, repetition of the Jeongseon Limestone and the Pyeongan supergroup defines NNE-trending thrust and EW-trending tear fault. In southern part of the study area, map-scale folds including the NS-trending Jidongri anticline and the NNE-trending Nambyeongsan syncline have different hinge orientations at western limb of the Jeongseon Great syncline. In the central part of the study area, thickness variations in the Jeongseon Limestone exist at the western limb of the Jeongseon Great syncline.

More detailed field survey and structural interpretation of the study area

will provide better understanding the structural geometry of the Pyeongchang area. This, together with structural interpretation of adjacent regions such as the basement thrusts at Jucheon-Pyeongchang area (Lee, 2016) and the thrust duplex at Yeongweol area (Jang et al., 2015), will help to figure out the structural evolution of the Okcheon belt, and will play an important role to construct the tectonic evolution model of East Asia.

References

- Cheong, C.H., Lee, D.Y., Yu, Y.S., and Kang, K.W., 1979a. Explanatory text of the geological map of Pyeongchang and Yeongweol sheet (1:50000). Korea Research Institute of Geoscience and Mineral Resources, Seoul, 19 pages (In Korean with English summary).
- Dongah Geological Consultant Co., 1978. Geology of the Pyeongchang coalfield. Korea Research Institute of Geoscience and Mineral Resources, Seoul, 32 pages (In Korean with English summary).
- Geological Investigation Corps of Taebaeksan Region (GICTR), 1962. Report on the geology and mineral resources of the Taebaeksan Region. The Geological Society of Korea, Seoul, 89 pages (In Korean).
- Hong, S.H., Hwang, S.G., Cho, D.L., 1995. Geological report of the Changdong sheet (1:50000). Korea Research Institute of Geology, Mining and Materials, 27 pages (In Korean with English summary).
- Jang, Y., Kwon, S., Yi, K., 2015. Structural style of the Okcheon fold-thrust belt in the Taebaeksan Zone, Korea. *Journal of Asian Earth Sciences* 105, 140-154.
- Kim, J.H., Son, Y.C., and Koh, H.J., 1999. Characteristic of the so called Banglim Fault and structures of its adjacent area, Pyeongchang, Korea. *Journal of the Geological Society of Korea*, v.35, no. 2, 99-116.
- Lee, H., 2016. Structural geometry and kinematics of the Jucheon-Pyeongchang area of the Okcheon belt, Korea. Master's thesis, Yonsei University, 158 pages (In Korean with English abstract).

Subduction record of the East African Orogen in a whole plate topological framework

Alan S. Collins^{a*}, Andrew Merdith^b, John Foden^a, Donnelly Archibald^a, Morgan Blades^a, Brandon Alessio^a, Haytham Sehsah^a, Simon Williams^b, Dietmar Müller^b

^a Tectonics, Resources and Exploration (TRaX), Department of Earth Sciences, University of Adelaide, SA 5005, Australia

^b Earth Byte Group, School of Geosciences, The University of Sydney, New South Wales, 2006, Australia

Here we present new U-Pb, O and Hf zircon and Nd whole rock isotopic data from Ethiopia, Egypt, Oman, Madagascar, Saudi Arabia and India that, along with published data from other workers, constrain the subduction history of the Mozambique Ocean, and from that the nature of the plate boundaries between Neoproterozoic India, Azania and both the Congo-Tanzania-Bangweulu Block and Sahara Metacraton of Africa. These form the core of a new global plate topological reconstruction that has been constructed using GPlates and incorporates the limited well-constrained palaeomagnetic record for

the Neoproterozoic as well as considerable geological information as to the nature and evolution of the plate margins.

The reconstruction forms an imperfect early version. More complementary data will enhance the reconstruction and we encourage the collection and publication of these data to improve this model. The production of full-plate topological reconstructions now allows tectonic geographic controls on other earth systems to be investigated, such as the possible role of volcanism on initiation of the Cryogenian, or the nature of Mantle convection in the Neoproterozoic.

Characterization of the crystalline basement in Voktipur, Northwest Bangladesh

Sudeb Chandra Das^a, S. M. Mahbubul Ameen^{b*}, Zahidul Bari^b, Mohammad Nazim Zaman^c, Md. Sakaouth Hossain^b, Al-Tamini Tapu^d

^a Morning Glory School and College, Savar Cantonment, Savar, Dhaka-1342, Bangladesh

^b Department of Geological Sciences, Jahangirnagar University, Savar, Dhaka-1342, Bangladesh

^c Institute of Mining, Mineralogy and Metallurgy (IMMM), BCSIR, Joypurhat, Bangladesh

^d Economic Geology, Oulu Mining School, University of Oulu, Oulu, Finland

*Corresponding Author e-mail: ameensmm@juniv.edu

The crystalline basement in Voktipur, northwest Bangladesh occurs in drillhole GDH 53, beneath ~420m of Cenozoic clastic rocks. We present the first account of petrography and geochemistry of the basement rocks from Voktipur, which lies about 50km northeast of the 1.73-1.72Ga Maddhapara diorite-tonalite basement in the Dinajpur block (Ameen et al., 2007; Hossain et al., 2007). The crystalline basement in Voktipur area comprises dominantly felsic rocks with minor leucogranite, felsic gneisses, mafic schists and dykes. Felsic rocks include granodiorite, tonalite and diorite, which were dissected by subordinate mafic (lamprophyre, hornblendite and picrite porphyry) dykes. The picrite porphyry is reported for the first time in the basement in Bangladesh.

The felsic rocks are leuco to mesocratic, exhibit hypidiomorphic, medium to coarse-grained interlocking

texture. They are composed primarily of variable amount of quartz, plagioclase, K-feldspar, amphibole, and biotite. The picrite porphyry is hemicrystalline, melanocratic, and shows porphyritic texture and composed mainly of olivine, pyroxene and biotite as phenocrysts in fine-grained groundmass of mafic minerals and plagioclase. Texturally lamprophyre is almost similar to picrite porphyre, with euhedral phlogopite surrounded by fine-grained groundmass of plagioclase, calcite, mafic and opaques. Hornblendite shows melanocratic, medium- to fine-grained, hypidiomorphic, inequigranular texture and composed mostly of amphibole with biotite, pyroxene and olivine. Gneisses are medium-grained rocks showing gneissic as well as xenomorphic granular texture and mineralogically similar to the felsic rocks. Mafic schists are represented by hornblende and hornblende biotite schist, are fine-grained, show schistose and

granulitic texture and consist of amphibole, biotite, plagioclase and quartz with minor opaques.

Apart from the leucogranite, felsic rocks show a moderate range in SiO₂ (52.3-65.3%), Al₂O₃ (13.04-18.45%), K₂O (2.81-7.70%), Na₂O (1.37-3.70%) and have variably high Fe₂O_{3t} (4.82-12.24%) and MgO (1.51-5.97%) contents. The leucogranite is high in silica (73.67%), alumina (15.81%) and K₂O (5.71%) and low in Na₂O (1.82%), Fe₂O_{3t} (1.32%) and MgO (0.14%). The high Mg# (53-63), moderate Cr (50-80 ppm) and Ni (21-63 ppm) contents in most of the felsic rocks are in the range of high-Mg diorite, granodiorite. The felsic rocks are metaluminous, calc-alkaline in nature, low in ASI values and have pronounced I-type affinity. The Voktipur granitoid rocks are characterized by strong [(La/Yb)_{CN} = 5.10-15.42] enrichment in large ion lithophile elements and distinct negative Nb and Ti and nil to weakly negative Eu anomalies. Trace element characteristics suggest that the parental melt of the granitoid rocks would have generated from a weakly fractionated source in an ocean-continent subduction zone. Assimilation of some mafic material in the source may have contributed to the high-Mg # values and Cr, Ni contents in these rocks. The mafic dykes are characterized by low SiO₂ (45.59-49.58%) and high TiO₂ (0.61%-6.7%), Fe₂O_{3^t} (8.89-16.41%) and MgO (6.47-18.02%). They also have variably high Mg# (50-80), moderately high Ni (41-247ppm) and high Cr (111-626ppm). Considering the chemical characteristics, the mafic rocks were suggested to have originated in a near primitive mantle to mantle wedge environment by mantle

metasomatism aided by prolonged differentiation processes and emplaced within the I-type Voktipur granitoid as late dykes. When compared with the data of the granitoids of the adjacent northeast Indian cratons, the current state of knowledge of the granitoid rocks in Voktipur, Bangladesh does not allow a direct correlation among these rocks from the two crustal blocks. The petrographic, chemical and genetic characteristics of the Voktipur granitoid rocks show similarity to those of the basement in Maddhapara (~50km SW of Voktipur) and therefore suggest that felsic rocks in these two locations may represent either two parts of a single granitoid, or different pulses of felsic magmatism/s of similar characteristics. Precise U-Pb age dating and isotopic study of these rocks are required to constrain the temporal relation and source characteristics of the granitoid lithologies from adjacent areas of northwest Bangladesh and the Indian Shield.

References

- Ameen, S.M.M., Wilde, S.A., Kabir M.Z., Akon, E., Chowdhury K.R and Khan, M.S.H., 2007, Palaeoproterozoic granitoids in the basement of Bangladesh: A piece of the Indian shield or an exotic fragment of the Gondwana jigsaw? *Gondwana Research*, vol. 12, 380-387.
- Hossain, I., Tsunogae, T., Rajesh, H.M., Chean, B., and Arakawa, Y., 2007, Paleoproterozoic U-Pb SHRIMP zircon age from basement rocks in Bangladesh: a remnant of magnetization associated with the Columbia supercontinent. *Comptes Rendus Geosciences*, vol. 339, 979-986.

Petrology and crystallization condition of granitic rocks in Wang Nam Khiao area, Nakhon Ratchasima, Northeastern Thailand

Alongkot Fanka¹, Toshiaki Tsunogae² and Chakkaphan Sutthirat^{1,*}

¹Department of Geology, Faculty of Science, Chulalongkorn University, Pathumwan, Bangkok 10330, Thailand

²Graduate School of Life and Environmental Sciences, University of Tsukuba, Ibaraki 305-8572, Japan

*Corresponding author e-mail: c.sutthirat@gmail.com; chakkaphan.s@chula.ac.th

Granitic rocks have been exposed in Wang Nam Khiao area of Nakhon Ratchasima Province, northeastern Thailand. These rocks are mainly characterized by hornblende-biotite granite and biotite granite which belong to the Eastern Granite Belt of Thailand. The hornblende-biotite granite is dominated by plagioclase, K-feldspar, quartz, hornblende, biotite and accessory minerals including zircon, sphene, and opaque minerals. The biotite granite also comprises similar assemblage except absences of hornblende and sphene. Geothermobarometry, according to amphibole-plagioclase thermometry and Al in hornblende barometry, indicates that crystallization may have P-T constraint between 2.4–5.8 Kb and 580–800°C.

Mineral chemistry of biotite and amphibole, dominant ferromagnesian minerals, indicates process of crystal fractionation of the magma. The biotite composition also suggests the magma origin related to calc-alkaline series involved by subduction. Moreover, amphibole composition also yields consistent result of crystallization process within the arc affinities. This study results are comparable to the arc magmatism of Loei Fold Belt which appears to have associated with the subduction between Palaeo-Tethys beneath Indochina Terrane.

A geophysical over view of the lithospheric structure and evolution of the sahyadris of Central Kerala, India

Ajayakumar P^{1*} and Mahadevan T. M²

¹Department of Marine Geology and Geophysics, Cochin University of Science and Technology, Cochin, India, 682 016.

² Sree Bagh, Ammankovil Road, Cochin, India, 682 035

*Corresponding author e-mail: ajaycochin@cusat.ac.in

In this work an effort is made to synthesise gravity, aeromagnetic and ground magnetic signatures with the geological features over a part of Western Ghats, Midlands and Lowlands in central Kerala to generate insights into their deep continental structure and evolution. The study area covers about 15,000 sq. km between Latitude 9°30'00" N to 10°45'00" N and Longitude 76°00'00" E to 77°30'00" E. The area is bound by the Palghat-Cauvery lineament in the north, and the Kambam lineament in the east, both of which are of Precambrian age (Fig.1a). In the west, the bounding West Coast fault is related to episodic Mesozoic rifting and Deccan volcanism and its precursors. The region has a bi-temporal evolution, a polyorogenic evolution in the Precambrian and a more passive evolution in the Late Mesozoic-Cenozoic. Precambrian formations of high metamorphic facies, namely charnockites and associated gneisses dominate the region. They have a

Pre-Cambrian history of exhumation from lower to mid-crustal levels and accompanying retrogression to amphibolite facies. The area is dissected by significant tectonic lineaments of which the Periyar, Idamalayar and Kerala and Todupuzha dyke lineaments have the most prominent surface expressions. These lineaments host small swarms of late Mesozoic dykes (~ 90 - 65 Ma in age) and bear witness to the Late Mesozoic continental magmatic (basaltic) events and distensional fracturing that overprinted the Pre-Cambrian continental margin. (Ajayakumar et al, 2016, *in press*).

Coastal Tertiary sediments extending westwards from the present coast line include the Cenozoic rifted basins of sedimentation, such as the Cochin and Konkan basins,. These form surface loads that have contributed to flexural isostatic uplift of the Sahyadris.in the late Cenozoic. Gravity modelling along a profile in the Sahyadris of central Kerala

and adjoining regions has revealed that the upper layer containing exhumed lower crustal rocks (2.76 gm/cc) is more or less homogeneous, except for variations in intracrustal layers of decharnockitised hornblende gneisses and intrusive granite bodies. Below this layer is a denser layer (2.85 gm/cc) of unknown composition overlying the MOHO. The Moho depth of the order of 40-41 km below the Periyar plateau has a tendency to thin up to 34-35 km along the West Coast (Ajayakumar et al., 2006), possibly due to the rifting of the

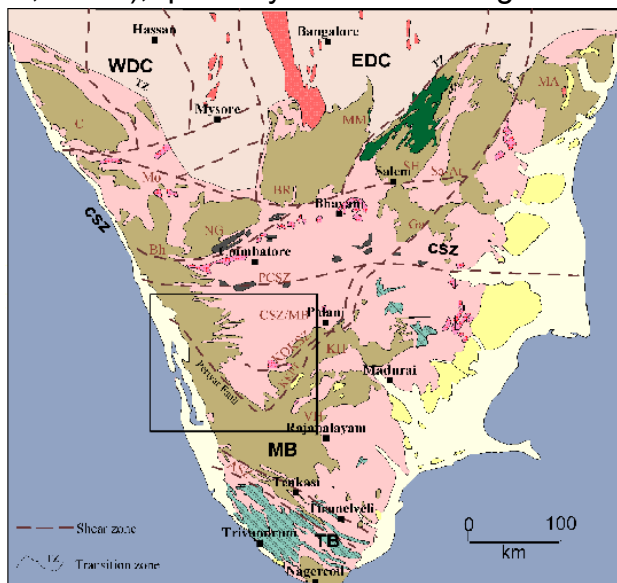


Figure 1a. Simplified south Indian geology map (after GSI and ISRO, 1994) and present study area shown within the rectangular as inset.

The structure below the region is compared with that of two other segments of the SGT from which it differs markedly. The Wynad plateau, north of the Periyar block, forming part of the Sahyadris along the presence of high density (2.98 gm/cc) material in the mid-to-lower crustal portions, bounded by a 2.85 gm/cc density

West Coast during the 65 million year episode of coastal evolution synchronising with Deccan magmatism. In view of the high concentration of dykes in the high-gradient zone southwest of the Periyar lineament, the 2.85 gm/cc layer (Layer A) overlying the MOHO (Fig.1b), could possibly be a zone of underplating with sill-like emplacement of basalts that, among other factors, may have contributed to enhancing the density of the original 2.76 gm/cc layer.

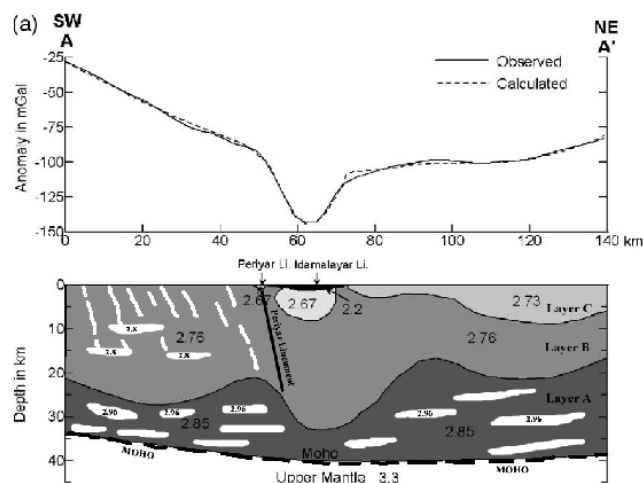


Figure 1b. Interpreted schematic crustal models along a profile in the Periyar plateau region of Sahyadris, central Kerala (White patches show the undertaplating high density materials as sills and dykes).

the western part of the Northern Block of the SGT is characterised by a heterogeneity due to the presence of contrasting crustal blocks on either side of the Bavali shear zone, and layer comparable to the Periyar region (Radhakrishna et al., 2003).

The crust below the Kuppam–Palani

geo-transect is reported to have a four-layer crustal structure with a mid-crustal low velocity (density) layer (Reddy et al., 2003; Singh et al., 2003). The crustal structure below the Kuppam–Palani geo-transect corridor is distinct from that below the Sahyadris and is not representative of the SGT as a whole. The distinctive crustal structure of the Sahayadris of central Kerala and adjoining regions is largely due its Precambrian history of large scale

References

- Ajayakumar P, Baiju K.R and T. M. Mahadevan, 2016. Status of Karur-Kambam-Painavu-Trichur shear zone, Southern Granulite Terrain (SGT) in the context of Late Mesozoic dynamic evolution of Western Ghats: A geophysical – geological perspective. *Current Science (in press)*.
- Ajayakumar P, P. John Kurian, S. Rajendran, M. Radhakrishna, C. G. Nambiar and T. M. Mahadevan, 2006. Heterogeneity in crustal structure across the Southern Granulite Terrain (SGT): Inferences from an analysis of gravity and magnetic fields in the Periyar plateau and adjoining areas. *Gondwana Research*, 10, 18-28.
- Radhakrishna, M., Kurian, P.J., Nambiar, C.G., Murty, B.V.S., 2003. Nature of the crust below the Southern Granulite Terrain (SGT) of Peninsular India across the Bavali shear zone based on analysis of gravity data. *Precambrian Res.* 124, 21–40.
- exhumation of the deep lower crust and the Mesozoic tectono-thermal overprinting. It is suggested that gravity interpretations in areas subjected to Late Mesozoic continental basaltic magmatism and intra-continental comparisons should take into account the possible modification in the deep continental structure due to superposed Late Mesozoic magmatic regimes.
- Reddy, P.R., Rajendra Prasad, B., Vijaya Rao, V., Sain, Kalachand, Prasada Rao,P., Khare, Prakash, Reddy, M.S., 2003. Deep seismic reflection and refraction/wide-angle reflection studies along Kuppam–Palani transect in the Southern Granulite Terrain of India. In: Ramakrishnan, M. (Ed.), *Tectonics of Southern Granulite Terrain: Kuppam–Palani Geotransect*. Geol. Soc. of India, Mem. 50, 79-106.
- Singh, A.P., Mishra, D.C., Vijaya Kumar, V., Vyaghreswara Rao, M.B.S., 2003. Gravity-magnetic signatures and crustal architecture along Kuppam–Palani geotransect, South India. In: Ramakrishnan, M. (Ed.), *Tectonics of Southern Granulite Terrain: Kuppam–Palani Geotransect*. Geol. Soc. of India, Mem. 50, 137-163
- GSI and ISRO, 1994. Project Vasundhara: Generalised Geological Map (Scale 1:2 Million). Geological Survey of India & Indian Space Research Organization, Bangalore.

Petrology and geochemistry of orthogneisses from Austhovde in the Lützow-Holm Complex, East Antarctica: implications for arc magmatism and high-grade metamorphism

Kazuki Takahashi^a, Toshiaki Tsunogae^b, Yusuke Takamura^c, Yohsuke Saitoh^c

^aCollege of Geosciences, University of Tsukuba, Ibaraki 305-8572, Japan

^bFaculty of Life and Environmental Sciences, University of Tsukuba, Ibaraki 305-8572, Japan

^cGraduate School of Life and Environmental Sciences, University of Tsukuba, Ibaraki 305-8572, Japan

The Lützow-Holm Complex (LHC) of East Antarctica exposes various Neoproterozoic high-grade metamorphic rocks formed by complex accretion-collision events related to the amalgamation of Gondwana Supercontinent. Previous petrological studies on metasedimentary and metabasic rocks of the complex suggested an increase in the metamorphic grade from northeast (amphibolite facies) to southwest (granulite facies) (Hiroi et al., 1991; Tsunogae et al., 2015). Recent petrological and geochronological data from the complex indicate that the LHC is a complex collage of Neoproterozoic (ca. 2.5 Ga) and Early Neoproterozoic (ca. 1.0-0.85 Ga) arcs and microcontinents developed through multiple subduction-accretion-collision history (Shiraishi et al., 2008; Tsunogae et al., 2015, 2016, Kazami et al.,

2016). However, detailed studies on the western margin of the complex around Austhovde and Innhovde have not been done. Here, we present new petrological, mineralogical, and geochemical data of granulites from Austhovde and compare the results with those in the other parts of the LHC.

The dominant lithologies in Austhovde are charnockite (quartz + K-feldspar + plagioclase + biotite + orthopyroxene ± garnet ± clinopyroxene), felsic orthogneiss (quartz + plagioclase + K-feldspar + biotite ± garnet ± corundum ± sillimanite ± spinel), intermediate orthogneiss (plagioclase + biotite + quartz + pargasite ± orthopyroxene ± clinopyroxene ± K-feldspar), mafic granulite (plagioclase + orthopyroxene + clinopyroxene ± pargasite ± biotite ± garnet ± quartz), ultramafic rock/pyroxenite

(clinopyroxene + pargasite + plagioclase ± orthopyroxene ± biotite), pelitic gneiss (garnet ± quartz ± biotite ± K-feldspar ± plagioclase ± sillimanite ± spinel-magnetite ± pargasite), garnet-biotite gneiss (garnet + biotite + plagioclase ± K-feldspar ± magnetite-ilmenite ± orthopyroxene ± clinopyroxene ± spinel), quartzite (quartz ± biotite ± K-feldspar ± plagioclase ± sillimanite ± garnet), impure marble (magnesite + olivine + serpentine + biotite), calc-silicate rock/skarn (clinopyroxene ± scapolite ± plagioclase ± amphibole ± quartz ± titanite ± biotite ± olivine ± calcite ± dolomite ± magnesite), and intrusive granite/pegmatite (quartz + K-feldspar + plagioclase ± biotite ± orthopyroxene ± clinopyroxene). The peak metamorphic condition of garnet-bearing mafic granulite (metagabbro) was estimated based on phase equilibrium modeling in NCFMASHTO system as 7.3-8.4 kbar and 800-870°C. The peak stage was probably followed by near isothermal decompression along a clockwise *P-T* trajectory, which is supported by decompression textures around garnet (orthopyroxene + plagioclase symplectite around garnet). The new *P-T* data from Austhovde are nearly consistent with those from other part of the LHC, although it is slightly lower than that from Rundvågshetta which corresponds to the highest metamorphic grade region in the LHC (Yoshimura et al., 2008).

Available geochemistry data of orthogneisses from Austhovde suggest that felsic orthogneiss was formed through felsic to intermediate arc magmatic activity, and its protolith corresponds to monzonite, whereas protoliths of mafic granulites are both volcanic-arc basalt and E-MORB. The results of this study suggest that Austhovde

region corresponds to a part of magmatic arc formed by Neoproterozoic or Early Neoproterozoic arc magmatism, and subsequently underwent granulite-facies metamorphism during the Gondwana assembly.

References

- Hiroi, Y., Shiraishi, K., Motoyoshi, Y., 1991. Late Proterozoic paired metamorphic complexes in East Antarctica, with special reference to the tectonic significance of ultramafic rocks. In: Thomson, M.R.A., Crame, J.A., and Thomson, J.W. (eds) *Geological Evolution of Antarctica*, Cambridge University Press, Cambridge, 83-87.
- Kazami, S., Tsunogae, T., Santosh, M., Tsutsumi, Y., Takamura, Y., 2016. Petrology, geochemistry and zircon U-Pb geochronology of a layered igneous complex from Akarui Point in the Lützow-Holm Complex, East Antarctica: Implications for Antarctica-Sri Lanka correlation. *Journal of Asian Earth Sciences*, doi: 10.1016/j.jseaes.2016.04.025.
- Shiraishi, K., Dunkley, D.J., Hokada, T., Fanning, C.M., Kagami, H., Hamamoto T., 2008. Geochronological constraints on the Late Proterozoic to Cambrian crustal evolution of eastern Dronning Maud Land, East Antarctica: a synthesis of SHRIMP U-Pb age and Nd model age data. *Geological Society, London, Special Publications* 21-67.
- Tsunogae, T., Yang, Q. Y., Santosh, M. 2015. Early Neoproterozoic arc magmatism in the Lützow-Holm Complex, East Antarctica: Petrology, geochemistry, zircon U-Pb

geochronology and Lu–Hf isotopes and tectonic implications. *Precambrian Research* 266, 467–489.

Tsunogae, T., Yang, Q.Y., Santosh, M., 2016. Neoproterozoic – Early Paleoproterozoic and Early Neoproterozoic arc magmatism in the Lützow-Holm Complex, East Antarctica: insights from petrology, geochemistry, zircon U-Pb geochronology and Lu-Hf isotopes. *Lithos*,

doi:10.1016/j.lithos.2016.02.010.

Yoshimura, Y., Motoyoshi, Y., Miyamoto, T., 2008. Sapphirine + quartz association in garnet: implication for ultrahigh-temperature metamorphism in Rundvågshetta, Lützow-Holm Complex, East Antarctica. *Geological Society of London Special Publication* 308, 377-390.

***P-T* fluid evolution of partially retrogressed pelitic granulite: A case study of the southern marginal zone of the Neoproterozoic Limpopo Complex, South Africa**

Tatsuya Koizumi^a, Toshiaki Tsunogae^{a, b}, Dirk D. van Reenen^b

^a Graduate School of Life and Environmental Sciences, University of Tsukuba, Ibaraki 305-8572, Japan

^b Department of Geology, University of Johannesburg, Auckland Park 2006, South Africa

Infiltration of H₂O-bearing fluid into middle to lower crustal level probably gives rise to intensive hydration, metasomatism, and/or partial melting of adjacent anhydrous rocks. Such hydrated/metasomatized/partially-molten rocks may record important information for understanding fluid process in middle to lower crust as well as exhumation history of high-grade metamorphic terranes, which provides important insights on the crust evolution in convergent margin. The Hout River Shear Zone (HRSZ), which marks the boundary between the granulite-facies Limpopo Complex (LC) to the north and the amphibolite-facies Kaapvaal Craton (KC) to the south in South Africa, has been regarded as a north-dipping deep-crustal shear zone along which H₂O-bearing fluid infiltrated during the last stage of orogeny (van Reenen et al., 2014). The southern margin of the LC, which corresponds to the hanging wall of the shear zone, was regionally (>4500 km², 8-18 km in

thickness) affected by the influx of H₂O-bearing fluids along the fluid channel during the exhumation (retrograde) stage at 2.62-2.69 Ga (van Reenen et al., 2014), causing partial hydration of anhydrous mineral assemblages in various rocks (e.g., Opx + Qtz + H₂O => Ath). However, the quantity of water in such retrograde fluids necessary to drive the hydration reactions is unknown. Here, we report new petrological data for partially hydrated pelitic granulites from the Southern Marginal Zone (SMZ) of the Neoproterozoic Limpopo Complex in South Africa, and estimate pressure-temperature condition as well as H₂O content of the rock in mole (M(H₂O)) in order to evaluate *P-T*-fluid evolution of high-grade metamorphic rocks along the HRSZ.

Two new partially-hydrated pelitic granulites examined in this study (samples LCK2-3A and LCK2-3B) were collected from an outcrop within the granulite sub-zone located about 30 km north from the

HRSZ. Although the locality is outside the hydration zone, some hydration textures have been reported in previous studies. Sample LCK2-3A is the dominant rock type of the outcrop, and contains quartz (25-35 vol.%), plagioclase (25-35 vol.%), orthopyroxene (20-25 vol.%), biotite (20-25 vol.%), cordierite (<5 vol.%), gedrite (<5 vol.%) and sillimanite/kyanite (<5 vol.%) with accessory ilmenite, apatite and zircon. Cordierite is pseudomorphic and partly or completely replaced by aggregates of kyanite/sillimanite + gedrite + quartz, suggesting the progress of following hydration reaction: (1) cordierite + H₂O => kyanite/sillimanite + gedrite + quartz, which has been commonly observed in many pelitic granulites in the zone of rehydration and the granulite sub-zone of the SMZ (van Reenen et al., 2014). The mineral assemblage of sample LCK2-3B is similar to that of sample LCK2-3A except the occurrence of coarse-grained subidioblastic garnet (up to 5 cm) surrounded mostly by quartz. The rock is composed of quartz (30-35 vol.%), plagioclase (30-35 vol.%), garnet (15-20 vol.%), biotite (5-10 vol.%), cordierite (5-10 vol.%), orthopyroxene (<5 vol.%), gedrite (<5 vol.%) and sillimanite/kyanite (<5 vol.%) with accessory apatite and zircon. It also shows a hydration texture formed by the progress of reaction (1). The estimated retrograde *P-T-M*(H₂O) conditions of the two samples based on phase equilibria modelling using THERMOCALC in the system NCKFMASH and NCKFMASHTO

indicate the hydration reaction (1) took place at 620-670 °C and 5.0-6.0 kbar, possibly caused by a slight increase of molar H₂O (0 to 1.0 mol.%) with decreasing H₂O activity ($\alpha_{\text{H}_2\text{O}}$) of fluid from 0.2 to 0.1. Although the estimated hydration conditions are nearly consistent with the result of pelitic granulite from the granulite sub-zone (e.g., Bandelierkop quarry), the conditions are slightly lower than those of the rehydration zone (H₂O = 2.0-2.5 mol.%, $\alpha_{\text{H}_2\text{O}}$ = 0.2-0.3; Koizumi et al., 2014). The result of this study indicates that, although the effect of hydration is most significant along the pathway of H₂O-bearing fluids along the HRSZ, the fluid also affected granulites more than 30 km apart from the shear zone.

References

- Koizumi, T., Tsunogae, T., van Reenen, D.D., 2014. Fluid evolution of partially retrogressed pelitic granulite from the Southern Marginal Zone of the Neoproterozoic Limpopo Complex, South Africa: Evidence from phase equilibrium modelling. *Precambrian Research* 253, 146-156.
- van Reenen, D.D., Smit, C.A., Huizenga, J.M., Roering, R., 2014. Fluid-rock interaction during high-grade metamorphism: instructive examples from the Southern Marginal Zone of the Limpopo Complex. *Precambrian Research* 253, 63-80.

U-Pb geochronology of detrital zircon from Sri Lanka and East Antarctica: Implications for the regional correlation of Gondwana fragments

Yusuke Takamura^a, Toshiaki Tsunogae^{a, b}, M. Santosh^{c, d}, Sanjeewa Malaviarachchi^{e, f}, Yukiyasu Tsutsumi^g

^a Graduate School of Life and Environmental Sciences, University of Tsukuba, Ibaraki 305-8572, Japan

^b Department of Geology, University of Johannesburg, Auckland Park 2006, South Africa

^c School of Earth Sciences and Resources, China University of Geosciences Beijing, 29 Xueyuan Road, Beijing 100083, China

^d State Key Laboratory of Continental Dynamics, Department of Geology, Northwest University, Xi'an 710069, China

^e Department of Geology, Faculty of Science, University of Peradeniya, Peradeniya 20400, Sri Lanka

^f Postgraduate Institute of Science, University of Peradeniya, Peradeniya 20400, Sri Lanka

^g Department of Geology and Paleontology, National Museum of Nature and Science, Ibaraki 305-0005, Japan

Neoproterozoic-Cambrian high-grade metamorphic rocks exposed in Sri Lanka and East Antarctica have been regarded as important materials for unraveling the processes of ocean closure and continent-continent collision during Gondwana amalgamation. The Highland Complex (HC), Sri Lanka, and the Lützow-Holm Complex (LHC), East Antarctica, are considered to have been juxtaposed and developed as a depositional basin before the final collision (Shiraishi et al., 1994). In the recent studies, the HC has been proposed as a suture zone formed by double-sided subduction during Neoproterozoic based on petrological and

geochronological data of meta-igneous rocks (e.g. Santosh et al., 2014; He et al., 2016). Similar subduction-related features and Early Neoproterozoic magmatic ages have been reported from meta-igneous rocks in the LHC, based on which it is suggested that the HC and the LHC possibly developed under similar subduction-related setting during Early Neoproterozoic (e.g. Tsunogae et al., 2015; Kazami et al., 2016). However, the LHC also have unique features different from the HC; (i) increase of metamorphic grade from amphibolite-facies in the northeast to granulite-facies in the southwest, (ii) remnants of Neoarchean (ca. 2500 Ma)

magmatic arcs occur adjacent to Neoproterozoic terranes. In order to further evaluate Sri Lanka-Antarctica correlation, detailed geological, petrological, and geochronological investigations on the two complexes are necessary.

Geochronological investigations of detrital zircon and comparison of their age spectra with those of adjacent terranes are common approaches to understand the evolution of orogen and crust, and continent reconstruction. Although some geochronological data suggesting Archean to Paleoproterozoic (ca. 3200-1800 Ma) and Neoproterozoic (ca. 1000-700 Ma) ages have been published from the HC and the LHC (e.g. Kröner et al., 1987; Shiraishi et al., 1994; Dharmapriya et al., 2016), they may not be sufficient to compare the age spectra of the HC and the LHC, and to precisely constrain the provenances of the complexes. In this study, we report new geochronological data on detrital zircons in metasediments from the HC and the LHC, and compare the age spectra of detrital zircons for unraveling the correlation of Sri Lanka and East Antarctica.

The detrital zircon cores from the HC samples show predominant Neoarchean to Paleoproterozoic (ca. 2700-1700 Ma) and minor Neoproterozoic (ca. 800-600 Ma) ages, which is consistent with the results of previous studies. We also found very minor Paleoarchean (ca. 3500 Ma) and Mesoproterozoic (ca. 1200 Ma) zircon grains that have not been reported in previous studies. The main source region is considered to be the Congo-Tanzania-Bangweulu Block in East Africa because Neoarchean to Paleoproterozoic and minor Mesoproterozoic terranes exist in this block. Neoproterozoic detrital

zircons also can be sourced from magmatic suites of the adjacent Wannai, Vijayan and Kadugannawa Complexes, Sri Lanka. The age spectra of the HC are similar to those of the northern Madurai Block, and potentially the Trivandrum Block, southern India (e.g. Plavsa et al., 2014) suggesting strong correlation between the HC and southern Indian terranes.

In contrast, the detrital zircon cores in metasediments from Tenmondai Rock, northeastern part of the LHC, show predominant Neoproterozoic (ca. 1000-700 Ma) and very minor Paleoproterozoic (ca. 2000, 1600 Ma) ages, obviously different from the results of previous studies from the southwestern part of the complex (e.g. Shiraishi et al., 1994). The older components can be derived from Archean to Paleoproterozoic provenances similar to those of the HC, whereas Neoproterozoic detrital zircons are considered to have been sourced from magmatic terranes in the LHC and/or the Rayner Complex. Although the southwestern part of the LHC can be correlated with the HC because of their major Archean to Paleoproterozoic and minor Neoproterozoic detrital zircons, those from the northeastern part have unique age spectra different from the HC. The results of this study indicate the southwestern part of the LHC might be the extension of the HC, whereas the northeastern part can be a different block. The two micro-blocks were formed separately, and juxtaposed together Latest Neoproterozoic Gondwana amalgamation.

References

Dharmapriya, P.L., Malaviarachchi, S.P.K., Sajeev, K., Zhang, C., 2016. New LA-ICP-MS U-Pb ages of detrital zircons

- from the Highland Complex: Insights into Late Cryogenian to Early Cambrian (ca. 665-535 Ma) linkage between Sri Lanka and India. *International Geology Review* (in press).
- He, X.-F., Santosh, M., Tsunogae, T., Malaviarachchi, S.P.K., Dharmapriya, P.L., 2016. Neoproterozoic arc accretion along the 'eastern suture' in Sri Lanka during Gondwana assembly. *Precambrian Research* 279, 57-80.
- Kazami, S., Tsunogae, T., Santosh, M., Tsutsumi, Y., Takamura, Y., 2016. Petrology, geochemistry and zircon U-Pb geochronology of a layered igneous complex from Akarui Point in the Lützow-Holm Complex, East Antarctica: Implications for Antarctica-Sri Lanka correlation. *Journal of Asian Earth Sciences*, doi: 10.1016/j.jseaes.2016.04.025.
- Kröner, A., Williams, I.S., Compston, W., Baur, N., Vithanage, P.W., Perera, L.R.K., 1987. Zircon ion microprobe dating of high grade rocks in Sri Lanka. *Journal of Petrology* 95, 775-791.
- Plavsa, D., Collins, A.S., Payne, J.L., Foden, J.D., Clark, C., Santosh, M., 2014. Detrital zircons in basement metasedimentary protoliths unveil the origins of southern India. *Geological Society of America Bulletin* 126, 791-812.
- Santosh, M., Tsunogae, T., Malaviarachchi, S.P.K., Zhang, Z., Ding, H., Tang, L., Dharmapriya, P.L., 2014. Neoproterozoic crustal evolution in Sri Lanka: Insights from petrologic, geochemical and zircon U-Pb and Lu-Hf isotopic data and implications for Gondwana assembly. *Precambrian Research* 255, 1-29.
- Shiraishi, K., Ellis, D.J., Hiroi, Y., Fanning, C.M., Motoyoshi, Y., Nakai, Y., 1994. Cambrian orogenic belt in east Antarctica and Sri Lanka: implications for Gondwana assembly. *Journal of Geology* 102, 47-65.
- Tsunogae, T., Yang, Q., Santosh, M., 2015. Early Neoproterozoic arc magmatism in the Lützow-Holm Complex, East Antarctica: petrology, geochemistry, zircon U-Pb geochronology and Lu-Hf isotopes and tectonic implications. *Precambrian Research* 266, 467-489.

Decarbonation of carbonate and formation of incipient charnockite in South-Central Madagascar

Toshiaki Tsunogae^{a, b*}, Takahiro Endo^a, M. Santosh^{c, d}, E. Shaji^e, Roger A. Rambeloson^f

^a Graduate School of Life and Environmental Sciences, University of Tsukuba, Ibaraki, 305-8572, Japan

^b Department of Geology, University of Johannesburg, Auckland Park 2006, South Africa

^c School of Earth Sciences and Resources, China University of Geosciences Beijing, 29 Xueyuan Road, Beijing 100083, China

^d Centre for Tectonics Resources and Exploration, Department of Earth Sciences, University of Adelaide, SA 5005, Australia

^e Department of Geology, University of Kerala, Kariyavattom, Trivandrum, India

^f Département des Sciences de la Terre, Université d'Antananarivo, B.P 906 - 101 Antananarivo, Madagascar

More than fifty years ago, Pichamuthu (1960) first reported dark veins and irregular patches of charnockite (orthopyroxene-bearing granitic rock) within amphibole-biotite gneiss from a quarry near Kabbal village, Karnataka State in the Archean Dharwar Craton of southern India, and attributed the presence of orthopyroxene to localized prograde metamorphism. Since then, numerous occurrences of such 'incipient' charnockites have been reported from granulite terranes worldwide, particularly from latest Neoproterozoic – Cambrian high-grade terranes in southern India, Sri Lanka, and Madagascar, which corresponds to the collisional orogen formed during the final amalgamation of Gondwana Supercontinent. Previous fluid inclusion

studies on incipient charnockite reported the occurrence of abundant CO₂-rich fluid inclusions (e.g., Hansen et al., 1984; Santosh et al., 1991, and many others), based on which they argued infiltration of CO₂-rich anhydrous fluids resulted in the lowering of water activity and stabilization of orthopyroxene-bearing dry assemblage in charnockite. However, the origin of such CO₂-rich fluids is still not known. In this study, we report detailed petrological data of incipient charnockite within biotite gneisses from south-central Madagascar, and discuss the petrogenesis of the charnockite through decarbonation of adjacent calc-silicate rocks.

The incipient charnockites (biotite + orthopyroxene + K-feldspar + plagioclase + quartz + magnetite + ilmenite) occur as

brownish patches, lenses, and layers within host orthopyroxene-free biotite gneiss (biotite + K-feldspar + plagioclase + quartz + magnetite + ilmenite). The application of mineral equilibrium modeling on the charnockite assemblage in NCKFMASHTO system on coarse-grained charnockite defines a *P-T* range of 840-880°C and 4.5-10.4 kbar, which is nearly consistent with the inferred *P-T* condition of the study area. Our fluid inclusion study on the charnockite indicates that pure CO₂ fluid with melting temperatures around -56.6°C was trapped as secondary phases in plagioclase and quartz. The close association of calc-silicate rocks and the charnockite suggests that the CO₂-rich fluid that caused dehydration and incipient charnockite formation might have been derived through decarbonation of calc-silicate rocks during high-grade metamorphism.

References

- Hansen, E.C., Janardhan, A.S., Newton, R.C., Prame, W.K.B.N., Kumar, G.R.R., 1987. Arrested charnockite formation in southern India and Sri Lanka. *Contributions to Mineralogy and Petrology* 96, 225-244.
- Pichamuthu, C.S., 1960. Charnockite in the making. *Nature* 188, 135-136.
- Santosh, M., Jackson, D.H., Harris, N.B.W., Matthey, D.P., 1991. Carbonic fluid inclusions in South Indian granulites: evidence for entrapment during charnockite formation. *Contributions to Mineralogy and Petrology* 108, 318-330.

Petrology and geochemistry of orthogneisses from Austhovde in the Lützow-Holm Complex, East Antarctica: implications for arc magmatism and high-grade metamorphism

Kazuki Takahashi^a, Toshiaki Tsunogae^b, Yusuke Takamura^c, Yohsuke Saitoh^c

^aCollege of Geosciences, University of Tsukuba, Ibaraki 305-8572, Japan

^bFaculty of Life and Environmental Sciences, University of Tsukuba, Ibaraki 305-8572, Japan

^cGraduate School of Life and Environmental Sciences, University of Tsukuba, Ibaraki 305-8572, Japan

The Lützow-Holm Complex (LHC) of East Antarctica exposes various Neoproterozoic high-grade metamorphic rocks formed by complex accretion-collision events related to the amalgamation of Gondwana Supercontinent. Previous petrological studies on metasedimentary and metabasic rocks of the complex suggested an increase in the metamorphic grade from northeast (amphibolite facies) to southwest (granulite facies) (Hiroi et al., 1991; Tsunogae et al., 2015). Recent petrological and geochronological data from the complex indicate that the LHC is a complex collage of Neoproterozoic (ca. 2.5 Ga) and Early Neoproterozoic (ca. 1.0-0.85 Ga) arcs and microcontinents developed through multiple subduction-accretion-collision history (Shiraishi et al., 2008; Tsunogae et al., 2015, 2016, Kazami et al., 2016). However, detailed studies on the western margin of the complex around

Austhovde and Innhovde have not been done. Here, we present new petrological, mineralogical, and geochemical data of granulites from Austhovde and compare the results with those in the other parts of the LHC.

The dominant lithologies in Austhovde are charnockite (quartz + K-feldspar + plagioclase + biotite + orthopyroxene ± garnet ± clinopyroxene), felsic orthogneiss (quartz + plagioclase + K-feldspar + biotite ± garnet ± corundum ± sillimanite ± spinel), intermediate orthogneiss (plagioclase + biotite + quartz + pargasite ± orthopyroxene ± clinopyroxene ± K-feldspar), mafic granulite (plagioclase + orthopyroxene + clinopyroxene ± pargasite ± biotite ± garnet ± quartz), ultramafic rock/pyroxenite (clinopyroxene + pargasite + plagioclase ± orthopyroxene ± biotite), pelitic gneiss (garnet ± quartz ± biotite ± K-feldspar ± plagioclase ± sillimanite ± spinel-magnetite

± pargasite), garnet-biotite gneiss (garnet + biotite + plagioclase ± K-feldspar ± magnetite-ilmenite ± orthopyroxene ± clinopyroxene ± spinel), quartzite (quartz ± biotite ± K-feldspar ± plagioclase ± sillimanite ± garnet), impure marble (magnesite + olivine + serpentine + biotite), calc-silicate rock/skarn (clinopyroxene ± scapolite ± plagioclase ± amphibole ± quartz ± titanite ± biotite ± olivine ± calcite ± dolomite ± magnesite), and intrusive granite/pegmatite (quartz + K-feldspar + plagioclase ± biotite ± orthopyroxene ± clinopyroxene). The peak metamorphic condition of garnet-bearing mafic granulite (metagabbro) was estimated based on phase equilibrium modeling in NCFMASHTO system as 7.3-8.4 kbar and 800-870°C. The peak stage was probably followed by near isothermal decompression along a clockwise *P-T* trajectory, which is supported by decompression textures around garnet (orthopyroxene + plagioclase symplectite around garnet). The new *P-T* data from Austhovde are nearly consistent with those from other part of the LHC, although it is slightly lower than that from Rundvågshetta which corresponds to the highest metamorphic grade region in the LHC (Yoshimura et al., 2008).

Available geochemistry data of orthogneisses from Austhovde suggest that felsic orthogneiss was formed through felsic to intermediate arc magmatic activity, and its protolith corresponds to monzonite, whereas protoliths of mafic granulites are both volcanic-arc basalt and E-MORB. The results of this study suggest that Austhovde region corresponds to a part of magmatic arc formed by Neoproterozoic or Early Neoproterozoic arc magmatism, and subsequently underwent granulite-facies

metamorphism during the Gondwana assembly.

References

- Hiroi, Y., Shiraishi, K., Motoyoshi, Y., 1991. Late Proterozoic paired metamorphic complexes in East Antarctica, with special reference to the tectonic significance of ultramafic rocks. In: Thomson, M.R.A., Crame, J.A., and Thomson, J.W. (eds) *Geological Evolution of Antarctica*, Cambridge University Press, Cambridge, 83-87.
- Kazami, S., Tsunogae, T., Santosh, M., Tsutsumi, Y., Takamura, Y., 2016. Petrology, geochemistry and zircon U-Pb geochronology of a layered igneous complex from Akarui Point in the Lützow-Holm Complex, East Antarctica: Implications for Antarctica-Sri Lanka correlation. *Journal of Asian Earth Sciences*, doi: 10.1016/j.jseaes.2016.04.025.
- Shiraishi, K., Dunkley, D.J., Hokada, T., Fanning, C.M., Kagami, H., Hamamoto T., 2008. Geochronological constraints on the Late Proterozoic to Cambrian crustal evolution of eastern Dronning Maud Land, East Antarctica: a synthesis of SHRIMP U-Pb age and Nd model age data. *Geological Society, London, Special Publications* 21-67.
- Tsunogae, T., Yang, Q. Y., Santosh, M. 2015. Early Neoproterozoic arc magmatism in the Lützow-Holm Complex, East Antarctica: Petrology, geochemistry, zircon U-Pb geochronology and Lu-Hf isotopes and tectonic implications. *Precambrian Research* 266, 467-489.
- Tsunogae, T., Yang, Q.Y., Santosh, M., 2016. Neoproterozoic – Early Paleoproterozoic and Early

Neoproterozoic arc magmatism in the Lützow-Holm Complex, East Antarctica: insights from petrology, geochemistry, zircon U-Pb geochronology and Lu-Hf isotopes. *Lithos*, doi:10.1016/j.lithos.2016.02.010.

Yoshimura, Y., Motoyoshi, Y., Miyamoto, T.,

2008. Sapphirine + quartz association in garnet: implication for ultrahigh-temperature metamorphism in Rundvågshetta, Lützow-Holm Complex, East Antarctica. *Geological Society of London Special Publication 308*, 377-390.

Mylonites in the Achankovil shear zone, Southern India: Microstructural evolution and deformation mechanisms

Vikas C.^{1*}, Pratheesh P.²

¹ ONGC, FB, Cauvery Asset, Karaikal, Pondyerry, India.

² CGIST, University of Kerala, Thiruvananthapuram, Kerala- 695 581, India

*Corresponding Author e-mail: vikascnair@gmail.com

The NW-SE trending Achankovil shear zone (AKSZ), a major crustal discontinuity in Southern India, which extends for about 120 km through the states of Kerala and Tamilnadu, separates the granulite facies Madurai block to the north from the khondalite belt (Trivandrum block) to the south. Mylonite and mylonitic patches in sheared gneisses with numerous shear indicators have developed along the strike length of the shear zone. The general tectonic framework of the AKSZ indicates polyphase deformation and metamorphism, suggesting reactivation with domains on various scales exhibiting structures indicative of opposing shear senses. The sheared gneissic rocks exhibit a strongly developed penetrative foliation trending in the NW-SE direction with moderate dips towards SW. Detailed field and laboratory investigations reveal a complete sequence of relatively low strained and coarse grained protolith

outside the shear zone to highly strained and fine grained ultramylonite in the centre of the shear zone. Three principal types of microstructures were recognized: preserved fabrics outside the shear zone (Type-1), partly recrystallised shear zone fabrics (Type-2) and reequilibrated shear zone fabrics (Type-3). A strong tectonic L-S fabric has developed characterised by grain size reduction, increasing flattening, elongation and dimensional preferred orientation of constituent minerals corresponding to a progression in strain. The microstructural studies of mylonites indicate that AKSZ has undergone extensive ductile shearing accompanied by fluid induced retrograde metamorphism. The progressive evolution of mylonite causes a change in the deformation mechanisms from dislocation creep through grain boundary sliding to grain size dependent diffusional flow, leading to strain softening.

Mylonites are commonly formed by ductile deformation through crystal plastic grain size reduction and recrystallisation. Ductile shear zones offer a unique opportunity to study the progressive development of microstructures and fabrics with increasing strain. They also provide through these features, an insight into the deformation process associated with large strain deformation and strain-softening mechanism. The Achankovil shear zone (AKSZ), a NW–SE trending strike slip shear zone of late Proterozoic age, situated in the southern part of the Southern Granulite terrain (SGT) is conspicuous in the satellite imageries and aero magnetic data (Drury and Holt, 1980). It is 8-10 km wide and can be traced for about 120 km starting from the west coast (Prasannakumar, 1998). Within the SGT, AKSZ separates Trivandrum block (TB) which lies to the south of shear zone to Madurai block (MB) in the north. Achankovil shear zone is defined as a shear zone based on the change in rock types to the north and south, and by the sharp change from NE-trending structures north of the belt to NW-trending structures within and to the south of it (Drury et al. 1984). Shearing in the AKSZ has been described as dextral (Sacks et al. 1997) or sinistral (Rajesh et al. 1998) based on mesoscopic shear sense indicators and the kinematic evolution of this crustal-scale structure is debated. The systematic field investigations across the area, especially along a major part of length and width of the zone falling in the states of Kerala and Tamilnadu indicate that there exists a distinct zone of highly sheared gneisses with numerous kinematic indicators and hence it can be considered as a shear

zone. Even though AKSZ appear to be ductile in nature, the microstructural features are not extensively studied to support the same. In such cases, microfabrics, when used in conjunction with the mesoscopic fabrics, have proved to be significant proxies for tectonite fabrics. Hence, the present work is an attempt to understand the micro structural behaviour of the mylonites from the AKSZ and its tectonic significance.

Massive charnockites dominate the lithology in the MB while khondalites and leptynites represent dominant lithology in the TB. Rocks within the shear belt are represented by deformed and highly migmatized garnet-biotite gneiss, cordierite gneiss, mylonite, charnockite (both massive and patchy), pyroxene granulite, calc-granulite and marble. Granite, gabbro and dunite are found as later intrusives into the dominant rock types. These rocks have been mylonitised and retrogressed, especially along shear planes. A strong tectonic L-S fabric has developed and the mylonitic fabric is well exhibited by the quartzofeldspathic and calcareous rocks than charnockite and other rock types. Gneissic rocks exhibit a strongly developed penetrative foliation trending in the NW-SE direction with moderate dips towards SW.

Polyphase deformation and metamorphism accompanied by shearing has given rise to different textural variants of mylonites in AKSZ. Detailed field and laboratory investigations reveal a complete sequence of relatively low strained and coarse grained protolith outside the shear zone to highly strained and fine grained ultramylonite in the centre of the shear zone. The Type-1 fabric, marked by the rocks outside the shear zone, is broadly

gneissic in nature and contains large unoriented feldspar grains together with biotite and quartz. Microstructurally, protomylonites are much similar to the protolith. The protomylonite is coarse grained and has undergone little grain refinement. Quartz form large elongate monocrystalline ribbons (Fig.1a) or as thick polycrystalline aggregates showing weak undulose extinction. Feldspars show limited plastic deformation in the form of weak to strong undulose extinction, deformation twinning and kinking and at many places, they are fractured and displaced with mica recrystallisation along these fractures. At high temperature metamorphic conditions, curved and lobate grain boundaries between quartz and feldspar in gneisses may be taken as an evidence for grain boundary sliding and solid state diffusion creep experienced by mineral grains (Passchier and Trouw, 2005). Near the shear zone boundary, Type-2 fabric is represented by porphyroclastic mylonite (Fig.1b) and mylonite showing signs of dynamic recrystallisation and decrease in grain size as compared to the coarse-grained Type-1 fabric. Quartz has suffered greater recrystallisation and sub grain development as the result of shearing. The typical internal feature is chess-board undulatory extinction or prism subgrain boundaries oriented obliquely to ribbon margins (Fig.1c). Feldspars occur either as porphyroclasts or as small grains in the groundmass and show features typical of ductile deformation like wavy extinction, deformation twinning, kinking of twin lamellae and sub grain development. Some original muscovite occurs in the form of porphyroclasts and mica fish while smaller recrystallised grains of mica defining

mylonitic foliation are recognized. Thus the sub grain formation, wavy extinction and the development of quartz ribbons suggest that dislocation creep type mechanisms accompanied by dynamic recrystallisation form the dominant deformation mechanism (Passchier and Trouw, 2005) producing steady flow in the rock which led to grain refinement. High shear strain microstructures (Type-3 fabrics) are typical of centre of the shear zone where mylonite grades into ultramylonite (Fig.1d), characterised by uniform grain-size, well-equilibrated feldspar microstructure and mineral assemblage (biotite replacing garnet) indicating amphibolite facies retrograde conditions. Fluid influx associated with shearing results in extensive biotisation of ultramylonites. Grain boundary migration recrystallisation becomes important in this zone.

Healed up late intragranular fractures filled up with smaller recrystallised quartz grains indicate late pulse of brittle deformation. The presence of various reaction textures, coronas and symplectitic intergrowths of cordierite, K-feldspar and quartz after orthopyroxene and garnet are indicators of near isothermal decompression and rapid uplift ((Santosh, 1987). This supports the Fault zone model of Sibson (Sibson, 1983) stating the formation of mylonites by ductile deformation process at 300-4000 C and 10-15 km depth, which are now exposed to the surface due to uplift and erosion. The widespread retrogression and metasomatism has been caused by the deep seated fluids (H₂O and CO₂) which conduits through the fractures of AKSZ during the process of tectonic upliftment. During the initial stages of exhumation, the

interaction of H₂O influx with the granulites causes retrograde hydration and the retrogression effect of mylonites is syn to late stage phenomena of progressive mylonitization. Thus, the degree of mylonitisation varies from place to place, in the domain of a thin section to the scale of a map. The progressive evolution of mylonite would cause a change in the deformation mechanisms from dislocation creep through grain boundary sliding to grain size dependent diffusional flow, leading to strain softening.

References

- Drury, S.A., Holt, R.W., 1980. The tectonic frame work of South India. A reconnaissance involving LANDSAT Imagery. *Tectonophysics*, 65, 1-15.
- Drury, S.A., Harris, N.B.W., Holt, R.W., Reeves-Smith, G.J., Wightman, R.T., 1984. Precambrian tectonics and crustal evolution in South India. *Journal of Geology* 92, 3 - 20.
- Passchier, C.W., Trouw, R.A.J., 2005. *Microtectonics*. 2nd revised edition, Springer-Verlag, Berlin-Heidelberg, 371.
- Prasannakumar, V., 1998. Kinematics of Achankovil Shear Zone. *Gondwana Research* (Correspondence – Gondwana News letter section) 1, 407.
- Rajesh, H.M., Santosh, M., Yoshida, M., 1998. Dextral Pan African shear along the south western edge of the Achankovil shear belt, South India: Constraints on Gondwana reconstructions: A Discussion. *Journal of Geology* 106, 105 - 114.
- Sacks, P.E., Nambiar, C.G., Walters, L.J., 1997. Dextral Pan-African shear along the South western Edge of the Achankovil Shear Belt, South India: Constraints on Gondwana Reconstructions. *Journal of Geology* 105, 275 - 284.
- Santosh, M., 1987. Cordierite gneisses of Southern Kerala, India: Petrology, fluid inclusions and implications for crustal uplift history. *Contributions to Mineralogy and Petrology* 96, 343 - 356.
- Sibson, R.H., 1983. Continental fault structure and shallow earthquake source. *Journal of Geological Society of London* 140, 741–767.

PT-parameters and time UHT metamorphism in South-Western Siberian craton (Yenisei Ridge, Russia)

V.P. Sukhorukov^{1, 2} and O.M. Turkina^{1, 2}

¹ V.S. Sobolev Institute of Geology and Mineralogy SB RAS, Novosibirsk, Russia

² Novosibirsk State University, Novosibirsk, Russia

The southern part of the Yenisei Ridge (Angara-Kan terrane) belongs to the basement structures of the southwestern Siberian Platform. It consists predominantly of Early Precambrian Kan granulitic and Yenisei amphibolite–gneiss complexes. The high-temperature metamorphism of the Kan complex and associated granite emplacement were related to the formation of Paleoproterozoic (1.8–2.0 Ga) collisional orogens, traced in all the basement uplifts of the Siberian Platform (Aldan and Anabar Shields; Sharyzhalgay, Angara–Kan, and Biryusa Uplifts) (Rosen et al., 1994). According to U–Pb zircon dating, metamorphism of paragneiss and migmatization occurred at 1.87–1.89 Ga (Urmantseva et al., 2012). Afterward the postcollisional granites of the Taraka pluton (1837 ± 3 Ma) intruded the metamorphic rocks of the Kan complex (Nozhkin et al., 2003). The Kan metamorphic complex composes the central part of the Angara–Kan terrane and is intruded in the east by the Paleoproterozoic granitoids of the Taraka pluton (Fig. 1). The complex is

dominated by orthopyroxene, garnet–orthopyroxene, and garnet–biotite plagioclase and two-feldspar gneisses (Nozhkin and Turkina, 1993). High-Al cordierite- and sillimanite-bearing gneisses make up from 15 to 30% of the Kan granulites. The gneiss protoliths correspond mainly to terrigenous rocks from sandstones and graywackes to mature pelites (Nozhkin et al., 2010).

Granulites with UHT mineral associations were found on the right banks of the Yenisey River in the upper reach of the Kuzjeva River and her tributary of Malaya Kuzjeva and Anenskiy streams. UHT rocks include garnet-bearing orthopyroxene gneisses, orthopyroxene-feldspar gneisses and sillimanite-bearing charnokites. Mineral assemblages of granulites are $\text{Opx} + \text{Grt} + \text{Sil} + \text{Bt} + \text{Pl} + \text{Kfs} + \text{Qtz} (+ \text{Spf} + \text{Crn} + \text{Mgt} + \text{Ti-Mgt} + \text{Spl})$ and $\text{Opx} + \text{Pl} + \text{Kfs} + \text{Qtz} + \text{Ilm} (+ \text{Bt} + \text{Crd} + \text{Sill} + \text{Mt} + \text{Ti-Mgt} + \text{Spl})$, charnokites - $\text{Opx} + \text{Pl} + \text{Kfs} (+ \text{Bt} + \text{Sil} + \text{Crd} + \text{Ti-Mgt})$.

Orthopyroxene in garnet-bearing granulites contain up to 9.9 wt.% of Al_2O_3 .

Garnet usually forms rims around orthopyroxene and Spl-Mgt-Crn intergrowth. Feldspars are represented by perthitic Kfs, antiperthitic Pl and mesopertites. Mesopertites can form separate grains or rims around plagioclase grains. Mesopertites can contain vermicular inclusions of orthopyroxene with 7-8 wt.% of Al₂O₃. Ternary feldspar composition and Al content in orthopyroxene indicate peak metamorphic temperatures of \approx 1070-1100°C. Grt-Opx geothermometer and Grt-Opx-Pl geobarometer yield a temperature range of 890-955°C and pressure range from 7.5 to 10 kbar and indicate post-peak PT-conditions. Metamorphic zircons of granulites are variably enriched in Ti ranging from 69 to 18 ppm and based on Ti-in-zircon thermometer (Ferry, Watson, 2007) show wide temperature range between 1020 and 840°C.

Charnokites contain vermicular intergrowths of cordierite and K-feldspar with orthopyroxene and quartz. These intergrowths are often interpreted as replacement product of osumilite. Mineral association and microstructure observed in granulites show predominately cooling retrograde PT – path which was followed by decompression.

The SHRIMP age data were obtained for more than 100 zircon grains from different UHT rocks. All samples contain zircon grains with core-rim structure and rounded or soccer-ball zircons which are typical for granulites. Zircons have a large range of Th/U ratio (0.01-4.9). There are three age peaks for metamorphic zircons in studied rocks. The old age peak was revealed for zircons from garnet-bearing granulites (1886±14 Ma) and charnokites (1871±15 Ma). The second peak in range of 1798±7 to 1780±8

Ma was established in all UHT granulites. Zircons of this group show the highest Ti-in-Zrn temperatures (up to 1020°C) and probably reflect the time of UHT metamorphic event. The third group of zircons was found only in charnokite sample and yielded age of 1745±11 Ma.

Thus we suggest that the whole duration of high-temperature metamorphic evolution in Angara-Kan terrane was about 100 millions years between 1.89 and 1.78 Ga and included two distinct events. The first metamorphic event restricted 1.89-1.87 Ga was related with collisional tectonics and culminated by emplacement of post-collisional granites at 1.84 Ga (Nozhkin et al., 2003). Later UHT metamorphic event supposed to be related with extension and crustal heating due to asthenosphere rising. Zircon ages from granulites and charnokites show wide range from \approx 1.8 to \approx 1.75 Ga and indicate long duration of UHT metamorphism and charnokite intrusion.

This work was supported by grants 15-05-02964 and 14-05-00373 from the Russian Foundation for Basic Research.

References

- Ferry J.M., Watson E.B., 2007. New thermodynamic models and revised calibrations for the Ti-in-zircon and Zr-in-rutile thermometers. *Contrib. Mineral. Petrol.*, 154, 429-437.
- Nozhkin, A.D., Bibikova, E.V., Turkina, O.M., Ponomarchuk, V.A., 2003. U-Pb, Ar-Ar, and Sm-Nd isotope-geochronological study of porphyritic subalkalic granites of the Taraka pluton (Yenisei Range). *Geologiya i Geofizika (Russian Geology and Geophysics)* 44 (9), 879–889 (842–852).

- Nozhkin, A.D., Dmitrieva, N.V., Turkina, O.M., Maslov, A.V., Ronkin, Yu.L., 2010. Lower Precambrian metapelites of the Yenisei Range: REE systematics, provenances, paleogeodynamics. Dokl. Earth Sci. 434 (2), 1390–1395.
- Rosen, O.M., Condie, K.C., Natapov, L.M., Nozhkin, A.D., 1994. Archean and Early Proterozoic evolution of the Siberian craton: a preliminary assessment, in: Archean Crustal Evolution. Elsevier, Amsterdam, pp. 411–459.
- Urmantseva, L.N., Turkina, O.M., Larionov, A.N., 2012. Metasedimentary rocks of the Angara-Kan granulite-gneiss block (Yenisey Ridge, southwestern margin of the Siberian Craton): provenance characteristic, deposition and age. J. Asian Earth Sci. 49, 7–19.

Occurrence and characterization of ferberite: implications to tungsten mineralization in high temperature shear zone of the Eastern Ghats Mobile Belt, India

G. Parthasarathy*, T.R.K. Chetty and M. Satyanarayanan

CSIR- National Geophysical Research Institute, Uppal Raod, Hyderabad- 500007, Telangana, India.

*Corresponding Author e-mail: drg.parthasarathy@gmail.com

Tungsten is an important industrial metal with numerous applications in microwave scintillation, anodes in photoelectrolyses, optical modulation, magnetic devices, humidity sensors etc. Ferberite (FeWO_4) is an end member of the wolframite solid solutions series that constitutes an important part of tungsten mineralisation. This occurs in association with high and medium temperature hydrothermal quartz veins as well as in granite pegmatites. We report here about the occurrence, structure and electrical properties of Ferberite ($\text{Fe}_{0.98}\text{Mn}_{0.02}\text{WO}_4$) from the Tapasikonda tungsten bearing graphite deposit of the Eastern Ghats Mobile Belt (EGMB) of India.

Tungsten bearing graphite gneiss in association with quartz pegmatite is enclosed by garnet- sillimanite-quartz-feldspar rock popularly known as khondalitic rocks. Geological setting of the region was discussed earlier by other

workers elsewhere (Parthasarathy et al, 2006; Umathay and Pophare 2014). Composition of the samples were determined by EPMA and XRF at room temperature. The samples were found to have 2 mol % of huebnerite MnWO_4 . Powder X-ray diffraction measurements showed that the sample has an orthorhombic unit cell with cell parameters $a= 0.4727$ nm; $b=0.57$ nm; and $c= 0.495$ nm. It is well known that Ferberite is monoclinic structure with cell parameters $a= 0.475$ nm; $b=0.572$ nm; $c= 0.497$ nm and $\beta=90^\circ 10'$. The higher symmetry of the present sample indicates high temperature isomorphic phase transition. Further the purity of Ferberite has been independently verified with the dc electrical resistivity measurements in the temperature range of 300- 800 K. The four probe electrical resistivity measurements showed that the sample having resistivity value of 3.3×10^3 Ωcm and activation energy of 0.20

eV, which agrees well with the reported values for the pure synthetic FeWO_4 (5×10^2 to 10^5 μm and 0.15 to 0.32 eV respectively; Schmidbauer et al. 1991). Laser Raman spectroscopic studies showed strong peaks at 154, 208, 330, 401, 534, 777 and 880 cm^{-1} confirming the purity of Ferberite. Our present results on the purity of Ferberite composition and crystalline structure of FeWO_4 complements the findings of our earlier studies on fluid deposited rhombohedral graphite (Parthasarathy et al. 2006) from the same region of the Tapasikonda-Burugubanda shear zone of the EGMB, which might have experienced high temperature 1100- 1150 K fluid activity during Proterozoic period.

Acknowledgements:

We thank CSIR-SHORE, PLANEX, SAC-ISRO Government of India for funding. One

of us (TRKC) thanks DST for the financial support through book-writing program.

References

- Parthasarathy, G., Sreedhar, B., Chetty, TRK. (2006) Spectroscopic and X Ray diffraction studies on fluid deposited rhombohedral graphite from the Eastern Ghats Mobile Belt, India. *Current Science*, 90, 995-1000.
- Schmidbauer, E., Schanz, U., and Yu F.J., 1991, electrical transport properties of mono- and polycrystalline FeWO_4 . *J. Phys. Condensed Matter*. 3, 5341-5352.
- Umathay, R.M., and Pophare, A.M. (2014) Revisit to Graphite, Tungsten deposits of East Godavai District, Andhra Pradesh. *J. Geol.Soc. India* 84, 417-430.

Precambrian crustal growth in Kotri belt, Bastar Craton, Central India

C. Manikyamba^{a,*}, M. Santosh^{b, c}, B. Chandan Kumar^{a, d}, S. Rambabu^a, Li Tang^c,
Abhishek Saha^{a, e}, D.V. Subba Rao^a

^aNational Geophysical Research Institute (Council of Scientific and Industrial Research), Uppal Road, Hyderabad 500 007

^bCentre for Tectonics, Resources and Exploration, Department of Earth Sciences, University of Adelaide, SA 5005, Australia

^cSchool of Earth Science and Resources, China University of Geosciences, Beijing, China

^dKarnatak University, Pavatenagar, Dharwad-580007, India

^eNational Institute of Oceanography (Council of Scientific and Industrial Research), Regional Centre, Visakhapatnam 530017

*Corresponding author e-mail: cmaningri@gmail.com

The Precambrian crust of Central India as preserved in Bastar and Bundelkhand cratons are accreted in the northern and southern parts of Central Indian Tectonic Zone (CITZ). The Bastar Craton composed of cratonic components representing the geological events spanning from Mesoarchean to Neoproterozoic in age. One of the most prominent features in the central part of the craton is the N-S trending Kotri-Dongargarh belt where a thick sequence of volcano-sedimentary rocks is preserved which are distributed in the Amgaon, Bengpal, Bailadila and Nandagaon Groups. The Nandagaon Group has bimodal volcanic rocks in which the basalts exhibit

porphyritic to spherulitic texture with the presence of pyroxenes, plagioclase, actinolite, tremolite, chlorite \pm Fe oxides. The rhyolites display porphyritic texture consisting of K-feldspar, quartz and plagioclase as phenocrysts. The associated porphyritic granitoids have K-feldspar, microcline, plagioclase and biotite phenocrysts within a groundmass of similar composition. The mafic and felsic volcanic rocks have SiO₂ content varying from 47-54 wt. % and 67-76 wt. % respectively indicating bimodal composition. The MgO and CaO decreases with increasing SiO₂, and Al₂O₃, TiO₂, Fe₂O₃ and P₂O₅ decreases from mafic to felsic rocks, whereas Na₂O and K₂O increases with

increasing SiO₂, indicating fractional crystallization. Primitive mantle normalized basalts and rhyolites exhibit distinct negative anomalies for Nb-Ta and Ti with relative enrichment in Th and La whereas basalts are slightly fractionated to flat patterns in chondrite normalized REE diagram ((La/Yb)_N=1.26-8.92) with feeble Eu anomaly (Eu/Eu*=0.72-0.94). In contrast, the rhyolites have strongly fractionated patterns ((La/Yb)_N= 11.2-15.3) with significant negative Eu anomaly (Eu/Eu*=0.20-0.88). The geochemical features of the bimodal suite endorsing their generation in an island arc/back arc tectonic setting. The granitoids show high SiO₂ (69-78 wt.%), K₂O (6.3 - 7.4 wt. %) and Na₂O (2.8 - 3.7 wt. %) with molar Al₂O₃/CaO+Na₂O+K₂O (A/CNK) ranging from 0.92 - 1.13 and are classified as potassic granites. Primitive mantle normalized diagram display Th enrichment with significant negative Nb, Ta and Zr anomalies and the chondrite normalized REE patterns are highly fractionated ((La/Yb)_N= 12.9-22.2) with distinct negative Eu anomaly. The geochemical features of the associated granitoids indicate that these are potassic and classify as within plate A-type granites.

Zircons from the basalts show clear oscillatory zoning in their CL images. They cluster as a coherent group with ²⁰⁷Pb/²⁰⁶Pb spot ages ranging from 2446 to 2522 Ma and weighted mean age of 2471±7 Ma (Fig. 1). Zircons from the rhyolite samples are subhedral to euhedral and show simple oscillatory zoning with some heterogeneous fractured domains. The data from two samples define upper intercept ages of 2479±13 Ma and 2463±14 Ma (Fig. 1). Zircons grains in the

granite show clear oscillatory zoning and their U-Pb data define an upper intercept age of 2506±50 Ma. The Lu-Hf isotopic data on the zircons from the basalts show initial ¹⁷⁶Hf/¹⁷⁷Hf ratios from 0.280925 to 0.281018. Their ε_{Hf}(t) values are in the range of -10.0 to -6.7. The Hf depleted model ages (T_{DM}) are between 3038 Ma and 3171 Ma, and Hf crustal model ages (T_{DM}^C) varies from 3387-3589 Ma. The zircons from the rhyolites show initial ¹⁷⁶Hf/¹⁷⁷Hf ratios from 0.280919 to 0.281020 and 0.281000 to 0.281103 respectively with ε_{Hf}(t) values are varying from -10 to -6.4 and -7.5 to -3.9. Among these, one sample shows Hf depleted model ages (T_{DM}) between 3038 Ma and 3182 Ma, and Hf crustal model ages (T_{DM}^C) varies from 3377-3596 Ma whereas the other sample shows ages of 2925 Ma and 3072 Ma with Hf crustal model ages (T_{DM}^C) varies from 3208-3432 Ma. The initial ¹⁷⁶Hf/¹⁷⁷Hf ratios of the granites range from 0.280937 to 0.281062 with ε_{Hf}(t) values of -8.8 to -4.3. The Hf depleted model ages (T_{DM}) are between 2979 Ma and 3170 Ma, and Hf crustal model ages (T_{DM}^C) varies from 3269-3541 Ma. The dominantly negative ε_{Hf}(t) values of zircons from these rocks suggest that the source material was evolved from the Paleoarchean crust. The geological, geochemical and geochronological evidence suggests coeval tectonic and magmatic episodes of volcanic and plutonic activity in an island arc setting where the arc migrated towards the continental margin and played a significant role in the Neoproterozoic-Paleoproterozoic crustal growth of the Koteri belt of Central India (Manikyamba et al., 2016; Fig. 1).

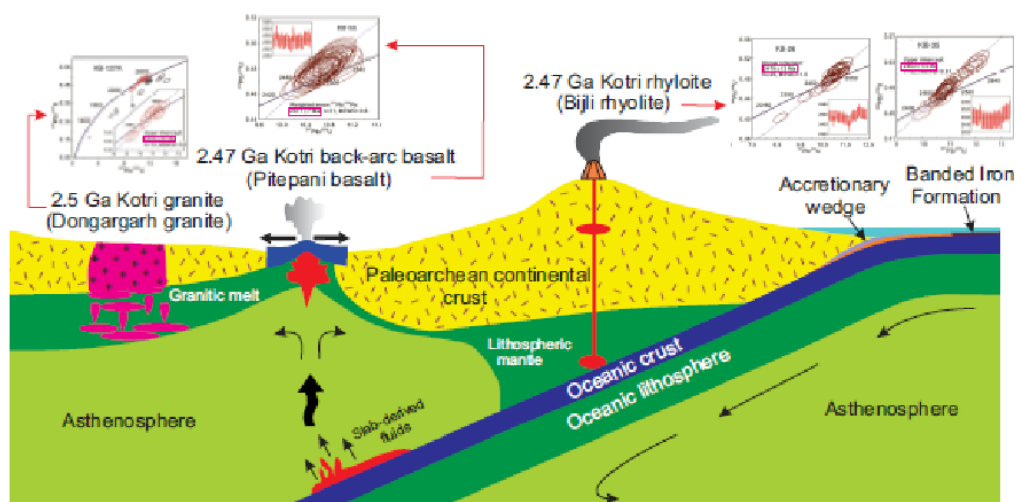


Figure 1. Schematic diagram showing synchronous volcanism of Bijli rhyolites in an active continental margin and Pitapani basalts in a continental back arc setting and anorogenic, within-plate granitoid emplacement in the Kotri belt.

Acknowledgements

The authors thank Dr. S. Chandrasekhar, Director, NGRI for permitting to publish this work. CM acknowledges the funds from Council of Scientific and Industrial Research (CSIR) to National Geophysical Research Institute through the projects of India Deep Earth Exploration Programme (INDEX). Dr. Kundan Banjara of Mines and Geology, Chhattisgarh is thanked for his help during the field work. Dr. Sohini Ganguly is thanked for helping in the preparation of the manuscript. Drs. M. Satyanarayanan, S. Sawanth, K.S.V. Subramanyam and A.K. Krishna are acknowledged for providing the geochemical data.

References

Asthana, D., Pophare, A.M., Rajalingam, S., Kumar, H., 2014. Neoproterozoic Dongargarh Rapakivi A-type Granites and its relationship to Pitepani tholeiites. *Gondwana Geological Magazine, Special Volume 16*, 25-40.
 Ghosh, J.G., 2004. 3.56 Ga tonalite in the

central part of the Bastar Craton, India: oldest Indian date. *Journal of Asian Earth Sciences* 23, 359–364.

Ghosh, J.G., Pillay, K.R., 2012. Evolution of the Kotri Linear Belt: A Late Archaean Continental Rift in the Bastar Craton, Central India. *Proceedings of the National workshop on “Recent advances in Geology of Dongargarh-Kotri belt, Central India and its Mineral potential”*. Gondwana Geological Society, Nagpur, p. 16.

Manikyamba, C., Santosh, M., Chandan Kumar, B., Rambabu, S., Tang, L., Abhishek Saha, Arubam C Khelen, Sohini Ganguly, Dhanakumar Singh, Th, Subba Rao, D.V., 2016. U-Pb zircon geochronology and Lu-Hf isotope systematics of bimodal volcanic rocks and associated granitoids: implications for Neoproterozoic-Paleoproterozoic crustal growth in Kotri belt, Bastar Craton, Central India. *Gondwana Research*, Doi 10.1016/j.gr.2015.12.008.

Mesoproterozoic Mafic complexes of south east central continental margin of Indian plate: Zircon trace element signatures and petrogenesis

K.S.V. Subramanyam^{a*}, M. Santosh^{b, c}, Qiong-Yan Yang^{b, c}, Ze-ming Zhang^d, V. Balaram^a, U.V.B. Reddy^e

^a CSIR-National Geophysical Research Institute, Uppal Road, Hyderabad, Telangana, 500 007, India

^b Department of Earth Sciences, University of Adelaide, Australia

^c School of Earth Science & Resources, China University of Geosciences, Beijing, China

^d Institute of Geology, Chinese Academy of Geological Sciences, Beijing, 100037, China

^e Department of Applied Geochemistry, Osmania University, Hyderabad, Telangana, 500007, India

Zircon U-Pb ages from three gabbro-anorthosite plutons namely Purimetla (PUR), Kanigiri (KG) and P CPalle (PCP) which intruded into the high grade rocks of the Prakasam Igneous Province in south east central continental margin of Indian plate were determined using LA-ICP-MS. U-Pb data on zircons from these plutons reveal prominent late Mesoproterozoic ages of 1334 ± 15 Ma, 1338 ± 27 Ma and 1251.2 ± 9.4 Ma. The cumulative $^{207}\text{Pb}/^{206}\text{Pb}$ mean age of 1315 ± 11 Ma is interpreted to represent the timing of mafic magmatism in the Prakasam Igneous Province (Subramanyam et al., 2016). Chondrite normalised Zircon REE distribution patterns these gabbro-anorthosite plutons show enrichment in HREE relative to LREE at a high degree of fractionation with

prominent Eu-negative and Ce-positive anomalies (Fig. 1 a,b,c).

Eu/Eu*, Ce/Ce*, Hf (ppm), U (ppm), Th (ppm), Ti (ppm), ΣREE (ppm) contents of zircons from these Mesoproterozoic mafic complexes constrain the following petrogenetic aspects; zircon crystallisation temperatures calculated based on Ti-contents in zircon after Watson et al., (2006) using equation $T(\text{°C}) = (5080 \pm 30) / ((6.01 \pm 0.03) - \log(\text{Ti})) - 273$. The minimum and maximum zircon crystallisation temperatures (in T °C) computed for individual zircon grains are found to be 571.3-769.0; 675.8-775.4 and 663.1-881.2 for PUR, KG and PCP plutons. A positive correlation is observed between Ti-contents and zircon crystallisation temperatures (Fig. 2). Marked variations are observed in zircon REE contents (ΣREE of Purimetla pluton 1808-6576 ppm; KG

pluton 1461-8168 ppm, and PC Palle plutons range from 2772-45723 ppm). Eu/Eu* in the range of 0.3-0.7, 0.1-0.3, 0.2-1.4; Ce/Ce* is in the range of 1-167.7, 1-165.2, 5.3-28.52 and Hf (ppm) range from 7784-11996, 7939-13179, 7349-15282 for PUR, KG and PCP plutons. Th/U is >0.1 (0.5-1.0 PUR; 0.6-1.2 KG and 0.23-2.2 PCP). Ta (ppm) ranges from 0.1-0.7, 0.2-0.5 and 0.7-3.6, whereas Nb (ppm) range 0.09-1.0, 0.3-1.7 and 0.8-9.9; Y (ppm) ranges from 1294-311, 265-1726 and 256-7399; Ti (ppm) ranges from 5.1-13.6, 4.5-49.3 and 3.8-40.6 for PUR, KG and PCP series of mafic plutons respectively. These trace element parameters indicate that the three plutons have evolved during fluctuating P-T conditions as well as fO₂ in around two million years span with repetitive magma additions, varying host melt composition, crystal mush replenishment and fractional crystallisation in an increasing thermal regime from PUR>KG>MCP. The wide range of variations in positive Ce- and negative Eu-anomalies indicate minor fluctuations in oxygen fugacity of crystallising melts (Fig. 1 a,b,c).

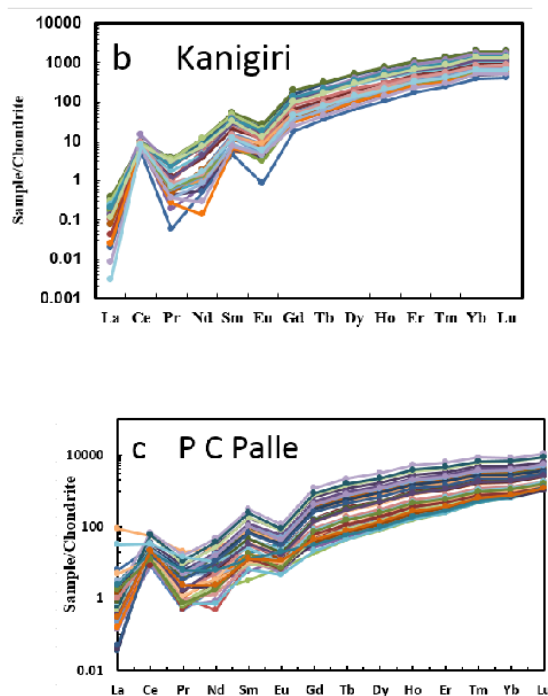
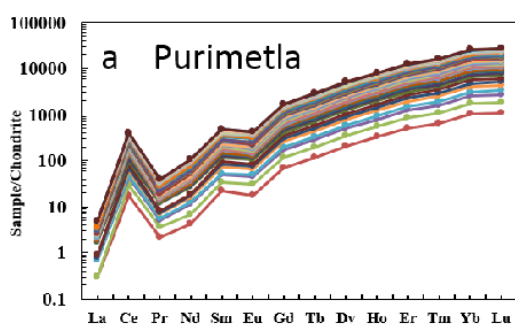


Fig.1: Chondrite normalised zircon REE distribution patterns of a) Purimetla b) Kanigiri c) P C Palle gabbro-anorthosite plutons

References

- Subramanyam, K.S.V., et al. Mesoproterozoic island arc magmatism along the south-eastern margin of the Indian Plate: Evidence from geochemistry and zircon U-Pb ages of mafic plutonic complexes. *Journal of Asian Earth Sciences* (2016), <http://dx.doi.org/10.1016/j.jaes.2016.05.016>.
- Watson, E.B., et al. Crystallization thermometers for zircon and rutile, *Contrib Mineral Petrol* (2006) 151: 413–433, DOI 10.1007/s00410-006-0068-5.

A re-evaluation of the Kumta Suture in Southwest India and its extension into Madagascar

Sheree. E. Armistead^a, Alan S. Collins^{a*}, William H. Mansfield^a, M. Santosh^a, E. Shaji^b

^a Tectonics, Resources and Exploration (TRaX), Department of Earth Sciences, University of Adelaide, SA 5005, Australia

^bDepartment of Geology, University of Kerala, Kariavattom, Trivandrum, India

It has long been recognised that Madagascar was contiguous with India until the Late Cretaceous, however the timing and nature of the amalgamation of these two regions is still highly contentious. Most workers agree that the Antongil Domain in Madagascar and the Western Dharwar Craton in India shared a common tectonic evolution since the Palaeo/Mesoarchaeon [e.g. 1, 2]. However, models differ to the origin and affinity of central Madagascar (the Antananarivo Domain). Some suggest that this too was part of a Neoproterozoic/Palaeoproterozoic Greater Dharwar Craton [e.g. 2], whereas others argue that the Antananarivo Domain and analogous terranes (collectively termed Azania by [3]) amalgamated with India during the latest Neoproterozoic/Cambrian formation of Gondwana, forming the Malagasy Orogeny [1].

The geology of west peninsular India is poorly constrained, with limited information available from geological

survey maps and published data. Currently available age data is insufficient to precisely correlate the southwest of India with eastern Madagascar. Despite this, it has recently been suggested that a newly defined, west-dipping, 15 km wide suture zone—the so-called Kumta Suture—separates a block centred on southern Goa, northwest Karnataka (the Karwar Block) from the Archaean Dharwar Craton, and which forms a continuation of the Betsimisaraka Suture of eastern Madagascar [4]. In this model it is proposed that the Karwar Block is a continuation of the Antananarivo Domain of central Madagascar. It is suggested that the Kumta Suture represents ocean closure during the amalgamation of Rodinia and occurred at c. 1380 Ma in the north; progressing toward the south at c. 750 Ma [4]. The implication that this subduction zone was active for an unlikely period of at least 630 million years has motivated us to re-evaluate the presence of the Kumta Suture; and its extension into

Madagascar.

Here we present preliminary U-Pb zircon data from five metasedimentary samples from the Karwar Block of India to further constrain the geology and depositional age/provenance in this area. New U-Pb data from detrital zircons yield two dominant age peaks at ~2.5 Ga and ~3.1 Ga. We have compared these detrital zircon age data to published data from elsewhere in Madagascar and India. To compare the data more quantitatively, we have used multi-dimensional scaling (MDS), which is a way of comparing distributional data between a large number of samples or regions. Our results indicate that detrital zircons from our samples in the Karwar Block are most similar to published detrital samples from the Antongil and Masora domains of Madagascar as well as the Dharwar Craton of India. Our new data are shown to be most dissimilar to samples from central and southern Madagascar. This is contrary to what would be expected from the recently proposed model by

Ishwar-Kumar et al. 2013.

We propose an alternative model whereby the Karwar Block is a continuation of the Antongil and Masora domains of Madagascar, and the Dharwar Craton of India, and not of the Antananarivo Domain in central Madagascar. This interpretation is consistent with the model of Collins and Windley 2002 that the Betsimisaraka Suture is a major boundary separating two distinct terranes with different detrital zircon spectra, and that the suture does not crop out in western India.

References

- [1] Collins, A.S. and Windley, B.F. (2002) *The Journal of Geology*, 110(3): 325-339

- [2] Tucker, R.D., et al. (2011) *Precambrian Research* 185(3-4): 109-130
- [3] Collins, A.S. and Pisarevsky, S. (2005) *Earth Science Reviews* 71: 229-270
- [3] Ishwar-Kumar, C., et al. (2013) *Precambrian Research* 236: 227-251

The Dhala crater, Madhya Pradesh, India: Impact crater or volcanic caldera?

Keerthy Suresh¹, K.S. Sajinkumar^{1, 2*}, M. Santosh^{3, 4}, S.P Singh⁵, G.K. Indu¹

¹Department of Geology, University of Kerala, Kariavattom 695 581, Thiruvananthapuram, India

²Department of Geological & Mining Engineering & Sciences, Michigan Technological University, 1400 Townsend Drive, Houghton, Michigan 49931, USA

³China University of Geosciences Beijing, Beijing 100083, P.R. China

⁴Department of Earth Sciences, University of Adelaide, Adelaide SA 5005, Australia

⁵Department of Geology, Bhundhelkhand University, Jhansi 284 128, Uttar Pradesh, India

*Corresponding author e-mail: sajinks@gmail.com

Bolide impact structures are common on the surface of planetary bodies in the Solar System, particularly in planets of the inner Solar System and their satellites. However these are rare features on the surface of the Earth due to the geologically active nature of the planet, with around 176 structures so far confirmed as impact structures. The Lonar in Maharashtra and Dhala in Madhya Pradesh are among the impact structures identified from the Indian Peninsula.

The Dhala Crater (N 25°17'59.7"; E 78°8'3.1"), considered to have formed by impact of an asteroid, is located in the Shivapuri district of Madhya Pradesh. The diameter of the structure is estimated as 11km. The basement rocks are predominantly composed of Archean granitoids. It is postulated that the impact occurred between 1.6 and 2.5 Ga, although this has not been confirmed by any precise geological or geochronological

studies. The Dhala structure is partly covered, in its central portions, by post impact sediments, presumed to belong to the Vindhyan Supergroup (Pati et al., 2008). The Dhala area is mainly composed of calc-silicate rocks, granitoids, large quartz veins/reefs and dolerite dykes, as well as sandy siltstone-silty sandstone with conglomerate lenses and an interclast shale-sandstone unit with a small exposure of bedded ash and laterite occurring on the top of the central hill, which is partly covered by Quaternary alluvium. The diagnostic evidence of shock metamorphism as observed in Dhala include impact melt breccias and the presence of the high-pressure polymorph reidite.

The present study aims at identifying more robust evidence like inverted rock layers, shatter cones, planar deformation features (PDF) and remnants of meteorite, if any. The study also aims at

precise geochemical fingerprinting and isotopic dating of the intrusive and extrusive magmatic units within the impact area to understand their petrogenesis, tectonic affiliation and timing with a view to address the question whether the crater represents an impact structure or a volcanic caldera.

Reference

Pati J., Reimold W.U., Koeberl C., Pati P. (2008) The Dhala Structure, Bhundhelkhandcraton, Central India, Eroded remnant of a large Paleoproterozoic impact structure. *Meteorites and Planetary Science* 43: 19-24.

Studying field geology in the Nepal Himalaya - The 5th student exercise tour in March 2016

Masaru Yoshida^{a, b}, Kazunori Arita^c, Tetsuya Sakai^d and Bishal Nath Upreti^{b, a}

^aGondwana Institute for Geology and Environment, Hashimoto, gondwana@oregano.ocn.ne.jp

^bDepartment of Geology, Tri-Chandra Campus, Tribhuvan University, Kathmandu

^cHokkaido University Museum, Sapporo

^dInterdisciplinary Faculty of Science and Engineering, Shimane University, Matsue

The Himalaya has been formed by the collision of the Indian and Eurasian Plates since ca 50 Ma. Geologic constitution of the Himalaya being composed of five geotectonic zones running parallel to the mountain range clearly reflecting the collision tectonics. Large uplifting rate of maximum 5 mm per year of the mountains even at present results in deep valleys and steep mountain slopes where land slide, debris flow, and river flood are often met with. The Himalaya is the living museum for students to study geology and natural hazards.

The N-S traverse of the Himalaya along the route connecting the Kaligandaki and Tinau valleys in west-central Nepal is the best geo-excursion course that discloses a full view of the Himalayan Orogen. We have been conducting the Japan-Nepal Student Himalayan Exercise Program (SHET-HP, 2016) every year since 2012, and so far five field tours under the program were successfully conducted

along the above course, and preparation for the sixth tour in next March is under the progress.

The Program include the following two major objectives.

1) To let participants to become familiar to the Himalayan geology as well as field geology.

2) To let participants to obtain the internationality including familiarity and understanding to other countries and the passion and skill to use English.

The 5th exercise tour was conducted for 11 days from 6th to 16th March 2016 in west-central Nepal along the above course. The tour team was composed of 17 people including 15 students and two teachers/leaders. The tour course was just the same as previous four tours, viz, Kathmandu- Pokhara - Muktinath - Pokhara - Tansen - Lumbini - Nayangadh - Mugling - Kathmandu, thus covering all major geologic zones of the Himalayan Orogen, i.e, the Tethys Himalayan, Higher

Himalayan, Lesser Himalayan, Sub Himalayan, and Terai zones and their boundary faults from the north to the south (Fig.1). The highlight of the tour this time was the observation and sketching of a group of large recumbent fold viewed on the eastern slope of Dhapudhon Data of Sandachhe Himal on the right bank of the Kaligandaki Valley, where almost all major Mesozoic Tethys formations were included. A discovery of a new outcrop of the South Tibetan Detachment System is also noteworthy. The logistic characteristics of the tour this time was the usage of 4 jeeps chartered in Pokhara for all northern courses from Pokhara including the section Pokhara-Beni-Jomsom-Muktinath-Jomsom- Pokhara. Because of this usage, the tour along the above courses has become easier to manage and participants were less strained than previous tours.

As a whole, the 5th exercise tour was completed successfully. A brief report of the tour appeared in the Geological Society of Japan News (Yoshida and Manandhar, 2016) in April and a full report book of the tour was delivered in May (Yoshida, 2016), both of which are uploaded on the above home page (SHET-HP, 2016). At the presentation, important data and characteristic photos of the tour will be displayed.

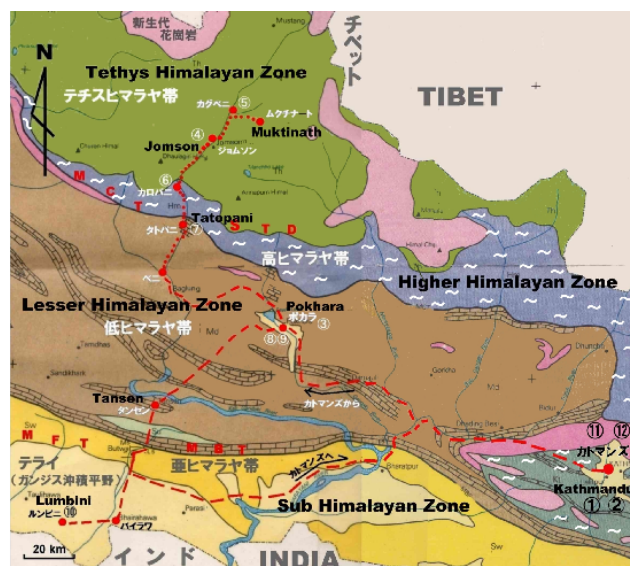


Fig. 1. Geologic outline of the exercise tour course area and route and itinerary of the tour. Dotted line: mainly by trekking. Dashed line: mainly by driving. Encircled numbers are night halts of the tour. (The base geologic map is referred after DMG, 1982).

References

- DMG, 1982, Geological Map of Nepal 1:1,000,000. Department of Mines and Geology, Nepal.
- SHET-HP, 2016, Home page of the Student Himalayan Exercise Program, http://www.geocities.jp/gondwanainst/geotours/Studentfieldex_index.htm
- Yoshida, M., 2016 (Ed), Traversing the Himalayan Orogen 2016-A record of the Fifth Student Himalayan Exercise Tour in March 2016. Field Science Publishers, Hashimoto, 165 pages (E-book).
- Yoshida, M., Paudel, M., 2016, Report of the 5th Student Himalayan Exercise Tour. Geological Society of Japan News, 19 (4), 8-9.

Radiogenic heat production and the formation of regional scale granulite and UHT metamorphic terranes through Earth history

Chris Clark

Department of Applied Geology, The Institute for Geoscience Research (TIGeR), Curtin University, GPO Box U1987, Perth WA 6845, Australia

It has been suggested that a major contributor to the generation of regional scale UHT conditions in collisional orogenesis the heat produced due to the decay of Heat Producing Elements (HPEs) in thickened crust. A good starting point to test the applicability of this mechanism to the generation of granulite and ultrahigh temperature (G-UHT) terranes through time is to see how it can be related to the observation that G-UHT metamorphism is cyclical in nature, and that there is a first order link between the supercontinent cycle and the generation and preservation of regional scale G-UHT terranes. For this model to be appropriate to the generation of G-UHT conditions in other G-UHT terranes throughout Earth history, a number of conditions must be satisfied.

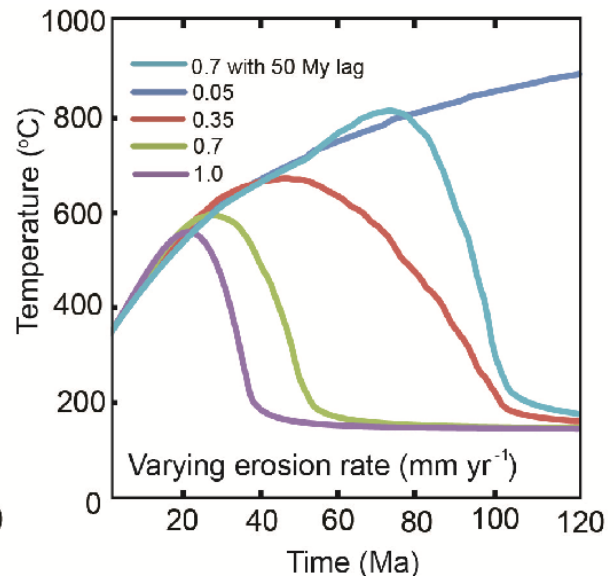
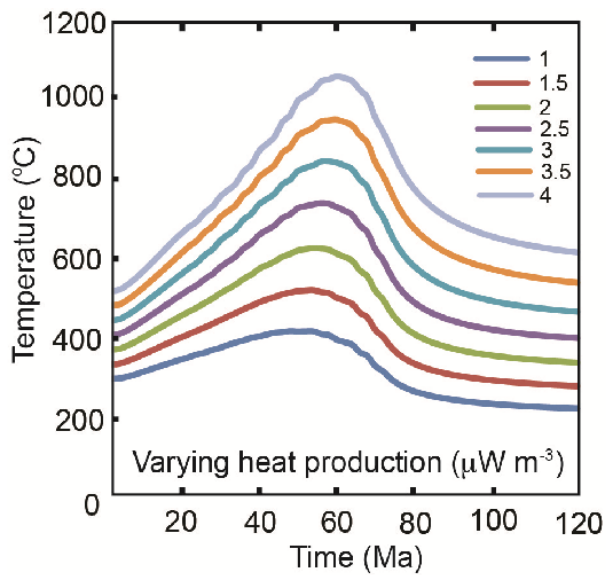
The primary requirement for radiogenic heat production to be the heat source for the generation of regional-scale G-UHT metamorphic conditions is that there is the requisite concentration of HPEs in the crustal column. The observed link

between the occurrence of G-UHT conditions and the terminal stages of supercontinent amalgamation may provide a mechanism for the enrichment of the crustal column in HPEs. It has been proposed that continents reorganize by two contrasting processes, known as extroversion or introversion, or by a combination of both. Extroversion is where a supercontinent rifts apart and then turns inside-out to form a second supercontinent along suture zones that correspond to the margins of the first supercontinent. In contrast, introversion, is where the first supercontinent rifts apart forming an internal ocean and then reassembles through the closure of the newly created ocean forming a second supercontinent. The process of extroversion, which is interpreted to be the driving mechanism for the formation and destruction of several past supercontinents in Earth history such as Vaalbara, Columbia, Rodinia and would have resulted in the development of large passive margins of material derived from

the erosive removal of the collisional mountain systems formed during continental collision. The reworking and redistribution of HPE within these collisional orogens, and their erosion and deposition at the margins of a supercontinent where they can be incorporated into the next supercontinent cycle, provides a mechanism for the heat source for the generation of regional scale G-UHT terranes. However, these ideas need to be tested in more detail through studies integrating geochronological and petrological data that focus on the duration and P - T conditions of metamorphism in each of these terranes.

Secondly, as partial melting acts as a heat sink during the evolution of a terrane to high temperatures, a requirement for a terrane to attain G-UHT conditions, effectively evolving from a regional scale migmatite terrane into a G-UHT terrane, is that the duration of orogenesis must be long enough (>60 Ma for average crustal heat productions of $3 \mu\text{W}^{-3}$) for the radiogenic heat source to provide the required thermal energy to overcome the thermal buffering effect of partial melting. This means that the orogen must be either large in scale or that erosion rates are slow enough to retard the removal of the HPEs. The observation that the age distribution of metamorphic belts that record regional scale G-UHT metamorphism is not uniform and can be broadly correlated with the amalgamation of the continental lithosphere into supercratons or supercontinents is suggestive of a correlation between the two processes. One school of thought suggests that G-UHT metamorphism is related to the generation of initially high geothermal gradient conditions in continental back-arc

regions prior to crustal thickening, we propose that G-UHT conditions actually relate to the final stage of amalgamation (i.e. continent-continent collision). The thickening of the crust during continental collision during the amalgamation of Gondwana has been likened to the generation of a Himalayan-scale continental collision system. This correlation between the terminal phase of collision during supercontinent amalgamation fulfils the requirement that a long-lived collisional system is integral to the cyclic generation of regional scale G-UHT conditions in nature.



While the scenario related to the formation and reorganisation of supercontinents described above fulfils a number of criteria in regard to the apparent cyclicity of G-UHT terranes it should also be noted that continental margins and other thick sedimentary basins on thinned crust and lithosphere, including continental

backarcs, are naturally enriched in HPE. Any collision involving a rifted continental margin, or closure of a continental back-arc basin, will result in thickened HPE-enriched sections and lead to the development of elevated geothermal gradients. Provided the crust remains thickened for long enough, there is the potential for the achievement of G-UHT conditions in any orogenic system of this type.

Vegetational changes in the late Palaeozoic-early Mesozoic sediments of Kashmir, Tethys Himalaya, India

Deepa Agnihotri¹ and Rajni Tewari¹

¹Birbal Sahni Institute of Palaeosciences, Lucknow-226007, India

*Corresponding author e-mail: deepa_agnihotri@bsip.res.in

The Jammu and Kashmir region contains the best developed and complete Palaeozoic, Mesozoic and Cenozoic stratigraphic successions. Lydekker (1883) divided the Palaeozoic rocks of the Kashmir region into the “Metamorphic”, Panjal and Zaskar systems. Later, Middlemiss (1910) discussed the general stratigraphy and palaeontology of the area and subdivided the Silurian–Triassic rocks into litho- and chronostratigraphic units, namely the “Older Silurian”, “Upper Silurian”, “Muth Quartzite”, “*Syringothyris* Limestone”, Passage Beds, “*Fenestella* Series”, “Agglomeratic Slates”, “Panjal Volcanic Flow”, “*Gangamopteris* beds”, Zewan beds, “Lower Triassic”, “Muschelkalk” and “Upper Triassic”. On the basis of plant fossil assemblages, Kapoor (1977, 1979) categorized the Permian strata of Kashmir into the Nishatbagh, Vihi, Marahoma, Munda and Mamal beds. Ahmad et al. (1978) and Singh et al. (1982) distinguished the plant-fossil-bearing beds below and above the Panjal Traps as the

Nishatbagh Formation and the Mamal Formation, respectively.

In the Kashmir region, the Carboniferous plant fossils are recorded from the *Fenestella* Shale Formation exposed at Kotsu village, Wallarama spur, Manigam spur (Pahalgam Area), Arbal and Gund villages (Banihal Area) by Pal (1978), Pal & Chaloner (1979), Singh et al. (1982), Singh et al. (2013) and Cleal et al. (2016). The plant fossil assemblage includes the orders Lepidodendrales, Equisetales, Filicales and Cordaitales. The palynoassemblage, recorded from the of *Fenestella* Shale Formation of Banihal Area includes 11 genera and 18 species. In the assemblage, the trilete spores and striate bisaccate pollen grains are scarce; monosaccate pollen taxa mainly - *Parasaccites*, *Plicatipollenites* and *Potonieisporites* are dominant. The assemblage is most similar to the *Parasaccites korbaensis* palynozone of the Lower Gondwana basins of Indian peninsula and the Stage 2 Palynozone

recorded from the late Carboniferous of east Australia.

The early Permian plant fossils have been recorded from the Nishatbagh Formation (early Artinskian) by Srivastava and Kapoor (1969), Kapoor (1977) and Singh et al. (1982). The floral assemblage of the Nishatbagh Formation is represented by *Gangamopteris kashmirensis*, *Glossopteris longicaulis*, *G. nishatbaghensis*, *Psymphyllum hollandii*, *Psymphyllum* sp., *Cordaites* sp. and *Nummulospermum* sp.

The flora of the Mamal Formation (early Kungurian) shows the presence of northern and southern mixed floral elements of the Permian Period and includes various orders like Equisetales, Sphenophyllales, Filicales, Glossopteridales, Cordaitales, Ginkgoales and Cycadales (Singh et al., 1982; Pant et al., 1984; Srivastava, 2004). The floral assemblage is comparable to that of the early Permian Barakar Formation of the Lower Gondwana basins of Peninsular India. Maheshwari et al. (1996) recorded monosaccate, striate disaccate and non-striate disaccate spores/pollen grains from this Formation.

The Zewan Formation, the uppermost sequence of the Permian Period in the Kashmir region contains well preserved faunal records. However, the sediments of the Zewan Formation are devoid of plant fossils. Palaeofire evidences have been recorded from the type locality of the Zewan Formation in the form of fragments of tracheids which show homogenized cell walls, a characteristic feature of charcoal (Jasper et al., 2016). The palaeo-wildfire studies provide important information about palaeoecological and palaeoenvironmental

conditions during the deposition of the sediments of the late Permian Zewan Formation.

Palynological studies from the world famous Permian-Triassic boundary section at Guryul Ravine reveal impoverished latest Permian spore-pollen assemblages in the uppermost Zewan Formation, a rich palynoassemblage from the basal Khunamuh Formation characteristic of the Permian–Triassic transition zone and depleted Triassic assemblages from higher in the Khunamuh Formation (Tewari et al. 2015). The collective assemblages are broadly correlated to the *Densipollenites magnicarpus* and *Klausipollenites decipiens* palynozones of peninsular India and to palynofloras spanning the Permian–Triassic boundary in other Gondwana countries.

References

- Ahmad, F., Chib, K.S. and Singh, A.J., 1978. Permian system in north and north eastern parts of Kashmir Himalayas. *Himalayan Geology* 8, 224–251.
- Cleal, C.J., Bhat, G.M., Singh, K.J., Dar, A.M., Saxena, A., Chandra, S. 2016. *Spondylodendron pranabii*-The dominant lycopsid of the late Mississippian vegetation of the Kashmir Himalaya. *Alcheringa* 40.
- Jasper A., Uhl D., Agnihotri D., Tewari R., Pandita S.K., Benicio J.R.W., Pires E.F., Augusto Stock Da Rosa A., Bhat G.D., Pillai S.S.K., 2016. Evidence of wildfires in the Late Permian (Lopingian) Zewan Formation of Kashmir, India. *Current Science* 110 (3), 419–423.
- Kapoor, H.M., 1977. Pastannah section of Kashmir with special reference to

- '*Ophioceras*' bed of Middlemiss. Journal of Palaeontological Society of India 20, 339–347.
- Kapoor, H.M., 1979. Gondwana of Kashmir – a reappraisal. In: Laskar, B., Raja Rao, C.S. (Eds.), Proceedings of the Fourth International Gondwana Symposium, Calcutta 1977 vol. 2. Hindustan Publishing Corporation, Delhi, pp. 443–462.
- Lydekker, R., 1883. The geology of Kashmir and Chambe territories and British District of Khagan. Memoirs of Geological Survey of India 22, 1–344.
- Maheshwari, H.K., Kapoor, H.M., Bajpai, U., 1996. Permian plant mega and palynofossils from Gondwana-equivalent sediments of Kashmir Valley. Palaeobotanist 43, 145–150.
- Middlemiss, C.S., 1910. A revision of the Silurian-Trias sequence in Kashmir. Records of Geological Survey of India 40, 206–260.
- Pal, A.K., 1978. Lower Carboniferous plant fossils from Kashmir Himalaya. Himalayan Geology 8, 119–43.
- Pal, A.K., Chaloner, W.G., 1979. A Lower Carboniferous *Lepidodendropsis* flora in Kashmir. Nature 281, 295–97.
- Pant, D.D., Nautiyal, D.D., Srivastava, D.D., 1984. The occurrence of Cathaysian elements in *Glossopteris* flora of Kashmir. Phytia 4 (5), 47–52.
- Singh, G., Maithy, P.K., Bose, M.N., 1982. Upper Palaeozoic flora of Kashmir Himalaya. Palaeobotanist 30, 185–232.
- Singh, K.J., Singh, R., Cleal, C.J., Saxena, A., Chandra, A., 2013. Carboniferous floras in siliclastic rocks of Kashmir Himalaya, India and evolutionary history of the Tethyan Basin. Geological Magazine 50, 577–601.
- Srivastava, P.C., 2004. Glimpses of Permian biodiversity in the Mamal bed of Kashmir Himalaya: Floristic analysis. Vistas in Palaeobotany and Plant morphology: Evolutionary and Environmental perspectives, P.C. Srivastava (ed.). Professor D.D. Pant memorial volume 133–169.
- Srivastava, J.P., Kapoor, K.M., 1969. Discovery of *Lepidostrobus* Brongniart from Lower Gondwana Formation of Kashmir. Journal of Palaeontological Society of India 12, 44–47.
- Tewari, R., Ram-Awatar, Pandita, S.K., McLoughlin, S., Agnihotri, D., Pillai, S.S.K., Singh, V., Kumar, K., Bhat, G.D., 2015. The Permian-Triassic palynological transition in the Guryul Ravine Section, Kashmir, India: implications for Tethyan-Gondwanan correlations. Earth Science Reviews 149, 53–66.

Detrital zircon age data from quartzites in the southern Madurai Block, India and their bearing on Gondwana assembly

G. Indu^{1*}, Shan-Shan Li², M. Santosh^{2, 3}, E. Shaji³, T. Tsunogae^{4, 5}

¹ Department of Geology, University of Kerala, Kariyavattom Campus, Trivandrum 695 581, India

² School of Earth Sciences and Resources, China University of Geosciences 6 Beijing, 29 Xueyuan Road, Beijing 100083, China

³ Department of Earth Sciences, University of Adelaide, Adelaide SA 5005, Australia

⁴ Graduate School of Life and Environmental Sciences, University of Tsukuba, Ibaraki 305-8572, Japan

⁵ Department of Geology, University of Johannesburg, Auckland Park 2006, South Africa

*Corresponding author e-mail: indoos209@gmail.com

Southern Peninsular India constituted the central segment of the Late Neoproterozoic supercontinent Gondwana and is composed of crustal blocks ranging in age from Mesoarchean to Late Neoproterozoic-Cambrian (Santosh et al., 2009; Santosh et al., 2015; Collins et al., 2014). Detrital zircon grains from a suite of quartzites accreted along the southern part of the Madurai Block were investigated through LA-ICPMS U-Pb geochronology (Shan-Shan Li et al., 2016). The data show multiple age populations of magmatic zircons, ranging from Mesoarchean to Paleoproterozoic (ca. 2980-1670 Ma, with peaks at 2900-2800 Ma, 2700-2600 Ma, 2500-2300 Ma, 2100-2000 Ma). Two quartzite samples carry magmatic zircons with dominantly Neoproterozoic (950-550 Ma) ages. Zircon grains of metamorphic origin from all the samples display ages in

the range of 580-500 Ma, correlating with the timing of metamorphism reported from the adjacent Trivandrum Block as well as from other adjacent crustal fragments within the Gondwana assembly. The Mesoarchean to Neoproterozoic age range of the zircon grains and their contrasting rare earth element features suggest that the detritus were sourced from multiple provenances involving a range of lithologies of varying ages. We interpret the data indicate that a branch of the Mozambique ocean might have separated the Paleoproterozoic basement rocks in central Madurai Block to the north and the Trivandrum and Nagercoil Blocks to the south. The ocean closure and associated high grade metamorphism were associated with the collisional assembly of Gondwana supercontinent during latest Neoproterozoic-Cambrian.

References

- Collins, A.S., Clark, C., Plavsa, D., 2014. Peninsular India in Gondwana: the tectonothermal evolution of the Southern Granulite Terrain and its Gondwanan counterparts. *Gondwana Research* 25, 190-203.
- Li, S.S., Santosh, M., Indu, G., Shaji, E., Tsunogae, T., 2016. Detrital zircon geochronology of quartzites from the southern Madurai Block, India: implications for Gondwana reconstruction *Geoscience Frontiers*, DOI: 10.1016/j.gsf.2016.07.002
- Santosh, M., Maruyama, S., Sato, K., 2009b. Anatomy of a Cambrian suture in Gondwana: Pacific-type orogeny in southern India? *Gondwana Research* 16, 321-341.
- Santosh, M., Yang, Q.Y., Shaji, E., Tsunogae, T., Ram Mohan, M., Satyanarayanan, M., 2015. An exotic Mesoproterozoic microcontinent: the Coorg Block, southern India. *Gondwana Research* 27, 165-195.

Facies distribution, heavy mineral sediment provenance and zircon geochronology of the Neoproterozoic succession of Oman: implications for tectonic setting and evolution of the Arabian peninsula

Irene Gomez-Perez^a, Andrew Morton^b and Dirk Frei^c

^a Petroleum Development Oman

^b Heavy Minerals Research

^c Stellenbosch University

The basement terranes of Oman were consolidated in the Late Neoproterozoic between ~860-520 Ma, but the exact timing of their attachment to the Arabian Peninsula remains unclear. Paleofacies maps have been combined with heavy mineral sandstone provenance and detrital zircon geochronology to better understand the sediment distribution patterns and tectonic setting of the Neoproterozoic-Early Cambrian succession of Oman. Ediacaran Nafun Group paleogeographies point to deposition along a non-volcanic passive margin facing a deep water basin to the west and south, with sediment source areas in the east-northeast. This followed deposition of the Cryogenian Abu Mahara Group in deep rift depocentres. Systematic heavy mineral provenance studies of the Neoproterozoic to Early Cambrian succession from both

the subsurface of South Oman and outcrops in north, central and south Oman indicate clastic sediment provenance from granitoid and mafic terranes, and sediment transport to the west-southwest. Detrital zircon geochronology indicates peak magmatism in the sediment source areas at ~830-780 Ma, secondary Paleoproterozoic sources, discrete activity at ~620 Ma, and renewed magmatic activity from ~550 Ma. These events match the nature of the Neoproterozoic basement exposed in Oman and beyond in Socotra, the Seychelles, northeastern Madagascar, Rajasthan and Pakistan. Magmatic events characteristic of the Arabian-Nubian Shield, peaking at ~640-620 Ma, are insignificant in the zircon populations of the Ediacaran succession of Oman. Renewed activity at ~550 Ma reflects incipient Angudan Orogeny.

Based on these observations and integration with studies of the basement and the sedimentary successions by different authors which position Oman at the eastern side of the Mozambique Ocean, we support that the Neoproterozoic succession of Oman was deposited at the passive, pericratonic western margin of the Greater India Shield, and that oblique

collision with Arabia only occurred during the latest Neoproterozoic Angudan-Malagasy Orogeny at ~538-520Ma. Latest Ediacaran-Early Cambrian marine basin closure is indicated by the gradual shallowing of the marine sedimentary succession of south Oman, followed by deposition of Ara Group evaporites, and by continental clastics of the Nimr Group.

Petrological characteristics of basement rocks in Voktipur, Rangpur District, Bangladesh

Md. Rezaul Islam^a, Ismail Hossain^{a,*}, Toshiaki Tsunogae^b, Mowsumi Nahar^a,

Md. Sazzadur Rahman^a

^aDepartment of Geology and Mining, University of Rajshahi, Rajshahi 6205, Bangladesh

^bGraduate School of Life and Environmental Sciences (Earth Evolution Sciences), University of Tsukuba, Ibaraki 305-8572, Japan

*Corresponding author e-mail: ismail_gm@ru.ac.bd

U–Pb SHRIMP zircon geochronological results of subsurface Maddhapara basement rocks in Bangladesh reveal the occurrence of Palaeoproterozoic age (~1.73 Ga). The common occurrences of similar ~1.7 Ga geologic units in the Central Indian Tectonic Zone (CITZ) and Meghalaya-Shillong Plateau in Indian Shield suggest their apparent continuation with a configuration of the Columbia supercontinent (Hossain et al., 2007). The Palaeoproterozoic basement rocks in NW Bangladesh, therefore, constitute an integral part of the collisional zone, it gets separated on or near the surface between the Chhotonagpur and Shillong Plateaus. Accordingly, the basement rocks from Rangpur district, Bangladesh show a large range of chemical variation of SiO₂ (38.53–64.98 wt %), Al₂O₃ (5.57–17.44 wt %), CaO (3.17–10.20 wt %), K₂O (2.12–7.87 wt %), Na₂O (0.76–3.69 wt %), MgO (1.5–14.8 wt %), TiO₂ (0.33–8.19 wt %), and P₂O₅ (0.06–3.68 wt %). The rocks of these areas

are broadly classified as ultrabassic, mafic and intermediate rock (Nahar et al., 2015). However, dominantly present intermediate rocks of the Voktipur area (borehole GDH-53), Rangpur show the SiO₂ variation (62.11–64.98 wt%) and these are mostly sub-alkaline/calc-alkaline, peraluminous categorized mainly as monzodiorite and quartz monzonite with lamprophyre variety. Dominant rocks are subhedral to euhedral, coarse to medium grained, hemicrystalline and showing inequigranular porphyritic with few poikilitic textures.

These rocks are mainly composed of plagioclase (13.2–54.6%), hornblende (15.5–33.2%), biotite (7–13%), quartz (0–5.8%), K-feldspar (11.8–40%) and accessory epidote, titanite, magnetite, zircon and chlorite. Hydrothermal alterations are also common. Undulation nature of some quartz grain, zoning of biotite and hornblende are present. Chemical analyses of amphibole, plagioclase, biotite, epidote and K-feldspar

in monzodioritic/monzonitic rocks were carried out by field emission electron probe microanalyzer (JEOL JXA-8530F) at the Chemical Analysis Division of the Research Facility Center for Science and Technology,

the University of Tsukuba, Japan. The results of representative analysis of minerals and their structural formulae are given in Table 1.

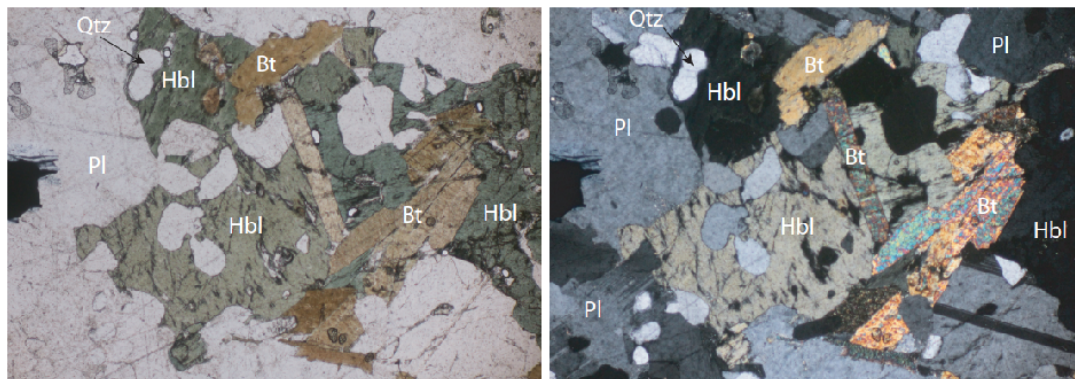


Fig. 1 Microphotographs (PPL and XPL) showing representative texture of monzodioritic rock with mineral assemblage and petrographic relationship among hornblende (Hbl), plagioclase (Pl), quartz (Qtz) and biotite (Bt).

Chemical compositions of amphiboles have clearly demarcated two varieties calcic amphibole in the examined monzodioritic/monzonitic rocks. These have a wide compositional variation in X_{Mg} ($Mg/[Fe+Mg] = (0.69-0.79)$ and $(0.35-0.37)$). Amphiboles of the sample SB13 (high Si content 7.15–7.83 pfu) of the present study are compositionally actinolite and magnesiohornblende, whereas ferroedenite in the sample SB15 (Si 6.47–6.51 pfu). Representative microprobe analyses of plagioclase, coexisting with ferroedenite, show a wide compositional range of An_{30-32} (andesine) with $\approx 2\%$ orthoclase component. K-feldspar in monzodioritic/monzonitic rocks shows a uniform orthoclase-rich composition in all samples ($Or_{90-92} Ab_{8-10}$). Biotite in monzodioritic/monzonitic rocks is Mg-rich ($X_{Mg} = 0.60-0.61$) and Mg-poor ($X_{Mg} = 0.41-0.42$). Its Ti contents also show low ($0.16-0.92$ wt% TiO_2) and high ($3.0-3.1$ wt% TiO_2) contents.

Hornblende is a luminous indicator of thermobarometry which provide vital information on the pressure and temperature (P-T) conditions of crystallization, the settlement depth. In these contexts, very few samples of monzodioritic/monzonitic rock fulfill an important prerequisite for application of aluminum-in-hornblende barometry as well as hornblende plagioclase thermometer (Stein and Dietl, 2001). The calculated P-T conditions of the studied rocks yielded about $696-711^\circ C$ and $5.5-6.24$ kbar. The average temperature calculated as $710^\circ C$ and pressure calculated as ~ 6 kbar which probably correspond to crystallization conditions of the Rangpur basement rocks. The pressure range enables us to estimate minimum emplacement depth of the dioritic rocks at $\sim 19-22$ km, if the rock density is assumed to be ~ 3 g/cm³. The result is nearly consistent with Maddhapara dioritic rocks (Hossain et al., 2009), pegmatite and aplite veins intruding the dioritic rocks in

Maddhapara, Bangladesh (~16 km/~4.8 kbar; Hossain and Tsunogae, 2008). Our study provides the P-T conditions and emplacement depth in the Rangpur

basement rocks in Bangladesh. The results will be useful in further understanding the tectonic activities in NW Bangladesh and adjoining areas in India.

Table 1. The results of representative analysis of minerals and their structural formulae

Sample No.	SB 13	SB1 3	SB1 3	SB1 3	SB1 3	SB1 3	SB1 3	SB1 5	SB1 5	SB1 5	SB1 5
Name	Kfs	Qtz	Hbl	Hbl	Hbl	Hbl	Bt	Qtz	Pl	Bt	Hbl
Analysis No.	n=3	n=1	n=2	n=3	n=6	n=2	b=4	n=1	n=3	n=3	n=3
SiO ₂	64.82	99.12	52.76	49.97	51.05	50.07	37.71	96.53	58.81	35.66	41.76
Al ₂ O ₃	18.55	0.03	3.49	5.96	4.68	5.82	14.63	0.06	24.28	14.51	10.92
TiO ₂	0.03	0.02	0.03	0.23	0.16	0.18	0.68	0.00	0.02	3.04	1.06
Cr ₂ O ₃	0.01	0.00	0.11	0.28	0.23	0.36	0.49	0.00	0.04	0.04	0.01
FeO*	0.04	0.06	10.11	11.56	10.83	11.70	16.32	0.07	0.15	22.10	21.17
MnO	0.01	0.00	0.55	0.48	0.51	0.55	0.37	0.00	0.00	0.36	0.57
MgO	0.01	0.03	16.52	14.89	15.93	15.16	14.16	0.01	0.03	8.84	6.74
CaO	0.00	0.08	11.85	11.84	11.75	11.94	0.08	0.14	6.36	0.09	10.97
Na ₂ O	0.98	0.08	0.74	0.97	0.82	1.19	0.13	0.06	7.64	0.19	1.64
K ₂ O	15.29	0.05	0.36	0.65	0.45	0.61	9.79	0.04	0.33	9.53	1.79
Total	99.80	99.47	96.56	96.86	96.47	97.65	94.41	96.93	97.68	94.36	96.62
Si	2.99	1.00	7.63	7.30	7.44	7.27	2.87	0.00	2.68	3.74	6.53
Al	1.01	0.00	0.59	1.03	0.81	1.00	1.31	0.00	1.31	1.80	2.01
Ti	0.00	0.00	0.00	0.03	0.02	0.02	0.04	0.00	0.00	0.24	0.12
Cr	0.00	0.00	0.01	0.03	0.03	0.04	0.03	0.00	0.00	0.00	0.00
Fe ²⁺	0.00	0.00	1.22	1.41	1.32	1.42	1.04	0.00	0.01	1.93	2.77
Mn	0.00	0.00	0.07	0.06	0.06	0.07	0.02	0.00	0.00	0.03	0.08

Mg	0.0 0	0.00	3.56	3.24	3.45	3.28	1.61	0.00	0.00	1.38	1.57
Ca	0.0 0	0.00	1.83	1.85	1.83	1.86	0.01	0.00	0.31	0.01	1.84
Na	0.0 9	0.00	0.21	0.27	0.23	0.33	0.02	0.00	0.68	0.04	0.50
K	0.9 0	0.00	0.07	0.12	0.09	0.11	0.95	0.00	0.02	1.28	0.36
Total	5.0 0	1.00	15.2 0	15.3 4	15.2 9	15.4 1	7.90	0.00	5.01	10.4 5	15.7 7

References

- Hossain, I., Tsunogae, T., Rajesh, H.M., Chen, B., and Arakawa, Y. (2007) Palaeoproterozoic U-Pb SHRIMP zircon age from basement rocks in Bangladesh: A possible remnant of the Columbia Supercontinent. *Comptes Rendus Geoscience*, v. 339, pp. 979–986.
- Nahar, M., Hossain, I., Zaman, M.N., Uddin, M.N., Tsunogae, T. (2015) Nature and origin of intermediate rocks with pyroxenite and lamprophyres in Bangladesh: an overview. *International Association for Gondwana Research Conference Series No. 21*, pp. 82–84
- Stein, E. and Dietl, C., (2001) Hornblende thermobarometry of granitoids from the Central Odenwald (Germany) and their implications for the geotectonic development of the Odenwald. *Mineralogy and Petrology*, v. 72 (1), pp. 185–207.
- Hossain, I., Tsunogae, T. and Rajesh, H.M. (2009) Geothermobarometry and fluid inclusions of dioritic rocks in Bangladesh: Implications for emplacement depth and exhumation rate. *Journal of Asian Earth Sciences*, v. 34 (6), pp. 731–739.
- Hossain, I. and Tsunogae, T. (2008) Fluid inclusion study of pegmatite and aplite veins of the Palaeoproterozoic basement rocks in Bangladesh: implications for magmatic fluid compositions and crystallization depth. *Journal of Mineralogical and Petrological Sciences*, v. 103, pp. 121–125.

Prograde and retrograde growth of monazite in migmatites: a Gondwanan example from the Nagercoil Block, Southern India

Tim E. Johnson^{a*}, Chris Clark^a, Richard J. M. Taylor^a, M. Santosh^b, Alan S.

Collins^c

^a Department of Applied Geology, The Institute for Geoscience Research (TIGeR), Curtin University, GPO Box U1987, Perth WA 6845, Australia

^b School of the Earth Sciences and Resources, China University of Geosciences (Beijing), 29 Xueyuan Road, Beijing 100083, China

^c Tectonics, Resources and Exploration (TRaX), Department of Earth Sciences, University of Adelaide, SA 5005, Australia

Data from a migmatized metapelite raft enclosed within charnockite provide quantitative constraints on the pressure–temperature–time (P–T–t) evolution of the Nagercoil Block at the southernmost tip of peninsular India. An inferred peak metamorphic assemblage of garnet, K-feldspar, sillimanite, plagioclase, magnetite, ilmenite, spinel and melt is consistent with peak metamorphic pressures of 6–8 kbar and temperatures in excess of 900 °C. Subsequent growth of cordierite and biotite record high-temperature retrograde decompression to around 5 kbar and 800 °C. SHRIMP U–Pb dating of magmatic zircon cores suggests that the sedimentary protoliths were in part derived from felsic igneous rocks with Palaeoproterozoic crystallisation ages. New growth of metamorphic zircon on the

rim of detrital grains constrains the onset of melt crystallisation, and the minimum age of the metamorphic peak, to around 560 Ma. The data suggest two stages of monazite growth. The first generation of REE-enriched monazite grew during partial melting along the prograde path at around 570 Ma via the incongruent breakdown of apatite. Relatively REE-depleted rims, which have a pronounced negative europium anomaly, grew during melt crystallisation along the retrograde path at around 535 Ma. Our data show the rocks remained at suprasolidus temperatures for at least 35 million years and probably much longer, supporting a long-lived high-grade metamorphic history. The metamorphic conditions, timing and duration of the implied clockwise P–T–t path is similar to that previously established for other

regions in peninsular India during the Ediacaran to Cambrian assembly of that part of the Gondwanan supercontinent.

1.6 billion years of granitoid magmatism and crustal growth in the Singhbhum craton: insights from zircon U-Pb-Hf isotopic study

Sukanta Dey

Department of Applied Geology, Indian Institute of Technology (Indian School of Mines), Dhanbad – 826 004, India
E-mail: geodeys@gmail.com

The Singhbhum craton in eastern India has a protracted (Palaeoarchaeon to Palaeoproterozoic) crustal evolutionary history. Yet, several issues related to the crustal growth in the craton remain unresolved. For example, the timing of juvenile crustal growth and reworking of older crust in the craton and their geodynamic significance are not well-known. Especially, correlation with other well-studied cratons is difficult due to dearth of precise geochronologic data. This work presents recently acquired whole-rock geochemical and zircon U-Pb age and Hf isotope data on granitoids of the Singhbhum craton to discuss their origin and role in crustal evolution.

The oldest granitoid magmatism in the Singhbhum craton is represented by a group of TTG (tonalite-trondhjemite-granodiorite) gneisses which formed at 3.53 and 3.47–3.45 Ga. These gneisses include both low-HREE (high-pressure) and high-HREE (low-pressure) TTGs. They are characterized by low Mg, Ni and

Cr contents and Mg# precluding direct involvement of mantle in their origin. The zircon Hf isotope signature ($\epsilon\text{Hf}_T = +2.1$ to $+4.8$) suggest a juvenile mafic source. This is followed by voluminous granitoid magmatism in several pulses at 3.37, 3.35–3.30 and 3.1–2.9 Ga. These granitoids, termed Singhbhum Granites, are interpreted to have originated by episodic crustal reworking. The earliest crustal reworking involved mostly mafic crust generating TTG melts. Successive crustal reworking events involved progressively greater amount of previously formed felsic crust forming more evolved, K-rich granites. Many of the granitoid suites display wide range of ϵHf_T (-1 to $+5.3$) which suggest addition of juvenile crust and attendant reworking of both juvenile and older crust. The process caused crustal differentiation and, finally, stabilization of the craton at 3.29 Ga. An oceanic plateau setting with repeated plume-related mafic-ultramafic magma underplating and intraplating inducing

recurrent crustal reworking is suggested for the Palaeoarchaeon crustal evolution of the Singhbhum craton. The situation is similar to that of the coeval East Pilbara Terrane and the Barberton Granitoid-Greenstone Terrain of the Kaapvaal Craton.

Several ~2.8 Ga anorogenic granites and rhyolites occur along the marginal part of the Singhbhum craton. They are K-rich, ferroan rocks rich in LILE and HFSE. Geochemical characteristics (negative Eu anomaly, flat HREE and low Sr/Y) and zircon Hf isotope composition ($\epsilon\text{Hf}_T = -2.7$ to $+0.1$) suggest an origin by shallow crustal melting of the Singhbhum Granite. This ~2.8 Ga A-type magmatism mark a significant crustal reworking event along the craton margin attendant to mantle-derived mafic magmatism in an extensional tectonic setting.

At 1.9 Ga several bodies of a high-silica, K-rich granite, termed Arkasani Granophyre, intruded the pelitic schists of the Singhbhum mobile belt. These granitoids originated through shallow crustal melting as suggested by their low MgO, Cr and Ni contents and Sr/Y ratios coupled with negative Eu anomaly and flat HREE pattern. The ϵHf_T values display wide range (-0.6 to $+6.3$) indicating a mixed source consisting of both juvenile material and older crust.

In conclusion, the Singhbhum craton records episodic crustal reworking and granitoid magmatism over a long period (3.5 to 1.9 Ga). These crustal reworking events can be linked to repeated mafic-ultramafic magma underplating and intraplating probably related to discrete mantle plume events.

Assessment of river banks in Kerala: A participatory approach

Shaji J

GIS Specialist, River Management Cell, Dept. of Revenue and Disaster Management, ILDM, Thiruvananthapuram
E-mail: shaji.jjohnson@gmail.com

Kerala is blessed with 44 rivers. The existence of state's economy, environment and people to a great extent depends on rivers. Nevertheless, they are in stress and at various stages of degradation due to unscientific and indiscriminate sand mining from river bed, encroachment of river banks for settlements, and pollution. An efficient management plan to revive the rivers in the state warrants ground level data which is lacking at present.

Mapping of river banks to human scale is a method to obtain ground level information about the current status of river banks and their conservation requirements. The River Bank Mapping Programme of Government of Kerala is an initiative in this direction. The programme was introduced in 2012 for the twenty major rivers of the state and implemented in a participatory way involving government organizations, educational institutions, and NGO's under the supervision of River Management Cell and National Centre for Earth Science Studies. The present paper tries to consolidate and highlight the salient outcomes of the programme in generating

ground level information of river banks in Kerala by selecting 8 rivers: Kallada, Pamba, Periyar, Meenachil, Chaliyar, Kuttiyadi, Anjarakandy and Kadalundi.

The methodology for the programme has been put forward by National Centre for Earth Science Studies, Thiruvananthapuram. This involves the field survey of river banks applying Cadastral maps and collection of data on physical, landuse and manmade features present in the river banks for individual survey plots using standard data format designed for the purpose. These data are field cross checked to ensure its quality by River Management Cell and then prepares three different sets of maps covering physical, landuse and manmade features present in the river bank on cadastral scale (1:4,000 or 1:5,000) using Geographic Information System (GIS) for every panchayat. Only the main trunk of the river excluding forest area and coastal regulation zone is chosen for mapping. The length of rivers affected by erosion and also the length without riparian vegetation are separately computed for framing out

suitable management strategies. The study reveals that out of the 481 km long river banks mapped 90.85 km on the right bank and 86.87 km on the left bank are erosion

affected. It is expected that the data generated will assist in evolving a sustainable river bank development plan for each river in the state.

Petrology and geochemistry of dacites from the Coorg Block, Southern India

S G Dhanil Dev^{a*}, S Chinchu Nair^a, E Shaji^a, Mifthah Koya Thangal^a

^a Dept of Geology, University of Kerala, Kariavatom campus, Trivandrum-695 581, India

* Corresponding author e-mail: devetan@gmail.com

We report a rare meta-volcanic (dacite) rock within the TTG from Majakkad quarry of Coorg Block. Petrology and geochemistry of the rock has been studied. The rock is very fine grained, grey to greenish in colour with minerals like hornblende, biotite, plagioclase, epidote, feldspar, calcite and quartz. It has an aphanitic to porphyritic texture and is intermediate in composition between andesite and rhyolite. Xenocrysts are less abundant in the dacites than in the mafic layers, which contain thin, remnant quartz and feldspar grains. The rock is totally devoid of vesicles or amygdaloids. This rock contains garnet as phenocrysts. Microscopically the rock shows typical igneous texture. The rock can be considered as vitrophyric hornblende dacite. Euhedral to subhedral crystals of hornblende is bordered with deformed small grains of plagioclase and quartz. The groundmass of fresh dacites consists essentially of light gray volcanic glass with sparse plagioclase microlites,

clinopyroxene and rare zircon. The Majakkad dacite is calc-alkaline and I-type in composition, have uniform silica contents ($\text{SiO}_2 = 63.77$ to 64.97 wt. %) and relatively low Mg#. The alumina saturation index suggests they are metaluminous and ferroan types. A comparison between dacite from Majakkad and Dacite from South China using the variation diagram MgO (wt. %) vs SiO_2 (wt. %) (Bin Li et al., 2016), indicates that they are similar in composition and could have formed as a result of thick lower crust derived adakite like rocks. Adakitic magmas derived directly from partial melting of the subducted oceanic slab usually show characteristics of high Na_2O rather than high K_2O , as demonstrated by experimental studies (e.g. Defant and Drummond, 1990). This subduction could have resulted in the upwelling of the asthenosphere beneath the Coorg Block, which induced partial melting of the mantle as well as the mafic lower crust, and formed an arc regime in the Coorg Block.

Migmatites, charnockites and crustal fluid flux: the Pan-African granulites of Southern India

I.C.W. Fitzsimons^a, C. Clark^b, M. Santosh^{b, c}

^aDepartment of Applied Geology and TIGeR, Curtin University, Bentley, Western Australia

^bCentre for Tectonics, Resources and Exploration, University of Adelaide, South Australia

^cChina University of Geosciences, Beijing, China

The Southern Granulite Terrain forms the high-grade crystalline basement of Peninsular India south of the Archean granite-greenstone assemblage of the Dharwar Craton (Collins et al., 2014). This classification stems from Fermor (1936), who divided Indian basement into “normal” regions of relatively low metamorphic grade, like the Dharwar Craton, and deeply-eroded “charnockitic” regions to the south and east. The latter regions were named for their abundant charnockite, an orthopyroxene-bearing felsic rock with even-grained structure and distinctive dark green–brown quartz and feldspar (Holland, 1900). Much charnockite in the Southern Granulite Terrain occurs as massive bodies interpreted as granitic plutons emplaced and/or metamorphosed under hot, dry conditions that promoted the stability of orthopyroxene in felsic compositions. Sedimentary protoliths are also widespread and dominated by aluminous garnet–sillimanite (\pm cordierite) gneiss (khondalite) and quartzofeldspathic garnet–biotite gneiss

(leptynite), although the interpretation of the latter as metasedimentary rather than meta-igneous remains controversial. Both khondalite and leptynite are commonly migmatitic, with abundant evidence for partial melting. Sm–Nd, U–Pb and Lu–Hf isotope geochronology has been used to subdivide the Southern Granulite Terrain into several blocks with different protolith ages, but they all share a protracted history of 630–490 Ma high- to ultra-high temperature metamorphism (Collins et al., 2014; Clark et al., 2015; Fitzsimons, 2016). Peak conditions of 0.7–1.3 GPa and 850–1050°C were developed at ca. 590–540 Ma, followed by decompression and melt crystallisation at 540–510 Ma and a regional hydrothermal overprint at 500–490 Ma. Crystalline basement blocks in Sri Lanka and southern Madagascar have identical protolith ages and metamorphic histories to those in the Southern Granulite Terrain, and these would have been a contiguous region of high-temperature granulites before Gondwana breakup. The 590–540 Ma age

of peak metamorphism corresponds to the “Pan-African” event that reflects assembly of the Gondwana supercontinent, while the 50 Myr duration of these extreme conditions suggests that metamorphism was driven by radiogenic heat accumulation beneath a long-lived orogenic plateau, and was terminated by plateau collapse at ca. 530 Ma (Fitzsimons, 2016). While this model can account for the timing and conditions of granulite metamorphism in the Southern Granulite Terrain and its Gondwana neighbours, there is one aspect of these rocks that is difficult to explain – namely the widespread development of “incipient” charnockite.

Incipient charnockites are coarse-grained centimetre- to metre-scale dark patches that overprint a finer-grained biotite- and or hornblende-bearing gneissic host (Rajesh and Santosh, 2014). These patches have quartz and feldspar with the same distinctive brown–green colour that typifies massive charnockite, contrasting with paler quartz and feldspar in the host gneiss. The dark patches contain variably retrogressed orthopyroxene and have markedly reduced biotite and/or hornblende contents compared to the host, which is always orthopyroxene-absent. These changes in mineral mode suggest the patches formed by dehydration of host gneiss as hydroxyl-bearing mica and amphibole were replaced by anhydrous pyroxene. The diffuse edges of the dark patches locally crosscut the gneissic foliation of their host, although gneissic structures can be traced into the alteration as a ghost foliation. The patches have elongate and irregular morphologies, but are often interconnected and follow distinct structural trends that resemble fracture networks. This is consistent with the

patches forming in response to volatile fluid flow, and reports of elevated carbon contents in these patches, either as CO₂ fluid inclusions or graphite, were taken as evidence that these fluids were CO₂ rich (e.g. Hansen et al. 1987), a conclusion that also explained why this fluid would dehydrate biotite and hornblende to stabilise orthopyroxene. Incipient charnockite is very common in biotite-bearing leptynite and hornblende-bearing orthogneiss of the Southern Granulite Terrain, and is also reported in Sri Lanka and Madagascar (e.g. Hansen et al. 1987; Nédélec et al., 2014). This widespread occurrence was used to support conceptual models that viewed dry granulite assemblages in the lower crust as the result of regional-scale flushing by mantle-derived CO₂ fluids (Newton et al., 1980). Such ideas conflict with widely-adopted fluid-absent models for lower crustal metamorphism (Thompson, 1983), in which anhydrous granulite assemblages are a simple consequence of prograde heating leading to progressive loss of H₂O, initially via subsolidus breakdown of hydrous minerals and culminating in partial melting which rapidly consumes any remaining free fluid phase. There is still no consensus on why incipient charnockite is widespread in the Pan-African granulites of southern India, Sri Lanka and Madagascar, or how it might have formed, but there are several overlooked features of these rocks that might suggest a solution.

Firstly, it has long been known that the dark colouration around orthopyroxene is due to fine-grained chlorite and other iron-rich hydrous minerals present along micro-fractures in quartz and feldspar (Howie, 1967; Oliver, 1968). This low-temperature alteration must post-date

orthopyroxene, and the shape and distribution of the dark patches will therefore reflect passage of late hydrothermal fluids rather than any fluid present during orthopyroxene growth. Secondly, the host gneiss is not homogeneous, but actually a migmatite with a foliated gneissic component and coarser-grained quartzofeldspathic segregations, both overprinted by the dark chloritic alteration. In the case of leptynites, the gneissic component comprises garnet–biotite–quartz–feldspar while segregations are dominated by quartz–feldspar with scattered or clustered garnet (e.g. Braun et al. 1996; Blereau et al., 2016). These two components represent gneissic protolith and segregated leucosome, implying that the rocks underwent partial melting before development of patchy fluid-controlled alteration. In areas unaffected by dark alteration, leucosome contains garnet interpreted as a solid (peritectic) product of the melt reaction, and has similar grain sizes and shapes to the charnockite patches. There is also some indication that garnet leucosome has the same increased abundance of CO₂ fluid inclusions seen in charnockite, weakening the link between carbonic fluid and orthopyroxene growth. These observations are more consistent with orthopyroxene forming in leucosome as a peritectic product of dehydration melting in bulk compositions with lower Al or Fe²⁺ than those that stabilised garnet. In this model the CO₂ inclusions are residual fluids left after extraction of H₂O-rich melt from both garnet- and orthopyroxene-bearing leucosome.

This model fails, however, to explain the spatial link between orthopyroxene growth and hydrothermal retrogression. Why is evidence for hydrothermal alteration

always present around orthopyroxene but never seen away from orthopyroxene? Perhaps the hydrothermal fluid passed through all rock types, but only caused visible alteration if it intersected orthopyroxene causing retrogression and release of FeO and other components into adjacent rock. Evidence in support of pervasive fluid through the Southern Granulite Terrain is provided by petrographic and geochemical evidence for widespread fluid-mediated dissolution–reprecipitation of monazite grains at ca. 525–490 Ma in khondalite and leptynite samples, as well as incipient charnockite (Taylor et al., 2014; Blereau et al., 2016). If this model is correct, the dark patches that dominate incipient charnockite are linked to orthopyroxene breakdown rather than orthopyroxene growth, and although incipient charnockites remain a spectacular example of mineral reaction driven by external fluid flux, this reaction is low-temperature hydration around pre-existing orthopyroxene rather than high-temperature dehydration that stabilises orthopyroxene. This model has no need for substantial flux of externally derived carbonic fluid and does not require any volatile-rich fluid phase to be present under peak granulite-facies conditions at all, making it easy to accommodate within orthodox fluid-absent models for high-temperature metamorphism. It does require pervasive influx of retrograde hydrothermal fluid during the final stages of metamorphism, but this is much less controversial given the likelihood that deep partial melt bodies would crystallise and release hydrous fluids late in an orogenic event. More contentious is the implication that the magmas that released these fluids must have underlain the entire Southern

Granulite Terrain to account for the near ubiquitous occurrence of dark charnockitic patches in rocks of suitable bulk composition. However, given geological and geophysical evidence that partial melt is widespread underneath present-day Tibet (Nelson et al., 1996), such a conclusion is entirely consistent with suggestions that the Pan-African granulites of southern India, Madagascar and Sri Lanka represent the mid-crustal levels of an exhumed orogenic plateau (Fitzsimons, 2016).

References

- Blereau, E., Clark, C., Taylor, R.J.M., Johnson, T.E., Fitzsimons, I.C.W., Santosh, M., 2016. Constraints on the timing and conditions of high-grade metamorphism, charnockite formation and fluid–rock interaction in the Trivandrum Block, southern India. *Journal of Metamorphic Geology* 34, 527–549.
- Braun, I., Raith, M.M., Ravindra Kumar, G.R., 1996. Dehydration—melting phenomena in leptynitic gneisses and the generation of leucogranites: a case study from the Kerala Khondalite Belt, southern India. *Journal of Petrology* 37, 1285–1305.
- Clark, C., Healy, D., Johnson, T.E., Collins, A.S., Taylor, R.J.M., Santosh, M., Timms, N.E., 2015. Hot orogens and supercontinent amalgamation: A Gondwanan example from southern India. *Gondwana Research* 28, 1310–1328.
- Collins, A.S., Clark, C., Plavsa, D., 2014. Peninsular India in Gondwana: The tectonothermal evolution of the Southern Granulite Terrain and its Gondwanan counterparts. *Gondwana Research* 25, 190–203.
- Fermor, L.L., 1936. An attempt at the correlation of the ancient schistose formations of Peninsular India. *Memoirs of the Geological Survey of India* 70, 1–51.
- Fitzsimons, I.C.W., 2016. Pan–African granulites of Madagascar and southern India: Gondwana assembly and parallels with modern Tibet. *Journal of Mineralogical and Petrological Sciences* 111, 73–88.
- Hansen, E.C., Janardhan, A.S., Newton, R.C., Prame, W.K.B.N., Ravindra Kumar, G.R., 1987. Arrested charnockite formation in southern India and Sri Lanka. *Contributions to Mineralogy and Petrology* 96, 225–244.
- Holland, T.H., 1900. The charnockite series, a group of Archaean hypersthenic rocks in Peninsular India. *Memoirs of the Geological Survey of India* 28, 119–249.
- Howie, R.A., 1967. Charnockites and their colour. *Journal of the Geological Society of India*, 8, 1–7.
- Nédélec, A., Guillaume, D., Cournède, C., Duran, C., Macouin, M., Rakotondrazafy, M.A.F., Giuliani, G., 2014. Incipient charnockitisation due to carbonic fluid transfer related to late Pan-African transcurrent tectonics in Madagascar; implications for mobility of Fe, Ti, REE and other elements. *Journal of African Earth Sciences* 94, 86–99.
- Nelson, K.D., Zhao, W., Brown, L.D., Kuo, J., Che, J., Liu, X., Klemperer, S.L., Makovsky, Y., Meissner, R., Mechie, J., Kind, R., Wenzel, F., Ni, J., Nabelek, J., Chen, L., Tan, H., Wei, W., Jones, A.G., Booker, J., Unsworth,

- M., Kidd, W.S.F., Hauck, M., Alsdorf, D., Ross, A., Cogan, M., Wu, C., Sandvol, E., Edwards, M., 1996. Partially molten middle crust beneath southern Tibet: synthesis of Project INDEPTH results. *Science* 274, 1684–1688.
- Newton, R.C., Smith, J.V., Windley, B.F., 1980. Carbonic metamorphism, granulites and crustal growth. *Nature* 288, 45–50.
- Oliver, R.L., 1968. Colour in Charnockites. *Mineralogical Magazine* 36, 1135–1138.
- Rajesh, H.M., Santosh, M. 2012. Charnockites and charnockites. *Geoscience Frontiers* 3, 737–744.
- Taylor, R.J.M., Clark, C., Fitzsimons, I.C.W., Santosh, M., Hand, M., Evans, N., McDonald, B., 2014. Post-peak, fluid-mediated modification of granulite facies zircon and monazite in the Trivandrum Block, southern India. *Contributions to Mineralogy and Petrology* 168, 1044–17.
- Thompson, A.B., 1983. Fluid-absent metamorphism. *Journal of the Geological Society* 140, 533–547.

Spatial variability in free phase gas dynamics Using common offset ground penetrating radar in South West Indian Peatlands

Devi K.* and Rajesh R. Nair

Petroleum Engineering Programme, Department of Ocean Engineering, IIT Madras, India

* Corresponding author e-mail: k.devi190@gmail.com

Ground penetrating radar (GPR) is a non-invasive hydro-geophysical method utilized comprehensively to investigate peatland studies. However, this technique has not been used to explore the distribution and release of biogenic gas in Indian Peatlands. In this backdrop, the current research aims to identify the presence and saturation of biogenic methane in humid tropical peatland of Southern Kerala Sedimentary Basin (SKSB) using GPR. The survey was conducted with the GSSI GPR system, using 100 and 200 MHz frequencies shielded antennas. The variations in electromagnetic wave velocity and amplitude of radar signals were analysed

to identify the thickness and geometry of the peat layer and presence of shadow zones. We have adopted GPR common offset measurements for the delineation of vertical and spatial variabilities of in-situ biogenic gas saturation with depth from the deviations in the two-way travel time of reflections and by petrophysical model. Our results show variations in biogenic gas content in shallow (2-4m) and deep (16-18m) portions of the stratigraphic column where peat has encountered and sandwiched between clay rich confining layers. The results are pertinent in the current scenario of unconventional energy resources and global methane dynamics to the atmosphere.

Metasomatic origin of some microcline granites in Northeast Botswana

K.V. Wilbert Kehelpannala*, L. Richard, B.A. Bathobakae and L. Mokane

Department of Geology, Faculty of Science, University of Botswana, Private Bag UB 00704
Gaborone, Botswana

* Corresponding author e-mail: kvwilbert@hotmail.com

Granite-looking, microcline granitoids form a major lithology in the south-western part of the Archaean Zimbabwe Craton exposed in NE Botswana and in the Central Zone of the Archaean Limpopo Mobile Belt. Some of these microcline granitoids (Fig. 1a-f) occur in the areas around Dagwi, Changate, Moshambale, Timbale, Domboshaba and Morokain the Botswana part of the Zimbabwe Craton (Litherland, 1975) and in the Phikwe and Mahalapye complexes of the Central Zones of the Limpopo Belt in NE Botswana (e.g. Key, 1976; Skinner, 1978). Recent preliminary work carried out by Kehelpannala (2013) suggests that most of these granite-looking, microcline granitoids are products of post-metamorphic K-metasomatism of nearby metatonalites and metadiorites. Here we demonstrate that granites and granitic rocks exposed in the areas around Moroka and Domboshaba in the SW part of the Zimbabwe Craton and in the Mahalapye Complex of the Limpopo Belt, NE Botswana are, in fact, products of post-metamorphic K-metasomatism.

The main metasomatic transformation

is very similar to that of the Sri Lankan K-metasomatism (e.g. Kehelpannala, 2013) and is characterized by the formation of metasomatic microcline (mostly perthitic), myrmekite and minor albite in the presence of externally-derived K^+ ions. Three main mechanisms of K-metasomatism are recognized (Kehelpannala and Ratnayake, 1999). These are: (i) in-situ replacement of plagioclase by microcline, (ii) replacement of plagioclase by microcline through myrmekitization of the former and (iii) replacement of co-existing plagioclase-quartz by microcline through the reaction between these two minerals in the presence of K^+ ions. Almost all the microcline grains in these granite-looking rocks are of metasomatic origin, and the degree of metasomatism is directly proportional to the modal abundance of metasomatic microcline and myrmekite (Kehelpannala and Ratnayake, 1999). For naming these metasomatic rocks, we use the nomenclature suggested by Kehelpannala and Ratnayake (1999).

The Moroka Granite is an elongated, granite-looking rock body occurring in the area around Moroka, ~70 km N of

Francistown, NE Botswana, in the SW part of the Zimbabwe Craton. This granitic body within Botswana is more than 25 km long and about 10-15 km wide. The Moroka Granite is associated with metatonalite and metagabbro. A faint foliation is clearly visible in the granite at mesoscopic scale (Fig. 1a, b). At outcrop scale, it is a medium- to coarse-grained, more or less homogeneous rock characterized by the presence of quartz (~20-35%), plagioclase (~35-45%), microcline (~10-40%), biotite (~2-6%), chlorite (~2-5%) and minor amount of myrmekite and albite. Sphene, calcite, apatite and zircon occur as accessories. Quartz and plagioclase grains are fine to medium-grained and show irregular grain boundaries. Almost all quartz grains have developed subgrains, indicating their high temperature deformation, while some plagioclase grains show deformation twinning (albite twinning). Most of the plagioclase grains in the granite are altered to sericite. Microcline is very fine- to very coarse-grained and mostly forms irregular grains. Very coarse microcline grains vary in size from ~10 mm to ~30 mm and form porphyroblasts (Fig. 1a). Field and thin section studies demonstrate that all the microcline grains in the granite are metasomatic in origin and have grown through the replacement of plagioclase and some quartz.

Textural studies and microscopic examinations show that the granite is not an intrusive rock, but formed by K-metasomatism of nearby metatonalite with which the granite is associated. Mesoscopic to microscopic relicts of the parent metatonalite are clearly visible in the granite, which show diffuse contacts with the host granite (Fig. 1b). The parent metatonalite, which is strongly deformed

and metamorphosed under amphibolite-facies conditions, is well exposed around the Habangana area, ~7 km west of Moroka. This metatonalite had undergone at least three deformation represented by a flattening foliation, isoclinal folds and crenulation of the foliation prior to its metasomatism. The major minerals of the parent metatonalite are plagioclase (~45-65%), quartz (~30-45%) and biotite (~5-10%). Quartz and plagioclase show more or less equilibrium grain boundaries. Microcline was not found in unaffected parent metatonalite. Most of the quartz grains show subgrains due to ductile deformation under high-grade metamorphic conditions.

The major mineral formed during the K-metasomatism is fine- to very coarse-grained microcline. Chlorite, myrmekite, rim albite and have been formed as minor minerals. Relicts of quartz and plagioclase are found in the metasomatic microcline (Fig. 1g, h), and most of the plagioclase relicts have thin rims of albite or myrmekite (Fig. 1g). Neither microcline nor myrmekite are deformed as they grew after all the ductile deformations. However, relicts of quartz in metasomatic microcline show subgrains as it was deformed prior to the growth of the host microcline (Fig. 1h). Metasomatic microcline has grown by the replacement of plagioclase and of co-existing plagioclase-quartz according to the three mechanisms mentioned above. The most dominant mechanisms of K-metasomatism that produced the Moroka Granite from the surrounding metatonalite are the above (i) and (iii), and the second mechanism plays a minor role. The degree of the K-metasomatism is not uniform everywhere in the Moroka metasomatic rocks: some parts are strongly

metasomatized, while other parts are slightly affected. Where the metasomatism is strong, the rock is granitic, and where it is slightly affected it has a granodioritic composition. Therefore, the Moroka Granite is not a product of anatexis of the surrounding granitoid gneisses as suggested by Litherland (1975), but it is a product of post-metamorphic K-metasomatism of the nearby metatonalite. We consider the slightly metasomatized parts as pseudo granodiorite and the strongly metasomatized parts as pseudo granite following the nomenclature of Kehelpannala and Ratnayake (1999).

The Domboshaba Granite is a microcline-bearing, granite-looking rock body (Fig. 1c, d) having a shape of a mango as seen on the Geology Map of Litherland (1975) from the SW part of the Zimbabwe Craton. This granitic body occurs ~25 km SW of the Moroka Granite and covers an area of ~20 km² around Domboshaba, ~65 km NW of Francistown. The constituent minerals of the granitic rock are microcline (~20-60%), quartz (~10-35%), plagioclase (~10-40%), chlorite (~5-10%) and minor myrmekite and albite. Sphene, calcite, apatite and zircon occur as accessories. Microcline, quartz and plagioclase have irregular grain boundaries. The latter two minerals are fine- to coarse-grained, while microcline is very fine- to very coarse-grained. Our field and thin section studies clearly demonstrate that the Domboshaba Granite is a product of K-metasomatism of the nearby Kalakamate metatonalite, which has undergone deformation and metamorphism under amphibolite-facies conditions. All the microcline grains, myrmekite and albite are product of this metasomatism. We, therefore, rule out the

intrusive origin suggested for this granite by (Litherland, 1975).

The parent Kalakamate metatonalite had undergone, at least, three ductile deformations prior to its metasomatism. The first deformation of this metatonalite has produced the strong foliation, and the second deformation has given rise to isoclinal folds as seen in many metatonalite outcrops. The third ductile deformation of this parent rock is the crenulation of the above foliation. The parent metatonalite contains plagioclase (~50-60%), quartz (~30-40%) and biotite (~10-20%) as major minerals, and zircon and apatite are found as accessories. No microcline was found in the parent metatonalite, except where it is slightly metasomatized. Although the Kalakamate metatonalite has not yet been dated, the Domboshaba Granite has yielded a U-Pb zircon age of 2647±4 Ma (Bagai et al., 2002). We interpret this age as the intrusive age of the of the Kalakamate metatonalite from which the Domboshaba Granite has been derived through K-metasomatism. The metatonalite has not completely undergone metasomatism, and relicts of this rock can be seen within the metasomatic rocks (Fig. 1c, d). The most dominant metasomatic transformation mechanisms that produced the Domboshaba Granite from the Kalakamate metatonalite are the above (i) and (iii), and the second mechanism plays a minor role. As it is formed by metasomatism, it is considered as pseudogranite.

The Mahalapye Granite is a granite-looking rock body (Fig. 1e, f) in the Mahalapye Complex of the Central Zone of the Limpopo Belt in Botswana. The rock body covers an area of about 2000 km² around Mahalapye. The granite is a

medium- to very coarse-grained microcline-bearing, pink-coloured rock. It contains variable amount of quartz, plagioclase and microcline as major minerals. Chlorite, an alteration product of hornblende and biotite, is present as a subordinate mineral. The minor mineral present in the granite are myrmekite, albite and calcite. This granitic rock has been considered by some workers as a post-tectonic intrusion that crystallized at 2023 ± 7 Ma (McCourt and Armstrong, 1998; Milloning et al., 2010). However, here we demonstrate that this granite is not an intrusive rock body, but a product of strong K-metasomatism of once deformed and metamorphosed tonalite in the Mahalapye Complex.

The Mahalapye Granite is closely associated with metatonalite, which has quartzo-feldspathic layers of variable thickness. Field and thin sections studies show that the granite has been derived from the metatonalite through K-metasomatism of the latter. At mesoscopic scale, the parent metatonalite shows evidences for at least three ductile deformation represented by a strong foliation, tight to isoclinal folds and crenulation of the foliation. This metatonalite had undergone deformation and metamorphism under amphibolite- to granulite-facies conditions (Milloning et al., 2010) before it underwent K-metasomatism to produce the Mahalapye Granite. Microcline, myrmekite, albite, chlorite and calcite are the products of this metasomatism. Microcline is fine- to very coarse-grained and contains numerous

relicts of plagioclase and quartz. Relicts of plagioclase inclusions in this microcline have either rim albite or rim myrmekite. Remnants of the parent metatonalite are clearly visible in the strongly metasomatized part of the rock (Fig. 1e, f). A ghost foliation, which is inherited from parent metatonalite, is clearly visible even in strongly metasomatized parts of the rock (Fig. 1f). As in the other granite described above, the dominant mechanisms of metasomatism of the metatonalite to form the Mahalapye Granite are the above mechanisms (i) and (iii). As it is formed by metasomatism, the Mahalapye granitic rock is considered as pseudogranite.

All three granitic bodies studied from NE Botswana, regardless of their wide geographical distribution, are metasomatic in origin. In all three cases the original parent rocks are deformed and metamorphosed tonalite. The original rocks had undergone, at least, three ductile deformation and high-grade metamorphism prior to K-metasomatism. The metasomatic transformation in all the granite studied are (i) in-situ replacement of plagioclase by microcline, (ii) replacement of plagioclase by microcline through myrmekitization of the former and (iii) replacement of co-existing plagioclase-quartz by microcline through the reaction between these two minerals in the presence of K^+ ions derived from some external sources (Kehelpannala, 2013; Kehelpannala and Ratnayake, 1999). The first and third mechanisms dominate over the second mechanism in all the case.

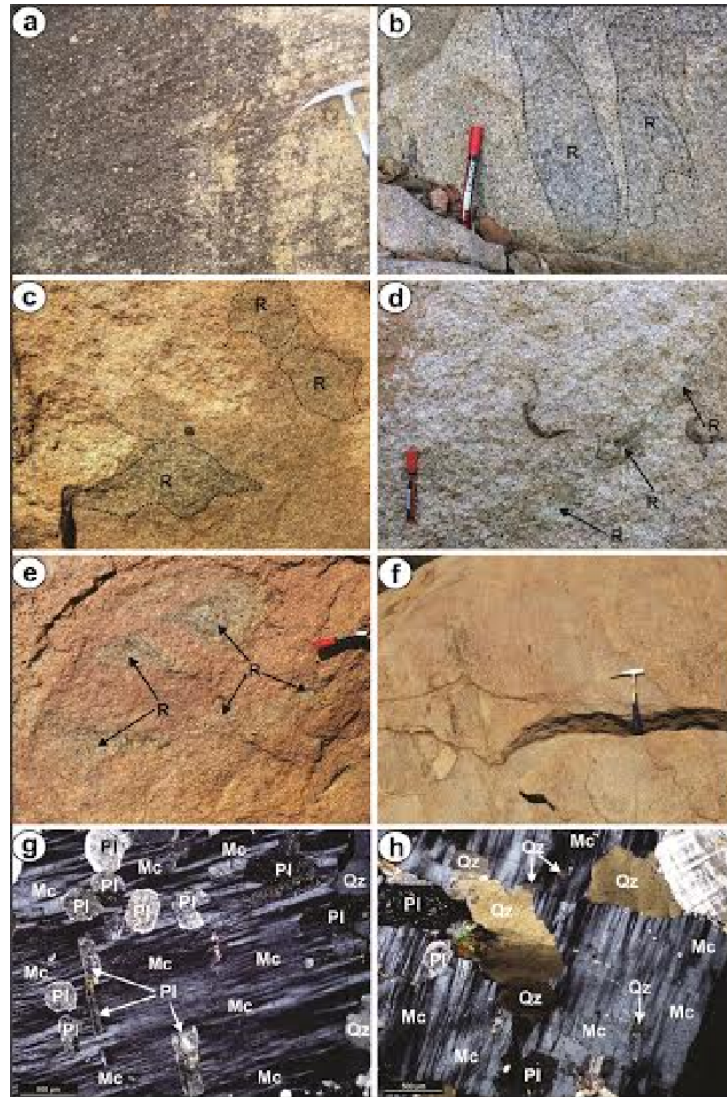


Figure 1. (a)-(f) Field photographs showing the studied granitic bodies. (a)-(b) The Moroka Granite withghost foliations. (c)-(d) The Domboshaba Granite withremnants (**R**) of the parent metatonalite. (e)-(f) The Mahalapye Granite. Note remnants (**R**) of the original metatonalite with foliations in (e) and ghost foliations in (f). In (b)-(e) the ghost foliations in the metasomatic rocksand those of the remnants of the parent rocks are parallel. Note the remnants of the original metatonalite in (b)-(e) are slightly-moderately metasomatized.(g)-(h) Photomicrographs showing metasomatic microcline (Mc) with relicts of plagioclase (Pl) and quartz (Qz). Note relicts of deformed quartz with subgrains in microcline in (h).

References

- Bagai, Z., Armstrong, R., Kampunzu, A.B., 2002. U Pb single zircon geochronology of granitoids in the Vumba granite greenstone terrain (NE Botswana): Implications for the evolution of the Archaean Zimbabwe. *Precambrian Research* 118, 149-168.
- Kehelpannala, K.V.W., 2013. Post metamorphic K-metasomatism of cratonized rocks: Evidence from NE Botswana: *International Association for Gondwana Research Conference Series* 16, 76-78.

- Kehelpannala, K.V.W., 2014. Post metamorphic K-metasomatism in time and space. International Association for Gondwana Research Conference Series 18, 45-47.
- Kehelpannala, K.V.W., Ratnayake, N.P., 1999. Evidence for post-metamorphic metasomatism of high-grade orthogneisses from Sri Lanka. Gondwana Research 2, 167-184.
- Litherland, M., 1975. The geology of the area around Maitengwe, Sebina and Tshesebe, Northeast and Central Districts, Botswana. District Memoir.2, Geological Survey Department, Botswana, 133pp.
- McCourt, S., Armstrong, R.A., 1998. SHRIMP U-Pb zircon geochronology of granites from the Central Zone, Limpopo Belt, southern Africa: Implications for the age of the Limpopo Orogeny. South African Journal of Geology 101, 329-338.
- Milloning, L., Zeh, A., Gardes, A., Klemd, R., Barton, J.M., Jr, 2010. Decompressional heating of the Mahalapye Complex (Limpopo Belt, Botswana): a Response to Palaeoproterozoic magmatic underplating? Journal of Petrology 51, 703-729.
- Skinner, A.C., 1978. The geology of the Mahalapye area. Botswana Geological Survey Department Bulletin 9, 30pp.

Petrological study of rodingite of the ophiolite belt of Manipur, Northeastern India

Kakchingtabam Anil Sharma* and Bidyanada Maibam

Department of Earth Sciences, Manipur University, Canchipur, Imphal-795003, India

* Corresponding author e-mail: anilkak11@gmail.com

Manipur Ophiolite belt is part of the Indo Myanmar Ophiolite belt of Northeastern India which geologically evolved from convergence of Indian and Burmese plates form a belt extending about 200 km from Phokhpur (Nagaland) in the north to Moreh (Manipur) in the south. The Ophiolite belt consists of different igneous, metamorphism and sedimentary sequences. Ultramafic rocks forming the main component of the belt are consisting of mantle sequences of tectonised peridotite with mafic intrusives, volcanic rocks, pelagic sediments (Bhattacharjee, 1991). The rodingites associated with the ultramafic rocks of the Indo Myanmar Ophiolite located in Manipur states of India provide a good opportunity to carry out petrological study of these rocks.

Rare and discontinuous occurrences of rodingites have been recorded all along the ophiolite belt (Shukla, 1989, Ghose et al., 1986). Rodingite were collected from the Kwatha, Chandel District of the ophiolite belt. They occur as discontinuous lenses, pocket veins and pods and abundant in the vicinity of highly serpentized zones. In the field,

rodingite could be distinctly identified as a white, weathered and conspicuous from the dark-coloured ultramafic host. Rodingites of Manipur Ophiolite belt are mainly fine grained dense, white or greenish coloured rocks. Mineral assemblage of the finer grained rocks could not be possible to identify with petrological microscope.

We have analysed the phase chemistry of the samples with electron microprobe analysis and identified the mineral phases such as grossular (garnet), epidote, diopside, idocrase, chlorite, prehnite, apatite, rutile, ilmenite and sphene (titanite). Representative mineral chemistry of the studied samples is presented in Table 1. Garnet analyses from the rock samples Si contents 5.8, Ca value 6.1 and Al value 3.9 are mainly grossular, the end member grossular molecule ranges between 95% to 99% and andradite range from 2 to 3%. Clinopyroxene are low in Al_2O_3 , FeO, Na_2O but CaO and MgO are high. Prehnites, an early product of rodingitization, is chemically homogeneous shows low Fe content. This Fe-poor prehnite in the rock

sample indicates that originated from the fluid which was involved in serpentinisation process (Sivell et al., 1986). Chlorite is an important mineral phases in rodingite which believed to be altered from clinopyroxene. The analyzed chlorite crystals are rich in Mg and are mostly of clinochlore and ripidolite with Si content ranging between 5.9 and 6.1. Whole rock geochemical data

is generated using X-ray Fluorescence (XRF) and the SiO₂ ranges between 41.6 to 43.63 wt. %, Al₂O₃ from 11.00 to 16.47, FeO between 5.8 to 11.4 wt. %, TiO₂ (1.8 to 3.0 wt. %) and high CaO between 29.00 to 38.41 wt %. Based on the geochemical dataset, it can be inferred that the rodingite samples from the Manipur Ophiolite are formed from different protoliths.

Table 1: Representative phase chemistry of rodingite samples from the Manipur Ophiolite

<i>Oxides</i>	<i>Garnet</i>		<i>Diopside</i>		<i>Epidote</i>		<i>Chlorite</i>	
<i>SiO₂</i>	38.02	38.07	50.80	53.39	37.12	38.32	27.28	28.85
<i>Al₂O₃</i>	21.93	21.84	1.38	0.62	26.64	26.52	25.31	22.05
<i>Na₂O</i>	0.00	0.00	0.02	0.00	0.26	0.14	0.02	0.01
<i>MgO</i>	0.00	0.03	15.33	17.18	3.07	3.45	25.39	25.87
<i>K₂O</i>	0.00	0.00	0.00	0.03	0.01	0.02	0.00	0.03
<i>CaO</i>	37.86	37.21	25.07	24.78	22.91	22.67	0.02	0.13
<i>TiO₂</i>	0.46	0.38	0.01	0.01	0.00	0.04	0.03	0.02
<i>NiO</i>	0.00	0.00	0.00	0.00	0.00	0.00	0.00	0.00
<i>MnO</i>	0.15	0.10	0.48	0.72	0.02	0.01	0.05	0.06
<i>FeO</i>	0.81	0.83	2.07	2.02	1.38	1.28	7.55	10.41
<i>CoO</i>	0.00	0.00	0.00	0.00	0.00	0.00	0.00	0.00
<i>ZnO</i>	0.00	0.00	0.00	0.00	0.00	0.00	0.00	0.00
<i>V₂O₃</i>	0.00	0.00	0.00	0.00	0.00	0.00	0.00	0.00
<i>Cr₂O₃</i>	0.06	0.07	0.00	0.03	0.00	0.08	0.04	0.03
<i>Total</i>	99.23	98.53	95.16	98.78	91.41	92.53	87.69	87.46

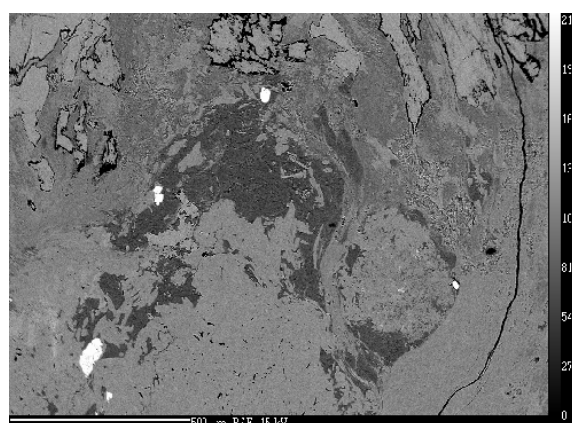


Fig 1. Representative Back Scattered Image of studied rodingite sample.

References

- Bhattacharjee, C.C., 1991. The ophiolites of northeast India – a subduction zone ophiolite complex of the Indo-Burman orogenic belt. *Tectonophysics*, 191, pp. 213-222.
- Ghose, N.C., Agrawal, O.P., Singh, R.N., 1986. Geochemistry of the ophiolite belt of Nagaland, N.E. India, ophiolite and Indian plate margin. In: Ghose, N.C. (Ed.), *Phanerozoic Ophiolites of India and Associated Mineral Resources*. Suman Publication, Patna, pp. 241–293.
- Shukla, R., 1989. Occurrence of rodingite in the ophiolite belt of Manipur. In: Ghose N.C., (Ed.) *Phanerozoic ophiolite belt of India*, Sumna Publ., Patna, pp. 189–196.
- Sivell, W.J., Waterhouse, J.B., 1986. The geochemistry, origin and tectonic significance of rodingite from the Dun Mountain Ultramafic, D'Urville Island, New Zealand. *New Zealand Journal of Geology and Geophysics*, 29, pp. 9-27.

Deformation along southeastern margin of Cauvery Suture Zone: Critical consequences related to evolution of Southern Granulite Terrain

D.P. Mohanty

Dept. of Geology, Savitribai Phule Pune University, Pune, India
E-mail: dpmohanty@unipune.ac.in

The high-grade terrain occurring at the southern tip of India, popularly known as the Southern Granulite Terrain (SGT), consists mainly of late Archaean charnockites, quartzo-feldspathic gneisses, high-grade supracrustals and a variety of younger intrusions such as alkaline-anorthositic rocks and granitoids. SGT comprises a group of fragmented and separated into different imbricate blocks by crustal-scale Cauvery Shear Zone system, recently reported as Cauvery Suture Zone (CSZ) and the Achankovil Shear Zone (AKSZ) (Santosh et al., 2009; Mohanty and Chetty, 2014; Mohanty, 2016; Chetty et al., 2016 and references there in). The CSZ constitutes high-angle thrust represented by the Moyar-Bhavani-Mettur Shear Zone at the northern margin and many sub-parallel shear zones to the south representing back thrusts, which are together visualized as a crustal-scale 'flower structure' (Chetty and Bhaskar Rao, 2006). The CSZ has also been extended to Madagascar coinciding with sinistral Ranatsora shear zone of Madagascar, and

to east Antarctica joining with the junction between Napier complex and Rayner complex of Enderby Land (Colins et al., 2007). A wide variety of migmatites and deformed structures are very common in CSZ in general and along its southeastern margin in particular (Mohanty, 2016) which is the prime focus of this study. This work involves the structural and petrological investigation of Precambrian high grade gneisses of the basement complex along the south eastern margin of CSZ and highlights the finite strain geometry, pattern of deformation and grade of metamorphism preserved within the rock. The structural elements preserved within the high grade gneissic rocks in this area are extremely exciting. Multi scale structural analysis has helped in understanding the structural geometry particularly in the migmatitic rocks and their inter relations with the associated rock types. Structural fabrics include: numerous mesoscopic as well as map scale shear zones, boudinaged competent layers displaced by melt lubricated shear zones, complex pattern of

shearing in the presence of melt and disruption of mafic layers, riedel shear geometry and C-S fabrics etc.. Besides, the complex fold structures observed in this region are most significant, which involves tight isoclinal folds, ptygmatic folds, narrow limb and broad hinge folds, plunging anticlines and synclines, open to gentle folds, sheath folds and superimposed fold patterns predominately the Type-2 and Type-3 interference pattern of folding. Various structural cross sections made through different traverses of the area shows the northward dipping of the rock units and superposed folding as well. The north dipping and southerly verging thrust surfaces mark the back thrust zone of the CSZ section. Systematic petrographic studies have helped in redefining field based terminologies to *sēnsū strictō* nomenclatures of the rock types observed. Eg. Quartzo feldspathic gneiss to Bt-Amph gneiss to Migmatitic gneiss. This classification also helped in coming to a concluding point that the deformation intensity of the rocks are increasing when we go from north to south in the study area. This also suggests that, the granulites from the boundary regions are not similar in nature rather showing different characteristics when we move from north to south. The granulites in the northern margin have both garnetiferous and non-garnetiferous where as in western margin they are having eclogitic in nature containing atoll garnets within them. The granulites in the southern margin are showing very high grade metamorphism as the grain sizes are comparatively finer. So, from this it is clear that, there is an increase in metamorphic grade when we move from north to south of the study area. The present study reports a critical

consequence related to the evolution of the entire Southern Granulite Terrain of Indian peninsula. The results from this study along with the available geochemical, geochronological data enhances the evidences of subduction tectonics involved during Gondwana amalgamation (Santosh et al., 2009).

References

- Chetty et al., 2006, Crustal architecture and tectonic evolution of the Cauvery Suture Zone, southern India. Journal of Asian Earth Science, In press.
- Chetty, T.R.K., Bhaskar Rao, Y.J., 2006a. The Cauvery shear zone, Southern Granulite Terrain, India: a crustal-scale flower structure. Gondwana Res. 10, 77–85.
- Chetty, T.R.K., Yellappa, T., Mohanty, D.P., Nagesh, P., VenkataSivappa, V., Santosh, M., Tsunogae, T. 2012. Mega-Sheath Fold of the Mahadevi Hills, Cauvery Suture Zone, Southern India: implication for accretionary tectonics. Journal of Geological Society of India 80, 747–758.
- Collins, A.S., Clark, C., Sajeev, K., Santosh, M., Kelsey David, E., Matin, H., 2007. Passage through India: Mozambique Ocean suture, high pressure granulites and Palghat-Cauvery shear zone system. Terra Nova 19, 41–147.
- Mohanty, D.P. 2016. Study of Mesoscopic structural features along the margins of Cauvery Suture Zone, Southern India, Shear Zones and Crustal Blocks of Southern India, V. 3, 14-23.
- Mohanty, D.P. and Chetty, T.R.K. 2014. Possible Detachment Zone in Precambrian rocks of Kanjamalai Hills, Cauvery Suture Zone, Southern India:

- Implications to accretionary tectonics. *Journal of Asian Earth Sciences*, 88, 50-61.
- Santosh, M., Maruyama, S., Sato, K., 2009. Anatomy of a Cambrian suture in Gondwana: Pacific-type orogeny in southern India? *Gondwana Res.* 16 (2), 321–341.
- Yellappa, T., Santosh, M., Chetty, T.R.K., Sanghoon Kwon, Chansoo Park, Nagesh, P., Mohanty D.P, Venkatasivappa, V. 2012. A Neoproterozoic dismembered ophiolite complex from southern India: Geochemical and geochronological constraints on its suprasubduction origin, *Gondwana Research*, 21,246-265.

Geochronological and geochemical study of detrital zircons from the Naga Metamorphites, Northeastern India: Provenance and Paleogeographic implications

Bidyananda Maibam^{a *}, Stephen F. Foley^{b, c} and Klemens Link^{b, d}

^aDepartment of Earth Sciences, Manipur University, Canchipur, Imphal-795003, India

^bGeocycles Research Centre, University of Mainz, 55099 Mainz, Germany

^cCCFS and Department Earth and Planetary Sciences, Macquarie University, North Ryde, NSW 2109, Australia

^dGübelin Gem Lab, Lucerne, Switzerland

* Corresponding author e-mail: bmaibam@yahoo.com

Zircon is an attractive proxy for provenance because of its durability and remarkable chemical stability. Detrital zircons are widely used for provenance study since they are relatively difficult to destroy and they provide a record of magmatic history that is developed further through each sedimentary cycle. The processes of weathering, fluvial activity and gravitation over the time have separated and concentrated a statistically more meaningful sample than is achievable by conventional single-rock sampling, and thus can provide a more comprehensive coverage of rock types in the region (Belousova et al., 2009). The analysis of large numbers of grains obtained from detrital concentrates generates U–Pb age spectra in which peaks can be used to recognise major episodes of magmatic activity.

Indo-Myanmar ophiolite in the northeastern India is bounded to the east by a west-directed thrust that places the mid-Cretaceous limestone of the Nimi Formation together with the Naga Metamorphics over the ophiolite. The Naga Metamorphics (Brunnschweiler, 1966) are an assemblage that includes pelites, psammites, phyllitic schists, quartz-chlorite-mica-schists, marbles, granite gneisses and quartzose gneisses. It is presumed to be an exotic lithounit attached to the Indo-Myanmar ophiolite belt. We have carried out combined U–Pb geochronology and trace element geochronological study of the detrital zircons separated from the lithounits of Naga metamorphic rocks using a laser ablation inductively coupled mass spectrometry (LA-ICPMS). The objective of our study is to characterize the detrital zircons associated with the Naga

Metamorphics to decipher probable provenance of the geologically little known area.

The samples were crushed into centimeter-sized chips and were thoroughly washed after eliminating the weathered portions. We have carried out conventional zircon separation using the heavy liquid, followed by magnetic separation using a Frantz isodynamic separator. Zircon grains were handpicked using a binocular microscope. Individual clear, unfractured and less coloured zircons were selected and were mounted on a double-sided tape, cast in epoxy and sectioned by polishing. Transparent zircons with simple internal structure were documented in detail. The grains recovered from the studied samples are inclusion free

subhedral to subrounded, colourless to brownish.

U–Pb isotopes were analysed by LA-ICPMS using an Agilent 7500ce quadrupole inductively coupled mass spectrometer linked to a New Wave NWR193-excimer-laser system with 193 nm wavelength housed at the University of Mainz. After pre-ablation, analyses were conducted using a 25 micrometer crater diameter with 20 second warm up-, 30 second dwell- and 30 second washout-time. Analyses were standardized using the GJ-1 zircon (Jackson et al., 2004). The reproducibility was controlled by measuring the zircon standards ‘Plešovice’ (Sláma, et al., 2008) and ‘91500’ (Wiedenback et al., 1995) as blind samples and measured values deviated less than 2% from the accepted values.

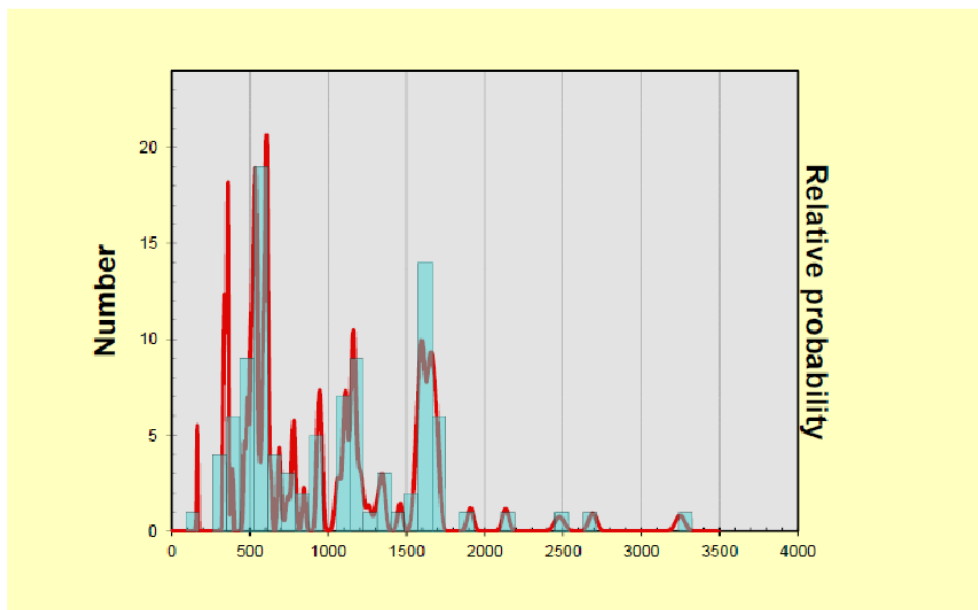


Fig. 1. Representative probability distribution curve of detrital zircons Naga Metamorphic rock

U–Pb geochronological data show that the detrital zircons from the studied rocks are ranging between 120 to 3300 Ma with age peaks in the range 500–650,

1000–1200, 1500–1700 Ma. Representative probability distribution curve is shown in Fig. 1. Detrital age spectrum reflects the probable magmatic

activity of the provenance. The trace element compositions of magmatic zircon can be used to recognise broad categories of magmatic rocks that represent the crystallized melts from which the zircons crystallized (Belousova et al., 2002). Based on the various zircon trace element diagrams, it can be inferred that the detrital zircons probably derived from continental marginal granitoids. During the presentation, possible source terrains and their implications in the framework of available tectonic models for the region would be discussed.

References

- Belousova, E.A., Griffin, W.L., O'Reilly, S.Y., Fisher, N.I., 2002. Igneous zircon: trace element composition as an indicator of source rock type. *Contributions to Mineralogy and Petrology* 143, 602–622.
- Brunnschweiler, R.O., 1966. On the geology of the Indo-burman ranges Arakan Coast and Yoma, Chin Hills, Naga Hills. *Journal of the Geological Society of Australia*, 13, 137–194
- Jackson, S.E., Pearson, N.J., Griffin, W.L., Belousova, E.A., 2004. The application of laser ablation-inductively coupled plasma mass spectrometry to in situ U–Pb zircon geochronology. *Chemical Geology* 211, 47–69.
- Wiedenbeck, M., Alle, P., Corfu, F., Griffin, W.L., Meier, M., Oberli, F., Quadt, A., Roddick, J.C., Spiegel, W., 1995. Three natural zircon standards for U–Th–Pb, Lu–Hf, trace element and REE analyses. *Geostandards and Geoanalytical Research* 19 (1), 1–23.

Seismic imaging of a new Gondwana basin around Vinjamuru region of Nellore Schist Belt, south Indian shield and its possible geodynamic implications

O. P. Pandey* and K. Chandrakala

CSIR-National Geophysical Research Institute, Uppal Road, Hyderabad -500 007, India

* Corresponding author e-mail: om_pandey@rediffmail.com

Eastern part of the Dharwar craton (EDC) is considered a key element in India- east Antarctica correlation within the Gondwanaland assembly. It remained geodynamically quite active during the entire course of geologic history, having undergone oceanic subduction, continent-continent collision, multi-stage accretional growth, besides multiple deformation and metamorphism. In spite of many geological and geophysical investigations in the last two decades, the nature of deep crustal structure and the geodynamic evolution of this region remain an enigma. In view of this, we made a new attempt to seismically image this region, encompassing intracratonic Proterozoic Cuddapah basin, Nellore Schist Belt (NSB), Ongole domain of the Eastern Ghats Belt and adjacent East Coast Terrain, using Deep Seismic Sounding (DSS) data.

An important new finding of this study has been the detection of a thin

sequence (~200 m) of Gondwana sediments with a distinct velocity of 4.20 km/s, which has a lateral dimension of about 40 km around Vinjamuru and Kaligiri region of NSB. Its estimated velocity closely conforms to DSS derived velocities in other Gondwana grabens like Bengal, Mahanadi, Krishna-Godavari and central India. Incidentally, this is possibly the first report of the occurrence of Gondwana sediments in an intracratonic setting. Till now, their presence have been reported mainly from the rifted Gondwana grabens, situated along the peripheries of various Archean-Proterozoic cratons like Dharwar, Bastar, Singhbhum etc, which were perpetual weak zones formed consequent to the separation/amalgamation of the cratonic blocks time and again. These Gondwana sediments, which we name as Vinjamuru Gondwanas, are found to be underlain possibly by thick Proterozoic sediments, having velocities 5.3 and 5.5 km/s, which compare well with the

velocities of upper and lower Cuddapah sediments respectively.

It appears that during the Gondwana period, entire eastern segment of EDC, have been persistently rifting, uplifting and eroding together with other Gondwana grabens in India, thereby leaving behind only a thin veneer of Gondwana sediments at many places, as recent drill hole studies would suggest. In view of the presence of number of Gondwana basins all along the east coast, it is felt that the rifting during the Gondwana period may have been a prelude to India- Antarctica breakup, with

final separation between the two taking place much later during mid to late Cretaceous period. Presence of Gondwana sediments over the NSB region of EDC, puts forward a question, whether the intra-cratonic parts of the shield terrains were also rifting during the Gondwana period, which will challenge the widely believed theory of the stability of shield terrains since Neoproterozoic era. If so, continued rifting could have been a major cause for substantial thinning of the Indian shield lithosphere to about 100 km in comparison to 250-300 km in other shields elsewhere.

Lifestyles of the Palaeoproterozoic stromatolite builders in the Vempalle Sea, Cuddapah Basin, India

Sarbani Patranabis-Deb

Geological Studies Unit, Indian Statistical Institute, 203, B.T.Road, Kolkata 700108, India

The Vempalle Limestone Formation of the Cuddapah Basin of the east Dharwarcraton, India, was deposited on an extensive Palaeoproterozoic passive margin ramp type carbonate platform. The formation can be physically traced for about 250 km along the south western arcuate margin of the Papaghni Sub basin, with ~2 km preserved thickness. The platform is composed of heterolithic carbonate mudstone and siltstone at the lower part of the succession and almost entirely of fine-grained lime-mudstone, oolite and dolomite with development of wide range of columnar, domal and stratiform microbialite facies in the upper part of the formation. Sedimentological investigation reveals several facies association which are depth partitioned and range from supratidal to subtidal regime. Algal laminites dominate in the lower part of the Vempalle succession, often with tepee

structure, desiccation cracks filled with lime mud or sand, molar-tooth structure and rhombic halite casts and intraformational limeclast conglomerate. The upper part of the succession is dominated by bedded dolomites which occur as lens-shaped bodies, slightly convex upward, shoaling-up bars with isolated stacked hemispheroidal (SH) stromatolites to laterally linked hemispheroidal (LLH) type stromatolites. Successive stromatolite beds are separated by muddy intervals, which occur in a well-defined cyclic arrangement in the stratigraphic profile. The cyclicity is interpreted here as evidence of eustatic sea-level fluctuations leading to variable changes in accommodation space. The distribution of the microbialite facies from stratiform to columnar type is with increase in synoptic relief of columnar stromatolites point to marine transgression.

New views on the composition and character of earth's mantle: Insights from ophiolites

Paul T. Robinson^{1, 2}, Jian-Wei Li¹, Jingsui Yang², Mei-Fu Zhou³, and Fahui Xiong²

¹Faculty of Earth Sciences, China University of Geosciences, Wuhan

²Institute of Geology, Chinese Academy of Geosciences, Beijing

³Department of Earth Sciences, The University of Hong Kong SAR, China

Most of the evidence for the composition and character of Earth's mantle comes from indirect studies, such as seismic information and experimental studies of mineral stability and melting conditions of presumed mantle phases, as well as the composition and isotopic character of mantle-generated magmas. Outcrops of mantle rocks are mostly limited to the seafloor and to ophiolites, both of which are thought to have been formed at shallow levels. In recent years a totally unexpected collection of exotic phases, including ultrahigh pressure phases (diamond), highly reduced native elements and alloys and a range of crustal minerals, has been recovered from both peridotites and chromitites of ophiolites that suggests a highly heterogeneous mantle in which such phases can be preserved. The presence of diamonds suggests formation at depths of at least 130 km and perhaps as deep as 380 km, but clearly these minerals were able to persist during transport to shallow-

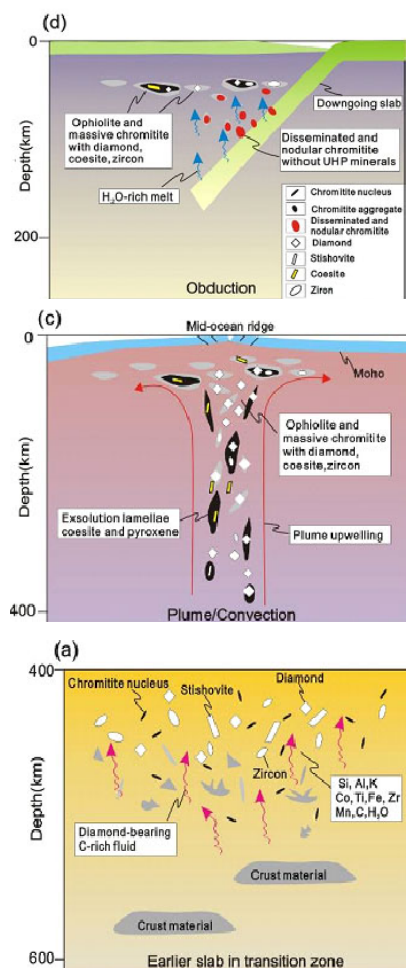
level peridotites and high-temperature chromitites without being converted to graphite. The many native elements, metallic (Ni, Co, Mn) alloys, and alloys indicate formation under super-reducing conditions and yet many are enclosed in grains of magnesiochromite that presumably crystallized under oxidizing conditions to form chromitites. Both the diamonds and super-reduced minerals are accompanied by a wide range of silicate minerals of presumed crustal origin, such as K-feldspar, Na-plagioclase, amphibole, biotite, muscovite, garnet, corundum, zircon, rutile, quartz (and coesite). The crustal minerals must have been introduced into the mantle by subduction of oceanic and continental lithosphere but their preservation under mantle conditions is difficult to understand. Zircon is a particularly useful mineral because it shows that the ophiolitic peridotites and chromitites contain grains with a wide range of age, commonly from Archean to Mesozoic.

Many of the older zircon grains are rounded and contain inclusions of common crustal minerals indicating derivation from reworked continental crust.

The presence of these unexpected minerals in mantle rocks has generated many competing models to explain their origin and preservation. We prefer a model in which the UHP and super-reduced minerals are formed at depths above the transition zone where they can be encapsulated in grains of magnesiochromite. Crustal minerals may also have been introduced to similar depths by subduction, but their preservation favors introduction at shallower levels, perhaps in suprasubduction zone mantle wedges. Fluids and melts generated in such SSZ environments react with the host peridotites to mobilize and recrystallize magnesiochromite grains in the peridotites to form chromitites. The exotic minerals are preserved during this process presumably because they are incorporated as inclusions in the magnesiochromite grains, although many of the exotic minerals in the peridotites are not hosted in such grains.

Our model for evolution of the mantle is given below. In the first step (a) slabs of oceanic lithosphere containing continentally derived sediments and/or fragments of continental crust are subducted into the mantle transition zone or even deeper and the material is disseminated in the mantle peridotites. Crystallization of chromite grains above the transition zone at pressures <14 GPa encapsulates the UHP, super-reduced and crustal minerals facilitating their preservation. Upwelling beneath ocean spreading centers (c) carries the mantle peridotites and disseminated chromitites to shallow levels. Later subduction (d) produces

suprasubduction zone mantle wedges in which massive chromitite bodies are formed with dunite envelopes. Many of the crustal minerals may be introduced into the mantle during this later subduction. Eventual emplacement of some of these SSZ mantle wedges on continental margins and in island arcs results in the formation of ophiolites.



This model suggests that the oceanic mantle is more heterogeneous than previously thought and that a wide range of minerals can exist metastably in this environment. If this model is correct, many of the exotic minerals, particularly the UHP and super-reduced phases should exist widely in in-situ oceanic peridotites.

Petrology and geochemistry of basement rocks in Bangladesh: Implications for Paleoproterozoic tectonic evolution

Ismail Hossain^{1*}, Toshiaki Tsunogae² and Most Momotaz Khatun¹

¹Department of Geology and Mining, University of Rajshahi, Rajshahi 6205, Bangladesh

²Graduate School of Life and Environmental Sciences (Earth Evolution Sciences), University of Tsukuba, Ibaraki 305-8572, Japan

*Corresponding author e-mail: ismail_gm@ru.ac.bd

The Palaeoproterozoic (1.73 Ga) basement rocks from Bangladesh composed mainly of diorite, quartz diorite, monzodiorite, quartz monzonite and granite (Hossain et al., 2007, Hossain and Tsunogae 2014). These rocks also show a large range of chemical variations (e.g. SiO₂ = 50.7–74.7 wt%, Fe₂O₃* = 1.23–10.08 wt%, MgO = 0.20–6.57 wt%). Plagioclase forms the dominant feldspar in diorite (~48%) and monzodiorite (~47%), while alkali feldspar predominate the modal assemblage of granite (~50–76%) and quartz monzonite (~40%). Amphibole and biotite form the dominant mafic minerals in the most rock types. The pluton overall displays metaluminous, calc-alkaline orogenic suite; mostly I-type suites formed within subduction-related magmatism. The observed major elements show general trends for fractional crystallization. Trace element contents also indicate the possibility of a fractionation or assimilation; explain the entire variation from diorite to monzonite, even granite. Major, trace and REE

abundances and patterns affected the evolution of the basement rocks of Bangladesh. The pluton may have evolved the unique chemical features by a process that included partial melting of calc-alkaline lithologies and mixing of mantle-derived magmas, followed by fractional crystallization, and by assimilation of country rocks. The pluton shows evidence of crystal fractionation involving largely plagioclase, amphibole and possibly biotite. Some of the fractionated magmas may have mixed with more potassic melts from distinct parts (metagrewackes) of the continental lithosphere to produce granites and/or pegmatites. It is possible that magmas generated deeper in the crust had a larger component of mantle-derived melt (e.g. diorite), and magma generated higher in the mid-crust contained a larger contribution of sialic material (e.g. quartz monzonite, granite). Parallel REE patterns indicate similar source of basement rocks. The main trend of the pluton, from diorites to granites, is thought to represent a wide

variety of interactions with crustal components, and especially the combined effects of assimilation-fractional crystallization (AFC).

The consistent magmatism is also common in the Central Indian Tectonic Zone (CITZ), India, the Transamazonian of South America, Bohemian Massif and the Svecofennian, Poland, have identified the sequential growth of the continent

through the amalgamation of juvenile terrains, succeeded by a major collisional orogeny (Lauria et al., 2012). Subduction-related batholiths in the Albany-Fraser belt in Australia have similar counterparts in the Windmill islands and Bungar Hills in Antarctica, suggest that such crust were actively contributing to magmatism in the Palaeoproterozoic supercontinent.

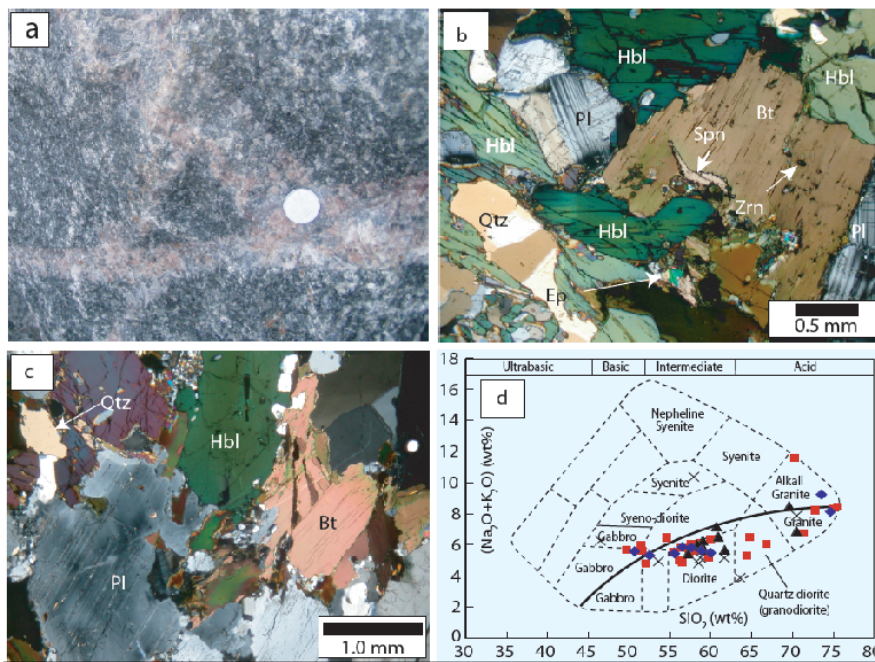


Fig. 1 (a) Diorite with cross-cutting pinkish granitic-pegmatite, (b and c) Microphotographs showing representative texture of quartz diorite with mineral assemblage and petrographic relationship among hornblende (Hbl), plagioclase (Pl), quartz (Qtz), biotite (Bt), titanite (Ttn), epidote (Ep), and zircon (Zrn), and (d) The chemical classification and nomenclature of basement rocks in Bangladesh using the total alkalis versus silica (TAS) diagram of Cox et al. (1979) adapted by Wilson (1989) for plutonic rocks (the curved solid line subdivides the alkalic from subalkalic rocks).

References

Cox, K.G., Bell, J.D., Pankhurst, R.J., 1979. The Interpretation of Igneous Rocks. George Allen and Unwin, London.

Hossain, I., Tsunogae, T., 2014. Crystallization Conditions and Petrogenesis of the Palaeoproterozoic Basement Rocks in Bangladesh: An Evaluation of Biotite and Coexisting Amphibole Mineral Chemistry. *Journal of Earth Science*, v. 25 (1), pp. 87–97

Hossain, I., Tsunogae, T., Rajesh, H.M., Chen, B., Arakawa, Y., 2007.

Palaeoproterozoic U-Pb SHRIMP zircon age from basement rocks in Bangladesh: A possible remnant of the Columbia Supercontinent. *Comptes Rendus Geoscience*, v. 339, pp. 979–986.

Lauria, L.S., Mikkolab, P., Karinena, T., 2012. Early Paleoproterozoic felsic and mafic magmatism in the Karelian province of the Fennoscandian shield. *Lithos* 151, 74–82.

***Glossopteris* flora from the Pali formation, Johilla coalfield, Umari District, Madhya Pradesh: Palynological implications for a late Permian age**

S.Suresh Kumar Pillai

Birbal Sahni Institute of Palaeosciences, Lucknow 226007 India
E-mail: suresh_pillai2000@rediffmail.com

The Johilla Coalfield is one of the important coalfields of South Rewa Gondwana Basin producing around 2.061 lakh tonnes of coal per year. The Gondwana sediments in this Coalfield consist of Talchir, Barakar, Pali, Tiki, Parsora and Hartala formations. The term “Supra-Barakar” was initially used by Hughes (1881) for the sedimentary sequence above the Barakar Formation. The age and consequently the order in which the “Supra-Barakar” formations occur has been a matter of debate within the scientific community.

On the basis of lithological and palynological evidences, the Pali Formation has been assigned varying ages ranging from middle Permian to middle Triassic (Tarafdar *et al.* 1993, Ram-Awatar 2003) and late Permian (Mukhopadhyay *et al.* 2010, Mukherjee *et al.* 2012). To resolve the debate regarding the age of the Pali Formation, several excursions were undertaken to the Johilla Coalfield for collection of plant fossils and rock samples for recovery of palynomorphs. As a result, a rich assemblage of plant fossils comprising different orders, namely, Glossopteridales,

Cordaitales and Filicales besides a scale leaf and several dispersed seeds was collected from a shale sequence of Pali Formation exposed along Pali-Manthar road section (latitude: N23°20.896' longitude: E 81° 04.935'), close to the Pali Village. The plant fossil assemblage comprising a typical *Glossopteris* flora includes the taxa *Glossopteris bosei*, *G. communis*, *G. gondwanensis*, *G. indica*, *G. intermedia*, *G. intermittens*, *G. leptoneura*, *G. longicaulis*, *G. searsoliensis*, *G. spathulata*, *G. stricta*, *G. subtilis*, *G. tenuifolia*, *G. tenuinervis*, *G. vulgaris*, *Neomariopteris hughesii*, *Vertebraria indica*, *Utkaliolepis indica*, dispersed seeds like *Cordaicarpus zeilleri*, *Rotundocarpus striatus*, *Samaropsis goraiensis*, *Samaropsis feistmantelli* indicating a Permian age. The palynological analysis (quantitative and qualitative) of sediments indicates dominance of striate disaccate pollen-grains. chiefly species of *Striatopodocarpites* and *Faunipollenites* in association with *Striatites*, *Verticypollenites*, *Densipollenites*, *Lahiritites*, *Crescentipollenites*, *Distriatites*, *Arcuatipollenites*, *Scheuringipollenites*,

Decussatisporites and sporadic occurrence of some stratigraphically significant taxa like *Guttulapollenites*, *Alisporites* and *Weylandites* which shows a late Permian affinity.

of the Pali Formation is comparable with those of the non-coaliferous beds of Kamthi and Bijori formations of Mahanadi and Satpura Gondwana basins, respectively, which are considered younger than the Raniganj Formation (Srivastava & Agnihotri, 2010). The lithological attributes of the Pali Formation are also shared with the Kamthi and Bijori formations and the Pachhwarra Formation of the Rajmahal Basin. The palynoflora of the Pali Formation can be correlated with the late Permian palynofloras of Pachhwarra Formation, Rajmahal Basin (Tripathi, 1996 & Vijaya 2009), Bijori Formation, Satpura Basin (Bharadwaj et al., 1978) and Kamthi Formation, Godavari and Mahanadi basins (Srivastava and Jha 1997, Meena 1998). On the basis of the palynological evidences, a late Permian age is suggested for the Pali Formation.

References

Bharadwaj, D.C., Tiwari, R.S. and Anand-Prakash 1978. Palynology of Bijori Formation (Upper Permian) in Satpura Gondwana Basin, India. *Palaeobotanist* 25, 72–78.

Hughes T.W.H. 1881. Notes on the South Rewa Gondwana basin. *Memoirs Geological Survey of India*. 14, 1-103.

Meena K.L. 1998. Palynological dating of sub-surface Kamthi sediments in Ib River Coalfield, Orissa. *Geophytology*, 27, 107–110.

Mukherjee, D., Ray, S., Chandra, S., Pal, S. Bandopadhyay, S., 2012. Upper Gondwana succession of the Rewa Basin, India: Understanding the interrelationship of lithologic and stratigraphic variables. *Journal of the*

This is the first detailed systematic record of the megafloral and the miofloral assemblages from the Pali Formation of Johilla Coalfield. The megafloral assemblage

Geological Society of India 79, 563–575.

Mukhopadhyay, G., Mukhopadhyay, S.K., Roychowdhury, M. Parui, P.K. 2010. Stratigraphic correlation between different Gondwana basins of India. *Jour. Geol. Soc. India* 76, 251-266.

Ram-Awatar, 2003. A Triassic palynoflora from Pali Formation, South Rewa Gondwana Basin, Madhya Pradesh, India. *Palaeobotanist* 52, 49-54.

Srivastava, A.K. and Agnihotri, D. 2010. Upper Permian plant fossil assemblage of Bijori Formation: A case study of *Glossopteris* flora beyond the limit of Raniganj Formation. *Journal of the Geological Society of India*, 76, 47–62.

Srivastava, S.C., jha, N. 1997. Status of Kamthi Formation: Lithological and Palaeobotanical evidences. *Palaeobotanist* 46,88-96.

Tarafdar, P., Sinha, P.K., Das, K.P., Kundu, A., Dutta, D.R., Rajaiya, V., Parui, P.K., Patel, M.C., Thanavelu, C., Kumar, A., Pillai, M.K., Agasty, A. Dutta, N.K. 1993. Recent advance in Post-Barakar stratigraphy in parts of Rewa Gondwana Basin. *Gondwana Geol. Mag., Spec. Vol.*, 60-69

Tripathi, A. 1996. Early and Late Triassic palynoassemblages from subsurface Supra-Barakar sequence in Talcher Coalfield, Orissa, India. *Geophytology* 26,109-118.

Vijaya, 2009. Palynofloral changes in the Upper Paleozoic and Mesozoic of the Deocha-Pachamari area, Birbhum Coalfield, West Bengal, India. *Science in China Series D: Earth Science* 52, 1932–1952.

Neoproterozoic lamprophyres from Halaguru area, Harohalli dyke swarm, Dharwar Craton, India: Insight on the Rodinia break-up and addition of juvenile crust

Kirtikumar Randive* and Shubhangi Lanjewar

Department of Geology, RTM Nagpur University, Nagpur-440001, India

*Corresponding author e-mail: randive101@yahoo.co.in

The Precambrian geologic history of Peninsular India covers nearly 3.0 billion years of time. It comprises several cratonic nuclei namely, Aravalli–Bundelkhand, Eastern Dharwar, Western Dharwar, Bastar and Singhbhum Cratons along with the Southern Granulite Province. Each of the major cratons was intruded by various age granitoids, mafic dykes and ultramafic bodies throughout the Proterozoic (Meert et al., 2010). The cratons are flanked by a fold belt, with or without a discernible suture or shear zone, suggesting that the cratons, as crustal blocks or microplates, moved against each other and collided to generate these fold belts (Naqui, 2005). Alternatively, these cratons could be the result of fragmentation of a large craton that constituted the Indian shield. In either case, rifting or splitting of cratons is documented by the presence of fold belts that are sandwiched between two neighbouring cratons. The cratons or microplates collided and developed the fold belts that occur peripheral to the cratonic areas of the Indian shield (Sharma, 2010).

The Archaean Dharwar craton is an extensively studied terrain of the Indian shield. It is a dominant suite of tonalite-trondhjemite-granodiorite (TTG) gneisses which are collectively described under the basket term peninsular gneisses. The TTG suite is believed to be the product of hydrous melting of mafic crust and last stage differentiates of mantle, accounting for crustal growth, both horizontally as well as vertically. The available geochronological data indicate that the magmatic protolith of the TTG accreted at about 3.4 Ga, 3.3–3.2 Ga and 3.0–2.9 Ga. The Pb isotope data of feldspar suggests near Haedian (>3.8 Ga) juvenile magmatism (Meen et al., 1992). The second category of rocks in the Dharwar craton is greenstones or schist belts with sedimentary associations (Sharma, 2010). The Dharwar Craton was initially divided into two blocks — the Western Block and the Eastern Block, separated by the Chitradurga Shear Zone (Swami Nath and Ramakrishna, 1981). Later, designated these blocks were named as Western and Eastern Dharwar Cratons (Naqui and Rogers, 1987).

The majority of intrusive events of the Eastern Dharwar Craton (EDC) are represented by mafic dykes, kimberlites and lamproites. There are five major dyke clusters known in the EDC, which are: (1) Hyderabad, (2) Mahbubnagar, (3) Harohalli/Bangalore, (4) Anantapur and (5) Tirupati (Meert et al., 2010).

The Harohalli/Bangalore swarm is located between the southwestern portion of the Cuddapah Basin and the southeastern limb of the Closepet Granite (Fig. 1). The dyke cluster is split into an older group made up of dolerites, trending E–W (Bangalore dyke swarm), and a younger group of alkaline dykes that trend approximately N–S (Harohalli alkaline dykes) (Pradhan et al., 2008). Bidadi-Harohalli area in Bangalore district is cut by many distinct suites of rocks, which are of different ages and petrographic types. These dyke swarms were broadly classified as metadolerites, metanorites, unmetamorphosed dolerites and alkaline types. They intrude country rocks that are dominantly made up of Peninsular gneiss and Clospet granite (Devaraju et al., 1995). Among the suites metanorites and metadolerites are older than the unmetamorphosed dolerites, which are dated around 2.42 Ga. These dykes were intruded by younger ~0.8 Ga (Ikramuddin and Stueber, 1976). This late igneous activity witnessed by the high-grade Archaean terrain of EDC is represented by dykes of lamprophyres, diorites, monzonites, tinguaites, solvesbergite, bostonites, granophyres and felsites (Devaraju et al., 1995; Le maitre, 2002).

All the lamprophyre dykes of Halaguru area are located in the proximity of Shimsha river. The dykes are usually thin (width ~ 25 cm to length 3 m) and patchy outcrops defining the trends of dykes could be traced up to 700 mts. However small clusters could be locally observed near Madhallidodgi, Torekadanahalli, and Valagerdoddi and that the fractional crystallization was more dominant process in the evolution of

Chillapura. Most prominent of the HL dykes is ~20 cm wide and could be traced up 15 meters. The lamprophyre dykes were identified in the field on the basis of their distinct phenocryst assemblage, radiating needles of amphiboles, presence carbonate ocelli, occasional xenoliths of quartz and/or country rocks embedded in the groundmass which is either aphyric or a crystallized mush, minor needles of amphiboles occur in the groundmass. A lamprophyre dyke also occurs in Matagalli Industrial area, close to the northeastern boundary of Mysore district and in the close proximity of Srirangapatna. Prominent feature of this dyke is presence of huge granite boulders and xenoliths. Although remaining portion of the dyke appears remarkably fresh.

Petrographic studies revealed that all the lamprophyre dykes are dominantly composed of amphiboles, which form well-developed phenocrysts showing porphyritic – panidiomorphic texture. Clinopyroxenes are also present but not in all the dykes, and their modal proportion also vary among the dykes. Olivine is totally absent and magnetites/titanomagnetites are scantily present. Feldspars show clear bimodal distribution, i.e. they are either albite or orthoclase, without much variation in their end-member compositions. Other minerals which occur profusely, but not considered to be of magmatic origin are chlorite – septachlorites, epidote, sphene, calcite and barite. An interesting petrographic feature of SKL dykes is that they are all influenced by carbothermal metasomatism. These fluids have been instrumental in crystallizing secondary amphiboles (edenite, pargasite and actinolite). Chemistry of different mineral phases brought forth the compositional zoning of clinopyroxenes and amphiboles. These patterns also indicate that the magma has experienced cryptic variations lamprophyric magma of Southern Karnataka lamprophyres.

Geochemical characters of SK lamprophyres do not deviate too much. They show almost consistent sodi-potassic characters (K_2O/Na_2O ratio near 1), calc – alkaline nature, and shoshonitic affinity. In the TAS diagram they fall in the fields of basalt, trachy- basalt, basaltic trachy–andesite, basaltic- andesite, trachy- andesite and trachydacite; altogether representing a calc-alkaline series. The trace elements show primitive

(MORB-like) characters. LILE and LREE both show only marginally enriched patterns (much depleted as compared to world-wide calc-alkaline lamprophyres); whereas HFSE and HREE show strongly depleted patterns (nevertheless HREE do not show much depletion as compared to world-wide calc- alkaline lamprophyres). These are probably distinguishing characters of SK lamprophyres from the world wide calc-alkaline lamprophyres.

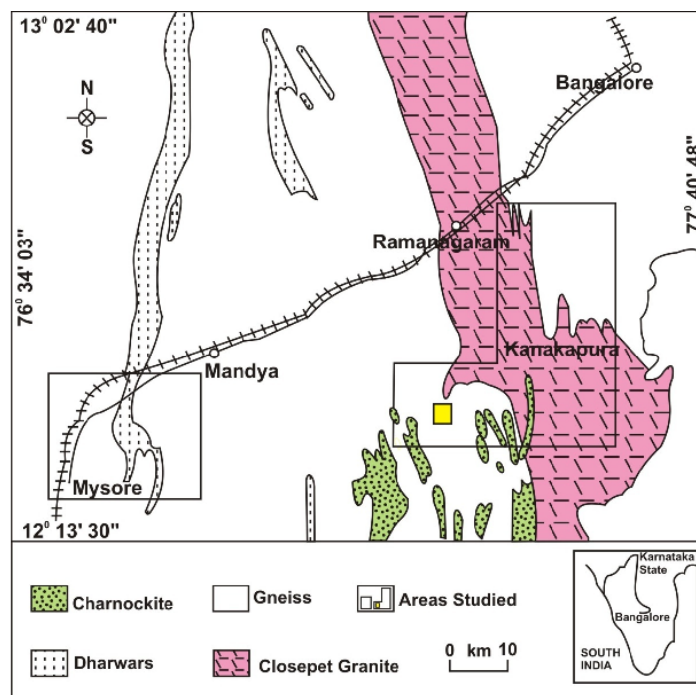


Fig.1 Geological Map of Neo-Proterozoic dyke swarm of southern Karnataka (*after* Devaraju, 1995)

Process identification criteria used during present study was based on petrography as well as geochemistry. Presence of compositional zoning in the mineral phases and geochemical proxies such as Ni versus Ce and La versus La/Sm indicates two fold influences, first (more valid for HL) is the fractional crystallisation and second (valid between HL and ML as one unit) is, relative degrees of partial melting. In the regional geologic sense, the SKL dykes are characterised by two major influences; namely, primary source region characteristic (which is geochemically more primitive, roughly falling within fields of

primitive - MORB and enriched- MORB) and second one is continental crust. The data points for all the SKL dykes distinctly show that they plot primarily near NMORB field and scatter towards the continental crust. Features like xenolith assimilation have definitely influenced the trace-elements characteristics of SKL dykes.

The data array also indicates that the SK lamprophyres are not related to subduction process. Therefore , the role of subduction related fluids should not be considered, although it is well known that the calc-alkaline lamprophyres are generally related to magmas generated by orogenesis. From the present study it has

now become evident that the Southern Karnataka Lamprophyres were derived from the rift-related (MORB-like) mantle source, which has been contaminated by the continental crust. The process identification diagrams have indicated that fractional crystallisation is a dominant mechanism. A graphical model has been presented which indicates that clinopyroxene was the main fractionating phase, with smaller role played by plagioclase and magnetite in the proportion Cpx (80%) : Mt (05) % : plg (15 %).

It is widely known that the Neoproterozoic period witnessed significant addition of the juvenile crust (~20%) all over the globe through a single cycle of supercontinent break-up (Rodinia) and reformation (Greater Gondwana and Pannotia) (Stern, 2008). Most of the activities were linked to the convergent margin settings; however, our data on SK lamprophyres indicate that they were formed in a rift related setting co-relatable to the break-up of Rodinia (~830 Ma) and not with the subduction related Pan-African (~600 Ma) event in the then adjacent East Antarctic orogen.

References

- Devaraju, T.C., Laajoki, K., Makkonen, H., Khandali, S.D., Ugarkar, A.G., Jamkhindi, M.S.R., 1995. Neoproterozoic Dyke swarms of Southern Karnataka. Part I: Field characters, petrography and Mineralogy, in: *Memoir Geological Society of India* No. 33. pp. 209–265.
- Ikramuddin, M., Stueber, A.M., 1976. Rb-Sr ages of Precambrian dolerite and alkaline dykes, Southeast Mysore State, India. *Lithos* 9, 235–241.
- Le maitre, R.W., 2002. *Igneous rocks; a classification and glossary of terms; recommendations of the International Union of geological Sciences Sub commission on the systematics of igneous rocks.* Cambridge, Cambridge University Press, United Kingdom.
- Meen, J.K., Rogers, J.J.W., Fullagar, P.D., 1992. Lead isotopic compositions of the Western Dharwar Craton, Southern India: Evidence for distinct middle Archean terranes in late Archean craton. *Geochemica Cosmochem. Acta* 56, 2455–2470.
- Meert, J.G., Pandit, M.K., Pradhan, V.R., Banks, J., Sirianni, R., Stroud, M., Newstead, B., Gifford, J., 2010. Precambrian crustal evolution of Peninsular India: A 3.0 billion year odyssey. *J. Asian Earth Sci.* 39, 483–515.
doi:10.1016/j.jseaes.2010.04.026
- Naqui, S.M., 2005. *Geology and Evolution of the Indian Plate.* Capital Publishing Company, New Delhi.
- Naqui, S.M., Rogers, J.J.W., 1987. *Precambrian Geology of India.* Oxford University Press, New York.
- Pradhan, V.R., Pandit, M.K., Meert, J.G., 2008. A cautionary note of the age of the paleomagnetic pole obtained from the Harohalli dyke swarms, Dharwar craton, southern India, in: Srivastava, R.K., Chalapathi Rao, N.V., Sivaji, C. (Eds.), *Indian Dykes: Geochemistry, Geophysics, and Geochronology.* Narosa Publishing Ltd., New Delhi, India, pp. 339–352.
- Sharma, R., 2010. *Cratons and Fold Belts of India, Lecture Notes in Earth Sciences.* Springer Berlin Heidelberg, Berlin, Heidelberg. doi:10.1007/978-3-642-01459-8
- Stern, R.J., 2008. Neoproterozoic crustal growth: The solid Earth system during a critical episode of Earth history. *Gondwana Res.* 14, 33–50.
doi:10.1016/j.gr.2007.08.006
- Swami Nath, J., Ramakrishna, M., 1981. The early Precambrian supracrustals of southern Karnataka. *Mem. Geol. Surv. India* 112, 350.

200 Myr history of crustal melting in Gongga Shan; constraints on the tectonics of eastern Tibet from the Triassic to present-day

Nick M W Roberts^{1*} and Michael P Searle²

¹NERC Isotope Geosciences Laboratory, British Geological Survey, Nottingham, UK

²Department of Earth Sciences, University of Oxford, Oxford, UK

*Corresponding author e-mail: nirob@bgs.ac.uk

Eastern Tibet and the surrounding regions comprise a complex assemblage of arcs and microcontinents of variable heritage, amalgamated and reworked from the Triassic to present-day. The Gongga Shan massif, located on the eastern edge of the Tibetan plateau, and reaching 7556 m, provides a record of crustal melting spanning some 200 Myrs. Here we will review the Triassic to present-day evolution of this region, using U-Pb geochronological and new Hf isotope data constraints from Gongga Shan to provide new insights into the causes of crustal melting, and the architecture of the Tibetan continental lithosphere.

Timing of Gongga Shan magmatism: For many years, Gongga Shan was believed to be a 12.8 Ma pluton, marking the onset of movement of the regional Xianshui-He fault that cross-cuts it (Roger et al., 1995). More recently, several studies (Li & Zhang, 2013; Li et al., 2015) including our own (Searle et al., 2016), have shown the evolution of the igneous

massif to be much more complex and protracted. Li & Zhang (2013) found ca. 32 and 27 Ma populations that they deemed to be related to migmatization and ca. 17 and 14 Ma ages that they relate to magmatism. Li et al. (2015) found much older magmatic ages across different parts of the batholith, ranging from ca. 216 to 204 Ma and at ca. 170 Ma, attesting to a complicated Triassic-Jurassic evolution. Searle et al. (2016) found further older ages, ranging from ca. 215 to 159 Ma. Old, i.e. ca. 170 Ma, and young ca. 15 and 5 Ma allanite ages, attest to variable tectonothermal reworking of the batholith. A sample with both ca. 14 and 5 Ma zircon age populations, and a ca. 5 Ma allanite population, provides the youngest magmatic age recorded thus far from the Tibetan plateau.

Sources of Gongga Shan magmatism: Our new Hf data from Gongga Shan provide constraints on the magmatic source. The ca. 800 Ma zircon core population from one sample has ϵ_{Hf}

ranging from +5 to +10, overlapping with the signature of the nearby Neoproterozoic Kangding complex (Zheng et al., 2007). Triassic to Jurassic age populations all fall within a range of ϵH_T of -4 to +2, indicating a similar source for all parts of the batholith at this time, irrespective of their I- or S-type characteristics. This isotopic signature can be explained by reworking of the 800 Ma source rocks alone. The younger 15-5 Ma age populations have ϵH_T ranging from -4 to +3 Ma. This signature can also be explained by reworking of the 800 Ma source, or by reworking of the Triassic-Jurassic rocks. Thus, overall the data can be interpreted as episodic closed-system reworking of a Neoproterozoic source region, similar to that of the nearby exposed Kangding Complex. However, input from Triassic Songpan-Garze flysch cannot be ruled out from the isotopic signatures. The inherited ages can provide additional constraints here. Songpan-Garze flysch sampled in the surrounding region has large age populations of Triassic and Ordovician, as well as Neoproterozoic and older (e.g. Weislogel et al., 2010). The inheritance in the Gongga Shan lacks Triassic to Ordovician ages, and is instead mostly Neoproterozoic. This evidence is not equivocal, but points to a likely magmatic source being dominantly Neoproterozoic, rather than derived from the Triassic Songpan-Garze flysch.

Triassic-Jurassic tectonics: The 216-159 Ma magmatism in Gongga Shan features both I- and S-type magmatism, and broadly splits into two episodes at 216-204 and 185-159 Ma. The exact tectonic setting of this magmatism remains uncertain. Regionally, Triassic orogenesis relates to the collision of the Qiangtang terrane and the North and South China

Blocks. The intervening Songpan-Garze basin, that hosted a thick sequence of Triassic sediments, was significantly shortened during this period. In the Danba area, Barrovian metamorphism related to this thickening and burial is dated at ca. 180 Ma (Weller et al., 2013). Granite bodies are found throughout many areas of the Songpan-Garze terrane, and are dated between 221-153 Ma (Roger et al., 2004, 2010). Variable models have been used to explain this magmatism, mostly defining them as syn- or post-collisional, and/or delamination-related. Whatever models are invoked, they need to explain the protracted and episodic nature of the 221-153 Ma magmatism. A simple model of crustal-thickening related melting cannot explain the earliest magmas, as these formed well before peak metamorphism. The protracted nature of the magmatism precludes a delamination model for all suites, and can only be used to explain single episodes. The range in magmatic products seen in Gongga Shan, including mafic enclaves, attests to the involvement of mafic magmas. To the west of the Songpan-Garze terrane, the Yidun arc was active at a similar timeframe, and comprises an overlapping Hf isotopic signature to Gongga Shan magmatic rocks. The Yidun arc may have formed from the rifting of the Neoproterozoic Yangtze craton during the preceding opening of Paleotethys (Roger et al., 2010). A geochemical study of Gongga Shan is warranted to help constrain models of its evolution, but we speculate that the older components of the Gongga Shan batholith may also represent Andean-type magmatism forming along a convergent margin located adjacent to the cratonic margin of the South China Block.

Cenozoic to present-day tectonics: The cause and nature of Cenozoic melt and migmatization events recorded in Gongga Shan is enigmatic, as evidence of Cenozoic shortening in the region is lacking. Most structures are related to the earlier Indosinian orogenic events. The structures, lack of regional metamorphism, and limited amount of regional crustal melts, preclude any channel flow operating in eastern Tibet, unlike the south Tibet-Himalayan region. Young crustal melts located in the Nyenchen Tanggla range, southern Tibet are thought to be exhumed partial melts, similar to the 'bright spots' seen in seismic studies (Weller et al., 2016). It is possible that Gongga Shan melts represent similar localised partial melts formed in the middle crust. It is worth noting however that the younger phases of Gongga Shan are not entirely all small-scale migmatite complexes, but include massive monzonite and porphyritic granitoids reflecting the accumulation of relatively large magma batches. The source of the young melts is isotopically indicated to be previously formed Triassic-Jurassic magmatic rocks, or older Neoproterozoic crust. Melting of either of these sources in the middle crust would have required an external heat source, or burial to temperatures where the most fertile sources could melt. We currently see no mechanism for the former, and suggest that the Neoproterozoic basement must comprise fertile compositions capable of crustal melting. Some addition of Triassic sedimentary source rocks cannot be ruled out, but these did not contribute to the zircon inheritance.

Implications for crustal architecture: The nature of the crust beneath the sedimentary upper crust of the Songpan-

Garze terrane is debated. The isotopic signature of the Gongga Shan batholith implies a Neoproterozoic source region, similar to the Kangding Complex on the edge of the Yangtze craton. Thus, we infer that the Triassic-Jurassic magmatism occurred on stretched Neoproterozoic continental crust of the Yangtze craton. The similar isotopic signature to other Triassic granitoids regionally, and to the Yidun arc to the west, suggests that this stretched crust may underlie vast portions of the Songpan-Garze terrane.

There is agreement in most models that Indian lower crust has been underthrust as far north as 31° N under the Lhasa Block in central-southern Tibet (e.g. Nábělek et al., 2009). In Eastern Tibet, the lower crustal/lithospheric architecture is less well-constrained. We postulate that the strong Indian lower crust has been underthrust as far north-northeast as the Xianshui-he fault. This underthrusting below the Asian crust has passively uplifted the Tibetan plateau, leading to its current doubled thickness. Additionally, we find no evidence for lower crustal flow beneath Eastern Tibet.

All of the granites of the Gongga Shan batholith are cut by the Xianshui-he fault. Our data suggest the fault was initiated after 5 Ma, because it cuts granites of that age. An earlier history is possible, but there is no record in the present exposures. It is noteworthy that ductile fabrics in the granites are cut by brittle fault strands, and that the granites are not connected to the strike-slip fault genetically, i.e. magmatism is related to crustal melting, and not to strike-slip faulting.

References

- Li, H. and Zhang, Y., 2013. Zircon U–Pb geochronology of the Konggar granitoid and migmatite: Constraints on the Oligo-Miocene tectono-thermal evolution of the Xianshuihe fault zone, East Tibet. *Tectonophysics*, 606, 127-139.
- Li, H., Zhang, Y., Zhang, C., Dong, S. and Zhu, F., 2015. Middle Jurassic syn-kinematic magmatism, anatexis and metamorphism in the Zheduo-Gonggar massif, implication for the deformation of the Xianshuihe fault zone, East Tibet. *Journal of Asian Earth Sciences*, 107, 35-52.
- Nábělek, J., Hetényi, G., Vergne, J., Sapkota, S., Kafle, B., Jiang, M., Su, H., Chen, J. and Huang, B.S., 2009. Underplating in the Himalaya-Tibet collision zone revealed by the Hi-CLIMB experiment. *Science*, 325, 1371-1374.
- Roger, F., Calassou, S., Lancelot, J., Malavieille, J., Mattauer, M., Zhiqin, X., Ziwen, H. and Liwei, H., 1995. Miocene emplacement and deformation of the Kongga Shan granite (Xianshui He fault zone, west Sichuan, China): Geodynamic implications. *Earth and Planetary Science Letters*, 130, 201-216.
- Roger, F., Jolivet, M. and Malavieille, J., 2010. The tectonic evolution of the Songpan-Garzê (North Tibet) and adjacent areas from Proterozoic to Present: A synthesis. *Journal of Asian Earth Sciences*, 39, 254-269.
- Roger, F., Malavieille, J., Leloup, P.H., Calassou, S. and Xu, Z., 2004. Timing of granite emplacement and cooling in the Songpan–Garzê Fold Belt (eastern Tibetan Plateau) with tectonic implications. *Journal of Asian Earth Sciences*, 22, 465-481.
- Searle, M.P., Roberts, N.M., Chung, S.L., Lee, Y.H., Cook, K.L., Elliott, J.R., Weller, O.M., St-Onge, M.R., Xu, X.W., Tan, X.B. and Li, K., 2016. Age and anatomy of the Gongga Shan batholith, eastern Tibetan Plateau, and its relationship to the active Xianshui-he fault. *Geosphere*, GES01244-1.
- Weislogel, A.L., Graham, S.A., Chang, E.Z., Wooden, J.L. and Gehrels, G.E., 2010. Detrital zircon provenance from three turbidite depocenters of the Middle–Upper Triassic Songpan-Ganzi complex, central China: Record of collisional tectonics, erosional exhumation, and sediment production. *Geological Society of America Bulletin*, 122, 2041-2062.
- Weller, O.M., St-Onge, M.R., Rayner, N., Searle, M.P. and Waters, D.J., 2015. Miocene magmatism in the Western Nyainqentanglha mountains of southern Tibet: An exhumed bright spot? *Lithos*, 245, 147-160.
- Zheng, Y.F., Zhang, S.B., Zhao, Z.F., Wu, Y.B., Li, X., Li, Z. and Wu, F.Y., 2007. Contrasting zircon Hf and O isotopes in the two episodes of Neoproterozoic granitoids in South China: implications for growth and reworking of continental crust. *Lithos*, 96, 127-150.

Late Paleozoic supra-subduction and intra-plate volcanism of the Tianshan-Junggar region: evidence for oceanic closure

I.Yu. Safonova^{1, 2}, V.A. Simonov^{1, 2}, A.V. Mikolaichuk³, A.V. Kotlyarov¹

¹ Institute of Geology and Mineralogy SB RAS, Koptyugaave. 3, Novosibirsk, 630090, Russia

² Novosibirsk State University, Pirogova St. 2, Novosibirsk, 630090, Russia

³ Institute of Geology NAS, Erkindikave. 30, Bishkek, 720481, Kyrgyzstan

The Junggar-Tianshan Region is located in the western part of the Central Asian Orogenic Belt, the world largest accretionary orogen, which has evolved during more than 800 Ma as a result of multiple episodes of subduction-accretion and collision. The region includes many fields of Late Paleozoic-Mesozoic supra-subduction and intra-plate continental basalts (e.g., Sobel and Arnaud, 2000; Simonov et al., 2014). The continental plume-related origin of the Meso-Cenozoic basaltic fields has been solidly proved based on detailed geological, geochronological, geochemical, and petrologic data (Simonov et al., 2014). The origin of the Late Paleozoic basalts remains debatable as different research teams consider them to be related to either an Andean-type continental margin or to a continental hotspot. The dilemma comes from the still disputable age of ocean closure and final continental collision in the region.

Late Paleozoic basalts occur within the Balkhash-Yili volcano-plutonic belt (Ryazantsev, 1999) or continental arc (Windley et al., 2007), geographically at the northern and southern mountain frames of the Yili basin, i.e., on the SW Junggar Ridge and northern Tianshan of south-east Kazakhstan, respectively. Some authors suggest that they may extend to East Kazakhstan and can be correlated with the Late Paleozoic supra-subduction volcanic series of the Char zone in East Kazakhstan and West Junggar of NW China (Yang et al., 2014; Kurganskaya et al., 2014).

There are three geochemically different groups of Late Paleozoic basalts in SE Kazakhstan: (1) LREE-Ti-Nb enriched alkaline basalt (SW Junggar), (2) Nb depleted basalts (south of the Junggar range and West Junggar) and (3) HFSE depleted basalts (N. Tianshan). Group 1 alkaline basalts are geochemically close to plume-related OIB-type basalts of oceanic islands or intra-continental rifts. Groups 2

and 3 are characterized by lower HFSE (Ti, P, Nb, Zr, Y) and higher Al_2O_3 . In general, they are compositionally similar to continental arc basalts, e.g. to alkaline and subalkaline mafic lavas of Andean-type active margins and/or marginal seas. Thus, the Late Cretaceous of the Tianshan-Junggar region of SE Kazakhstan) resemble both oceanic and continental intraplate basalts related to mantle plumes (Hawaii, Central Mongolia) and lavas erupted at Andean-type active margins or in passive margins/marginal seas.

The Late Paleozoic lavas of SE Kazakhstan yielded Ar-Ar ages of 282 Ma (Group 1), 305.2 ± 3.5 Ma (Group 2) and 311.9 ± 3.7 (Group 3). The volcanic rocks obviously erupted in sub-aerial conditions, and in terms of geochemistry they could have erupted in active margin and marginal sea. The Late Paleozoic orogens of the study area comprise the South Tianshan and Junggar-Balkhash orogenic belts. There are two models on their origin: on a convergent margin (island arc?) of the Kazakhstan consolidated continent (e.g., Yakubchuk, 2004; Biske and Seltmann, 2010) or in a post-orogenic continental environment (Simonov et al., 2014). The localities of basalts of different ages are separated from each other by local disconformities. We think that Late Carboniferous basalts of Groups 2 and 3, West Junggar and N. Tianshan, respectively, were derived from crustally contaminated mantle sources. Group 1 basalts (Early Permian) could be related to the manifestation of the Tarim Plume active at ca. 290-274 Ma (Li et al., 2011).

Thus, we recognize two stages of magmatism manifested in the Tianshan-Junggar region. The Late Carboniferous magmatism (312-305 Ma) produced

basaltic lavas geochemically similar to supra-subduction varieties of Andean-type convergent margins. That was probably the final stage of arc volcanism, which lavas erupted in an already reduced oceanic real or marginal sea. The eruption of Early Permian volcanics coincide with the time of the Tarim plume.

The available geological data suggest that the supra-subduction and intra-plate volcanic rocks erupted during final stages or after ocean closure, respectively. The northwestern circum-Junggar and South Tianshan orogens formed in place of the Junggar-Balkhash and Turkestan (or South Tianshan) Oceans, respectively, both were southern domains of the Paleo-Asian Ocean (Biske and Seltmann, 2010; Yang et al., 2014). The two oceans once separated the Kazakhstan and Siberian and the Kazakhstan and Tarim continental blocks, respectively, and probably closed in Late Carboniferous time (Windley et al., 2017; Xiao et al., 2011). More evidence for the Late Carboniferous ocean closure comes from (a) association of Late Carboniferous volcanics with coeval continental type deposits, (b) the transverse position of SE Kazakhstan volcanic belts hosting the basalt localities in respect to the strike of the collisional belts, (c) the intra-plate geochemical features of Permian granitoids in adjacent areas of the Tianshan (e.g., Konopelko et al., 2009), and (d) recent geochronological data from the adjacent areas in the Chinese Tianshan and East Kazakhstan (Xiao et al., 2011; Yang et al., 2014). All this suggests that the Late Carboniferous volcanics of the Tianshan-Junggar region erupted in a "remnant" marginal sea and continental setting and the formation of the Early Permian basalts

is related to a mantle plume. Contribution to IGCP#592 "Continental construction in Central Asia". Supported by the Russian Foundation of Basic Research (projects no. 14-05-00143, 16-05-00313).

References

- Biske Yu.S., Seltmann R., 2010. Paleozoic Tianshan as a transitional region between the Rheic and Urals–Turkestan oceans. *Gondwana Research* 17, 602–613.
- Konopelko, D., Seltmann, R., Biske, G., Lepekhina, E., Sergeev, S., 2009. Possible source dichotomy of contemporaneous post-collisional barren I-type versus tin-bearing A-type granites, lying on opposite sides of the South Tien Shan suture. *Ore Geology Reviews* 35, 206–216.
- Kurganskaya E.V., Safonov Yu., and Simonov V.A., 2014. Geochemistry and petrogenesis of suprasubduction volcanic complexes of the Char strike-slip zone, eastern Kazakhstan. *Russian Geology and Geophysics* 55, 69–84.
- Li, Z., Chen, H., Song, B., Li, Y., Yang, S., Yu, X., 2011. Temporal evolution of the Permian large igneous province in Tarim Basin in north-western China. *Journal of Asian Earth Sciences* 42, 917–927.
- Ryazantsev, A.V., 1999. The structures of the Middle Paleozoic active margin in Kazakhstan: lateral variability and migration. *Doklady Earth Sciences* 369, 659–663.
- Simonov V.A., Mikolaichuk A.V., Safonov Yu., Kotlyarov A.V., Kovyazin S.V., 2014. Late Paleozoic–Cenozoic intra-plate continental basaltic magmatism of the Tianshan–Junggar region in the SW Central Asian Orogenic Belt, Gondwana Research, <http://dx.doi.org/10.1016/j.gr.2014.03.001>.
- Sobel, E.R., Arnaud, N., 2000. Cretaceous–Paleocene basaltic rocks of the Tuyon basin, NW China and the Kirgiz Tian Shan: the trace of a small plume. *Lithos* 50, 191–215.
- Windley, B.F., Alexeiev, D., Xiao, W., Kroner, A., Badarch, G., 2007. Tectonic models for accretion of the Central Asian Orogenic Belt. *Journal of the Geological Society of London* 164, 31–47.
- Yakubchuk, A., 2004. Architecture and mineral deposit settings of the Altaid orogenic collage: a revised model. *Journal of Asian Earth Sciences* 23, 761–779.
- Yang, G., Li, Y., Safonova, I., Yi, S., Tong, L., Seltmann, R., 2014. Early Carboniferous volcanic rocks of West Junggar in the western Central Asian Orogenic Belt: implications for a supra-subduction system. *International Geology Review* 56, 823–844.
- Xiao, W.J., Windley, B.F., Allen, M.B., Han, C., 2013. Paleozoic multiple accretionary and collisional tectonics of the Chinese Tianshan orogenic collage. *Gondwana Research* 23, 1316–1341.

The mystery of Hadean Earth and primordial life

M. Santosh^{a, b}

^a China University of Geosciences Beijing, No. 29 Xueyuan Road, Beijing 100083, China

^b Department of Earth Sciences, University of Adelaide, SA 5005, Australia

The early history of the Earth during Hadean is shrouded in mystery. Earth-Moon system had many features in common during their birth stage in Hadean. Although anorthositic primordial continents on the Moon are largely preserved since their formation during Hadean, due to vigorous convection in the Earth and the onset of plate tectonics, these were disintegrated and dragged down to the deep mantle. Under extensive mantle convection, the primordial continents on the surface of the Earth which were penetrated by numerous mantle plumes from below could have been disrupted and destroyed by convection, particularly after the initiation of plate tectonics at 4.4 Ga. The formation of primordial continents on both Earth and Moon might have been linked to the magma ocean with the essential difference that on Earth, with nearly six times the gravity of Moon, extensive fractional crystallization might have been facilitated. A recent model proposes that the Earth was born dry as a 'Naked Planet' (Maruyama et al., 2013), without ocean and atmosphere through aggregation of dry enstatite chondrite at 4.56 Ga followed by the formation of Moon

through Giant Impact. Subsequently, hydrous asteroid bombardment occurred during the "Late Heavy Bombardment" stage delivering the primordial atmosphere and ocean. The advent of water and bio-elements (C-H-O-N) during asteroid bombardment initiated plate tectonics. The transient period from magma ocean to plate tectonics might have been marked by bombardment tectonics which extensively destroyed the surface and also deposited a thick veneer of chondritic debris, identical to the regoliths on the Moon with pulverized material which is a mixture of rock fragments from the primitive lunar crust together with glassy particles from the impact. Due to the small size of Moon, the volatiles delivered by the chondritic material escaped whereas in the case of Earth, the volatiles and ultra-high temperatures might have caused extensive mineral transformations in the underlying anorthositic crust to make it denser and to be dragged down into the deep mantle. The highly fractionated iron rich residual melts of the terrestrial magma ocean must have been enriched in P, K, and other elements, which along with the nutrients from primordial continents, might have

contributed to the prebiotic chemical evolution and the cradle of first life on this planet (Santosh et al., 2016).

References

Maruyama, S., Ikoma, M., Genda, H., Hirose, K., Yokoyama, T., Santosh, M., 2013. The naked planet Earth:

most essential pre-requisite for the origin and evolution of life.

Geoscience Frontiers 4, 141-165.

Santosh, M., Arai, T., Maruyama, S., 2016. Hadean Earth and primordial continents: the cradle of preboitic life. Geoscience Frontiers (under review).

Connecting India and Antarctica in Gondwanaiaiana – the Rauer-Rengali link

Saibal Gupta and Amol Dayanand Sawant

Saibal Gupta and Amol Dayanand Sawant

Dept. of Geology & Geophysics, IIT Kharagpur, Kharagpur – 721 302, India

Correlation of India and Antarctica in Gondwanaland has relied to a large extent on correlating the Eastern Ghats Province (EGP) in India with the Rayner Province (RP) in East Antarctica. The correlation has been based on exposures of granulite facies rocks of Grenvillian (~ 1.0 Ga) age in both terranes, with comparable peak metamorphic P-T conditions. An important element of the correlation has been the presence of the Mahanadi rift in the EGP that has been considered to be the conjugate of the Lambert rift in East Antarctica. These rifts host unmetamorphosed sedimentary rocks of Gondwana age. If the EGP and Rayner Province were indeed linked together, the area presently to the north of the EGP, known as the Rengali Province, should be correlatable with a corresponding part in East Antarctica, in the vicinity of Prydz Bay. This part of Antarctica is apparently composed of three distinct terranes – the Vestfold Hills block, the Prydz Bay region and the Rauer Group. The Vestfold Hills block is dominated by ~ 2.5 Ga orthogneisses, with a few c. 1.0 Ga ages also reported. On the other hand, granulite facies metamorphism in the Prydz Bay

region is of Pan-African age, but is believed to overprint an earlier Grenvillian (~ 1.0 Ga) thermal event, similar to parts of the Eastern Ghats Province. The intervening Rauer Group consists of Archaean orthogneisses (3.3-2.8 Ga) and Mesoproterozoic intrusives (~ 1.0 Ga), both of which record a tectonothermal overprint at 0.5 Ga. Major structural features within the Rauer Group show that the Archaean and Mesoproterozoic rocks are closely intercalated, and structural fabrics are sub-vertical, which is inconsistent with either regional-scale shortening or extension. The corresponding part in the Indian shield is the Rengali Province, which is sandwiched between the Archaean Singhbhum craton and the EGP. Interestingly, structural fabrics within the Rengali Province are also dominantly sub-vertical, as a consequence of a regional-scale strike-slip deformation that occurred around 500 Ma. Like the Rauer Group, the Rengali Province also contains closely juxtaposed slices of 2.8 Ga, 1.0 Ga and 500 Ma rocks. Given the location of the Rengali Province in the Indo-Antarctica amalgam, the structural evolution of the Rengali Province appears to explain the complicated intercalation

observed in the Rauer Group. We suggest that the strike-slip system to the north of the EGP continues into East Antarctica,

and is responsible for the juxtaposition of apparently temporally disparate units observed in the Rauer Group.

Geochemical and geochronological studies of the granitoids around chhota shigri area, Himachal Himalayas, India

Yengkhom Rajiv Singh^{a*}, Bidyananda Maibam^a, Anil D. Shukla^b, Jasper Berndt^c, A.L. Ramanathan^d

^aDepartment of Earth Sciences, Manipur University, Canchipur, Imphal-795003, India

^bPhysical Research Laboratory, Ahmedabad-680009, India

^cInstitut für Mineralogie, Westfälische Wilhelms-Universität Münster, D-48149 Münster, Germany

^dSchool of Environmental Sciences, Jawaharlal Nehru University, Delhi-110067, India

* Corresponding author e-mail: yrajboii@gmail.com

The Himalayan orogenic belt is characterized by numerous granitoid bodies of different ages associated with different geological setting. Many Paleoproterozoic granites with similar geological setting occur all along the 2000 km length of the Lesser Himalaya belt starting from Besham in Swat valley (NW Himalaya) to the Bomdila gneiss in Arunachal Pradesh (NE Himalaya) (Sharma, 1998). Chhota Shigri glacier lies in the Central Crystalline of the Pir Panjal range of the Indian Himalaya. This crystalline axis is comprised mostly of meso- to ketazonal metamorphites, migmatites and gneisses (Kumar et al., 1987). Pre-Himalayan granitoids are exposed in the Chhota Shigri area. A systematic study to characterize these rocks is lacking. We have carried out petrological, geochemical and

geochronological study to characterise the granitoids in the Chhota Shigri glacier area.

Phase chemistry of the granitoids is analysed using electron microprobe. Representative mineral composition of the rock is presented in Table 1. Major and trace element geochemical study was carried out for the granitoid samples at Physical Research Laboratory, Ahmedabad. The analysed granitoid samples show variable SiO₂ ranging between 64–78 wt.% and found to be ranging from granite to granodiorite with a high K calc-alkaline trend. Studied granites are medium to high-potassic with calc-alkaline affinity. The granites have fractionated nature of REE and minor negative Eu anomalies. The REE patterns of the studied granitoids are not much different. They are all slightly enriched in LREE (Lan/Lun=2–7). The REE enrichment

factor ranges from 40 x chondrite to 100 x chondrite, with distinct Eu anomalies. Various discrimination diagrams are used

to infer the probable tectonic setting of the studied granitoids.

Table 1. Representative mineral chemistry of Chhota Shigri granitoids.

Oxides	Plagioclase		K-feldspar		Biotite	
Na ₂ O	10.48	10.92	0.88	0.51	0.04	0.07
MgO	0.02	0.01	0.00	0.00	5.29	5.21
Al ₂ O ₃	21.10	20.13	17.67	17.86	17.42	17.43
SiO ₂	66.21	67.16	64.20	65.09	35.07	35.89
P ₂ O ₅	0.03	0.02	0.17	0.01	0.04	0.00
K ₂ O	0.18	0.15	15.56	15.84	9.20	9.50
CaO	2.24	1.22	0.22	0.01	0.00	0.00
TiO ₂	0.00	0.00	0.04	0.00	2.63	2.93
Cr ₂ O ₃	0.00	0.00	0.03	0.00	0.00	0.03
MnO	0.00	0.07	0.00	0.03	0.41	0.40
FeO	0.15	0.00	0.04	0.21	26.34	24.88
ZnO	0.00	0.01	0.00	0.00	0.33	0.00
Total	100.41	99.69	98.81	99.56	96.77	96.34

The processes of weathering, fluvial activity and gravitation over the time have separated and concentrated a statistically more meaningful sample than is achievable by conventional single-rock sampling, and thus can provide a more comprehensive coverage of rock types in the region (Belousova et al., 2009). The analysis of large numbers of grains obtained from detrital concentrates generates U–Pb age spectra in which peaks can be used to recognise major episodes of magmatic activity. To find out the age spectrum of the basement granitoids of the Chhota Shigri area, we have analysed detrital zircon brought down by the glacial melt water close to the base camp. Zircon grains were separated using conventional procedures

of the heavy liquid, followed by magnetic separation using a Frantz isodynamic separator. Zircon grains were handpicked using a binocular microscope. U–Pb isotope isotopes were analysed using a Thermo-Finnigan Element2 sector field ICP-MS coupled to a New Wave UP193HE ArF Excimer laser system at the Westfälische Wilhelms-Universität Münster. U–Pb geochronological data show that the detrital zircons from the studied rocks are ranging between 450 to 2729 Ma with known age peaks at 470, 750-850 and evidences of geological events at 1100, 1600 and 2730 Ma. Base on our preliminary geochronological dataset, it has confirmed episodic granitoid magmatism in the study area.

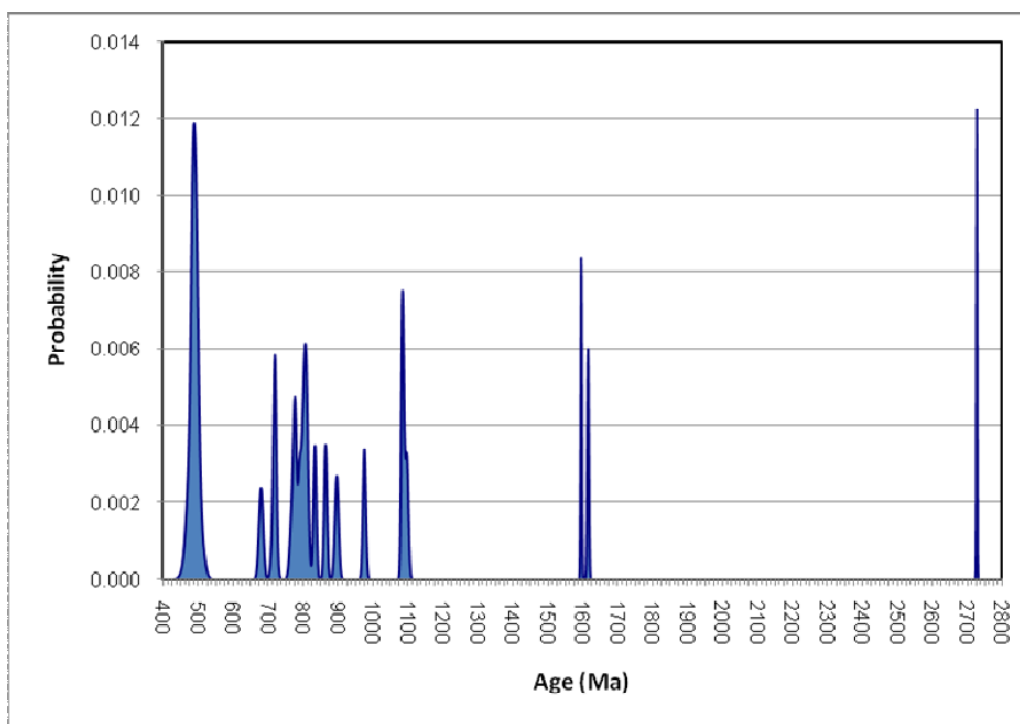


Fig. 1. Probability distribution curve of the analysed age of the detrital zircon from the Chhota Shigri glacial run off.

References

- Belousova, E.A., Griffin, W.L., O'Reilly, S.Y., Fisher, N.I., 2002. Igneous zircon: trace element composition as an indicator of source rock type. *Contributions to Mineralogy and Petrology* 143, 602–622.
- Kumar, S., Rai, H., Purohit K.K., Rawat, B.R.S. and Mundepi, A.K. (1987). Chhota Shigri Glacier, Technical report on Multi disciplinary glacier expedition to Chhota Shigri Glacier, Department of Science and Technology, 1:1-29.
- Sharma, K.K. (1998). Evidence of Paleoproterozoic orogeny (deformation, metamorphism and magmatism) from Satluj valley, NW Himalaya (Abstract volume, 13 HKT International Workshop, Peshawar, April 20-22, 1998). *Geol. Bull., University of Peshawar*, v.31, pp.181-182.

Permian-Triassic palynomorphs from Talcher Coalfield, Mahanadi Basin, India: Implications in biostratigraphy

Srikanta Murthy

Birbal Sahni Institute of Palaeobotany 53 University Road Lucknow 226007, India
E-mail: srikanta_murthy22@rediffmail.com

Mahanadi Basin is one of the major lower Gondwana basins of peninsular India and famous for its huge coal resources. It is located on the eastern part of India and constitutes five major coalfields such as Mand-Raigarh, Hasdo-Arand, Korba, Talcher and Ib-River. Talcher Coalfield, occupying an area of over 1800 sq.km, spreads in the south-eastern region of the Mahanadi Basin and is bounded between latitudes 20° 50' & 21° 15' N and longitudes 84° 20' & 85° 23' E. The Gondwana sediments in the Talcher Coalfield rest unconformably on the Precambrian basement rocks. The Permian- Triassic sedimentary rocks in Talcher Coalfield belong to Talchir, Karharbari, Barakar (early Permian) and the post Barakar formations which include Barren Measures (early late Permian) and Kamthi (late Permian/Triassic) formations. The Kamthi Formation is non coaliferous and represented by brown coloured, ferruginous, fine to coarse grained, gritty

sandstone and yellow clay sediments. On the basis of different proxies like Megafossils, palynofossils, lithology and mineralogy the Kamthi Formation has been considered as late Permian/early Triassic/Jurassic in age. Palynology is best suited for biostratigraphic studies of the Gondwana sediments because of the predominantly continental deposits. On the basis of palynological studies, delineation of Permian-Triassic boundary in Indian Gondwana basins of peninsular India have been attempted by several workers from different basins e.g. Damodar Basin (Tiwari and Singh 1982, 1983, 1986, Bharadwaj and Tiwari 1977, Tiwari and Tripathi 1992); Godavari Basin (Srivastava and Jha 1990, 1995, Jha and Srivastava 1996); Satpura Basin (Kumar 1996). In present study, palynological investigations have been carried out from late Permian and early Triassic sediments of Talcher Coalfield in order to delimit the Permian-Triassic boundary in the Mahanadi Basin.

The investigation on the non-marine sediments from bore core TTB-10 of Talchir Coalfield allowed for qualitative and quantitative palynological analysis. Three palynoassemblages have been identified; Palynoassemblage-I recorded between 30.15-159.00 m depth is characterized by the dominance of *Densipollenites* and striate bisaccate pollen grains such as *Striatopodocarpites* and *Faunipollenites*. The other stratigraphically significant palynotaxa are *Verticypollenites*, *Crescentipollenites*, *Falcisporites*, *Alisporites* and *Arcuatipollenites* which occur in low percentages and suggest a latest Permian (Lopingian) age for these rocks. Palynoassemblage-II is recorded between 24.15-30.15 m depth and exhibits mixed palynomorphs like cavate trilete spores, monosaccate, nonstriate, taeniate and striate bisaccate pollen taxa. This assemblage designates the Permian/Triassic transition. Palynoassemblage-III recorded between 7.65-16.40 m depth shows abundance of

cingulate cavate spores (*Lundbladispota* spp. and *Densoisporites* spp), monosaccate (*Playfordiaspora* spp.) and taeniate bisaccate (*Arcuatipollenites/Lunatisporites* spp) pollen grains. *Densipollenites* and striate bisaccate palynomorphs are not recorded at this depth. This palynoassemblage suggests an early Triassic age. Palynological changes through this succession successfully indicate Permo-Triassic boundary in the studied bore core TTB-10 (palynoassemblage-II). Age determination for the sequence has also been inferred by comparison with similar assemblages recorded by earlier worker from different lower Gondwana basins of India eg. Damodar, Satpura, South Rewa and Godavari basins. Additionally, general analysis of palynotaxa from the Talcher Coalfield favours a broad tentative correlation with the Permian- Triassic assemblages of South America, Africa, Antarctica and Australia.

Provenance, palaeoclimate and tectonic settings of the Gondwana sediments of the upper and lower Palar Basin, Southern India, Tamil Nadu

R. Subin Prakash* and S. Ramasamy

Department of Geology, University of Madras, Guindy Campus, Chennai 600025
Corresponding author e-mail: suban5geo@gmail.com

Palar Basin is considered as one of the pericratonic rift basins of East Coast of India. An integrated petrographic, clay mineralogic and heavy mineral studies of sandstone, shale and ironstone from the Upper and lower Palar Basin South India, Tamil Nadu have been carried out to decipher their provenance, palaeoclimate and tectonic setting. Texturally these studied samples are matured, well sorted grains which are rounded to subrounded. Majority of the samples contain monocrystalline grains with straight to undulose extinction at few amount of polycrystalline quartz. Using the classification diagram, the Palar Basin sandstones are classified as quartz arenite and sublitharenite types based on framework composition. A moderate content of feldspar especially plagioclase, orthoclase, perthite and microcline may imply rapid deposition of sediments from a nearby source rock. In modal analysis of sandstone quartz ranges from 83.06 to 96.55% with an average of 89.17%. The feldspar grain varies from 3.03 to 11% with

an average of 7.17%. Rock fragments in the studied sample ranges from 0.41 to 9.12% with an average of 3.88%. The detrital mode of these sandstones suggested that they were derived from continental and recycled orogen provenance with craton interior and transitional continental tectonic settings of the studied samples.

The heavy mineral suite displays rounded to subrounded as well as euhedral or angular grains of ilmenite, magnetite, zircon, tourmaline, garnet, rutile, sillimanite, kyanite, and staurolite in decreasing order of abundance. The calculated ZTR indices range from 73.42 to 95.16% with an average of 83.21%. The ZTR index and abundance of heavy minerals reflects that the Palar Basin samples are attained a moderate to high mineralogical maturity and these sediments have been originated mainly from granitic and metamorphic source areas with broad drainage basin. Clay mineral assemblage of the Palar Basin point out the dominance of rock derived minerals (illite and chlorite)

over soil derived clay minerals (Kaolinite and smectite). The high content of illite which indicates the sediment were derived from pre-existing rocks (granite and

gneisses), subjected to physical weathering over chemical weathering in a temperate climate (Hot/ Humid).

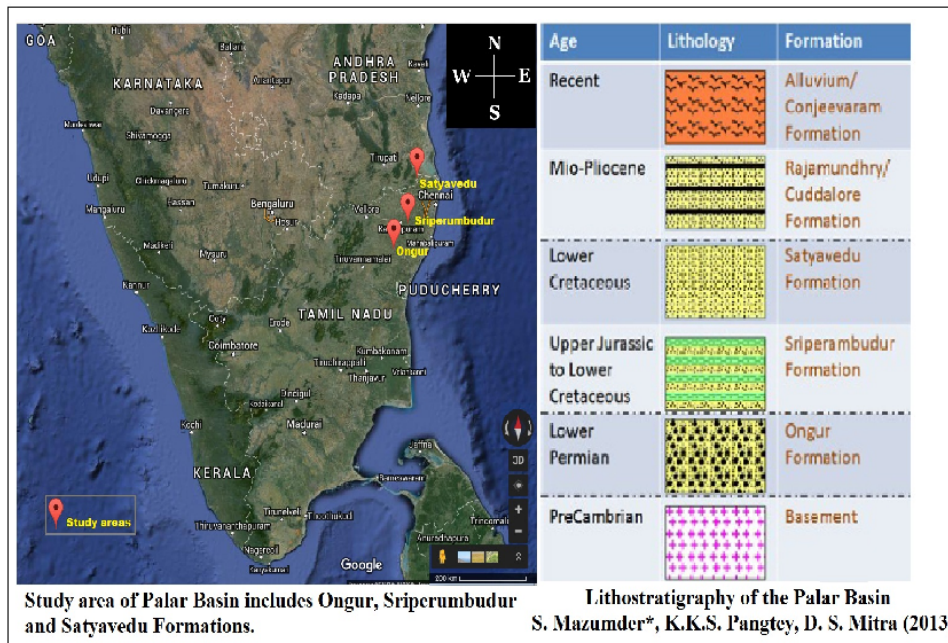


Table 1. Recalculated modal point counts of the Palar Basin sandstone samples

Sample	Q	F	R	Qm	F	Rt	Qt	F	Rt	Opq	F	R	Qpq	Qmu	Qm nu
PB1	93.6 4	3.9 5	2.4 2	86.9 6	8.0 9	4.95	88.0 4	7.42	4.54	40.66	36.81	22.5 3	8.52	80.6	88
PB4	83.0 7	7.8 1	9.1 2	67.7 1	14. 9	17.39	71.0 5	13.3 6	15.5 9	26.27	34.03	39.7 0	12.6 8	76.73	59
PB7	84.2 6	9.9 8	5.7 6	68.3	20. 09	11.61	72.8	17.2 4	9.96	34.26	41.67	24.0 7	16.3	75.77	93
PB8	86.3 5	8.7 4	4.9 1	73	17. 29	9.71	75.9 8	15.3 8	8.64	31.52	43.84	24.6 4	12.7	81.46	84
PB9	83.0 6	11.0 0	5.9 3	69.3 2	19. 93	10.75	71.0 3	18.8 2	10.1 5	16.11	54.50	29.3 8	7.26	89.96	78
PB12	84.9 8	10. 03	4.9 9	71.3 2	19. 15	9.53	73.8 8	17.4 4	8.68	25.49	49.75	24.7 5	10.7 9	89.21	
PB13	87.7 4	9.7 9	2.4 7	77.6	17. 89	4.51	78.1 5	17.4 5	4.4	10.24	71.69	18.0 7	3.09	88.36	55
PB14	87.6 5	7.6 5	4.6 9	76.7 7	14. 4	8.83	78.0 2	13.6 3	8.35	19.65	49.82	30.5 3	6.44	81.59	97
VK1	94.6 9	3.8 5	1.4 6	86.7 2	9.6 3	3.65	89.9 2	7.3	2.78	70.59	21.32	8.09	21.1 9	78.81	
VK3	96.5 5	3.0 3	0.4 1	92.3 1	6.7 7	0.92	93.3 3	5.87	0.8	66.67	29.33	4.00	12.5	87.5	
VK6	91.4 8	6.0 3	2.4 9	80.3	13. 94	5.76	84.3	11.11	4.59	56.38	30.87	12.7 5	19.4	79.45	15
P12	88.3 0	8.3 0	3.4 0	80.7 5	13. 66	5.59	84.3 4	11.11	4.55	54.41	32.35	13.2 4	18.1 4	81.86	
SV2	96.1 3	3.3 1	0.5 5	92.2 2	6.6 7	1.11	92.5 5	6.38	1.07	36.36	54.55	9.09	4.4	95.6	

Metamorphic zircon formation of Paleoproterozoic metasedimentary rocks in the Korla Complex, NW China: implications for the late Paleoproterozoic collisional orogenic event in the Tarim Craton

Wenbin Zhu*, Rongfeng Ge, Hailin Wu

School of Earth Science and Engineering, Nanjing University, Nanjing 210046, PR China

*Corresponding Author e-mail: zwb@nju.edu.cn

Widespread Paleoproterozoic supracrustal rocks in the northern Tarim Craton contain important information about its geological evolution and correlation with adjacent blocks. We present new in situ LA-ICP-MS zircon U–Pb and Lu–Hf isotopic data for six mica schist samples from the Korla Complex. Field and petrological studies indicate a pelitic to semi-pelitic protolith and a high pressure upper amphibolite-facies peak metamorphic condition ($T = 690 \pm 50^\circ\text{C}$ and $P = 11 \pm 2$ kbar) for these samples. CL-images reveal that zircons in these samples are dominantly metamorphic origin and only a few detrital zircons occur as relics in sample T1, the ages of which suggest a maximum deposition age of ca. 2.0 Ga and a sedimentary provenance from the Tarim Craton itself. All metamorphic zircons consistently record a metamorphic age of ca. 1.85 Ga, despite of various degrees of discordance probably due to later Pb-loss. Both recrystallization

and new zircon growth are recognized for the genesis of these metamorphic zircons. The metamorphic zircon domains in sample T1 show a relatively large range of initial $^{176}\text{Hf}/^{177}\text{Hf}$ ratios similar to the detrital cores, whereas those in the other samples show similar initial $^{176}\text{Hf}/^{177}\text{Hf}$ ratios (ca. 0.28140 ± 0.00010) regardless of their internal structures and degrees of discordance. The former is interpreted as a result of complete U–Pb resetting through fluid-mediated recrystallization, whereas the later probably implies a large-scale Hf isotopic homogenization during new zircon growth. Petrological and zircon isotopic evidence supports that the new zircon growth and Hf isotopic homogenization probably resulted from the mixing of Hf–Zr derived from dissolution of tiny detrital zircons and decom-position of garnet to chlorite in hydrothermal fluids during retrograde metamorphism. Accordingly, the ages of these new zircon growths may postdate the peak metamorphism, which

was probably related to a late Paleoproterozoic collisional orogenic event in the northern Tarim Craton. A compilation of available geological and geochronological data enables us to identify two Late Paleoproterozoic orogenic belts: theca. 1.9–1.8 Ga North Tarim Orogen and the ca. 2.0–1.9 Ga South Tarim Orogen. It is suggested that the Tarim Craton, including the Dunhuang and

Quanji Blocks, was correlative with the Alxa–Yinshan Block of the North China Craton, and they probably formed a coherent massif during the Neoproterozoic–early Paleoproterozoic, which collided with the Ordos Block and its western extension along the ca. 1.95 Ga Khondalite Belt–South Tarim Orogen to form a larger landmass in the Columbia Supercontinent.

Spatial and temporal provenance analysis of the Upper part of the Roper Group, Beetaloo Sub-basin, North Australia

Bo Yang, Todd Smith, Alan S. Collins

Tectonics, Resources and Exploration (TRaX), Department of Earth Sciences, University of Adelaide, SA 5005, Australia

The Mesoproterozoic Beetaloo Sub-basin of the McArthur Basin, North Australia, comprises a series of weakly deformed and metamorphosed shallow water clastic sediments and is interpreted as the depo-centre of the Roper Group. Being surrounded by different aged plate margin orogens the Beetaloo Sub-basin recorded the detailed paleotectonic history of the North Australian Craton.

In this research, new detrital zircon samples were collected from core drills

covering the whole Beetaloo Sub-basin. In these core drills, each formation of the upper part of the Roper Group was sampled. Coupled LA-ICP-MS U-Pb data and Hf isotopic analysis provide new constraints on the basin age and provenance. The spatial and temporal variation of provenance information reveals the regional paleo tectonic geography and evolution.

Continental growth through microblock amalgamation: example from the North China Craton

Qiong-Yan Yang^{1, 2}, M. Santosh^{1, 2, 3*}

¹School of Earth Sciences and Resources, China University of Geosciences Beijing, 29 Xueyuan Road, Beijing 100083, China

²Department of Earth Sciences, University of Adelaide, SA 5005, Australia

³Faculty of Science, Kochi University, Akebono-cho 2-5-1, Kochi 780-8520, Japan

* Corresponding author e-mail: msantosh.gr@gmail.com

The growth of continental fragments occurs through both vertical addition of magmas and lateral accretion involving arc-arc, arc-continent and continent-continent amalgamation. There were no large continental masses on the Archean Earth, and continent building occurred through the assembly of microcontinents, oceanic arcs and plateaus. The North China Craton (NCC) provides a typical case where at least six ancient microcontinental nuclei with distinct lithological features and independent tectonic histories were amalgamated into the cratonic framework at the end of the Archean. Here we evaluate the anatomy of one of these microblocks, the Jialiao Block which forms part of the composite Eastern Block of the NCC (Yang et al., 2016). Arc-related magmatic rocks are distributed along the western and southern periphery of this block. The southern periphery also preserves the remnants of Neoproterozoic

suprasubduction zone ophiolitic assemblages (Santosh et al., 2015). Petrological, geochemical and zircon U-Pb geochronological data from the charnockite suite, and associated amphibolites, metagabbros and orthogneisses from the Qianxi Complex along the western periphery of this rock attest to subduction-related magmatism. The felsic units straddle from diorite through syeno-diorite to granite with both alkalic and subalkalic affinity, with dominantly magnesian composition and arc-related features. In tectonic classification diagrams, the rocks plot in the VAG+syn-COLG field or the VAG area suggesting subduction-related origin. The magmatic zircons show upper intercept ages in the range 2587 ± 10 Ma to 2543 ± 17 Ma for the charnockite suite, 2556 ± 20 Ma for metagabbro and 2539 ± 9 Ma for amphibolite marking the timing of emplacement of the arc magmas (Yang et al., 2016). The overgrowth rims as well as

discrete neofomed grains formed during metamorphism and yield $^{207}\text{Pb}/^{206}\text{Pb}$ ages between 2533 Ma to 2490 Ma in charnockites, and 2449 ± 58 Ma to and 1845 ± 25 Ma in metagabbro. Zircon Lu-Hf data show dominantly positive $\epsilon\text{Hf}(t)$ values and combined with crustal residence ages, the data indicate Mesoarchean to Neoproterozoic juvenile crust formation in the NCC. The construction of the NCC is a result of the assembly of several microblocks or terranes at the end of Archean.

References

Yang, Q.Y., Santosh, M., Collins, A.S., Teng, X.M., 2016. Microblock amalgamation in the North China Craton: Evidence from Neoproterozoic magmatic suite in the western margin of the Jiaoliao Block. *Gondwana Research* 31, 96-123.

Santosh, M., Teng, X. M., He, X.F., Tang, L., Yang, Q.Y., 2015. Discovery of Neoproterozoic suprasubduction zone ophiolite suite from Yishui Complex in the North China Craton. *Gondwana Research*, doi:10.1016/j.gr.2015.10.017

Was there Neotethys Ocean's northern branch? A new look to Meso-Cenozoic tectono magmatic evolution of eastern Mediterranean region

Yener EYUBOGLU

Karadeniz Technical University, Department of Geological Engineering, 61080, Trabzon, Turkey

The Meso-Cenozoic geodynamic evolution of the Northern Turkey (Pontides Orogenic Belt), which is one of the most critical regions in the Alpine-Himalayan belt, is still controversial due to limited geological, geochemical and geochronological data. The most popular idea on the geodynamic evolution of Northern Turkey is that the Pontides Belt was shaped by a northward subduction of lithosphere belonging to northern branch of Neotethys ocean that opened as a back-arc basin during the southward subduction of Paleotethys lithosphere during early Jurassic and ended by a collision between Tauride and Pontide belts in Paleocene (Şengör and Yılmaz, 1981). In this model, the mafic-ultramafic lithologies exposed in the southern part of the belt represent the remnants of a Jurassic Penrose type ophiolite.

In a most recent paper, Eyuboglu et al. (2016) focused on the mafic intrusions cutting Kop ultramafic massif representing the ultramafic bodies exposed in the southern part of the Pontides Belt (Figure 1). The new zircon U-Pb age data from the

mafic lithologies indicated that there were at least three different phases of mafic igneous activity before the Jurassic time (Figure 2). The gabbro body representing the first phase is well exposed in the western part of the Kop ultramafic massif. The U-Pb age determinations of nine zircon grains from this sample yielded a weighted mean age of 432.5 ± 3.9 million years. Another phase of mafic-ultramafic magmatism in the Kop Mountain area is represented by non-metamorphic cumulate gabbros and wehrlites. Their contacts with the serpentinized Kop ultramafic rocks are intrusive. The U-Pb analyses of zircon grains extracted from a plagioclase-rich gabbroic sample representing this phase gave a weighted mean age of 325.1 ± 2.4 Million years. In addition, three zircon grains from a wehrlite sample yielded U-Pb isotopic ages of 328, 329 and 343 Million years which are concordant with the U-Pb ages of zircons from the gabbroic sample. Our dating studies in the entire belt indicate that intrusions of similar age also appear within the high-grade lithologies of Pulumet metamorphic massif. They are well known

as Alaskan-type mafic-ultramafic intrusions with their field and petrographical characteristics and also subduction-related chemistry (Eyuboglu et al., 2010). The third phase of mafic activity is represented by fine-grained gabbro dikes cutting both ultramafic rocks of unknown age and Carboniferous cumulate rocks. Thin section analyses reveal that the fine-grained rock consists predominantly of plagioclase and amphibole and minor clinopyroxene. The U-Pb age determinations on nine zircon grains from a representative sample (D-5)

yielded ages ranging from 264 to 285 and a weighted mean age of 282.9 ± 2.8 Million years (Permian). Considering all U-Pb age data from mafic-ultramafic lithologies in the Kop ultramafic massif representing the northeastward extension of Refahiye ultramafic massif, it is clear that the mafic ultramafic bodies exposed between Eastern Pontides and Tauride blocks are Paleozoic or older in age and they are not remnants of a Jurassic ocean that known as "Northern Branch of Neotetys".

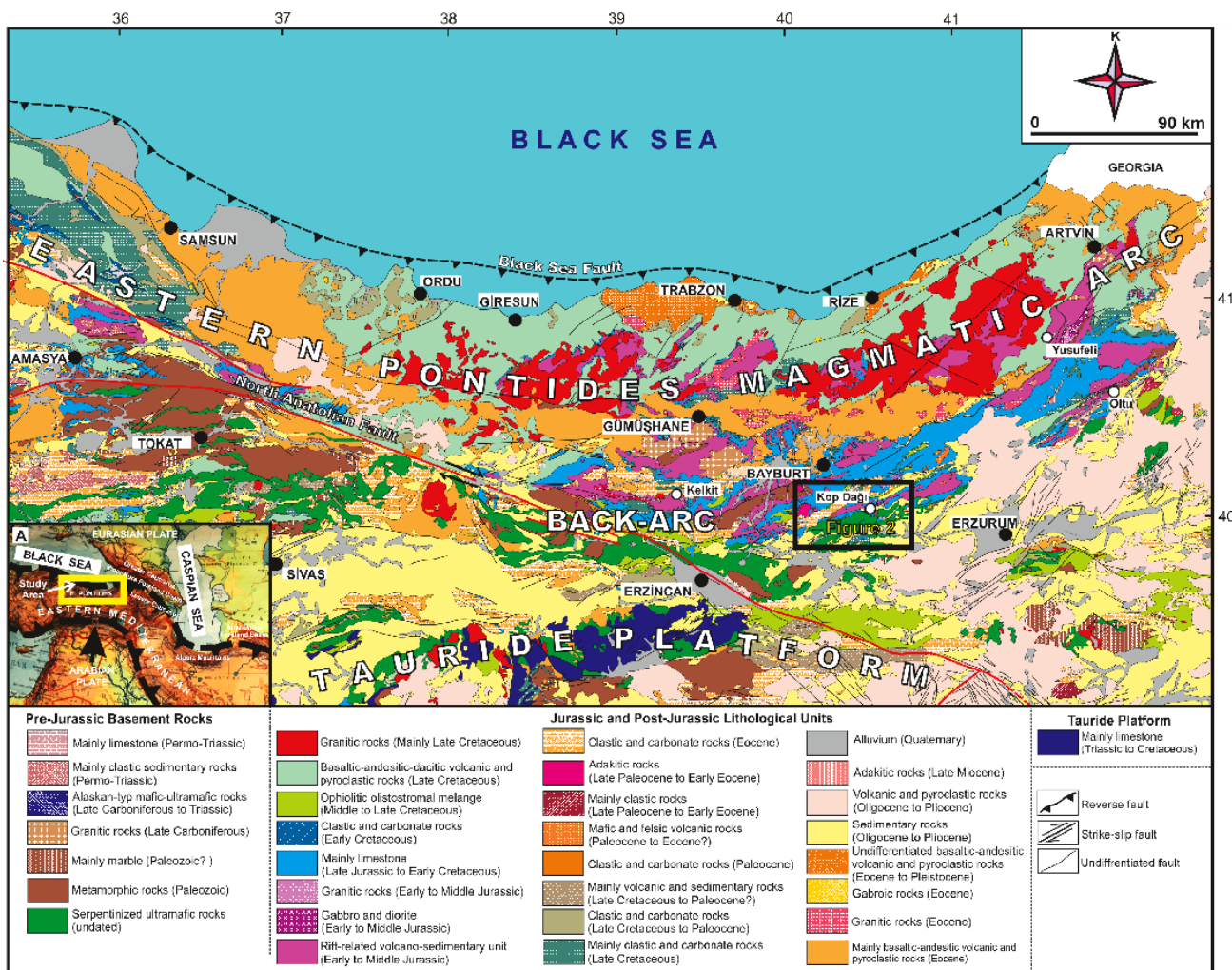


Figure 1: The main lithological units of the Eastern Pontides Orogenic Belt (modified from 1/500.000 scale geological map of Turkey prepared by MTA; Eyuboglu et al., 2016).

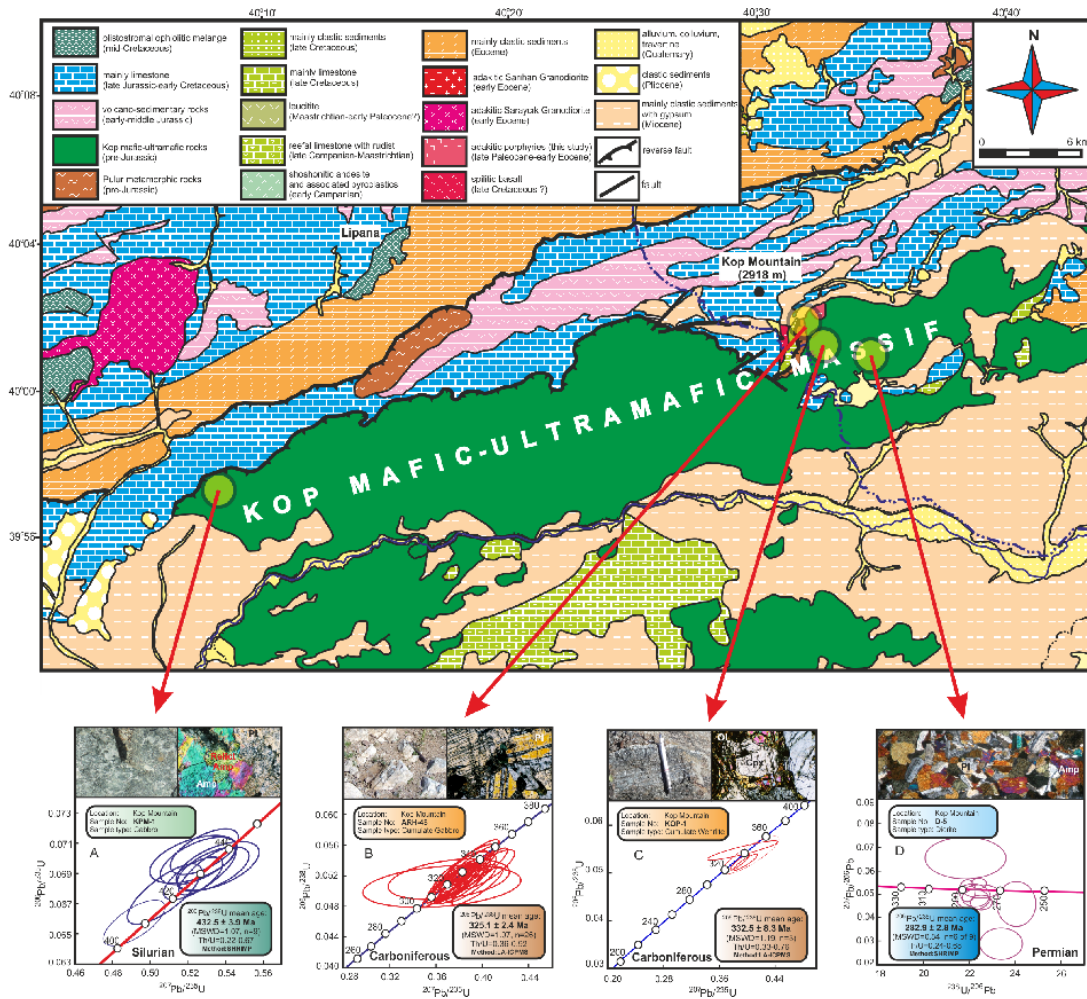


Figure 2: The geological map showing the main lithological units in Kop Mountain area and new U-Pb age data from mafic lithologies cutting Kop ultramafic masif (modified from Eyuboglu et al., 2016).

References

Eyuboglu, Y., Dilek, Y., Bozkurt, E., Bektaş, O., Rojay, B., Şen, C., 2010, Geochemistry and Geochronology of a Reversely-Zoned, Alaskan-type Ultramafic–Mafic Complex in the Eastern Pontides, NE Turkey. In: Santosh, M., Maruyama, S. (Eds.), A tribute to Akiho Miyashiro. *Gondwana Research* 18, 230-252.

Eyuboglu, Y., Dudas F.O., Santosh M., Xiao Y., Yi K., Chatterjee, N., Wu,

F.Y, Bektaş, O., 2016. Where are the remnants of a Jurassic Ocean in the eastern Mediterranean?. In: Eyuboglu, Y., Santosh, M. (Eds), *Convergent Margins and Related Processes. Gondwana Research* 33, 63-91.

Şengör, A.M.C., Yılmaz, Y., 1981. Tethyan Evolution of Turkey: a Plate Tectonic Approach. *Tectonophysics* 75, 181–241.

Mineral chemistry and petrology of mantle peridotites from the Guleman Ophiolite (SE Anatolia, Turkey): Evidence of a forearc setting

Mustafa Eren RIZELI^a, Melahat BEYARSLAN^{a*}, Kuo-Lung WANG^b, A. Feyzi BINGÖL^a

^a Firat University, Department of Geological Engineering, Elazig-TURKEY

^b Institute of Earth Sciences, Academia Sinica, Taipei, TAIWAN

*Corresponding author e-mail: m.erenrizeli@gmail.com

The Guleman ophiolite situated in SE Anatolia, Turkey is regarded as a fragment of Late Cretaceous oceanic lithosphere, consisting a core of mantle rocks overlain by an ultramafic sequence, layered and isotropic gabbros, sheeted dykes structurally overlies the Lower Miocene Lice Formation and is deposition ally overlain by sandstone sandshales of the Upper Maashtrichtian-Lower Eocene Hazar complex and Middle Eocene Maden Complex (Righo de Righi and Cortesini, 1964; Erdogan, 1977; Perinçek, 1979; Özkaya, 1978; Perinçek, and Çelikdemir, 1979; Bingöl, 1986; Beyarслан and Bingöl, 2014).

The mantle peridotites consist mainly of fresh and in place serpentized harzburgites with local bands and lenses of dunite and large-sized chromitite pods. The harzburgites contain 70-80 modal % of olivine and 15-25 modal % of

orthopyroxene. The minor phases are clinopyroxene (2-3 modal %) and chrome-spinel (2-3 modal %). They commonly display high-temperature deformation fabrics such as kink-bands in olivines. The main texture of the harzburgites is porphyroclastic texture, and occasionally mylonitic textures can be observed. Orthopyroxene and spinel are stretched in some samples. Chrome-spinel exhibits vermicular and xenomorphic, and rarely idiomorphic habits in peridotites. They contain 2-3% clinopyroxene as exsolution lammelles in orthopyroxene. The harzburgite and dunite have low CaO and Al₂O₃ abundances similar to Mariana fore-arc peridotite (Pearce et al. 1992). The average Cr-ratio = (Cr/(Cr + Al) atomic ratio) of Cr-spinels in harzburgites, and dunites is remarkably high (>0.63). The Fo content of olivine is between 90.9 to 92.3 in harzburgites and dunites. In the Mg

(Mg/(Mg+Fe²⁺)) versus Cr# in spinel diagram used to determine the degree of partial melting and the tectonical environment, the spinel plot in the fore arc peridotites field and the degree of the partial melting is > 35% (Fig.1). Orthopyroxene and clinopyroxene lamellae from the Guleman harzburgites have low CaO, Al₂O₃ and TiO₂ contents, resembling those of depleted harzburgites from modern fore-arc sand different from moderately depleted abyssal peridotites. Fore-arc peridotites are typically more depleted than abyssal peridotites, except for some lherzolites from the South Sandwich fore arc (Arai and Ishimaru, 2008; Pearce et al. 2000). In fertile abyssal lherzolites, spinels with Cr# < 30 are dominant (Dick and Bullen, 1984), while spinel in fore-arc peridotites may cover a slightly wider range, 40 < Cr# < 80 (Arai, 1994). The unusually depleted nature of fore arc peridotites requires unusual melting conditions: abnormally high temperature, volatile flux, or both. Highly depleted harzburgites, dunites and chromitites in the ophiolites form by melts of the mantle wedge overlying the new subduction zone (Shervais, 2001). These melts form in response to continued melting of previously depleted as the nose sphere brought about by increasing flux of fluids and melts from the subducting slab (Shervais, 2001). According to Whattam and Stern (2011), most ophiolites are fragments of exhumed fore arc sand that fore arcs form during subduction initiation allows us to use ophiolites to explore how subduction zones form. Consequently, we propose that the Guleman peridotites form in a fore arc setting during the subduction initiation that developed as a result of northward subduction of the southern

branch of the Neo-Tethys in response to the convergence between Arabian and Anatolian plates.

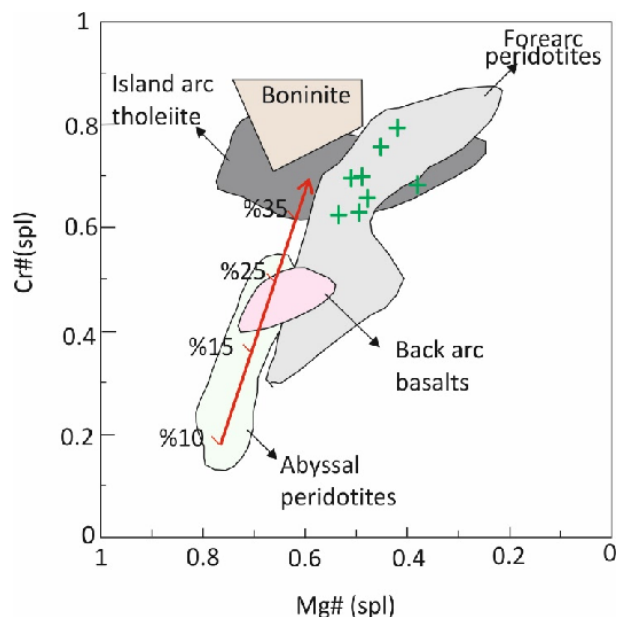


Figure 1, Composition of spinels in Guleman peridotites, plotted on Mg# [=Mg/(Mg+Fe²⁺) atomic ratio] versus Cr# [=Cr/(Cr+Al) atomic ratio] diagram. Abyssal peridotite and boninite field from Dick and Bullen (1984), fore arc peridotite field from Ishii et al. (1992); island arc tholeiite and back arc basin basalts field from Allan (1994), red arrow showing the percentage of the partial melting of peridotite from Hirose and Kawamoto (1995).

References

- Allan, J.F., 1994. Cr-spinel in depleted basalts from the Laubasin back-arc: petrogenetic history from Mg-Fe crystal-liquid exchange. In: Hawkins, J., Parson, L., Allan, J.F. et al. (Eds.), Proceedings of the Ocean Drilling Program. Scientific Results, vol. 135. p. 565-583.
- Arai, S., 1994. Characterization of spinel peridotites by olivine-spinel

- compositional relationships: review and interpretation. *Chemical Geology* 113, 191-204.
- Arai, S. And Ishimaru, S. 2008. Insight in to petrological characteristics of the lithosphere of mantle wedge beneath arcs through peridotite xenoliths: a review. *Journal of Petrology* 49, 665–95.
- Beyarslan, M. ve Bingöl, A.F., 2014. Petrology of the Ispendere, Kömürhan and Guleman Ophiolites (Southeast Turkey): Subduction Initiation Rule (SIR) Ophiolites and Arc Related Magmatics. 3rd Annual International Conference on Geological and Earth Sciences, proceedings., 22-23 September, Singapore.
- Bingöl, A.F., 1986. Petrographic and petrologique characteristic of the Guleman Ophiolite (Eastern Taurus-Turkey), *Gesound*, 13/14, 41-57.
- Dick, H.J.B., Bullen, T., 1984. Chromianspinel as a petrogenetic indicator in abyssal and alpine-type peridotites and spatially associated lavas. *Contributions to Mineralogy and Petrology* 86, 54-76.
- Hirose, K., Kawamoto, T., 1995. Hydrous partial melting of lherzolite at 1 Gpa: the effect of H₂O on the genesis of basaltic magmas. *Earth and Planetary Science Letters* 133, 463-473.
- Ishii, T., Robinson P.T., Maekawa, H., Fiske, R., 1992. Petrological studies of peridotites from diapiric serpentinite sea mounts in the Izu-Ogasawara-Mariana fore arc, Leg 125. In: Fryer, P., Pearce, J.A., Stokking, L.B. et al. (Eds.), *Proceedings of the Ocean Drilling Program Scientific Results*, vol. 125. pp. 445-486.
- Pearce, J.A., Vander Laan, S.R., Arculus, R.J., Murton, B.J., Ishii, T., Peate, D.W., and Parkinson, I.J., 1992. Boninite and harzburgite from Leg 125 (Bonin-Mariana fore arc): A case study of magma genesis during the initial stages of subduction, in Fryer, P., et al., *Proceeding of the Ocean Drilling Program, Scientific Results, Site 778–786, Bonin-Mariana Region: College Station, Texas, Ocean Drilling Program*, p. 623–659.
- Pearce, J.A., Barker, P.F., Edwards, S.J., Parkinson, I.J., and Leat, P.T., 2000. Geochemistry and tectonic significance of peridotites from the South Sandwich arc-basin system, South Atlantic: Contributions to Mineralogy and Petrology, v. 139, p. 36–53, doi:10.1007/s004100050572.
- Shervais, J. W., 2001. Birth, death, and resurrection: The life cycle of supra subduction zone ophiolites: *Geochemistry, Geophysics, Geo systems*, v. 2. Page number 2000GC000080.
- Whattam, S.A., Stern, R.J., 2011. The ‘subduction initiation rule’: a key for linking ophiolites, intra-oceanic fore arc and subduction. *Contributions to Mineralogy and Petrology*. doi:10.1007/s00410-011-0638-z.

Dehydration patches (Incipient charnockite) within the granite gneiss: A report from Munnar area Southern India

S Rajesh* and A.P. Pradeepkumar

Department of Geology, University of Kerala, Trivandrum, India, 695581

*Corresponding Author e-mail: georajeshmunnar@gmail.com

Orthopyroxene-bearing, dark green metamorphic dehydration zones (popularly known as incipient charnockites) occurring within granite gneiss (Fig.1) in munnar area in the western domain of the Madurai block of southern granulite terrain. Such localized dehydration zones, occurring over a scale of centimeters to a few meters, have been already documented in the southern granulite terrain (Santosh, 1986; Rajesh, 2004; Ravindra Kumar, 2004). This incipient Charnockite patches contains subhedral coarse to medium grained plagioclase, quartz, K-feldspar, orthopyroxene, biotite, and hornblende and the granite gneiss contain subhedral quartz, K-feldspar, plagioclase, hornblende and biotite (Fig. 2) and which are coarse to medium grained, showing hypidiomorphic granular texture also shows a wide grain size variation from fine to coarse. Field investigations reveal that the rocks in Munnar include granite, hornblende biotite gneiss, cordierite gneiss, granite gneiss, carbonatite, syenite and migmatite. The Munnar granite has a U–Pb zircon age of

740±30 Ma (Odom, 1982). The E-W trending irregular pink granite near Munnar (Fig. 3) shows variations from a medium-grained marginal intermediate phase to a medium coarse grained interior felsic phase. The Munnar granite contains hornblende (±biotite) gneiss and calc-silicate enclaves. The presence of pegmatites and quartz veins of varying dimensions (5–100 cm) in granites suggests that the residual magma was volatile rich. The internal fabrics and pluton margins crosscut the regional fabric developed in the surrounding rocks, indicating the post-tectonic nature of the granites.

Based on the petrographic fluid inclusion studies of the surrounded area gives an evidence for the involvement of immiscible CO₂- and H₂O-bearing Cl-rich brine in the dehydration process at a local scale.

The common spatial association of large biotite-bearing, granite pegmatites and dehydration zones in the munnar granite gneiss suggests that they are an

obvious candidate to test in terms of the fluid carrier. However, the lack of CO₂-rich fluid inclusions and the diffuse contact relationships with the Munnar granite gneiss rule out the granite pegmatites as the carrier of the dehydrating fluids.

Granitic melts can contain very small quantities of CO₂ and Cl but these components will be overwhelmed by the H₂O given off by crystallization of the pegmatite.

Based on the field occurrence, the Munnar granite gneiss collected from the metasomatized zone, which is more leucocratic than the surrounded migmatized gneiss sample, it can be inferred that the fluids most probably moved along grain boundaries parallel to the gneissic fabric observed in the Munnar

granite gneiss. Dehydration of the wall-rocks occurred where the permeability was sufficient for fluid penetration. It is thus suggested that H₂O-CO₂ - brine fluids derived from an external source were lithologically or structurally channeled; these then interacted with the Munnar granite gneiss, triggering dehydration with the formation of orthopyroxene.

The occurrence of minor monzonitic (An igneous intrusive rock composed of approximately equal amounts of plagioclase and alkali feldspar, with less than 5% quartz) domains surrounding the dominant orthopyroxene-bearing domains in the hornblende veins suggest the possibility of partial melting accompanying fluid-rock interaction.

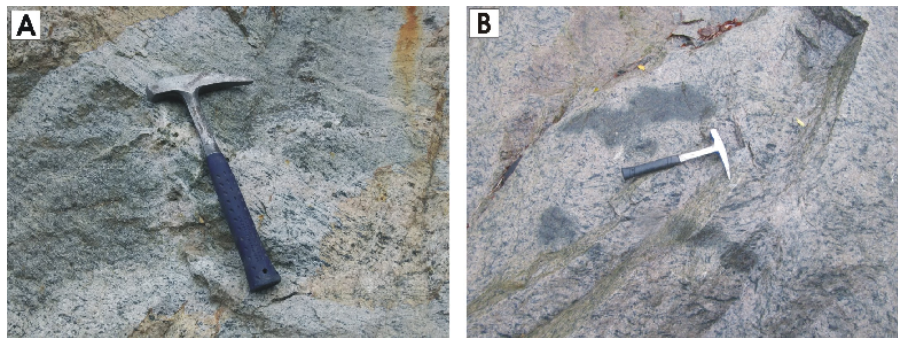


Fig 1. Dehydration patches developed in Manner granite

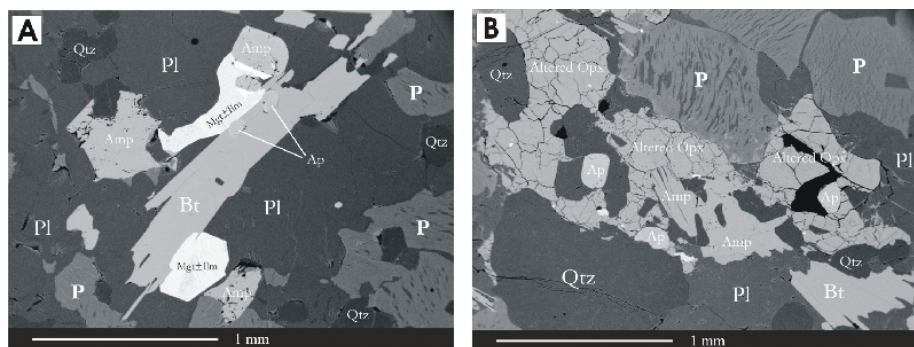


Fig 2. Back-scattered electron images (BSE) of granite and charnockite patch. A) Granite mineral assemblage B) Dehydration zone mineral assemblage: Bt (or Amp) + $Qtz \Rightarrow Opx + H_2O$

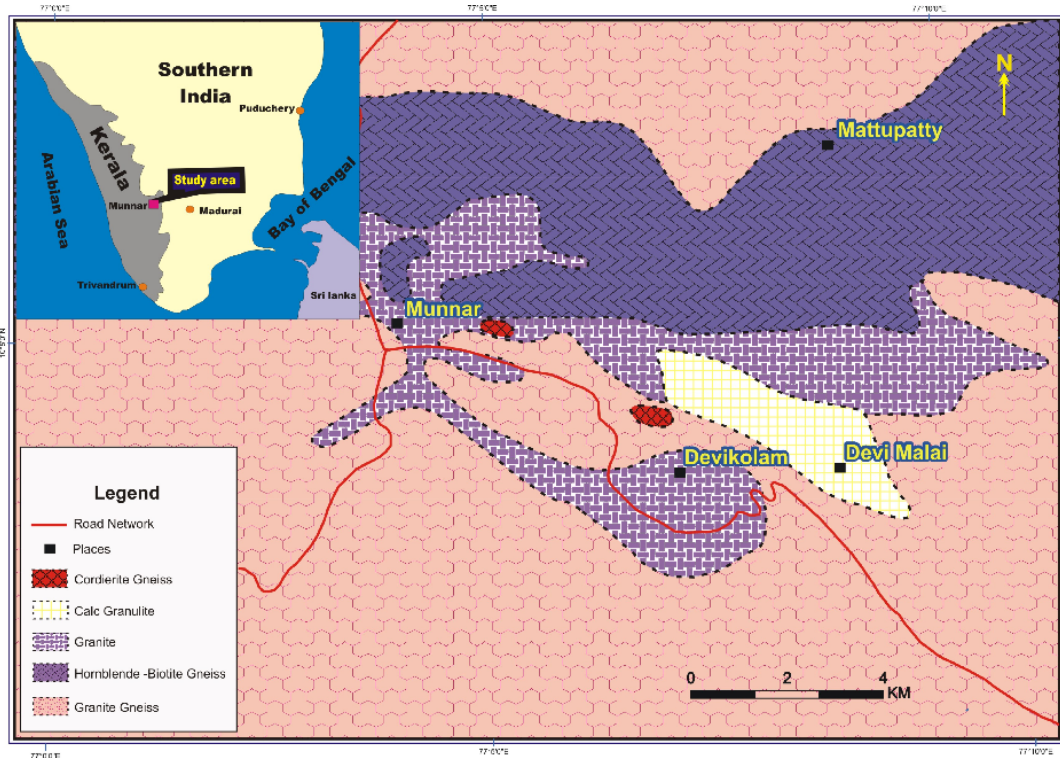


Fig 3. Geological map of the Munnar area in the western part of the Madurai block

References

- Santosh, M. (1986). Carbonic metamorphism of charnockites in the south western Indian shield: a fluid inclusion study. *Lithos* 19, 1-10.
- Rajesh, H. M. & Santosh, M. (2004). Charnockitic magmatism in southern India. *Journal of Earth System Science* 113, 565-585.
- Ravindra Kumar, G. R. (2004). Mechanism of arrested charnockite formation at Nemmara, Palghat region, southern India. *Lithos* 75, 331-358.
- Odom, A.L., 1982. Isotope age determinations of rock and mineral samples from Kerala, India. Unpublished Final Report UN Case No 81-10084, KMEDP. Trivandrum, 10.

Evidences of extensive crustal melting in the Kerala Khondalite Belt, southern India during assembly of Eastern Gondwana

V Nandakumar¹, SL Harley², Vinod Samuel³, J K Tomson¹, Jayanthi J L¹,
Batuk Joshi¹ & Nilanjana Sorcar¹

¹ Crustal Processes Group, National Centre for Earth Science Studies, ESSO-NCESS, Trivandrum- 695011, Kerala, India

² School of Geosciences, University of Edinburgh, Kings Buildings, Edinburgh UK

³ Earth Sciences, Indian Institute of Science, Bangalore, India

*Corresponding Author e-mail: v.nandakumar66@gmail.com

We evaluate the geochemical signatures resulting from processes associated with the partial melting of paragneisses during Neoproterozoic-Cambrian (565-515 Ma) granulite facies metamorphism in the Kerala Khondalite Belt (KKB). Simple whole rock geochemical relationships referenced against SiO₂ allow the discrimination of restite material (SiO₂: 56-60 wt %), migmatite (SiO₂: 60-66 wt%), leucosomes (SiO₂: 66-70 wt%) and well-segregated leucogranites (SiO₂: 70-75 wt%) (Fig.1). Major element systematics also show that the leucosomes and leucogranites are peraluminous and calc-alkaline to alkaline-calcic. Restite and migmatite show complementary enrichments in all major elements apart from SiO₂ and K₂O relative to leucosome

and leucogranite. CIPW norm calculations applied to the four rock types demonstrate that they are all corundum normative, consistent with a sedimentary protolith for the paragneisses. LIL and HFS incompatible element enrichments are consistent with extensive melting. Major and trace element tectonic discrimination diagrams, which are applicable only to leucosomes and leucogranites that can be deduced from other chemical parameters to have been largely liquid prior to final crystallisation, are consistent with syn-orogenic magmatism when such filters are applied. The Leucogranites are seldom just simply 'melts' - they vary due to some fractionation, but more importantly they are liquid + crystal mixes, with minor / moderate residual material (e.g. Grt + Bt +

Sill. maybe Qz) in some, peritectic Grt (and ilm?) in others, all of these perhaps in some, and only in a few cases is the result simply crystallised melt (forming minimum-melt compositions of Qz-Kfs-Plag-Grt-Ilm-Apat / Mnz etc). REE patterns overall approximate to post-Archaean shale composite in terms of fractionated LREE, and flat (ish) HREE, but there is considerable variability within this, and it is not appropriate to simply conclude that extracted leucogranites/ leucosomes are always enriched in LREE and heat producing elements.

As part of our studies to verify the role of fluids in the generation of melts a preliminary study on fluids in the leucosome, restite and migmatitic portions

have been conducted. In general, the fluid inclusions are abundant in the leucosome portions compared to the restitic and migmatitic portions. The most common type of inclusions are carbonic inclusions (vapour-liquid) containing a dense and sometimes dark CO₂ rich fluids which completely fills the inclusion. FIs are abundant in minerals like quartz and feldspar. Garnets have ovoidal and diamond shaped fluid inclusions. The leucosome have basically two generation of FIS where as with densities from 0.7 to 0.6 g cm⁻³. All the other minerals are having CO₂ inclusions of typical density approximating to 0.9- 0.8 gcm⁻³. Raman studies have also been initiated and the Raman peak of CO₂ is shown (Fig. 2) at 1385 cm⁻¹.

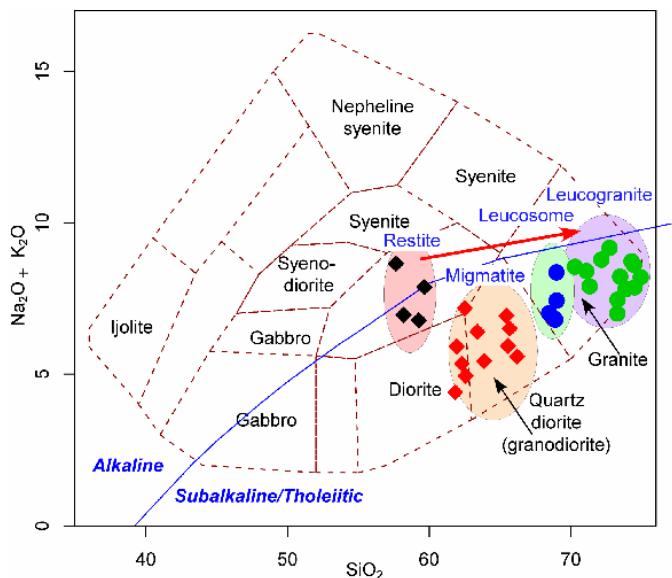


Fig. 1. Discrimination diagram using major element data. **A**, total alkali (Na₂O+K₂O) vs. SiO₂ diagram after Le Maitre et al. (1989).

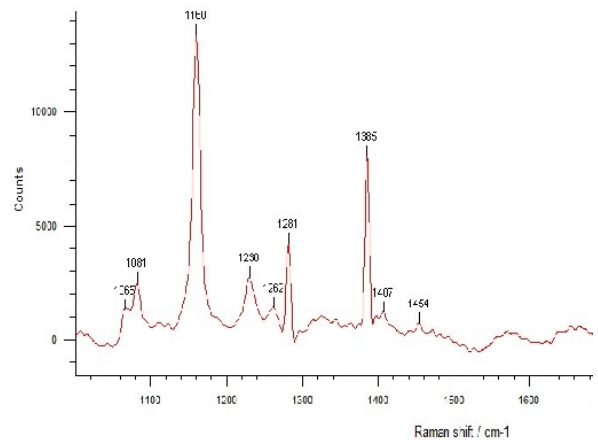


Fig.2. Analysis of fluid inclusions using Raman shows the peak of CO₂ at 1385 cm⁻¹

HT-UHT metamorphism of the Kerala Khondalite Belt: Complexity and interpretations

Durgalakshmi^a, I.S. Williams^b, V. Samuel^c, V.J. Rajesh^d and K. Sajeev^c

^aDepartment of Studies in Earth science, University of Mysore, Mysuru

^bResearch School of Earth Sciences, Australian National University, Canberra

^cCentre for Earth Sciences, Indian Institute of Science, Bengaluru

^dDepartment of Earth and Space Sciences, Indian Institute of Space Science and Technology, Thiruvananthapuram

The Kerala Khondalite Belt (KKB) lies to the south of the Achankoil Shear Zone and to the north of the Nagercoil Block in the Southern Granulite Terrain, southern India (Taylor et al., 2014). The KKB exposes granulite grade metasedimentary rocks (e.g., Chacko et al., 1987; Nandakumar and Harley, 2000) that were subjected to high- and ultrahigh-temperature metamorphism (Chacko et al., 1987; Nandakumar and Harley, 2000;; Morimoto *et al.*, 2004, Harley and Nandakumar, 2016) during the latest Neoproterozoic to Cambrian times (Braun et al. 1998; Cenki et al., 2004; Shabeer et al., 2005; Santosh et al., 2005; Harley and Nandakumar, 2014; Taylor et al., 2014 and references therein) .

Samples of highly migmatized paragneiss were collected from a quarry at Poolanthara (N 8°38'23.7" E 076°53'29.6"). The leucosome consists of quartz and feldspar with euhedral to subhedral garnet and minor fine grained biotite flakes as ferromagnesium phases. Restite, which

forms the melanosome, consists of porphyroblastic resorbed garnet, coarse needles of sillimanite, and cordierite, spinel and biotite. Retrograde rims of cordierite around garnet are slightly deformed. Sillimanite and biotite are abundant in the melanosome. The contact between leucosome and melanosome is diffused—possibly evidence of partial melting. Cordierite is present in both leucosome and melanosome. The common mineral assemblage is Crd+Grt+Sil+Bt±Spl. Silimanite-absent cordierite-rich melanosome domains are also present.

A sample of cordierite rich metapelite with the mineral assemblage Crd+Grt+Sil+Bt+Spl+Qtz was selected for U-Pb geochronology, Ti-in-zircon thermometry and REE analysis by Sensitive High Resolution Ion Microprobe (SHRIMP). The near peak assemblage identified in the matrix was Spl+Qtz, associated with resorbed garnet. Peak-metamorphic conditions are calculated to have been $T \approx 900^\circ\text{C}$ at $P = 0.6\text{--}0.7$ MPa.

Zircon was analysed both as separated grains and in-situ in thin-sections. Monazite grains separated from the same sample were analysed for U-Pb geochronology. The separated zircon was divided into two grain sizes, < 70 and > 70 μm , in an unsuccessful attempt to concentrate new-grown zircon during the metamorphic event. The zircon analysed in thin-section mostly was > 70 μm and occurred within cordierite. A very few grains were inside a garnet porphyroblast.

Cathodoluminescence (CL) images of the zircon (both separated and in-situ) mostly showed a bright white rim, inside and outside of which were darker zones, and an inner core. In the few grains without a white rim, the zone outside the core or any metamorphic layer was assumed to have formed inside the white rim. These textural distinctions were used to guide the ion probe analyses.

On the basis of the chondrite-normalised Yb-Tb ratio, the REE patterns were categorized as 'very low' (<0.2), 'low' (0.3–1.0), 'flat' (1.1–2.7) or 'high' (6–25). The zircon cores all had a 'high' REE pattern. All zones between the core and the white rim had a 'flat' pattern. The REE pattern of the white rim was 'very low' and that of the zones outside white rims was 'low'.

There was a correlation between the REE patterns and U and Th contents, Th/U, Ti content, Zr/Hf and age. The zones with 'flat' patterns had a limited range in Th and U content and consistently very low Th/U (most 0.030–0.035), indicators of crystallisation in the presence of garnet and probably monazite. There was a wide range in Ti content, however (9.5–19.7 ppm). Zones with 'low' REE patterns had a much wider range of Th/U (up to ~

0.3) but a relatively narrow range of $^{206}\text{Pb}/^{238}\text{U}$ age (560–530 Ma). Th/U was higher (0.36–0.53) in the bright zones with 'very low' REE patterns and the range in $^{206}\text{Pb}/^{238}\text{U}$ age was similar (525–490 Ma). The cores, with 'high' patterns, had a wide range of apparent ages (2.3–1.3 Ga).

These relationships between texture and composition were used to interpret the data from a large number of additional spots on which only U-Th-Pb were measured. The U-Pb analyses of cores were consistently weakly to strongly discordant, indicative of isotopic disturbance. $^{207}\text{Pb}/^{206}\text{Pb}$ ages ranged from 2.6 to 1.0 Ga. The zones with 'flat' REE patterns adjacent to the cores, despite their homogeneity in U and Th, showed extreme heterogeneity in radiogenic Pb content on the nanometre scale, evident as extreme variability in Pb count rates during the ion probe analysis of a single spot. This was evidence of the presence of Pb nanonuggets, presumably produced by Pb clumping (Kusiak et al., 2013) during the UHT metamorphism. Determining the age of these zones was not possible. The white rims, in contrast, had relatively uniform Pb/U, giving a weighted mean $^{206}\text{Pb}/^{238}\text{U}$ age of 497.7 ± 8.2 Ma. The zones with 'low' REE patterns outside the white rims were expected to give even lower Pb/U ages, but instead gave two groups of higher ages, 540 ± 4.9 and 508 ± 5.8 Ma (95% c.i.), possibly because the white rims were produced by late recrystallisation. Monazite also gave dispersed $^{206}\text{Pb}/^{238}\text{U}$ results, indicative of an age of 582 ± 16 or 565.3 ± 5.4 Ma, depending on whether the oldest or dominant age group was selected. The $^{208}\text{Pb}/^{232}\text{Th}$ age of the dominant group was 558 ± 6.5 Ma. Metamorphic monazite crystallised before metamorphic zircon.

The ages measured on the metamorphic zircon and monazite from the Poolanthara sample are consistent with the few ages for metamorphism in the area that have been published previously. They coincide in time with the protracted orogenic event that marked the final amalgamation of the Gondwana supercontinent, the Pan-African Orogeny.

References

- Braun, I., Montel, J.-M., Nicollet, C., 1998. Electron microprobe dating monazites from high-grade gneisses and pegmatites of the Kerala Khondalite Belt, southern India. *Chemical Geology* 146, 65–85
- Cenki, B., Braun, I., Bröcker, M., 2004. Evolution of the continental crust in the Pan-African mobile belt of southernmost India: evidence from Nd isotope mapping combined with U–Pb and Rb–Sr geochronology. *Precambrian Research* 134, 275–292.
- Chacko, T., Ravindra Kumar, G.R., Newton, R.C., 1987. Metamorphic P-T conditions of the Kerala (South India) Khondalite belt: a granulite-facies supracrustal terrain. *Journal of Geology* 96, 343–358.
- Harley, S.L., Nandakumar, V., 2014. Accessory mineral behaviour in granulite migmatites: a case study from the Kerala Khondalite Belt. *Indian Journal of Petrology* 55, 1965–2002.
- Harley, S.L., Nandakumar, V., 2016. New evidence for Palaeoproterozoic high grade metamorphism in the Trivandrum Block, Southern India. *Precambrian Research* 280, 120–138
- Morimoto, T., Santosh, M., Tsunogae, T., Yoshimura, Y., 2004. Spinel + quartz association from the Kerala Khondalites, southern India: evidence for ultrahigh temperature metamorphism. *Journal of Mineralogical and Petrological Sciences* 99, 257–278.
- Nandakumar, V., Harley, S.L., 2000. A reappraisal of the pressure-temperature path of granulites from the Kerala Khondalite Belt, southern India. *Journal of Geology* 108, 687–703.
- Santosh, M., Collins, A.S., Morimoto, T., Yokoyama, K., 2005. Depositional constraints and age of metamorphism in southern India: U-Pb chemical (EPMA) and isotopic (SIMS) ages from the Trivandrum Block. *Geological Magazine* 142, 255–268.
- Shabeer, K.P., Satish-Kumar, M., Armstrong, R., Buick, I.S., 2005. Constraints on the timing of Pan-African granulite-facies metamorphism in the Kerala Khondalite Belt of Southern India: SHRIMP mineral ages and Nd isotope systematics. *Journal of Geology* 113, 95–106.
- Taylor, R.J.M., Clark, C., Fitzsimons, I.C.W., Santosh, M., Hand, M., Evans, N., McDonald, B., 2014. Post-peak, fluid-mediated modification of granulite facies zircon and monazite in the Trivandrum Block, southern India. *Contributions to Mineralogy and Petrology* 168, 1–17.

Metamorphism and plate tectonic implications of the BIF, TTG and associated rocks of the Nilgiri Block, with special reference to Calicut District, Kerala, South India

R. S. Prasanth* and A. P. Pradeepkumar

Department of Geology, University of Kerala, Trivandrum, India – 695 581

*Corresponding Author e-mail: prashanthgeo@gmail.com

The Study area lies to the south of the Coorg Block, and is dominantly composed of charnockites and their variants, together with metagabbros, TTG gneisses and slivers of BIF. The Moyar-Bhavani shear zone (MBSZ) defines the northern and eastern limits of the Nilgiri Block (Fig 1). The banded iron formations of the study area, associated with plunging synforms and antiforms, occur at Cherupa, Eliyottimala, Nanminda, Naduvallur, Alampara, Kakkayam, East and West Hills (Fig 2). Extensive magmatism along convergent margin settings marks the late Neoproterozoic tectonics in the northern segment of the Southern Granulite Terrane (SGT) in Peninsular India. Here we investigate a suite of magmatic rocks (TTG, charnockite and amphibolite) together with accreted banded iron formation (BIF) from the western margin of the Nilgiri Block. The petrologic features of these rocks, including the presence of

gruneritic amphiboles, suggest crystallization from calc-alkaline magmas typical of those derived from slab melting. The focus of the study is the petro-mineralogical characterisation of the iron formations. Rare earth element geochemistry of the iron formation will provide insights into the composition of contemporaneous seawater and evolution of the atmosphere, hydrosphere and lithosphere system. The zircon grains in all the rock types show clear magmatic features including well-crystallized prismatic features, oscillatory zoning and high Th/U values. The study also aims to illustrate the plate tectonic settings of the iron formations in the light of new proposals on subduction-accretion-collision history at the margins of the Archean cratons in southern India, thereby revealing the mechanism of formation of the iron ores and the metamorphic history of the associated lithologies and hence

constraining the plate tectonic setup. The geochronological data based on

$^{207}\text{Pb}/^{206}\text{Pb}$ suggest major late Neoproterozoic magmatism between ca. 2.6 and 2.5 Ga.

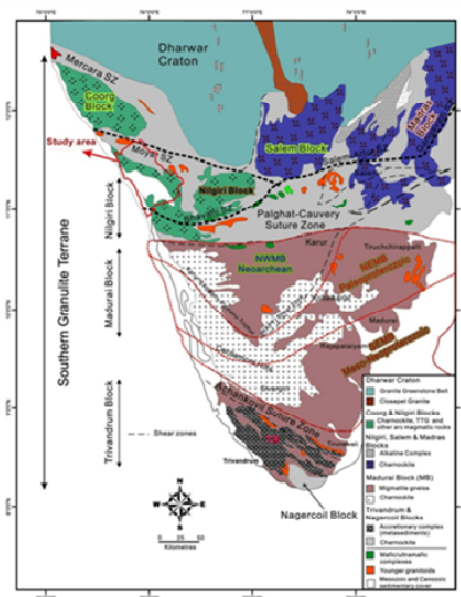


Fig. 1 Geological framework of the Southern Granulite Terrain, India (after Santosh et al., 2015; Collins et al., 2014)

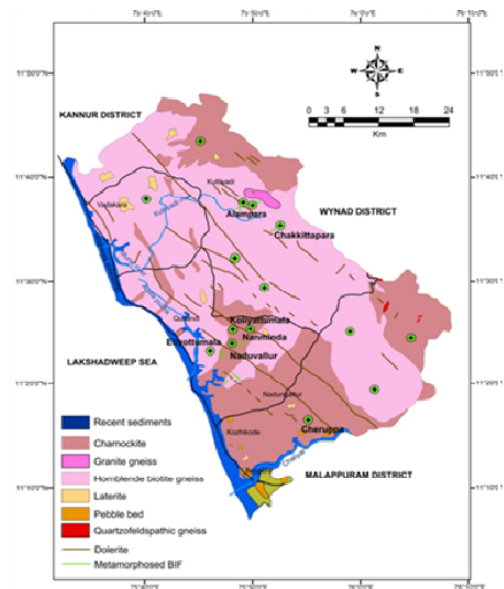


Fig. 2 Geological map of the Coimbatore district showing sample locations of present study.

Representative field photographs



(a) 100% gneiss with distinct compositional banding. (b) Amphibolite lenses within 100% gneiss. (c) Charnockite. (d) Banded iron formation.

Geochemistry and metamorphism of the migmatized gneiss and dehydrated charnockite around Marthandam, Tamil Nadu, India

J. Remya* and A. P. Pradeepkumar

Department of Geology, University of Kerala, Trivandrum, India – 695 581

*Corresponding Author e-mail: jremya11@gmail.com

Geochemistry and metamorphism of migmatized gneisses and charnockite in the northwestern part of the Nagercoil Block (NGB), within the southern fringe of Southern Granulite Terrain, in and around Marthandam has been studied in detail (Fig 1, Fig 2). It is believed to be rifted continental margin of the Indian Peninsula, and mainly composed of gneisses and charnockites. The rocks are invariably interrelated and are seen to be formed at the same time by the metamorphism of pelitic sediments. Geochemistry reveals that the gneisses are peraluminous to moderately peraluminous and alkali-calcic variety while massive charnockite and incipient charnockite samples fall in the peralkaline and peraluminous field respectively. Generally strongly peraluminous magmas are formed by mixing of mature pelitic sediments with the initial melt and produce S-type igneous rocks. But the gneisses of Marthandam are not so intensely peraluminous, discounting them being categorised as metapelitic. The source rocks could as well

be intermediate to felsic igneous rocks as well as products of partial melting of metaluminous mafic material. The area has experienced a minimum P-T condition of 8.5 kilobars and 800°C. Based on the coexisting mineral assemblages in the gneisses, charnockite and associated rocks, it is found that the rocks of the area have undergone granulite facies metamorphism.



Photo 1: Felsic aggregation and melt like pockets parallel to the foliation of the GBG

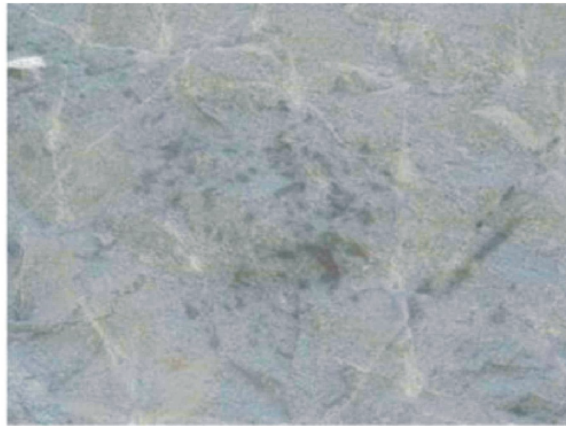


Photo 2: Dehydration patches in the GBG

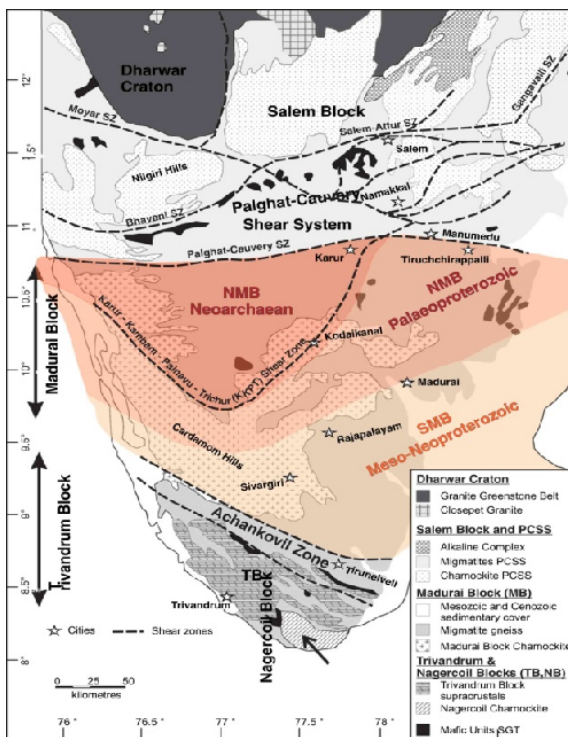


Fig.1 Map of southern India modified from Geological Survey of India (1994) and Plavsa et al. (submitted for publication) with the study area marked. NMB = Northern Madurai Block, SMB = Southern Madurai Block, PCSS = Palghat Cauvery Shear

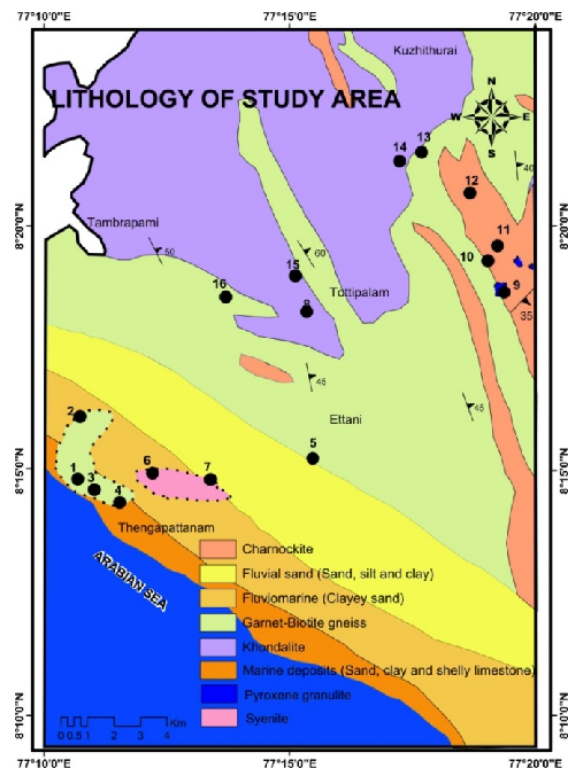


Fig.2 Location map of Marthandam area

Mineral magnetic characterisation of tropical soil profiles from Northern Kerala, India

Linu Babu^{1*} and Reethu Mohan²

¹ School of Environmental Sciences, Mahatma Gandhi University, Kottayam 686 560, India

² Department of Geology, University of Kerala, Kariavattom, Trivandrum 695 581, India

*Corresponding Author e-mail: linubabu1990@gmail.com

Regolith is the surficial blanket of material including weathered rock, sediments, soils and biota that forms by the natural processes of weathering, erosion, transport and deposition with a vary in thickness from a few centimeters to hundreds of meters. It is a good record of paleoclimatic variations. So it needs much more attention. Mineral magnetism is an efficient tool to discover the environmental processes governed by a combination of factors including formation, transportation, deposition and post-depositional alterations. The study area is located at Kannur district, in the northern part of Kerala, and subject to humid tropical monsoonal climate. The area is a plane terrain like a plateau with hard cap of laterite on the surface. Three core samples (KC-1, KC-2, and KC-3) were collected from this area which contains laterite/bauxite, clay, iron formations, peat formation, sand and hornblende gneiss with a distance of 600 m interval. The upper parts of the lateritic rocks are characterized by lateritic soils. The three soil profiles contain both insitu and transported sediments. Insitu sediments are present just above the hard rock. All other sediments are transported in origin. Redness rating index and mineral magnetic characteristics were determined

for each sediment in the soil profiles. Iron in soils is present in the form of oxides (magnetite, titanomagnetite, hematite and maghemite), sulphides (greigite and pyrrhotite) and hydroxides (goethite and limonite). Magnetic analyses included low-frequency dependent susceptibility (χ_{LF}), susceptibility of anhysteretic remanent magnetism (χ_{ARM}), the saturation isothermal remanent magnetism (SIRM) and the isothermal remanent magnetism (IRM) reverse were performed for the three sediment cores.

43 m core sample (KC-1) above the hard rock (base) composite profile of sediments, clay, laterites and bauxitic laterites and peat shows a major change in mineral magnetic parameters matching with ~20 m depth. This depth coincides with the change in facies from majority of gray to majority of reddish brown. The B (0) CR and S-Ratio mark this change more remarkably by showing the changeover from ferromagnetic to antiferromagnetic mineralogy. Amongst the other parameters the χ_{ARM} / χ shows an anomalous peak at ~30 m depicting the enrichment of SD magnetites. This horizon encounters a peat deposition anticipating the in situ formation of SD magnetites under reducing conditions. Peak antiferromagnetic compositions

occur at the top horizons showing laterite and lateritic bauxites. It is therefore inferred that the major climatic change has occurred at ~20 m level from reductive and wet to oxidative warm humid climates further leading to the intensive lateralization. The 42 m core (KC-2) displaying similar composite lithology but variation in thicknesses of the layers and placements of some layers. The Gray brownish changeover occurs at ~22 m depth with the peat horizon occurring at ~25 m. The S-Ratio and B (0) CR rightly reflect the changeover ferri- to antiferromagnetic mineralogy at ~25 m coinciding with the observations as above. There is an anomalous peak in the parameters showing antiferromagnetic All the soil horizons designate the dominance of authigenic mineralogy and the absence of stable single domain grains. A change in grayish to reddish brown and ferromagnetic to antiferromagnetic mineralogy is observed at a depth of ~25 m in all the stratigraphic columns which indicate a climatic change from reductive and wet to oxidative and warm humid condition further leading to the intensive lateralization. The mass specific susceptibility (χ_{LF}), mean coercivity ($(B_0)_{CR}$), χ_{ARM}/χ_{LF} , HIRM, the mean S-ratio, S-ratio 2, and S-ratio % indicates purely hard antiferromagnetic mineralogy with interplay of hematite and goethite. The result of Munsell colour

mineralogy at ~6 m which coincides with the laterite horizon. Further up also the antiferromagnetic mineralogy becomes abundant indicating lateritization up to top. The longest core sample with 49.5 m (KC-3) shows the grey to brownish red transformation at 30 m, however there the peat occurrence is observed at ~18 m while the anomalous peak in ARM/χ_{LF} occur at ~24 m within the sandy horizon. Further although the ferri to antiferromagnetic change occurs at ~30 m, the conditions are largely fluctuating as compared to the above two cores. An anomalous peak in HIRM, H and $SIRM/\chi_{LF}$ occur at ~12 m with iron concretions. The large fluctuations in all these parameters depict fluvial influence in this core. notations in dry and wet conditions and redness rating are also confirms the presence of hematite in three core samples.

Acknowledgements

Linu Babu gratefully acknowledges the Kerala State Council for Science Technology (KSCSTE)'s PhD fellowship and Reethu Mohan acknowledges the KSCSTE's Masters Dissertation support through the Student Project Scheme. Prof Sangode of Pune University is thanked for hosting and supervising us in his magnetism lab and Dr AP Pradeepkumar for guidance.

**2016 Annual Convention &
13th International Conference on
Gondwana to Asia**

Trivandrum, India

November 18-22, 2016

Field Excursion Guide Book



Organized by

University of Kerala, Trivandrum, India

**2016 Annual Convention & 13th International Conference on Gondwana to Asia
18-22 November 2016**

Field Excursion Guide Book

Contributed by

E. Shaji (University of Kerala), M. Santosh (CUGB, Beijing) Chris Clark (Curtin University, A. P. Pradeepkumar (University of Kerala) V. J. Rajesh (IIST, Trivandrum) V. Nandakumar (NCESS, Trivandrum) , and K. Sajeev, (IISc, Bangalore)

Welcome to the 2016 Annual Convention & 13th International Conference on Gondwana to Asia fieldtrip to the important charnockite-leptynite-khondalite localities of Trivandrum Block and the Achankovil Tectonic Zone of the Southern Granulite Terrane of India. On 21 Nov 2016 (Monday), we will start our trip from Trivandrum with a visit to what could be considered as the type area of the khondalites (aluminous metapelites) at Koliakodu. The second locality is Kakkodu quarry, where we will get a chance to discuss the relationships between different lithologies (leptynites, khondalites and “incipient charnockites”) that are uniquely exposed here.

On 22 Nov 2016, after an early morning visit to one of the most famous Ganesh temples in India, we will visit what is probably the best-known outcrop in the Trivandrum Block – the incipient charnockites at the Kottavattom Quarry. This locality has been the focus of a number of geochemical, petrological and isotopic studies that have resulted in the “charnockite controversy”. At this locality we hope to continue this debate by providing some additional data that can be discussed in the context of the source of the fluids – be they melts or CO₂-rich, derived from the mantle or crystallising granites – that are involved in the progressive change from leptynite to charnockite in what can be seen as an unambiguously structurally controlled process.

We will end the trip at Kovalam Beach, and will examine the Paleoproterozoic charnockite exposures near the beach. We then drive back to Trivandrum.

Itinerary

21-11-2016 Day 1

Trivandrum to Kottarakkara

08.00 AM: Check-out and board vehicle from Residency Tower Hotel

09:30: Stop 1 – Koliakodu Quarry GPS - 76° 53'27" E 80 38'21" N

Geology: Typical khondalite (grt-sill-crd-bio-gneiss)

Lunch on the way

02:00 PM Stop 2 Kakkodu quarry GPS 76°49'7" E 8° 45'53" N

Geology: Incipient charnockite + leptynite + khondalite

Stay at Kottarakkara at Hotel High Lands

22-11-2016 Day 2

6:00 AM: Visit to Kottarakkara Ganesh temple [optional, this is a traditional Hindu temple and those who visit has to follow the norms of the temple]

Check out and start from hotel: 08:30 AM

09:30 AM; Stop 1 – Kottavattom GPS -76° 52' 42" E 9° 00' 24" N

Geology: Incipient charnockite + leptynite

Lunch on the way, long drive

03:30 PM: Stop 2 Kovalam GPS- 76° 58' 44" E 08° 24' 03" N

Geology. Massive charnockite

Safety information

All quarries are working and please be aware of hazards including – depressions, rough and narrow roads without side walls, deep valleys, slippery ground etc. Please do not attempt to climb the rock cliff, and please always move as a group.

Part 1 - Introduction to the geology of the Southern Granulite Terrane, India

The Southern Granulite Terrane (SGT) is a collage of crustal blocks to the south of the Archean Dharwar Craton. These blocks were joined together at various geological times from Mesoarchean to latest Neoproterozoic–Cambrian (Santosh et al., 2015; Collins et al., 2014; Santosh et al., 2009) and exposes mid and lower levels of continental crust. These tectonic blocks (Coorg, Nilgiri, Salem, Madurai, Trivandrum and Nagercoil Blocks) are dissected by crustal scale shear zones (Drury and Holt, 1980; Nutman et al., 1992; Peucat et al., 1993, 2013; Harris et al., 1994; Chetty et al., 2003; Bhaskar Rao et al., 2003, 2008; Ghosh et al., 2004; Tomson et al., 2006; Santosh et al., 1992, 2003, 2009, 2012, 2013b; 2015; Clark et al., 2009a; Collins et al., 2014). Major shear/suture zones in the SGT are the Mercara Shear Zone, Moyar Shear Zone (MBSZ), Palghat-Cauvery Shear Zone (PCSZ) and Achankovil Shear Zone (ACSZ) Santosh et al., 2009a; Sajeev et al., 2009; Rajaram and Anand, 2014; Collins et al., 2014). The detail of the Blocks is given below.

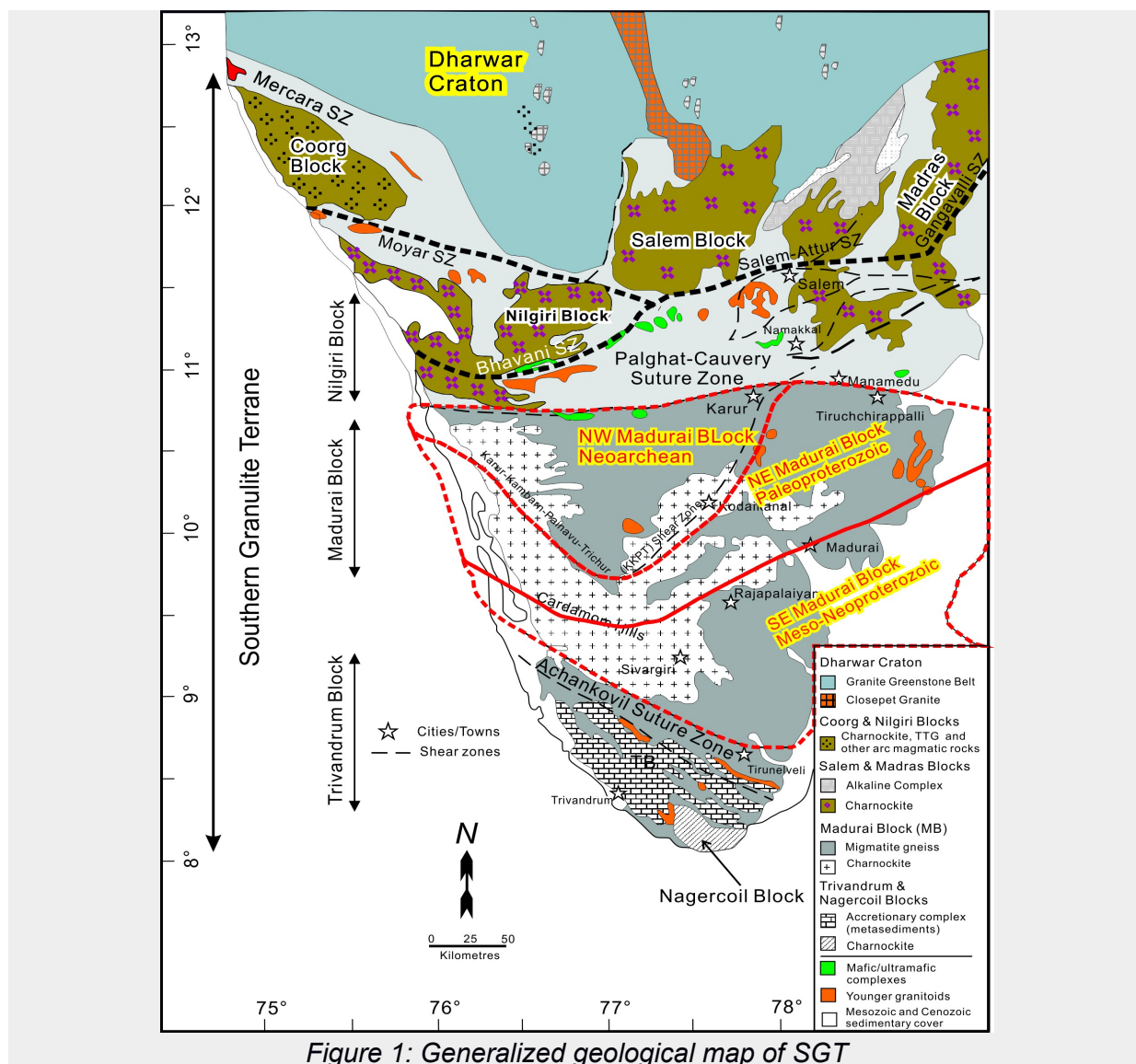


Figure 1: Generalized geological map of SGT

Nagercoil Block

The southern tip of the SGT is represented by the Nagercoil Block. The dominant rock types in this Block are massive charnockite, metapelites and calc silicates. The rocks have experienced high grade metamorphism which occurred firstly at 1.8 Ga and secondly at 500–550Ma (Santosh 1996; Santosh et al., 2003; Kroner et al., 2015). Age spectra of zircons and monazites from the charnockites are similar to those from meta-sedimentary gneisses of the Trivandrum Block suggesting that they lie in the same tectonic unit (Santosh et al., 2006). U–Pb zircon data from the charnockites also demonstrate that they have protolith ages similar to the Paleoproterozoic protoliths reported from the old charnockites in the Trivandrum Block (Ghosh et al., 2004; Kroner et al., 2012) consistent with Nd model ages of 2.2-2.6 Ga obtained by Cenki et al. (2004).

Trivandrum Block

The Trivandrum Block (also known as Kerala Khondalite Belt) is one of the largest supracrustal sequences occupying the major part of the southernmost segment in the SGT. The Achankovil shear zone separates the Madurai Block from the Trivandrum Block. The Trivandrum Block is dominated by metasedimentary gneisses that include garnet bearing felsic gneisses (leptynites) and garnet-cordierite-sillimanite gneisses (khondalites). The latter gave the name the 'Kerala Khondalite Belt' for the Block (Chacko et al., 1987). Collins et al. (2007) showed that the protolith to many of the metasedimentary gneisses in the Trivandrum Block were sourced from Paleoproterozoic and Neoproterozoic rocks and that the rocks were deposited some time after c.1900 Ma. Kroner et al. (2012, 2015) suggested the presence of Paleoproterozoic igneous protoliths for the charnockites in the northern Trivandrum Block and these may be the source of some of the detrital metasedimentary grains. Potential sources of the Paleoproterozoic zircons and monazites are rare in peninsular India north of the Southern Granulite Terrain. Collins et al. (2007) pointed out the similarity to Paleoproterozoic sedimentary rocks in Central Madagascar and suggested that they both were sourced from the same east African rocks (Collins et al., 2003)

Madurai Block

The Madurai Granulite Block occurs immediately south of the PCSZ and north of ACSZ. This is the largest crustal block of SGT and comprises dominantly of charnockite massifs intercalated with tonalitic/granodioritic gneisses, metasedimentary rocks including quartzites, metamorphosed carbonates, iron formations and pelites. The Karur-Kambam-Painavu-Trissur (KKPT) Shear Zone runs within the Madurai Block (MB). The MB can be lithologically divided into a western region and an eastern region; Madurai Block in Kerala (MBK) and Madurai Block in Tamil Nadu (MBTN). The MBK is characterized by two different groups of hornblende-biotite and orthopyroxene-biotite (charnockite) gneisses, one being quartz rich and the other feldspar rich. The eastern part, MBTN is composed of massive charnockites, quartzites and calc silicate series of rocks.

The northwest of the Madurai Block is composed of charnockite massifs with Sm-Nd and Rb-Sr whole rock model ages in the range of 2200-3170 Ma (Bartlett et al., 1998). U-Pb zircon ages from charnockites in this north-west Madurai Block have yielded a consistent range of crystallization ages between 2.55 and 2.50 Ga (Brandt et al., 2011; Ghosh., 2004; Plavsa et al., 2012). These charnockites are well exposed in the Kodaikanal massif where they structurally underlie metasedimentary gneisses that dominate the southern and eastern Madurai Block. Metasedimentary enclaves occurring within the charnockites contain detrital zircons with 2.5 Ga age (Brandt et al., 2011)

Salem Block

The Salem Block is composed of orthogneisses and charnockitic equivalents, with some minor mafic granulite and metasedimentary rocks. Large charnockitic massifs occur at the north of the Salem Block. They are surrounded by granitic orthogneisses and para gneisses that have experienced amphibolite to granulite grade metamorphism (Anderson et al., 2012; Clark et al., 2009b; Ghosh et al., 2004; Janardhan et al., 1982; Sato et al., 2011a). It is suggested that these northern granulites are the metamorphosed equivalents of the Dharwar Craton without distinct lithological or tectonic contact between the two (Fermor 1936; Harlov 2007; Janardhan et al., 1982; Mojzsis et al., 2003). The isotopic studies of the Salem Block protoliths show Mesoarchaeon to Neoproterozoic rocks that stretch far south of the Palghat Cauvery Shear Zone (PCSZ) (Bartlett et al., 1998; Bhaskar Rao et al., 2003; Friend and Nutman 1992; Ghosh et al., 2004). The ages as young as ~2.5 Ga has been obtained from rocks in the Nilgiri hills and in the southern part of the Salem Block (Bartlett et al., 1998; Tomson et al., 2006). Cryogenian alkali plutons cut the northeast Madurai Block and have been dated as 755 Ma (Miyazaki et al., 2000). The Salem Block was metamorphosed to granulite facies in the late Archean to early Proterozoic (Anderson et al., 2012; Clark et al., 2009b; Peucat et al., 1993; Sato et al., 2011a) and was subsequently deformed along the Salem-Attur shear zone (Chetty 1996; Chetty and Bhaskar Rao, 1998; Anderson et al., 2012). Some of the oldest high pressure metamorphic conditions have been reported from the Salem Block (14-16 kbar and 820-8600 C at ~2490 Ma) at Kanjamalai near Salem. Salem-Attur shear zone is the eastern continuation of Moyar-Bhavani shear zone. Sithampundi layered ultramafic complex (Subramaniam, 1956) lies within the southern Salem Block and dates back to the Mesoarchaeon. It also experienced the ~2.5 Ga metamorphism (Bhaskar Rao et al., 1996) similar to that of Kanjamalai (Anderson et al., 2012) and contains extremely rare omphacite inclusions in garnet that suggest extreme metamorphic conditions of ~20 kbar and 1020°C (Sajeev et al., 2009).

Nilgiri Block

The Nilgiri Block marks the meeting point of two mountain ranges in southern Peninsular India – the Eastern and Western Ghats. The northern boundary of the Nilgiri Block is flanked by the Archean Dharwar Craton, south by the Madurai Block and in the east with Biligirirangan, Shevroy and Salem Blocks. The Nilgiri hills represent a triangular prism of crustal block uplifted up to 2500 m above sea level. It has its base at

the western part and apex at the east, with the longest side along the southern boundary. This block is bordered by two major shear zones: the Moyar shear zone to the north and the Bhavani shear zone to the south (Srikantappa, 1996; Raith et al., 1999). Both these shear zones converge at the eastern tip of the Nilgiri Block and extend to the east as the Salem-Attur shear zone (Bhaskar Rao et al., 1991, 2003; Harris et al., 1994; Chetty et al., 2003; Ghosh et al., 2004).

Coorg Block

The Coorg Block is bound on the north by the Mercara Shear Zone and the south by the WNW-ESE trending Bavali-Moyar Shear Zone (BMSZ) (Chetty et al., 2012, Santosh et al., 2015). The Mercara Shear Zone welds the Coorg Block with the Dharwar Craton to the north and is marked by steep gravity gradients (Sunil et al., 2010) which suggest the presence of underplated high-density slab in the lower crust. Previous studies considered the Coorg Block as the higher grade southern extension of the Western Dharwar Craton, with its continuity into the Biligirirangan Hills. The Coorg–Nilgiri–Biligirirangan–Salem–Madras Blocks were previously grouped together, and considered to have witnessed a common granulite facies metamorphism (ca. 2500 Ma) (Raith et al., 1990, 1999; Janardhan et al., 1994, 1996; Devaraju and Janardhan, 2004; Bernard-Griffiths et al., 1987; Peucat et al., 1993; Bhaskar Rao et al., 1992, 2003; Santosh et al., 2003; Ghosh et al., 2004; Clark et al., 2009; Sato et al., 2011b). However, Santosh et al. (2015) reports that the Coorg is an exceptional block within the Southern Granulite Terrain without any signature of the 2.5 Ga regional metamorphism that affected all the other blocks in this region. The geochronological data (Santosh et al., 2015, 2016) have shown that this block has an exotic entity within the dominantly Mesoarchean to Neoarchean collage in the northern domain of the SGT. Rocks belonging to WDC are particularly well exposed in the Coorg region and in the Biligirirangan and Mahadeswara ranges. The zircon in the rock samples from the western flank of Biligirirangan and the northern part of the Coorg massif yield Mesoarchean crystallisation ages ≥ 3.3 Ga, with the oldest concordant zircons at 3.39 and 3.38 Ga (Vijaya Kumar et al., 2013). These samples are the oldest yet studied from the SGT. Hf(t) for the Mesoarchean zircon ranges between -5 and $+4$, while Hf-depleted mantle model ages range between 3.35 and 3.70 Ga, pointing to Mesoarchean juvenile magmatism and involvement of Neoarchean crustal components in the generation of charnockite protoliths.

Field trip localities

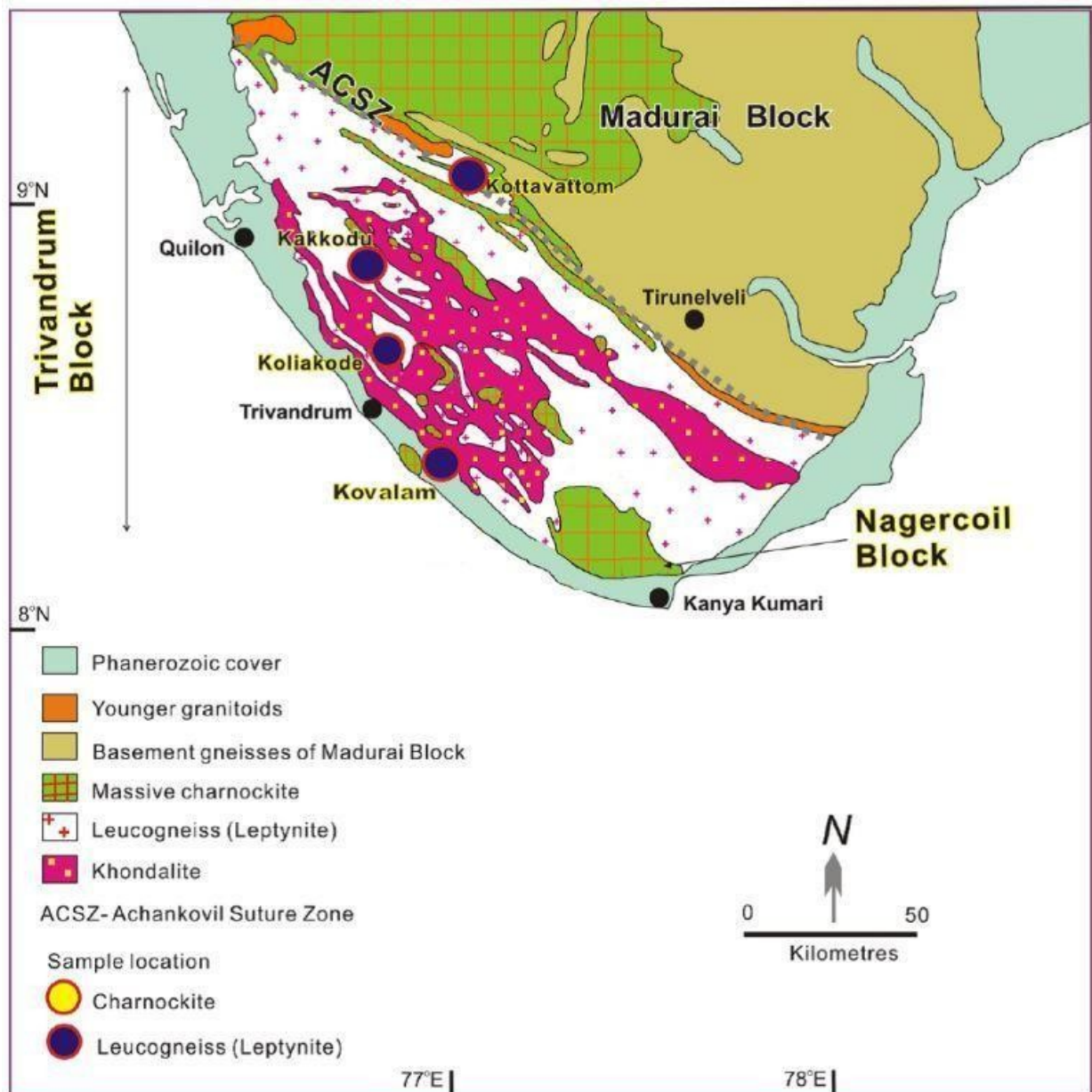


Figure 2: Location Map

Day 1: Monday 21nd of November, Trivandrum Block

Locality 1 –Koliakodu Quarry GPS - 76° 53'27" E 8° 38'21" N

Geology: Typical khondalite (grt-sill-crd-bio-gneiss) (Trivandrum Block)

At Koliakodu, a large active quarry provides fresh exposures of granulite-facies metapelites. The rocks predominantly comprise garnet–sillimanite–spinel– cordierite-bearing metapelites that occur as bands of varying width ranging from a few centimetres to more than 2 meters intercalated within garnet- and biotite-bearing felsic

gneisses. They are deformed into tight isoclinal folds and rootless intrafolial folds. Cordierite occurs along the compositional layers and also as large purple/blue crystals. Graphite occurs in a variety of associations in this locality. Thin flakes and fine disseminated graphite within the metapelite bands represent the conversion of biogenic material trapped within host sediments during high-grade metamorphism as indicated by their carbon isotope composition (Santosh and Wada, 1993). Coarse flakes and flaky aggregates of graphite occurring with patches, veins and late shears/fractures have isotopic compositions characterized by enrichment in heavier carbon indicating precipitation from magmatically derived CO₂-rich fluids (Santosh and Wada, 1993). The Koliakodu quarry preserves quartzite bands and metapelites without any melt signature. These features, abundance of sillimanite and cordierite are good indicators of sedimentary protolith.

The most common assemblage of the Koliakodu metapelite is Grt+Sil+Crd+Spl+Kfs+Bt+Qtz+Pl with accessory zircon and monazite. Aluminous melanosomes are characterized by the assemblage Grt+Sil+Crd+Bt+Kfs±Spl±Ilm±Gr, and alternate with felsic leucosomes containing mostly Kfs+Qtz+Bt+Pl. Zircon (100–250 μm) and monazite (up to 300 μm) occur mostly as inclusions within garnet and cordierite. Plagioclase and K-feldspar also sometimes carry zircon and monazite inclusions. Rarely, zircon and monazite also form inclusions within spinel and sillimanite. The K-feldspar is often mesoperthitic showing coarse exsolution lamellae of plagioclase. Some of the retrogressed assemblages also contain graphite as disseminations along foliation planes. Magnetite, ilmenite, zircon and monazite are ubiquitously present as accessories. The rocks exhibit various reaction textures including $Bt + Sil + Qz = Grt + Crd \pm Kfs$, $Grt + Sil + Qz = Crd$, $Grt + Crd + Sil = Spl + Qz$, $Spl + Qz = Crd$, and $Grt + Sil = Spl + Crd$.



Figure 3: Porphyroblasts of cordierite and garnet from Koliakodu Quarry (Kroner et al. 2015)

Locality 2 – Kakkodu quarry GPS 76° 49'7" E 8° 45'53" N

This is an oval shaped quarry located in the northern end of Trivandrum district. Several working quarries are located in the area. The dominant rock type within the quarry at Kakkod is pale-grey garnet–biotite gneiss. The gneiss has a centimeter-scale gneissic foliation defined by biotite with numerous pink garnet porphyroblasts. Garnet occurs mainly within 5–10 mm wide leucosome veins that are parallel to the regional foliation, as well as within larger leucogranite sheets that vary from 5 cm to 3 m in thickness. The leucogranite is coarser grained than the garnet–biotite gneiss and lacks biotite. The garnet in the leucogranite sheets typically occurs as grain aggregates 1–2 cm across and, less commonly, as large euhedral to subhedral grains 1.0–1.5 cm across. At the western end of the quarry a layer of migmatitic garnet–sillimanite–cordierite gneiss (metapelitic gneiss) is exposed. No direct contact between the garnet–biotite gneiss and the metapelitic gneiss is exposed. The two rock types are always separated by a thin (5–10 cm) garnet-bearing leucogranite sheet that is similar in mineralogy to the leucogranite described above. A number of small dykes (~10–12 cm wide) of undeformed coarse grained monazite- and biotite-bearing but garnet-absent pegmatite crosscut the foliation within the garnet–biotite gneiss. Incipient charnockites at Kakkod are characterized by the occurrence of diffuse, irregular dark patches that occur exclusively within the garnet–biotite gneiss. These patches comprise orthopyroxene-bearing quartzo-feldspathic granofels ranging from 50 cm to 2 m across and have no clear preferred orientation. A 2–5 cm transition zone between the garnet–biotite gneiss and the charnockite is characterized by a decrease in the abundance of biotite and a gradual change in colour into the darker green charnockite. Incipient charnockites rarely crosscut the leucogranite, although charnockite patches occur commonly at the margins of some of the larger leucogranite bodies.

Blereau et al. (2016) conducted a detailed study in the quarry and established that phase relationships in all three rock types at Kakkod (garnet–biotite gneiss, charnockite, and metapelitic gneiss) are consistent with peak metamorphic conditions of c. 830–925 °C and 6–9 kbar. Peak metamorphism was followed by high-T decompression best recorded by retrograde growth of cordierite and/or biotite in the metapelitic gneiss. The onset of high-grade metamorphism is dated at c. 590 Ma with melt crystallization starting at c. 540 Ma. The majority of zircon grew at 540– 510 Ma, which is taken as when most of the melt at Kakkod crystallized. Orthopyroxene-bearing charnockite assemblages replaced local patches of the garnet–biotite gneiss at or soon after peak metamorphism. They must reflect local compositional heterogeneities in the garnet–biotite gneiss, although we cannot determine if these heterogeneities were inherited from the protolith or introduced by high-T fluid influx. Five P–T–X sections highlight the sensitivity of orthopyroxene stability in metafelsic rocks to the local oxidation state, but this does not seem to have been the controlling factor in charnockite formation at Kakkod.

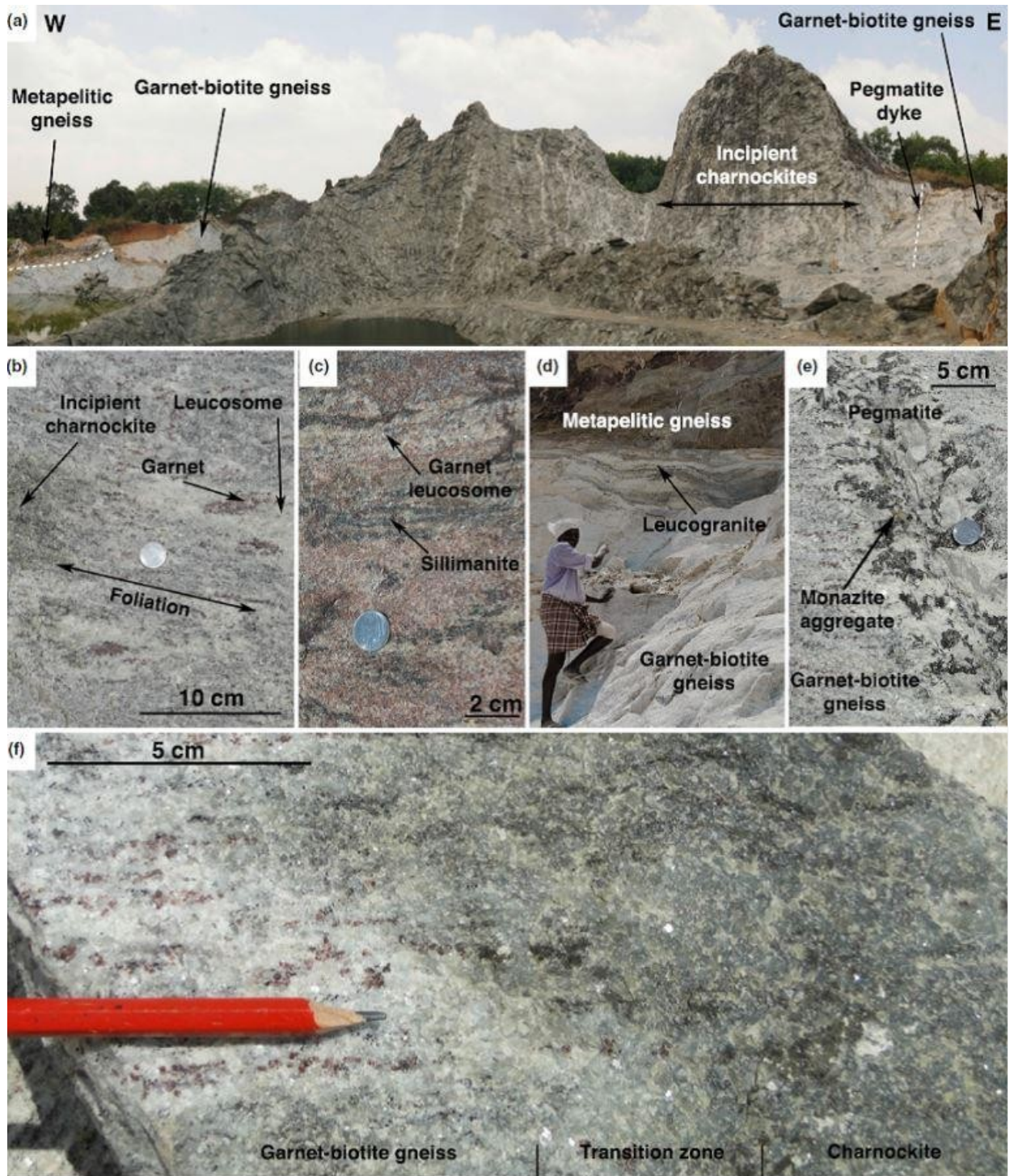


Figure 4: Rock types from Kakkodu quarry (after Blereau et al., 2016)

Lower temperature fluid influx at c. 525–490 Ma led to coupled dissolution–reprecipitation of monazite and variable resetting of its U–Pb isotope system. Based on comparisons with monazite textures in experiments, we follow Taylor et al. (2014) in suggesting that these fluids were aqueous and perhaps rich in alkalis. The presence of coupled dissolution–reprecipitation textures in monazite from all samples at Kakkod indicates that late fluid flux was pervasive throughout the outcrop. It is likely to have driven hydrous retrogression of the charnockite, but played no role in its stabilization. The timing of monazite modification at Kakkod is very close to final melt crystallization

ages from this and other localities. This suggests that fluid influx was linked to cooling and solidification of local (and possibly deeper) melt systems, and could be related to the pegmatite dyke at Kakkod with a crystallization age of c. 512 Ma.

Locality 3 – Kottavattom

The quarry at Kottavattom lies in the northern part of the Trivandrum Block, close to the boundary with the Achankovil Zone. The dominant lithology at the quarry is garnet-biotite gneiss that contains garnet-bearing, quartzo-feldspathic leucosomes aligned with the gneissic foliation. Overprinting the gneissic fabric and leucosomes are metre-scale garnet-amphibole-bearing patches with dark green feldspars that create a marked colour contrast against the light-grey gneiss. Previous studies at this and other localities have identified these patches as containing orthopyroxene with varying degrees of hydrous alteration (Pichamuthu 1953; Raith and Srikantappa 1993; Endo et al. 2012), resulting in these zones being referred to as charnockite. It is likely that the amphibole in the sample studied here was originally orthopyroxene making it a granulite facies mineral assemblage, but it will be referred to here as garnet-amphibole patch to maintain consistency with its current mineral content. Garnet amphibole patches are particularly common within certain horizons of the garnet-biotite gneiss, but in other parts of the quarry the patches occur along two perpendicular orientations, each at approximately 45° to the orientation of the metamorphic fabric. These field relationships have been used to infer structural control over patch formation (Raith and Srikantappa 1993), but this pattern is not seen in all parts of the quarry and no brittle deformation structures have been identified within the garnet-amphibole patches.

The dominant lithology at the quarry is garnet-biotite gneiss that contains garnet-bearing, quartzo-feldspathic leucosomes aligned with the gneissic foliation. Overprinting the gneissic fabric and leucosomes are metre-scale garnet-amphibole-bearing patches with dark green feldspars that create a marked colour contrast against the light-grey gneiss. The Kottavattam quarry exposes fairly homogeneous, light-coloured garnet-biotite gneiss of granitic composition (the regional leptynites). Garnet is present predominantly within the granitic leucosomes, which are aligned within the gneissic foliation. This suggests that partial melting in these rocks was synchronous with deformation and was most likely related to biotite dehydration-melting at near-peak metamorphic conditions.

On the fresh faces of the quarry, a spectacular regular pattern of charnockite development is most striking due to the marked colour contrast between the light-grey leptynitic gneiss and the dark-brown charnockite. Gneiss 'horizons' with a dense network of more or less continuous charnockite zones following a set of planes which intersect at almost right angles as well as the foliation plane, alternate with zones where only a few randomly distributed charnockite patches are developed. The structural control of localized charnockite development is obvious. Its spatial variation in intensity cannot be related to variations in bulk composition, since the gneiss is homogeneous within the scale of the outcrop. There is no indication of localized ductile shear deformation preceding or accompanying the process of charnockitization. This

suggests that the planar charnockite network developed along a system of conjugate fractures, when the gneiss unit attained semi-brittle to brittle behavior (Raith and Srikantappa, 1993). In the charnockite zones (generally 10-15 cm wide), the foliation and migmatitic structure of the gneisses is completely obliterated due to thorough recrystallization and considerable grain-size coarsening. Generally, the unaltered gneiss is separated from the orthopyroxene-bearing charnockite by a 2-3-cm-wide transition zone in which biotite has disappeared but garnet remains. In the central part of the charnockite zone, however, garnet is mostly absent.

Zircon in the garnet-biotite gneiss sample has a variety of morphologies and ranges in size up to 500 μm in the longest dimension. Cathodoluminescence (CL) images of zircons from this sample display a variety of textures. The majority of grains have a low CL response with very few internal features and weak zonation. Other grains have cores with a bright CL response and typically elongate morphologies, and in most cases, these latter grains display oscillatory zoning, or simple, broad zonation with a high CL response. Some core material has low CL response rims that slightly truncate the original zoning, whilst a small number of cores show strong resorption textures with crosscutting embayment textures with low CL response. In most cases, these low CL response zones crosscut the pre-existing zoning showing sharp boundaries with the original grain texture. Bright CL cores gave predominantly discordant results, with the oldest $^{207}\text{Pb}/^{206}\text{Pb}$ spot age being $1,994 \pm 9$ Ma. Ten zircon rims from the garnet biotite gneiss show a younger group giving a concordia age of 523.1 ± 7.0 Ma.

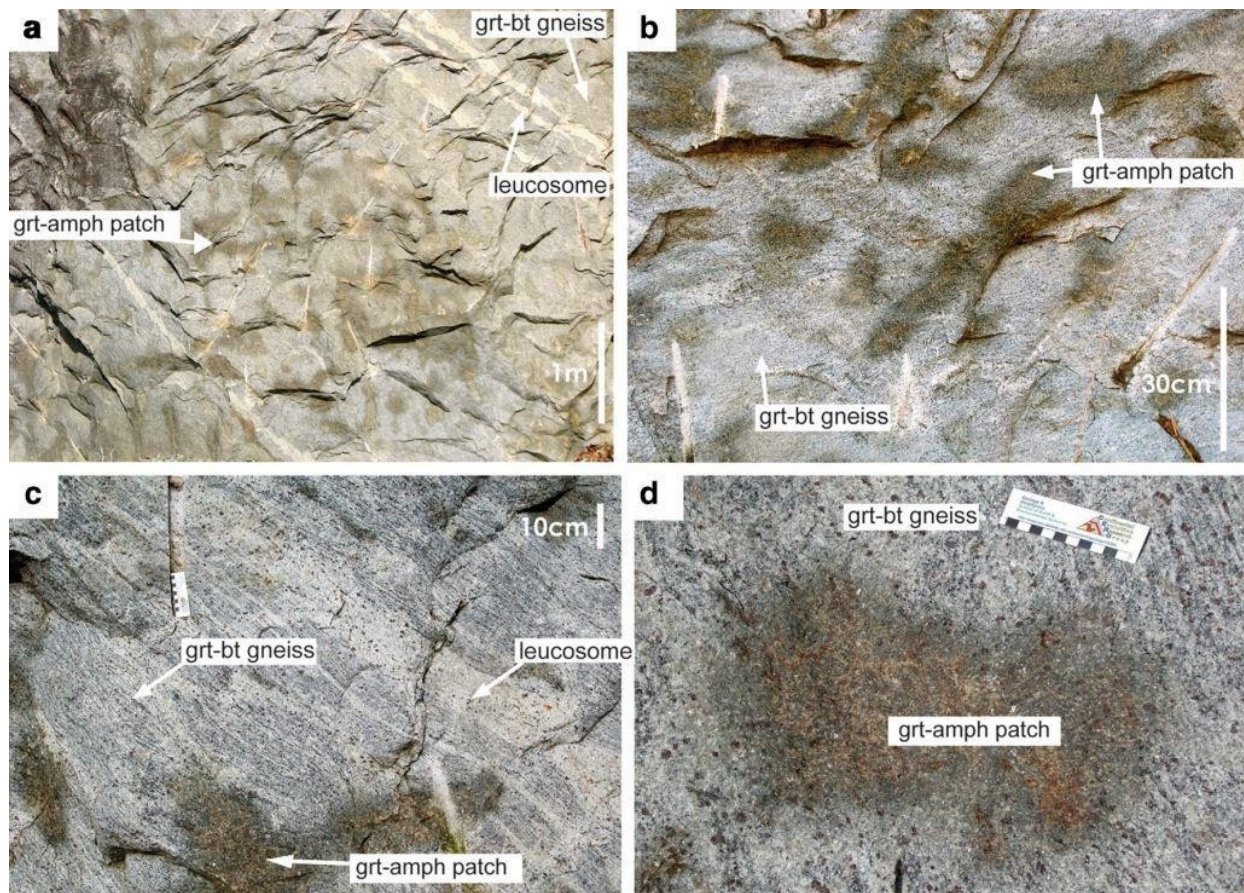


Figure 5: Field photographs showing patches of dark green/brown garnet-amphibole incipient charnockite within pale grey granitic gneiss at various scales (after Taylor et al. 2014)

U–Pb analyses of monazite from the garnet-biotite gneiss covered a large variety of the textures revealed by BSE imaging. The darker BSE cores give the oldest ages, $^{206}\text{Pb}/^{238}\text{U}$ spot ages from 608 ± 17 to 520 ± 10 Ma, whilst the rims show a younger range with $^{206}\text{Pb}/^{238}\text{U}$ spot ages from 535 ± 10 to 472 ± 10 Ma. Core analyses, with Th/U ratios < 49 , form a population with a concordia age of 587.5 ± 9.5 Ma. The most extreme Th/U ratios give the youngest spot ages, and a single population was obtained from the monazite analyses with Th/U > 95 and gave a concordia age of 496.9 ± 3.4 Ma (Taylor et al., 2014).

Garnet-amphibole patches in Kotavattam were subjected to U–Pb analyses on zircon grains. The overall results are very similar to those from the garnet-biotite gneiss with core analyses showing varying degrees of discordance, and the oldest $^{207}\text{Pb}/^{206}\text{Pb}$ spot age being 2088 ± 96 Ma. The full range of U–Pb ages from individual zircon rims ranges from 563 ± 10 to 499 ± 6 Ma. Monazite U–Pb analyses for the garnet-amphibole patch give the oldest ages from 606 ± 11 to 567 ± 10 Ma (Taylor et al. 2014).

Locality 4–Kovalam GPS- $76^{\circ} 58' 44''$ E $08^{\circ} 24' 03''$ N

At Kovalam, in and around the beach, medium- to coarse-grained greenish-grey charnockite can be observed. It is comprised of a granoblastic assemblage of orthopyroxene–garnet–perthitic K-feldspar-plagioclase-quartz with accessory biotite and Fe–Ti oxides. Apatite and zircon occur as accessory minerals. The charnockite shows a massive, magmatic texture, overprinted by a weak metamorphic foliation defined by the preferred alignment of garnet and biotite. The charnockite locally incorporates enclaves of granodiorite. The charnockite is distinctly different from the ‘incipient charnockites’ that were visited at Kottavattom. The charnockite is similar to the massive-type charnockites within the Madurai Block to the north and the Nagercoil Block to the south.

Zircon populations are indistinguishable from the Nagercoil charnockites. Magmatic zoning is common in the large and well-rounded zircon crystals (and so is thin metamorphic overgrowth on the magmatic grains). Seven grains were analyzed of which four define a near-concordant array with a mean $^{207}\text{Pb}/^{206}\text{Pb}$ age of 2074.9 ± 1.3 Ma. The three discordant analyses are well aligned, and all data define a discordia line with a lower Concordia intercept at 506 ± 240 Ma, indicating Pan-African Pb-loss and or recrystallization as in all previous samples. The analysis of one metamorphic rim yielded a concordant $^{206}\text{Pb}/^{238}\text{U}$ age of 561 ± 8 Ma, more precisely defining zircon growth near the peak of granulite-facies metamorphism (Kroner et al. 2014).

Hf isotopic analysis from charnockite sample from the Kovalam quarry yields strongly variable but positive $\epsilon\text{Hf}(t)$ values for an age of 2075 Ma, ranging from $+0.4$ to $+6.1$ and corresponding to Hfc model ages of 2.27 to 2.57 Ga.

References

- Anderson, J. R., Payne, J. L., Kelsey, D. E., Hand, M., Collins, A. S., & Santosh, M. (2012) High-pressure granulites at the dawn of the Proterozoic. *Geology*, 40(5): 431-434.
- Bartlett, J. M., Dougherty-Page, J. S., Harris, N. B., Hawkesworth, C. J. and Santosh, M., (1998) The application of single zircon evaporation and model Nd ages to the interpretation of polymetamorphic terrains: an example from the Proterozoic mobile belt of south India. *Contributions to Mineralogy and Petrology*, 131(2-3): 181-195.
- Berman, R. G. and Bostock, H. H. (1997) Metamorphism in the northern Taltson Magmatic Zone, Northwest Territories. *Canadian Mineralogist*, 35:1069-1091.
- Bernard-Griffiths, J., Jahn, B.-M., Sen, S. (1987) Sm–Nd isotopes and REE geochemistry of Madras granulites, India: an introductory statement. *Precambrian Research*, 37: 343-355.
- Bhaskar Rao, Y.J., Griffin, W.L., Ketchum, J., Pearson, N.J., Beyer, E. and O'Reilly, S.Y. (2008) An outline of juvenile crust formation and recycling history in the Archaean western Dharwar craton, from zircon in situ U–Pb dating and Hf-isotopic compositions. Abstract, Goldschmidt Conference 2008. *Geochimica Cosmochimica Acta*, 72: A81.
- Bhaskar Rao, Y.J., Janardhan, A.S., Kumar, T.V., Narayana, B.L., Dayal, A.M., Taylor, P.N. and Chetty, T.R.K. (2003) Sm–Nd model ages and Rb–Sr isotopic systematics of charnockites and gneisses across the Cauvery shear zone, southern India; implications for the Archaean Neoproterozoic terrane boundary in the Southern Granulite Terrain. *Memoir—Geological Society of India*, 50: 297-317.
- Bhaskar Rao, Y.J., Naha, K., Srinivasan, R. and Gopalan, K. (1991) Geology, geochemistry and geochronology of the Archaean Peninsular gneiss around Gorur, Hassan district, Karnataka, India. *Proceedings of the Indian Academy of Sciences-Earth and Planetary Sciences*, 100(4): 399-412.
- Bhaskar Rao, Y.J., Sivaraman, T.V., Pantulu, G.V.C., Gopalan, K. and Naqvi, S.M. (1992) Rb–Sr ages of Late Archean meta volcanics and granites, Dharwar Craton, South India and evidence for Early Proterozoic Thermo tectonic events. *Precambrian Research*, 59: 145-170.
- Blereau, E., et al. Constraints on the timing and conditions of high-grade metamorphism, charnockite formation and fluid–rock interaction in the Trivandrum Block, southern India. *Journal of Metamorphic Geology* (2016).
- Brandt, S., Raith, M. M., Schenk, V., Sengupta, P., Srikantappa, C. and Gerdes, A. (2014) Crustal evolution of the Southern Granulite Terrane, south India: New geochronological and geochemical data for felsic orthogneisses and granites. *Precambrian Research*, 246: 91-122.
- Brandt, S., Schenk, V., Raith, M. M., Appel, P., Gerdes, A., and Srikantappa, C. (2011) Late Neoproterozoic PT evolution of HP-UHT granulites from the Palni Hills (South India): New constraints from phase diagram modelling, LA-ICP-MS zircon dating and in-situ EMP monazite dating. *Journal of Petrology*, 52(9): 1813-1856.
- Cenki, B., Braun, I. and Brocker, M. (2004) Evolution of the continental crust in the Kerala Khondalite Belt, southernmost India: evidence from Nd isotope mapping, U–Pb and Rb–Sr geochronology. *Precambrian Research*, 134(3): 275-292.
- Chacko, T., Ravindra Kumar, G.R. and Newton, R.C. (1987) Metamorphic P–T conditions of the Kerala (South India) Khondalite Belt, a granulite facies supracrustal terrain. *Journal of Geology*, 95: 343-358.
- Chetty, T. R. K. (1996). Proterozoic shear zones in southern granulite terrain, India. *The Archaean and Proterozoic Terrains in Southern India within East Gondwana*, 3: 77-89.
- Chetty, T. R. K. and Rao, Y. B. (1998) Behaviour of stretching lineations in the Salem-Attur shear belt, southern granulite terrane, South India. *Geological Society of India*, 52(4): 443-448.
- Chetty, T. R. K. and Rao, Y. B. (2006) The Cauvery shear zone, Southern Granulite Terrain, India: a crustal-scale flower structure. *Gondwana Research*, 10(1): 77-85.

- Chetty, T. R. K., Vijay, P., Narayana, B. L., and Giridhar, G.V. (2003) Structure of the Nagavali shear zone, Eastern Ghats Mobile Belt, India: correlation in the East Gondwana reconstruction. *Gondwana Research*, 6(2): 215-229.
- Chetty, T.R.K., Mohanty, D.P. and Yellappa, T. (2012) Mapping of shear zones in the Western Ghats, Southwestern part of Dharwar Craton. *Journal of the Geological Society of India*, 79: 151-154.
- Clark, C., Collins, A. S., Santosh, M., Taylor, R. and Wade, B. P. (2009a) The PT architecture of a Gondwana suture: REE, U–Pb and Ti-in-zircon thermometric constraints from the Palghat Cauvery shear system, South India. *Precambrian Research*, 174(1):129-144.
- Clark, C., Collins, A.S., Kinny, P.D., Timms, N.E. and Chetty, T.R.K. (2009b) SHRIMP U–Pb age constraints on charnockite magmatism and high grade metamorphism in the Salem Block, Southern India. *Gondwana Res*, 16: 27-36.
- Clark, C., Santosh, M., Taylor, R., Fitzsimons, I., Nandakumar, V. and Shaji, E. (2013) Granulites and Granulites 2013 – Field guide to the charnockites, khondalites and leptynotes of the Kerala Khondalite Belt, Southern Granulite Terrane, India, 21–26 January 2013. Curtin University, Perth, Australia, 63.
- Collins, A. S., Fitzsimons, I. C., Hulscher, B. and Razakamanana, T. (2003a) Structure of the eastern margin of the East African Orogen in central Madagascar. *Precambrian Research*, 123(2): 111-133.
- Collins, A. S., Johnson, S., Fitzsimons, I. C., Powell, C. M., Hulscher, B., Abello, J. and Razakamanana, T. (2003b) Neoproterozoic deformation in central Madagascar: a structural section through part of the East African Orogen. *Geological Society, London, Special Publications*, 206(1): 363-379.
- Collins, A. S., Santosh, M., Braun, I. and Clark, C. (2007) Age and sedimentary provenance of the Southern Granulites, South India: U-Th-Pb SHRIMP secondary ion mass spectrometry. *Precambrian Research*, 155(1): 125-138.
- Collins, A.S., Clark, C. and Plavsa, D. (2014) Peninsular India in Gondwana: the tectonothermal evolution of the Southern Granulite Terrain and its Gondwana counterparts. *Gondwana Research*, 25(1): 190-203.
- Devaraju, J. and Janardhan, A.S. (2004) Metamorphic history of staurolite–kyanite–garnet–cordierite-bearing pelites of Mangalore-Mercara lineament, South India. *Journal of the Geological Society of India* 63: 555-561.
- Drury, S.A., Holt, R.W., (1980) The tectonic framework of South Indian craton: a reconnaissance involving Landsat imagery. *Tectonophysics* 65, T1–T15.
- Endo, T., Tsunogae, T., Santosh, M. and Shaji, E. (2012) Phase equilibrium modeling of incipient charnockite formation in NCKFMASHTO and MnNCKFMASHTO systems: a case study from Rajapalayam, Madurai Block, Southern India. *Geoscience Frontiers*, 3(6), 801-811.
- Endo, T., Tsunogae, T., Santosh, M., Shimizu, H. and Shaji, E. (2013) Granulite formation in a Gondwana fragment: petrology and mineral equilibrium modeling of incipient charnockite from Mavadi, southern India. *Mineralogy and Petrology*, 107(5): 727-738.
- Friend, C. R. L., & Nutman, A. P., (1992) Response of zircon U– Pb isotopes and whole-rock geochemistry to CO₂ fluid-induced granulite-facies metamorphism, Kabbaldurga, Karnataka, South India. *Contributions to Mineralogy and Petrology*, 111(3): 299-310.
- Friend, C.R.L. (1981) Charnockite and granite formation and influx of CO₂ at Kabbaldurga *Nature*, 294: 550-552.
- Ghosh, J.G. (2004) Age and tectonic evolution of Neoproterozoic ductile shear zones in the Southern Granulite Terrain of India, with implications for Gondwana studies. *Tectonics*, 23P.
- Ghosh, J.G., DeWrr, M.J. and Zartman, R.E. (2004) age and tectonic evolution of Neoproterozoic ductile shear zones in the Southern Granulite Terrain of India, with implications for Gondwana studies. *Tectonics*, 23.
- Harris, N. B. W., Santosh, M. and Taylor, P. N. (1994) Crustal evolution in South India: constraints from Nd isotopes. *The Journal of Geology*: 139-150.
- Janardhan, A.S. Anto, K.F. (1996) Evolution of granulite blocks of Southern India and their relation to the East Gondwana continent. *Journal of African Earth Sciences*, 23: 6-9.

- Janardhan, A.S., Jayanada, M. and Shankara, M. A. (1994) Formation and tectonic evolution of granulites from the Biligirirangan and Nilgiri Hills, S-India-geochemical and isotopic constraints. *Journal of the Geological Society of India*, 44: 27-40.
- Kroner, A., Santosh, M. and Wong, J. (2012) Zircon ages and Hf isotopic systematics reveal vestiges of Mesoproterozoic to Archaean crust within the late Neoproterozoic–Cambrian high-grade terrain of southernmost India. *Gondwana Research*, 21(4): 876-886.
- Kroner, A., Santosh, M., Hegner, E., Shaji, E., Geng, H., Wong, J., Xie, H., Wan, Y., Shang, C.K., Liu, D. and Sun, M. (2015) Palaeoproterozoic ancestry of Pan-African high-grade granitoids in southernmost India: Implications for Gondwana reconstructions. *Gondwana Research*, 27(1): 1-37.
- Kröner, A., Santosh, M., Hegner, E., Shaji, E., Geng, H., Wong, J., and Sun, M. (2015). Palaeoproterozoic ancestry of Pan-African high-grade granitoids in southernmost India: Implications for Gondwana reconstructions. *Gondwana Research*, 27(1), 1-37.
- Kroner, A., Wan, Y., Liu, X and Liu, D. (2014). Dating of zircon from high grade rocks: Which is the most reliable method?. *Geoscience Frontiers*, 5(4), 515-523.
- Miyazaki, T., Kagami, H., Shuto, K., Morikiyo, T., Mohan, V. R., & Rajasekaran, K. C. (2000). Rb-Sr geochronology, Nd-Sr isotopes and whole rock geochemistry of Yelagiri and Sevattur syenites, Tamil Nadu, south India. *Gondwana Research*, 3(1): 39-53.
- Nutman, A. P., Chadwick, B., Ramakrishnan, M. and Viswanatha, M. N. (1992) SHRIMP U-Pb ages of detrital zircon in Sargur supracrustal rocks in western Karnataka, southern India. *Geological Society of India*, 39(5): 367-374.
- Peucat, J. J., Jayananda, M., Chardon, D., Capdevila, R., Fanning, C. M. and Paquette, J. L. (2013) The lower crust of the Dharwar Craton, Southern India: Patchwork of Archean granulitic domains. *Precambrian Research*, 227: 4-28.
- Peucat, J.J., Mahabaleswar, B. and Jayananda, M. (1993) Age of younger tonalitic magmatism and granulitic metamorphism in the South Indian transition zone (Krishnagiri area); comparison with older Peninsular gneisses from the Gorur-Hassan area. *Journal of Metamorphic Geology*, 11(6): 879-888.
- Pichamuthu, C. S. (1953) The charnockite problem. Mysore geologists' association.
- Plavsa, D., Collins, A. S., Foden, J. F., Kropinski, L., Santosh, M., Chetty, T. R. K. and Clark, C. (2012) Delineating crustal domains in Peninsular India: age and chemistry of orthopyroxene-bearing felsic gneisses in the Madurai Block. *Precambrian Research*, 198, 77-93.
- Raith, M. M., Srikantappa, C., Buhl, D. and Kaehler, H. (1999) The Nilgiri enderbites, south India: Nature and age constraints on protolith formation, high grade metamorphism and cooling history, *Precambrian Res*, 98.
- Raith, M., and Srikantappa, C. (1993) Arrested charnockite formation at Kottavattam, southern India. *Journal of Metamorphic Geology* 11.6, 815-832.
- Raith, M., Srikantappa, C., Ashamanjari, K.G. and Spiering, B. (1990) The granulite terrane of the Nilgiri Hills (Southern India): characterization of high-grade metamorphism. In *Granulites and crustal evolution*. Springer Netherlands, 339-365.
- Rajaram, M. and Anand, S. P. (2014) Aeromagnetic signatures of Precambrian shield and suture zones of Peninsular India. *Geo science Frontiers*, 5(1):3-15.
- Rajesh, H. M. (2008) Petrogenesis of two granites from the Nilgiri and Madurai blocks, southwestern India: Implications for charnockite–calc-alkaline granite and charnockite–alkali (A-type) granite link in high-grade terrains. *Precambrian Research*, 162(1): 180-197.
- Rajesh, H. M. and Santosh, M. (1996) Alkaline magmatism in Peninsular India. In: Santosh, M and Yoshida M. (Eds.) *The Archaean and Proterozoic terrains in Southern India within East Gondwana*. Gondwana Res. Group Mem. No.3, Field Sci. Publ., Osaka, pp. 91-115.
- Rajesh, H. M., Santosh, M. and Yoshikura, S. (2011) The Nagercoil charnockite: a magnesian, calcic to calc-alkalic granitoid dehydrated during a granulite-facies metamorphic event. *Journal of Petrology*, 52(2):375-400.
- Rajesh, H.M. (2012) A geochemical perspective on charnockite magmatism in Peninsular India. *Geoscience Frontiers*, 3(6): 773-788.
- Rajesh, H.M. and Santosh, M. (2004) Charnockitic magmatism in southern India. *Journal of Earth System Science*, 113: 565-585.

- Rajesh, H.M. and Santosh, M. (2012) Charnockites and charnockites. *Geoscience Frontiers*, 3: 737 -744.
- Rajesh, H.M., Santosh, M. and Yoshikura, S. (2011) The Nagercoil charnockite: a magnesian, calcic to calc-alkalic granitoid dehydrated during a granulite-facies metamorphic event. *Journal of Petrology*, 52(2): 375-400.
- Sajeev, K., Windley, B. F., Connolly, J. A. D. and Kon, Y. (2009) Retrogressed eclogite (20 kbar, 1020°C) from the Neoproterozoic Palghat–Cauvery suture zone, southern India. *Precambrian Research*, 171(1): 23-36.
- Santosh, M. (1987) Cordierite gneisses of Southern Kerala, India: Evidence from fluid inclusion. *Jour. Geosciences, Osaka City University*, 54: 1-53.
- Santosh, M. (1996) The Trivandrum and Nagercoil granulite blocks. *Gondwana Research Group Memoir*, 3: 243-277.
- Santosh, M. and Collins, A. S. (2003) Gemstone mineralization in the Palghat-Cauvery shear zone system (Karur-Kangayam Belt), southern India. *Gondwana Research*, 6(4): 911-918.
- Santosh, M., and Wada, H. (1993). Microscale isotopic zonation in graphite crystals: Evidence for channelled CO influx in granulites. *Earth and Planetary Science Letters* 119.1 19-26.
- Santosh, M., Collins, A. S., Tamashiro, I., Koshimoto, S., Tsutsumi, Y. and Yokoyama, K. (2006) The timing of ultrahightemperature metamorphism in Southern India: U–Th–Pb electron microprobe ages from zircon and monazite in sapphirinebearinggranulites. *Gondwana Research*, 10(1): 128-155.
- Santosh, M., Harris, N.W., Jackson, D.H. and Matthey, D.P. (1990) Dehydration and incipient charnockite formation: a phase equilibria and fluid inclusion study from South India. *The Journal of Geology*, 915-926.
- Santosh, M., Kagami, H., Yoshida, M. and Nandakumar, V. (1992) Pan-African charnockite formation in East Gondwana: geochronologic (Sm-Nd and Rb-Sr) and petrogenetic constraints. *Indian Geol.Assoc. Bull*, 25:1-10.
- Santosh, M., Liu, D., Shi, Y. and Liu, S.J. (2013) Paleoproterozoic accretionary orogenesis in the North China Craton: A SHRIMP zircon study. *Precambrian Research*, 227: 29-54.
- Santosh, M., Liu, S. J., Tsunogae, T. and Li, J. H. (2012) Paleoproterozoic ultrahigh-temperature granulites in the North China Craton: implications for tectonic models on extreme crustal metamorphism. *Precambrian Research*, 222: 77-106.
- Santosh, M., Maruyama, S. and Sato, K. (2009) Anatomy of a Cambrian suture in Gondwana: Pacific-type orogeny in southern India, *Gondwana Research* 16 :321-341.
- Santosh, M., Tagawa, M., Taguchi, S. and Yoshikura, S. (2003) The Nagercoil Granulite Block, southern India: petrology, fluid inclusions and exhumation history. *Journal of Asian Earth Sciences*, 22(2): 131-155.
- Santosh, M., Tanaka, K., Yokoyama, K. and Collins, A. S. (2005) Late Neoproterozoic-Cambrian felsic magmatism along transcrustal shear zones in southern India: U-Pb electron microprobe ages and implications for the amalgamation of the Gondwana supercontinent. *Gondwana Research*, 8(1): 31-42.
- Santosh, M., Yang Q., Shaji, E., Tsunogae, T., Ram Mohan, M. and Satyanarayanan, M. (2015) An exotic Mesoproterozoic microcontinent: The Coorg Block, southern India. *Gondwana Research*, 27:165-195.
- Santosh, M., Yang, Q. Y., Shaji, E., Mohan, M. R., Tsunogae, T. and Satyanarayanan, M. (2016) Oldest rocks from Peninsular India: evidence for Hadean to Neoproterozoic crustal evolution. *Gondwana Research*, 29(1), 105-135.
- Santosh, M., Yokoyama, K., Bijusekhar, S. and Rogers, J.J.W. (2003) multiple tectonothermal events in the granulitic blocks of southern India revealed from EPMA dating; implications for the history of supercontinent. *Gondwana Res*, 6.
- Sato, K., Santosh, M., Tsunogae, T., Chetty, T. R. K. and Hirata, T. (2011a) Laser ablation ICP mass spectrometry for zircon U-Pb geochronology of metamorphosed granite from the Salem Block: Implication for Neoproterozoic crustal evolution in southern India. *Journal of Mineralogical and Petrological Sciences*, 106(1):1-12.
- Sato, K., Santosh, M., Tsunogae, T., Chetty, T. R. K. and Hirata, T. (2011b) Subduction–accretion–collision history along the Gondwana suture in southern India: a laser ablation ICP-MS study of zircon chronology. *Journal of Asian Earth Sciences*, 40(1): 162-171.

- Srikantappa, C., (1996) The Nilgiri granulites The Archaean and 1990. The granulite terrane of the Nilgiri Hills (Southern Proterozoic terrains of southern India within East-India): characterisation of high-grade metamorphism. In: Gondwana, Santosh, M., Yoshida, M. (Eds.), Gondwana Vielzeuf, D., Vidal, Ph. (Eds.), Granulites and Crustal Evo-Res. Group Memoir, 3: 185-222.
- Subramaniam, A.P. (1956) Mineralogy and petrology of the Sittampundi Complex, Salem district, Madras state, India. Geol. Soc. Am. Bull, 67: 317-390.
- Sunil, P. S., Radhakrishna, M., Kurian, P. J., Murty, B. V. S., Subrahmanyam, C., Nambiar, C. G. and Mohan, S. K. (2010) Crustal structure of the western part of the Southern Granulite Terrain of Indian Peninsular Shield derived from gravity data. Journal of Asian Earth Sciences, 39(6): 551-564.
- Taylor, R.J., Clark, C., Fitzsimons, I.C., Santhosh, M., Hand, M., Evans, N., and Mc Donald, B. (2014) Post-peak, fluid-mediated modification of granulite facies zircon and monazite in the Trivandrum Block, southern India." Contributions to Mineralogy and Petrology 168.2 1-17.
- Tomson, J. K., Rao, Y. B., Kumar, T. V. and Rao, J. M. (2006) Charnockite genesis across the Archaean-Proterozoic terrane boundary in the South Indian Granulite Terrain: Constraints from major-trace element geochemistry and Sr-Nd isotopic systematics. Gondwana Research, 10(1): 115-127.
- Tomson, J.K., Rao, Y.B., Kumar, T.V. and Choudhary, A.K. (2013) Geochemistry and neodymium model ages of Precambrian charnockites, Southern Granulite Terrain, India: constraints on terrain assembly. Precambrian Research, 227: 295-315.
- Vijaya Kumar, T., BhaskarRao, Y.J., Clark, C., Taylor, R., Tomson, J.K., Sreenivas, B., Babu, E. and VijayaGopal, B. (2013) Zircon U-Pb ages and Hf-isotopic compositions of Late Archean charnockites from the BiligiriRangan, Nilgiri, Vythiri and Coorg granulite massifs, the Southern granulite Terrain, S. India: constraints on terrane assembly and charnockite precursors. In: Fitzsimons, I., Clark, C. (Eds.), Granulites & Granulites 2013, Hyderabad, 63.

Abdullah, R., 75
 Agnihotri, D., 131
 Ajayakumar, P., 92
 Akçay, M., 68
 Alessio, B., 88
 Alshamsia, D., 19
 Amal Dev, J., 16
 Amaldev, T., 71
 Ameen, S.M.M., 75, 89
 Anilsharma, K., 161
 Archibald, D., 88
 Arita, K., 126
 Arman, H., 19
 Armistead, S.E., 122
 Arungokul, J., 80
 Asthana, D., 32
 Babu, L., 225
 Baiju, K.R., 71
 Balaram, V., 120
 Balush, S.A., 19
 Balusi, H.W.A., 19
 Bari, Z., 75, 89
 Basak, K., 42
 Bathobakae, B.A., 155
 Berndt, J., 194
 Berzina, A.P., 82
 Berzina, A.N., 82
 Beyarslan, M., 210
 Bhattacharya, S., 30, 56
 Bingöl, A.F., 210
 Blades, M., 88
 Bose, S., 65
 Chandra Das, S., 75, 89
 Chandrakala, K., 170
 Chen, N.H.C., 1
 Cheng, B., 5
 Cheong, H.J., 86
 Chetty, T.R.K., 9, 115
 Clark, C., 128, 142, 149
 Collins, A.S., 88, 172, 142, 204
 Cui, J., 40
 Dev, S.G.D., 148
 Devi, K., 154
 Dey, S., 144
 Dharmapriya, P. L., 56
 Dong, S., 40
 Dong, Y.P., 5, 66
 Durgalakshmi, 219
 Endo, T., 103
 Evans, N., 68
 Fanka, A., 91
 Fitzsimons, I.C.W., 149
 Foden, J., 88
 Foley, S.F., 167
 Frei D., 136
 Galli, A., 56
 Ganai, J.A., 58
 Ganguly, S., 28
 Gimon, V.O., 82
 Gomez-Perez, I., 136
 Goswami, S., 63
 Gümrük, O., 68
 Guo, N., 24
 Gupta, S., 192
 Gupta, S., 65
 Hames, W.E., 20
 Harley SL., 217
 He, D. F., 5
 Hossain, I., 138, 175
 Hossain, Md. Sakawat., 75, 89
 Hussein, S.M., 19
 Indu, G., 134
 Indu, G.K., 37, 124
 Islam Md. Rezaul., 138
 Jahan, H., 75
 Jang, Y., 2
 Jayanthi, J.L., 217
 Johnson, E.T., 142
 Johnston, S., 40
 Jonckheere, R., 20
 Joshi, B., 217
 Jourdan, F., 68
 Karaođlan, F., 20
 Kehelpannala, K.V.W., 155
 Khatun, M.M., 175
 Khatun, M.M., 175
 Koizumi, T., 98
 Kotlyarov, A.V., 187
 Kriesman, L., 56
 Krivonogov, 45
 Kumar, B.C., 117
 Kumar, K.S., 36
 Kumar, S., 32,
 Kwon, S., 2, 86,
 Kwon, S., 86
 Lanjewar, S., 179
 Li Jian-Wei., 173
 Li Shan-Shan., 134
 Li, J., 40
 Li, W., 5
 Link, K., 167
 Liu, X., 66
 Liu, X.M., 5
 Mahadevan, T.M., 92
 Maibam B., 167, 194
 Maibam, B., 161
 Malaviarachchi, S, P.K., 56, 100
 Manikyamba, C., 28, 117
 Mansfield, W.H., 122
 McInnes, B., 68
 Merdith, A., 88
 Mikolaichuk, V.A., 187
 Mohan, R., 225
 Mohanty, D.P., 164
 Mokane, L., 155
 Morton, A., 136

Müller, D., 88
Murad, A.A., 19
Murthy, S., 197
Nahar, M., 138
Nair, R.R., 154
Nair, S.C., 148
Nandakumar, V., 217
Nandy, S., 42
Noh, J., 86
Osanai, Y., 56
Pandey, O.P., 170
Parthasarathy, G., 115
Patranabis-Deb, S., 172
Phani, P.R.C., 38
Pillai, S.S.K., 177
Pradeepkumar, A.P., 213, 221, 223
Pradeepkumar, T., 71
Prakash, R.S., 200
Prasanth, R.S., 221
Pratheesh, P., 108
Rajesh S., 213
Rajesh, V.J., 30, 37, 215
Rajiv Singh, Y., 194
Ramanathan, A.L., 194
Ramasamy, S., 200
Rambabu, S., 117
Rambelason R. A., 103
Randive, K., 179
Rashid, S.A., 58
Ratheeshkumar, R.T., 52
Reddy, U.V.B., 120
Remya, J., 223
Renjith, M.L., 13, 60
Richard, L., 155
Rizell, M.E., 210
Roberts, N.M.W., 182
Robinson, P.T., 173
Rongfeng Ge., 202
Safonova, I.Yu., 187
Saha, A., 117
Saitoh, Y., 95, 105
Sajeev, K., 56,71, 215
Sajinkumar, K.S., 37, 124
Sakai, T., 126
Samuel, V., 217, 219
Santosh, M., 24, 26, 28, 55, 71, 80, 100, 103, 117, 120, 122, 124, 134, 142, 149, 190, 205
Satyanarayanan, M., 60, 71, 115
Sawant, A.D., 192
Saxena, A., 63
Sazzadur, R. M., 138
Searle, M.P., 182
Sehsah, H., 88
Sengupta, S., 42
Shahriar Md. Shams., 75
Shaji J., 146
Shaji, E., 16, 80,103,122,134,148
Shu, L., 7
Shukla, A.D., 194
Simonov, V.A., 187
Singh, K.J., 63
Singh, S.P., 60, 124
Smith, T., 204
Sorcar, N., 217
Subba Rao, D.V., 60, 117
Subrahmanyam, K.S.V., 120
Sukhorukov, V.P., 112
Turkina, O.M., 112
Sun, S., 66
Sun, S.S., 5
Suresh, K., 37,124
Sutthirat. C., 91
Takahashi,K., 95, 105
Takamura, Y., 95, 100, 105
Tang Li., 26
Tang Li., 117
Tapu Al-Tamini., 75, 89
Taylor Richard, J. M., 142
Tessalina, S., 68
Tewari, R., 47, 131
Thangal. M.K., 148
Tomson, J.K., 217
Tsunogae, T., 26, 56, 71, 91, 95, 98, 100, 103, 105, 134, 138, 175
Tsutsumi, Y., 100
Uddin, Md. Nehal., 75
Upreti, B.N., 126
Uthup, S., 30
vanreenen, D.D., 98
Vikas, C., 108
Wang Kuo-Lung., 210
Wang, G., 24
Williams, I.S., 219
Williams, S., 88
Wu, H., 202
Xin, Y., 40
Xiong, F., 173
Yang B., 204
Yang, F., 24
Yang, J., 173
Yang, Q.Y., 80, 120, 205
Yang, Z., 5, 66
Yao, J., 7
Zaman, M.N., 89
Zhang, F.F., 5
Zhang, Y., 40
Zhang, Z. M., 120
Zhao, G., 1, 40
Zhou Mei-Fu., 173
Zhou, X., 66
Zhou, X.H., 5
Zhu, D.C., 20
Zhu, W., 202

